4 January 2008 | $10

Science

The Cosmic Web

AAAS

CONTENTS

Volume 319, Issue 5859

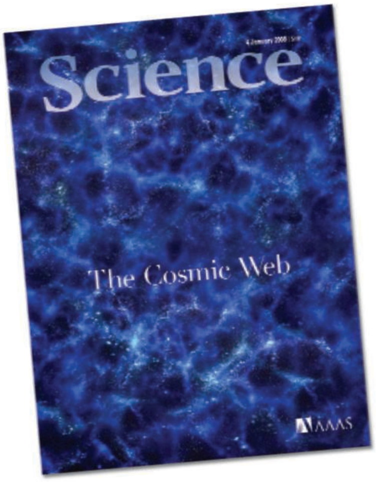

COVER

The universe is filled with filamentary structures of dark and visible matter that make up the "cosmic web," as suggested in this artist's rendering of cosmic bubbles and connected clumps. A special section beginning on page 46 considers the latest research into the origins and evolution of the cosmic web.

Image: Shigemi Numazawa/Atlas Photo Bank/Photo Researchers Inc.

DEPARTMENTS

EDITORIAL

SPECIAL SECTION

Cosmic Web

INTRODUCTION

NEWS

PERSPECTIVES

47

NEWS OF THE WEEK

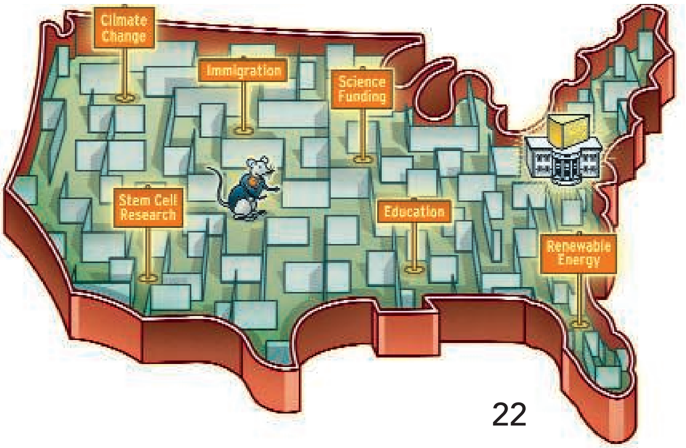

22

NEWS FOCUS

U.S. Presidential Candidates

CONTENTS continued >>

CONTENTS

SCIENCE EXPRESS

www.sciencexpress.org

BIOPHYSICS

Three-Dimensional Super-Resolution Imaging by Stochastic Optical Reconstruction Microscopy
B. Huang, W. Wang, M. Bates, X. Zhuang
Three-dimensional fluorescence images of cellular structures in fixed cells are realized at 20- to 30-nm lateral and 50-nm axial resolution, without scanning.
10.1126/science.1153529

BIOCHEMISTRY

Direct Observation of Hierarchical Folding in Single Riboswitch Aptamers
W. J. Greenleaf et al.
Optical trapping reveals that activation by adenine stabilizes the weakest helix in a riboswitch, after which secondary and tertiary structures are formed sequentially.
10.1126/science.1151298

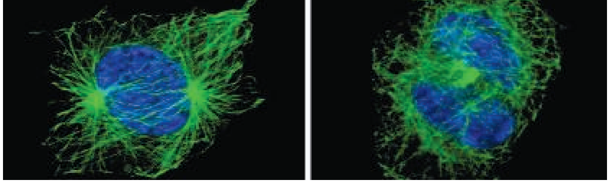

GENETICS

Mutations in the Pericentrin (*PCNT*) Gene Cause Primordial Dwarfism
A. Rauch et al.
In humans, an inherited condition with small brain size and near-normal intelligence is caused by mutations that disrupt chromosome separation during cell division.
10.1126/science.1151174

CLIMATE CHANGE

The Spatial Pattern and Mechanisms of Heat Content Change in the North Atlantic
M. S. Lozier et al.
Warming and cooling in different parts of the North Atlantic since 1950 reflect variable atmospheric circulation, complicating our understanding of anthropogenic changes.
10.1126/science.1146436

LETTERS

BOOKS *ET AL.*

POLICY FORUM

PERSPECTIVES

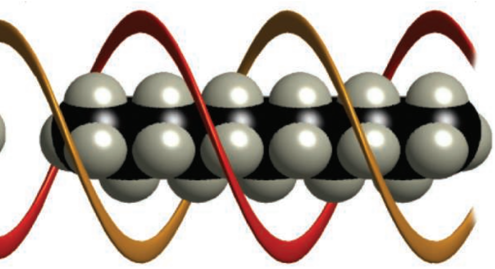

41 & 69

TECHNICAL COMMENT ABSTRACTS

PALEONTOLOGY

BREVIA

EVOLUTION

Rarity of Males in Pea Aphids Results in Mutational Decay 58
J. A. Brisson and S. V. Nuzhdin
Genes used preferentially by female pea aphids are under stronger selection than those used by males, probably because females mainly reproduce asexually.

EVOLUTION

Physiological Sex Predicts Hybrid Sterility Regardless of Genotype 59
J. H. Malone and P. Michalak
An apparent violation of Haldane's rule (in hybrid organisms the heterogametic sex tends to be sterile) in frogs can be explained by postulating that males have evolved faster.

RESEARCH ARTICLES

PALEOCLIMATE

Reduced North Atlantic Deep Water Coeval with the Glacial Lake Agassiz Freshwater Outburst 60
H. F. Kleiven et al.
Data on deep water formation in the North Atlantic indicate that the sudden draining of a huge glacial lake south of Hudson Bay led to dramatic cooling 8200 years ago.

GENETICS

The *Physcomitrella* Genome Reveals Evolutionary Insights into the Conquest of Land by Plants 64
S. A. Rensing et al.
Comparison of the moss genome sequence with those of other plants reveals hallmarks of colonization of land, including genes to manage terrestrial stresses such as dehydration.

CONTENTS continued >>

Published by AAAS

REPORTS

CHEMISTRY

Hidden Degrees of Freedom in Aperiodic Materials 69

B. Toudic et al.

Neutron diffraction shows how a host-guest crystal can undergo a phase transition that affects only higher-dimensional parameters that relate two simple sublattices. *>> Perspective p. 41*

CHEMISTRY

Nonadiabatic Interactions in the Cl + H_2 Reaction Probed by ClH_2^- and ClD_2^- Photoelectron Imaging 72

E. Garand et al.

Comparison of high-resolution spectra with theoretical simulations reveals that electronically excited ions subtly participate in an elementary reaction. *>> Perspective p. 40*

GEOCHEMISTRY

Helium and Neon Abundances and Compositions in Cometary Matter 75

B. Marty et al.

The amount and isotopic composition of helium and neon in Stardust samples imply that comet Wild 2 acquired these gases in a high-energy environment near the young Sun.

PLANETARY SCIENCE

Temperature and Composition of Saturn's Polar Hot Spots and Hexagon 79

L. N. Fletcher et al.

Cassini observations show that Saturn's atmosphere has stable, unusually hot vortices around both poles, even though its north pole is shrouded in darkness.

PALEONTOLOGY

The Avalon Explosion: Evolution of Ediacara Morphospace 81

B. Shen, L. Dong, S. Xiao, M. Kowalewski

Earth's first complex life 575 million years ago rapidly encompassed the full range of ediacara morphologies before declining, a pattern like that in the later Cambrian explosion.

GEOPHYSICS

Intermittent Plate Tectonics? 85

P. G. Silver and M. D. Behn

Subduction may have stopped at times in Earth's past as supercontinents formed, thus slowing the planet's heat loss.

EVOLUTION

A Mosaic of Chemical Coevolution in a Large Blue Butterfly 88

D. R. Nash, T. D. Als, R. Maile, G. R. Jones, J. J. Boomsma

Because they are coated with a specific chemical, the larvae of a butterfly are adopted and cared for by an ant species, a relationship that shows signs of ongoing coevolution.

EVOLUTION

Polymorphic Y Chromosomes Harbor Cryptic Variation with Manifold Functional Consequences 91

B. Lemos, L. O. Araripe, D. L. Hartl

Unexpectedly, the Y chromosome exerts strong regulatory effects on X-linked and autosomal genes in *Drosophila*. *>> Perspective p. 42*

MOLECULAR BIOLOGY

Heterochromatin and RNAi Are Required to Establish CENP-A Chromatin at Centromeres 94

H. D. Folco, A. L. Pidoux, T. Urano, R. C. Allshire

Formation of the centromere, the specialized region by which chromosomes are pulled apart during cell division, requires the presence of RNAi-induced heterochromatin.

CELL BIOLOGY

Assembly Mechanism of the Contractile Ring for Cytokinesis by Fission Yeast 97

D. Vavylonis et al.

The contractile ring of cell division is powered by myosin motors on the cell equator, which capture and pull actin filaments growing randomly from the equator.

NEUROSCIENCE

Ongoing in Vivo Experience Triggers Synaptic Metaplasticity in the Neocortex 101

R. L. Clem, T. Celikel, A. L. Barth

During continuous sensory stimulation, NMDA receptors in the mouse cortex switch from enhancing synaptic potentiation to opposing it. *>> Perspective p. 39*

NEUROSCIENCE

Small Circuits for Large Tasks: High-Speed Decision-Making in Archerfish 104

T. Schlegel and S. Schuster

Archerfish shoot their insect prey with a stream of water and then use sensory information and just a few neurons to calculate how to retrieve their food.

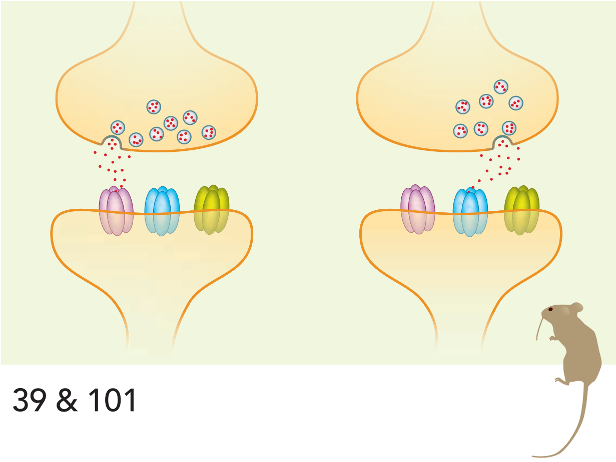

39 & 101

SCIENCE (ISSN 0036-8075) is published weekly on Friday, except the last week in December, by the American Association for the Advancement of Science, 1200 New York Avenue, NW, Washington, DC 20005. Periodicals Mail postage (publication No. 484460) paid at Washington, DC, and additional mailing offices. Copyright © 2008 by the American Association for the Advancement of Science. The title SCIENCE is a registered trademark of the AAAS. Domestic individual membership and subscription (51 issues): $144 ($74 allocated to subscription). Domestic institutional subscription (51 issues): $770; Foreign postage extra: Mexico, Caribbean (surface mail) $55; other countries (air assist delivery) $85. First class, airmail, student, and emeritus rates on request. Canadian rates with GST available upon request, GST #1254 88122. Publications Mail Agreement Number 1069624. SCIENCE is printed on 30 percent post-consumer recycled paper. **Printed in the U.S.A.**

Change of address: Allow 4 weeks, giving old and new addresses and 8-digit account number. **Postmaster:** Send change of address to AAAS, P.O. Box 96178, Washington, DC 20090–6178. **Single-copy sales:** $10.00 current issue, $15.00 back issue prepaid includes surface postage; bulk rates on request. **Authorization to photocopy** material for internal or personal use under circumstances not falling within the fair use provisions of the Copyright Act is granted by AAAS to libraries and other users registered with the Copyright Clearance Center (CCC) Transactional Reporting Service, provided that $20.00 per article is paid directly to CCC, 222 Rosewood Drive, Danvers, MA 01923. The identification code for *Science* is 0036-8075. *Science* is indexed in the *Reader's Guide to Periodical Literature* and in several specialized indexes.

CONTENTS continued **>>**

EDITED BY STELLA HURTLEY AND PHIL SZUROMI

THE ANT AND THE BUTTERFLY

Complex channels of chemical communication affect both the ecology and evolution of interactions among species. In Denmark, the Alcon blue butterfly larvae are adopted by ants of the genus *Myrmica*, which raise them preferentially to their own young. **Nash *et al.*** (p. 88) show that similarity in host and parasite surface chemistry explains a significant proportion of the variation in virulence of the parasite. Patterns of host cuticular chemistry are consistent with an ongoing coevolutionary arms race with one of its host ants (*Myrmica rubra*), but not with an alternative host (*Myrmica ruginodis*).

A Cooling Outburst

The generally stable climate of the North Atlantic region during the Holocene was interrupted by sudden intense cooling about 8200 years ago. It often is assumed that this event was the result of weaker ocean overturning circulation caused by the injection of large amounts of freshwater melt into the North Atlantic Ocean. **Kleiven *et al.*** (p. 60, published online 6 December), using an ocean sediment core from a location in the Northwest Atlantic well-suited to record a flood of fresh water from the Laurentide Ice Sheet, show that the bottom water chemistry and flow speed of Lower North Atlantic Deep Water changed markedly at approximately the same time as the catastrophic freshwater outburst from Lake Agassiz.

Motion in a Higher Plane

In host-guest materials, the lattices of the host framework and captured guests can differ in an incommensurate fashion along one or more dimensions. In such cases, the full crystal structure must be described by using a higher-dimensional superspace framework. **Toudic *et al.*** (p. 69; see the Perspective by **Coppens**) probed such an incommensurate system—a urea lattice encapsulating nonadecane—using neutron diffraction and uncovered a phase transition that exclusively involves rearrangement in the fourth, superspace dimension.

Supercontinents and Subduction

Mapping of the ocean basin and geologic reconstructions provides direct evidence for subduction that occurred continuously back to a few hundred million years ago. Older mountain belts and arc volcanoes clearly indicate that subduction events occurred 2 to 3 billion years ago. Has subduction necessarily occurred continuously since then? **Silver and Behn** (p. 85) argue that it may have ceased during times of supercontinent assembly several times in Earth's history, with consequences for cooling of the Earth.

How Mosses Made Their Move

Mosses represent an evolutionary intermediate between the aquatic algae and the dry-land angiosperms. **Rensing *et al.*** (p. 64; published online 13 December) present a draft genome sequence of the moss *Physcomitrella patens*, which gives insight into the evolution of plants from aquatic to terrestrial environments, the acquisition of certain hormone signaling pathways, and changes in life cycle.

Search and Capture

Cytokinesis, the physical process of separating two daughter cells, has resisted mechanistic understanding because it is not only complicated at the molecular level but it also involves the mechanical assembly of thousands of protein molecules into a regular structure. **Vavylonis *et al.*** (p. 97, published online 13 December) combined results from high-resolution observations of live cells and numerical simulations to suggest that the contractile ring assembles by a stochastic but remarkably reliable search-and-capture mechanism. Myosin motors in structures called nodes capture actin filaments growing randomly from other nodes. The motors pull on the attached node for a few seconds before releasing. These random movements condense the nodes into a continuous contractile ring around the equator of the cell.

The Shapes of Things Past

One measure of the diversity of life that is particularly useful in studying fossil assemblages is how organisms fill morphospace, which is a graphical representation of possible shapes or forms. This measure provides an approach that is complementary to taxonomic analyses. **Shen *et al.*** (p. 81) found that the early Ediacaran faunas, which represent Earth's first complex life, occupied all of the morphospace seen throughout the entire Ediacaran, and that later Precambrian fossils assemblages show a decline. This pattern is similar to that seen for the later Cambrian Explosion.

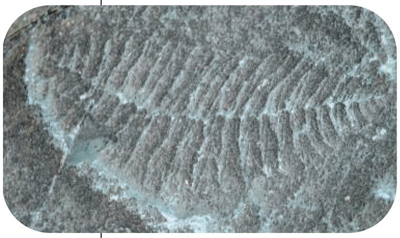

Small Brains, Big Decisions

The sophisticated cognitive performance of primates is usually associated with highly specialized brain areas containing enormous numbers of neurons in high densities and a plethora of synaptic contacts. **Schlegel and Schuster** (p. 104) provide a rather surprising example of a minute network in a fish that drives a highly sophisticated and plastic decision. Archerfish decision-making not only involves pinpointing the sensory configuration in a huge four-dimensional space and mapping it precisely onto a fine-tuned two-dimensional motor space. It also involves judging which of two targets is more rewarding by selectively attending to this target and then deciding when a response is unlikely to succeed.

CREDITS (TOP TO BOTTOM): DAVID NASH; BING SHEN AND SHUHAI XIAO/VIRGINIA POLYTECHNIC INSTITUTE

Published by AAAS

Donald Kennedy is the Editor-in-Chief of *Science*.

Science and God in the Election

THIS IS THE FIRST ISSUE OF THE NEW YEAR, AND GUESS WHAT? IT'S AN ELECTION YEAR IN THE United States, and other nations are watching the developments with interest. So *Science*'s News Focus section, beginning on p. 22, presents some of the major presidential candidates' views about science and science policy. We hope that these will give citizens of all countries a sense of how these aspirants would meet the essentially global challenges that rest on science and technology, including climate change, health policy, resource management, and energy conservation.

This election will be carried out amid new forces that have put the religious commitments of the candidates at the political center stage, a phenomenon now endemic to the United States but to few other non-Muslim nations. This contemporary dimension of presidential politics was brought into focus for me when a questioner in one of the "debates" brandished a copy of the Bible and asked the Republican candidates: "How you answer this question will tell us everything we need to know about you. Do you believe every word of this book?" It brought forth affirmative responses, with occasional limiting reservations about "metaphor" or "allegory," putting God right in the voting booth.

With respect to faith disclosures in politics, this is something new. This year, candidate Romney gave a speech to explain his Mormon faith, perhaps reassuring the evangelical Republican base by identifying Jesus Christ as "the son of God and the savior of mankind." Nearly 50 years ago, John Kennedy gave a speech in which he reassured the 1960 electorate about his Catholicism. He simply said that his religion would not affect his position as the U.S. president. Unlike Romney, he didn't give the voters an exegesis of his own faith; he clearly indicated that his private religious commitments would stay outside the Oval Office and were therefore not their business.

But these days, presidential candidates—even some Democrats—find it necessary to use religion to qualify their electability. The First Amendment of the U.S. Constitution is clear on prohibiting the establishment of a national religion. Yet in the election, we have been told repeatedly that the United States is a "Christian nation." This assertion might pass as the "free exercise" of religious preference as a fundamental right, a clause that has repeatedly clashed with the establishment clause. But when a candidate tries to persuade voters that his faith constitutes a claim on their vote, it surely touches on the establishment clause.

Given this new focus on religious disclosure, what does this U.S. election have to do with science? Everything. The candidates should be asked hard questions about science policy, including questions about how those positions reflect belief. What is your view about stem cell research, and does it relate to a view of the time at which human life begins? Have you examined the scientific evidence regarding the age of Earth? Can the process of organic evolution lead to the production of new species, and how? Are you able to look at data on past climates in search of inferences about the future of climate change?

Especially because we are in a new era of faith advertisement, we should demand that candidates provide thoughtful answers to such scientific questions. That religion has entered the political space should not produce a conflict between science and religion. Some of my scientist friends are religiously committed, others are actively disengaged, and both kinds are principled. Most of them are disinclined to join the religion versus science debate, which has become uncomfortably combustible.

But we share a right to press candidates about their views on the boundary. After all, determined efforts have been made to introduce scriptural versions of the age of Earth or of "intelligent design" in science classrooms. We need to know the candidates' qualifications for understanding and judging science, and for speaking intelligently about science and technology to the leaders of other nations in planning our collective global future. I don't need them to describe their faith; that's their business and not mine. But I do care about their scientific knowledge and how it will inform their leadership.

– Donald Kennedy

10.1126/science.1154211

CREDIT: COMSTOCK/CORBIS

www.sciencemag.org

Science

1200 New York Avenue, NW
Washington, DC 20005
Editorial: 202-326-6550, FAX 202-289-7562
News: 202-326-6581, FAX 202-371-9227

Bateman House, 82-88 Hills Road
Cambridge, UK CB2 1LQ
+44 (0) 1223 326500, FAX +44 (0) 1223 326501

Subscription Services For change of address, missing issues, new orders and renewals, and payment questions: 866-434-AAAS (2227) or 202-326-6417, FAX 202-842-1065. Mailing addresses: AAAS, P.O. Box 96178, Washington, DC 20090-6178 or AAAS Member Services, 1200 New York Avenue, NW, Washington, DC 20005

Institutional Site Licenses please call 202-326-6755 for any questions or information

Reprints: Author Inquiries 800-635-7181
Commercial Inquiries 803-359-4578

Permissions 202-326-7074, FAX 202-682-0816

Member Benefits AAAS/Barnes&Noble.com bookstore www.aaas.org/bn; AAAS Online Store http://www.apisource.com/aaas/ code MKB6; AAAS Travels: Betchart Expeditions 800-252-4910; Apple Store www.apple/eppstore/aaas; Bank of America MasterCard 1-800-833-6262 priority code FAA3YU; Cold Spring Harbor Laboratory Press Publications www.cshlpress.com/affiliates/aaas.htm; GEICO Auto Insurance www.geico.com/landingpage/go51.htm?logo=17624; Hertz 800-654-2200 CDP#343457; Office Depot https://bsd.officedepot.com/portalLogin.do; Seabury & Smith Life Insurance 800-424-9883; Subaru VIP Program 202-326-6417; VIP Moving Services http://www.vipmayflower.com/domestic/index.html; Other Benefits: AAAS Member Services 202-326-6417 or www.aaasmember.org.

science_editors@aaas.org	(for general editorial queries)
science_letters@aaas.org	(for queries about letters)
science_reviews@aaas.org	(for returning manuscript reviews)
science_bookrevs@aaas.org	(for book review queries)

Published by the American Association for the Advancement of Science (AAAS), *Science* serves its readers as a forum for the presentation and discussion of important issues related to the advancement of science, including the presentation of minority or conflicting points of view, rather than by publishing only material on which a consensus has been reached. Accordingly, all articles published in *Science*—including editorials, news and comment, and book reviews—are signed and reflect the individual views of the authors and not official points of view adopted by AAAS or the institutions with which the authors are affiliated.

AAAS was founded in 1848 and incorporated in 1874. Its mission is to advance science and innovation throughout the world for the benefit of all people. The goals of the association are to: foster communication among scientists, engineers and the public; enhance international cooperation in science and its applications; promote the responsible conduct and use of science and technology; foster education in science and technology for everyone; enhance the science and technology workforce and infrastructure; increase public understanding and appreciation of science and technology; and strengthen support for the science and technology enterprise.

Information for Authors

See pages 120 and 121 of the 5 January 2007 issue or access www.sciencemag.org/feature/contribinfo/home.shtml

EDITOR-IN-CHIEF **Donald Kennedy**
EXECUTIVE EDITOR **Monica M. Bradford**
DEPUTY EDITORS **R. Brooks Hanson, Barbara R. Jasny, Katrina L. Kelner**
NEWS EDITOR **Colin Norman**

Editorial supervisory senior editor Phillip D. Szuromi; **senior editor/perspectives** Lisa D. Chong; **senior editors** Gilbert J. Chin, Pamela J. Hines, Paula A. Kiberstis (Boston), Marc S. Lavine (Toronto), Beverly A. Purnell, L. Bryan Ray, Guy Riddihough, H. Jesse Smith, Valda Vinson, David Voss; **associate editors** Jake S. Yeston, Laura M. Zahn; **online editor** Stewart Wills; **associate online editors** Robert Frederick, Tara S. Marathe; **book review editor** Sherman J. Suter; **associate letters editor** Jennifer Sills; **editorial manager** Cara Tate; **senior copy editors** Jeffrey E. Cook, Cynthia Howe, Harry Jach, Barbara P. Ordway, Trista Wagoner; **copy editors** Lauren Kmec, Peter Mooreside; **editorial coordinators** Carolyn Kyle, Beverly Shields; **publications assistants** Ramatoulaye Diop, Chris Filiatreau, Joi S. Granger, Jeffrey Hearn, Lisa Johnson, Scott Miller, Jerry Richardson, Brian White, Anita Wynn; **editorial assistants** Carlos L. Durham, Emily Guise, Patricia M. Moore, Jennifer A. Seibert; **executive assistant** Sylvia S. Kihara; **administrative support** Maryrose Madrid

News senior correspondent Jean Marx; **deputy news editors** Robert Coontz, Eliot Marshall, Jeffrey Mervis, Leslie Roberts; **contributing editors** Elizabeth Culotta, Polly Shulman; **news writers** Yudhijit Bhattacharjee, Adrian Cho, Jennifer Couzin, David Grimm, Constance Holden, Jocelyn Kaiser, Richard A. Kerr, Eli Kintisch, Andrew Lawler (New England), Greg Miller, Elizabeth Pennisi, Robert F. Service (Pacific NW), Erik Stokstad; **intern** Elsa Youngsteadt; **contributing correspondents** Jon Cohen (San Diego, CA), Daniel Ferber, Ann Gibbons, Robert Irion, Mitch Leslie, Charles C. Mann, Virginia Morell, Evelyn Strauss, Gary Taubes; **copy editors** Rachel Curran, Linda B. Felaco, Melvin Gatling; **administrative support** Scherraine Mack, Fannie Groom; **bureaus** New England: 207-549-7755, San Diego, CA: 760-942-3252, FAX 760-942-4979, Pacific Northwest: 503-963-1940

Production director James Landry; **senior manager** Wendy K. Shank; **assistant manager** Rebecca Doshi; **senior specialists** Jay Covert, Chris Redwood; **specialist** Steve Forrester; **Preflight director** David M. Tompkins; **manager** Marcus Spiegler; **specialist** Jessie Mudjitaba

Art director Kelly Buckheit Krause; **associate art director** Aaron Morales; **illustrators** Chris Bickel, Katharine Sutliff; **senior art associates** Holly Bishop, Laura Creveling, Preston Huey, Nayomi Kevitiyagala; **associate** Jessica Newfield; **photo editor** Leslie Blizard

Science International

Europe (science@science-int.co.uk) **editorial: international managing editor** Andrew M. Sugden; **senior editor/perspectives** Julia Fahrenkamp-Uppenbrink; **senior editors** Caroline Ash, Stella M. Hurtley, Ian S. Osborne, Stephen J. Simpson, Peter Stern; **associate editor** Joanne Baker; **editorial support** Deborah Dennison, Rachel Roberts, Alice Whaley; **administrative support** Janet Clements, Jill White; **news: europe news editor** John Travis; **deputy news editor** Daniel Clery; **contributing correspondents** Michael Balter (Paris), John Bohannon (Vienna), Martin Enserink (Amsterdam and Paris), Gretchen Vogel (Berlin); **intern** Elizabeth Quill

Asia Japan Office: Asca Corporation, Eiko Ishioka, Fusako Tamura, 1-8-13, Hirano-cho, Chuo-ku, Osaka-shi, Osaka, 541-0046 Japan; +81 (0) 6 6202 6272, FAX +81 (0) 6 6202 6271; asca@os.gulf.or.jp; **asia news editor** Richard Stone (Beijing: rstone@aaas.org); **contributing correspondents** Dennis Normile (Japan: +81 (0) 3 3391 0630, FAX 81 (0) 3 5936 3531; dnormile@gol.com); Hao Xin (China: + 86 (0) 10 6307 4439 or 6307 3676, FAX +86 (0) 10 6307 4358; cindyhao@gmail.com); Pallava Bagla (South Asia: +91 (0) 11 2271 2896; pbagla@vsnl.com)

Africa Robert Koenig (contributing correspondent, rob.koenig@gmail.com)

EXECUTIVE PUBLISHER **Alan I. Leshner**
PUBLISHER **Beth Rosner**

Fulfillment Systems and Operations (membership@aaas.org); **director** Waylon Butler; **customer service supervisor** Pat Butler; **specialists** Laurie Baker, Latoya Casteel, LaVonda Crawford, Vicki Linton; **data entry supervisor** Cynthia Johnson; **specialists** Tarrika Hill, Erin Layne, Sheila Thomas

Business Operations and Administration director Deborah Rivera-Wienhold; **assistant director, business operations** Randy Yi; **senior financial analysts** Michael LoBue, Jessica Tierney; **financial analysts** Nicole Nicholson, Farida Yeasmin; **rights and permissions: administrator** Emilie David; **associate** Elizabeth Sandler; **marketing director** John Meyers; **marketing managers** Allison Pritchard, Darryl Walter; **marketing associates** Aimee Aponte, Alison Chandler, Mary Ellen Crowley, Marcia Leach, Julianne Wielga, Wendy Wise; **international marketing manager** Wendy Sturley; **marketing executive** Jennifer Reeves; **marketing/member services executive** Linda Rusk; **japan sales** Jason Hannaford; **site license sales director** Tom Ryan; **sales manager** Russ Edra; **sales and customer service** Mehan Dossani, Iquo Edim, Kiki Forsythe, Catherine Holland, Phillip Smith, Philip Tsolakidis; **electronic media: manager** Lizabeth Harman; **project manager** Trista Snyder; **assistant manager** Lisa Stanford; **senior production specialist** Walter Jones; **production specialists** Nichele Johnston, Kimberly Oster

Advertising director worldwide ad sales Bill Moran

Product (science_advertising@aaas.org); **consumer & sponsorship sales manager** Tina Morra: 202-326-6542; **midwest** Rick Bongiovanni: 330-405-7080, FAX 330-405-7081; **west coast/w. canada** Teola Young: 650-964-2266; **east coast/e. canada** Christopher Breslin: 443-512-0330, FAX 443-512-0331; **uk/europe/asia** Michelle Field: +44 (0) 1223-326-524, FAX +44 (0) 1223-325-532; **japan** Mashy Yoshikawa: +81 (0) 33235 5961, FAX +81 (0) 33235 5852; **senior traffic associate** Deiandra Simms

Commercial Editor Sean Sanders: 202-326-6430

Classified (advertise@sciencecareers.org); **us: recruitment sales manager** Ian King: 202-326-6528, FAX 202-289-6742; **inside sales manager: midwest/canada** Daryl Anderson: 202-326-6543; **northeast** Alexis Fleming: 202-326-6578; **southeast** Tina Burks: 202-326-6577; **west** Nicholas Hintibidze: 202-326-6533; **sales coordinators** Erika Foard, Rohan Edmonson, Shirley Young; **international: sales manager** Tracy Holmes: +44 (0) 1223 326525, FAX +44 (0) 1223 326532; **sales** Marium Hudda, Alex Palmer, Alessandra Sorgente; **sales assistant** Louise Moore; **japan** Mashy Yoshikawa +81 (0)3 3235 5961, FAX +81 (0)3 3235 5852; **advertising production operations manager** Deborah Tompkins; **senior production specialists** Robert Buck, Amy Hardcastle; **senior traffic associate** Christine Hall; **publications assistant** Mary Lagnaoui

AAAS
ADVANCING SCIENCE, SERVING SOCIETY

RANDOMSAMPLES

EDITED BY CONSTANCE HOLDEN

SMALL ROCK, BIG BANG

The Tunguska explosion, which in June 1908 leveled trees over a 5000-square-kilometer swath of Siberian forest, may have come from a much smaller meteorite than scientists had thought. A supercomputer simulation by scientists at Sandia National Laboratory in Albuquerque, New Mexico, showed that a much higher proportion of the total blast energy was transported to the surface than had been assumed. As a result, the team reported at last month's meeting of the American Geophysical Union in San Francisco, California, the explosion was likely between 3 and 5 megatons instead of the 10 to 20 megatons estimated earlier. Principal investigator Mark Boslough says the results suggest that small meteorites pose a greater threat to Earth than experts believed.

Hwang Back?

Disgraced stem cell scientist Woo-Suk Hwang is seeking to restart his human cloning research in South Korea.

No one in South Korea has worked in the field since Hwang was dismissed from Seoul National University in March 2006. But on 17 December, the Ministry of Health and Welfare announced that the Suam Biotechnology Institute outside Seoul has applied for permission to begin studies on cloning human embryos for research. Hwang is on the eight-member team but is not the principal investigator.

Suam received approval from the ministry in September as a "designated institute" qualifying to do human nuclear-transfer studies. Under the recently strengthened bioethics laws, women may not donate eggs directly; scientists have to use leftover eggs from fertility clinics. Hwang, still on trial for alleged embezzlement, bioethics violations, and fraud, began research on animal cloning at Suam in July 2006. He has recently been doing human-cloning research at a lab in Thailand.

"We're not sure if we will allow such research, in light of recent discoveries of more ethically safe alternatives and Hwang's reputation," said Byung-guk Yang, head of the ministry's bioethics safety department. The ministry must decide within 90 days of receiving the application.

Natufian Toolbox

Archaeologists have identified what they think are the remnants of a bag of tools used by a Natufian about 13,000 years ago for both hunting and harvesting.

Natufians were sedentary hunter-gatherer people who are of intense interest to archaeologists because they lived in the Mideast when people first started farming.

Phillip C. Edwards of La Trobe University in Victoria, Australia, who led excavations of the site—Wadi Hammeh 27—in the 1980s, reported in the December issue of *Antiquity* that a cluster of artifacts found there was probably all part of one Natufian's gear. The centerpiece was a sickle made of goat horn for cutting wild grains, with grooves in which sharp pieces of flint had been laid end to end like razorblades. There was also part of a bone handle, five beads made from gazelle foot bones, seven polished pebbles, 21 small flint crescent-shaped projectile points, and a core of the same flint.

The assemblage indicates that one person would set out for the day carrying materials for hunting, reaping, and toolmaking—evidence, Edwards says, that both sexes might have engaged in both hunting and gathering. "Natufian society was going through a profound change that encompassed every aspect of human life," says archaeologist Anna Belfer-Cohen of Hebrew University in Jerusalem, who agrees that probably included "gender role[s] and division of labor." Harvard University archaeologist Ofer Bar-Yosef calls the work a "major contribution to what we want to know about Natufian culture."

Lost Wax

Surfer Mike Ehlon found a chunk of beeswax in 2005.

For the past 300 years, chunks of amber-colored beeswax, some reportedly weighing as much as 54 kilograms, have occasionally washed up on the shores of Oregon's Nehalem Bay after a storm. In a few instances, exceptionally low tides have revealed a wooden hull. But the "beeswax wreck" has long been shrouded in mystery.

Now, a team of archaeologists, geologists, and historians intends to find the ship and excavate it. From radiocarbon dates of some of the wax and analyses of pieces of Chinese porcelain that have also washed up, they believe the vessel was a Spanish galleon that sank between 1650 and 1700 while plying the historic Manila-Acapulco trade route. Project leader Scott Williams of Washington state's Department of Archaeology and Historic Preservation says beeswax was a big trade item at the time, as the Catholic Church used only that substance for its candles. Because the New World lacked native honey bees, merchants shipped tons of wax made by bees in the Philippines.

Team members are now using remote sensing to look for the hull of the ship, which they believe is either the *Santo Christo de Burgos*, which sank in 1693, or the *San Francisco Xavier*, which disappeared in 1705. Progress is being tracked at www.archaeologychannel.org. Jon Erlandson, director of the University of Oregon Museum of Natural and Cultural History, notes approvingly that instead of wanting to ransack Spanish galleons for gold, this team wants "to really scientifically explore it."

CREDITS (TOP TO BOTTOM): RANDY MONTOYA; P. EDWARDS; RICK ROGERS/THE BEESWAX WRECK PROJECT

EDITED BY YUDHIJIT BHATTACHARJEE

People to Watch in 2008

THE COUNTDOWN >>

U.S. science policy could take a new turn after the fall elections. What are the chances that these six top science officials (pictured left to right) will be around in the next Administration? Here are our best guesses.

- Presidential science adviser **John Marburger**: The longest-serving science adviser in history and the only one who's held that job for George W. Bush says he has no plans to leave before January 2009—0%.
- NIH Director **Elias Zerhouni**: He's nearing the 5-year mark in an open-ended term that has required him to administer restrictions on embryonic stem cell research that he opposes. NIH insiders say he "plays his cards close to the chest"—20%.
- NSF Director **Arden Bement**: His 6-year stint runs until November 2010. And although he admits that a new president "could make things untenable," Bement says "as long as I'm doing a good job and having fun, I hope to complete my term"—50%.
- CDC Director **Julie Gerberding**: The infectious-disease expert began an open term as chief of a sleepy agency in 2002, instituting changes that sped the exit of many senior scientists. More recently, her forecast of climate-warming health consequences, softened by White House censors, drew fire—5%.
- NASA Administrator **Michael Griffin**: His promise to deliver a new rocket while keeping the rest of the agency healthy is meeting with increased skepticism within the Administration and Congress. Appointed nearly 3 years ago, observers expect him to stay until early 2009—20%.
- DOE science chief **Ray Orbach**: The longest-serving Bush science official after Marburger has enjoyed his nearly 6 years in Washington, D.C., long enough to wish for a reprieve from the normal political turnover. Insiders say he's working as though he has only a year left to finish his job—10%.

The Japanese government is hoping that Kyoto University's **Shinya Yamanaka** can keep the country in the forefront of stem cell research, building on his recent success in turning human skin cells into cells that behave like embryonic stem cells without the controversial use of embryos. The Ministry of Education is mulling building a center to help Yamanaka and others expand their work; there are no details yet on funding and staffing.

The first biologist to lead India's Council of Scientific and Industrial Research (CSIR) will be in the spotlight next year as he attempts to raise the profile of the $465 million, 38-lab network. **Samir Brahmachari**, who was appointed director general of the agency in November, spent the last decade transforming one of CSIR's less remarkable facilities into a leading research center for genome analysis. He is expected to play a role in guiding the government's recently announced plan for a 5-year, $1.6 billion investment in biotechnology research and training. CSIR's broad portfolio includes everything from aerospace engineering to oceanography. "The goal will be research for public good and strategic national needs," he says. "We've got lots of challenges—energy, transport, infectious diseases."

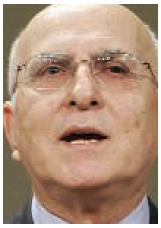

It's likely to be a key year for genetically modified (GM) crops in Europe—and for Greek politician **Stavros Dimas**, European commissioner for the environment. So far, only one GM crop—an insect-resistant maize variety—can be grown commercially, but several more are awaiting approval. In November, Dimas said he opposes two candidates, both maize strains equipped with a *Bt* gene to ward off insects. That puts him at odds with his own food safety agency and several pro-GM fellow commissioners. A formal decision on the two crops is expected sometime this year.

Over fierce student protests, France's higher education and research minister, **Valérie Pécresse**, last year pushed through a bill giving universities more freedom to handle their own affairs. But Pécresse says that much more is needed to make French science and education internationally competitive: She wants to lower the dropout rate among college students, reduce paperwork for researchers, increase project-based funding, and redefine the role of mammoth state-run labs like the National Centre for Scientific Research. Her reformist stance mirrors the approach taken by her boss, President Nicolas Sarkozy.

Volker ter Meulen will lead the Leopoldina as the 350-year-old organization takes on a new job as Germany's National Academy of Sciences. Ter Meulen, a virologist at the University of Würzburg, may need a bit of extra diplomacy as the Leopoldina fills its new role, which breaks with Germany's tradition of regional academies. He hopes to raise the scientific community's visibility in ongoing political debates on immigration, genetically modified crops, climate change, and energy.

CREDITS (TOP, LEFT TO RIGHT): SCIENCE; MARTY KATZ; RICK KOZAK; CDC; AP; DOE; (LOWER SECTION, TOP TO BOTTOM): CHRIS GOODFELLOW/GLADSTONE INST.; LANDOV; LANDOV; JENS SCHLÜTER/HALLE/SAALE; CSIR

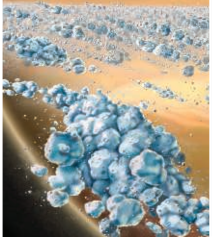

Saturn's old rings
21

Events to watch for in 2008
21

2008 U.S. BUDGET

Promising Year Ends Badly After Fiscal Showdown Squeezes Science

The U.S. science community's reaction to the 2008 federal budget adopted last month has been uniformly bleak. "A step backwards, … a missed opportunity, … a keen disappointment" declared press releases from advocates, including AAAS (which publishes *Science*), about a belated, $555 billion spending package (HR 2764) that was cobbled together and approved in a 4-day rush before the holidays. Those sad words are a reaction to the last-minute rollback of substantial planned increases for science that occurred after the Democratic-controlled Congress lost a showdown with the Republican White House.

The year began on a high note in February when President George W. Bush submitted his second straight request for large increases in the physical sciences at the National Science Foundation (NSF), the Department of Energy (DOE), and the National Institute of Standards and Technology (NIST), three agencies that constitute his American Competitiveness Initiative (ACI) (*Science*, 9 February 2007, p. 750). The good vibes continued with passage last summer of the America COMPETES Act, which contained even higher authorized spending levels for research, education and training, and innovation (*Science*, 10 August 2007, p. 736). Separate House and Senate spending panels working on the 2008 budget also matched or exceeded the president's request for several science agencies. But the legislation either languished in Congress or, in the case of a bill involving the National Institutes of Health (NIH), was vetoed by the president.

In the end, the numbers in the so-called omnibus spending bill (HR 2764) that was signed by President Bush the day after Christmas are much smaller than science boosters had thought likely for the 2008 fiscal year that began on 1 October. Research spending at NSF, for instance, will rise by only $56 million, to $4.8 billion, rather than by the $365 million requested back in February or by the even higher amounts the House and Senate had approved separately last fall. DOE's Office of Science saw a requested 15% increase in its $3.8 billion budget, which legislators had embraced, shrink by two-thirds. Programs in high-energy physics and fusion sciences were hit especially hard (for details, see *Science*NOW, www.sciencenow.org, for 18, 19, and 21 December 2007), and more than half of the growth is devoted to special projects earmarked by legislators. NIST winds up with a scant $6 million more for its core $434 million research programs instead of the $65 million boost that the president requested and legislators had approved earlier.

The pictures at other agencies not under the ACI umbrella are no brighter. NIH's $29.1 billion budget remains essentially flat once a $300 million transfer is subtracted; that's better than the 1% cut the president had sought but much less than a 3.7% rise Congress approved in the bill he vetoed this fall. NASA managed to hold onto the president's requested increase, a 3.1% jump to $17.3 billion. But it lost a $1 billion bump that legislators had previously adopted. Within that total, its $5.57 billion science budget, up $111 million, is eroded by millions of dollars in earmarks and directed spending for specific missions the agency hadn't requested.

Why did science fall short? Despite bipartisan support for boosting research budgets, larger forces prevailed. By threatening to veto any bills that exceeded his bottom line of $932 billion for domestic programs—which includes all research spending outside the Department of Defense—President Bush succeeded in

The Vision … and the Reality

AGENCY	FY 2007	FY 2008 Request	FY 2008 Final	% Change
National Institutes of Health	29,128*	28,849	29,456	+1.1%†
National Science Foundation	5,917	6,429	6,065	+2.6%
Research	4,766	5,131	4,821	+1.1%
Education	698	750	725	+4.0%
NASA science	5,466	5,516	5,577	+2.0%
Department of Energy science	3,797	4,397	4,018	+5.8%
Defense Department				
Basic research	1,564	1,428	1,614	+3.2%
DARPA	3,115	3,086	2,816	–9.6%
Department of Commerce				
NIST labs	434	500	440	+1.4%
NOAA research	532	528	573	+7.2%
EPA science	561	540	542	–3.5%
USDA competitive research	191	257	191	0.0%
U.S. Geological Survey research	564	547	583	+3.4%

* All figures in millions of current dollars.
† Includes Global AIDS Fund.

SOURCE: CONGRESS, THE FEDERAL AGENCIES, AND AAAS

FOCUS

Science and the wannabe presidents

22

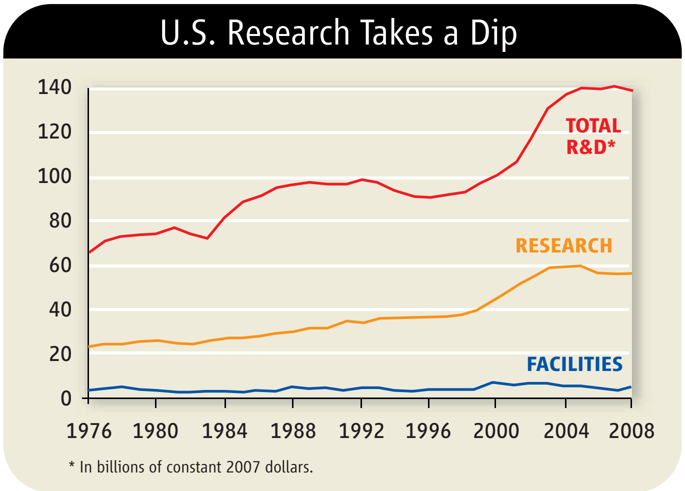

* In billions of constant 2007 dollars.

Going downhill. Research spending has failed to match inflation despite small increases this year for NSF, DOE, and NASA.

SOURCE: AAAS ANALYSES OF R&D SPENDING IN ANNUAL FEDERAL BUDGETS

forcing Democratic leaders to abandon $22 billion in additional proposed spending. The retreat affected almost every agency.

The legislators most intimately involved in the process—the chairs of the spending panels that assembled the individual pieces of the 1400-page bill—are no happier than their constituents. “The Commerce, Justice, Science Subcommittee agrees that the bill represents inadequate funding across the departments and agencies under our jurisdiction,” says Representative Alan Mollohan (D–WV), chair of the panel that oversees NSF, NASA, the National Oceanic and Atmospheric Administration, and NIST. “The House-passed bill,” Mollohan laments, “is far more representative of the committee’s priorities than is the omnibus.”

Presidential science adviser John Marburger says he’s also disappointed by the terms of the omnibus bill, although he says the president was pleased with its bottom line. “The most surprising aspect to me is the absence of any visible priority for basic research in the physical sciences … after the president asked for the money,” Marburger told *Science*. Mollohan’s comments are equally partisan. “Between the holes in President Bush’s budget request and his veto threats,” he says, the committee had little choice but to make “several rounds of unpleasant cuts.”

NSF’s budget reflects those last-minute changes. Only a few days before the final deal was announced on 15 December, NSF’s budget was still at the president’s request of $6.43 billion. It had survived a previous round of cuts imposed after Democratic leaders shaved $11 billion off their earlier total. But then the leadership ordered another $11 billion to be pared to satisfy the president’s demands. That’s when a $514 million overall increase for NSF, to $6.43 billion, shrunk to $150 million.

Traces of the promised largess can still be found in the report accompanying the massive bill, in language a staffer admits “was written before the cuts were taken.” The legislators urge NSF to give the biological sciences and the social, behavioral, and economic sciences “comparable growth” to what the math and physical sciences, computer sciences, and engineering directorates are receiving—although the budgets of all six research directorates are essentially flat. And two programs within those directorates receive special treatment. NSF was ordered “to provide the budget request” for operating all its ground-based telescopes, part of a strong lobbying campaign by supporters of the Arecibo radio telescope in Puerto Rico after NSF decided to reduce funding for the observatory (*Science*, 10 November 2006, p. 904). And legislators actually added $8 million to the $107 million requested for the Experimental Program to Stimulate Competitive Research, a long-running program to help 27 have-not states and territories.

NSF Director Arden Bement says those two directives “will pinch” other programs. As one NSF staffer notes, “those are all things that you can do with a $500 million increase. But we’re only getting $56 million [more for research].”

Despite the lower ceiling, Mollohan still made an effort to accommodate agencies’ wishes. NSF, for example, received all but $4 million of a $40 million requested increase in its $246 million account for salaries and operations. “I consider that to be a victory” for an overburdened merit-review system, says Bement, “and a sign that Congress realizes its importance.” Congressional aides say that Bement made clear it was a top priority.

Along with their scalpel, legislators also used an administrative fiat to meet the lowered spending ceiling. NSF must return $33 million, and NASA $192 million, from funds not spent during the 2007 fiscal year. DOE’s Office of Science was ordered to trim 0.9%, or a total of $33 million, from what it has received in fiscal year 2008 for current activities.

Some other legislative priorities scattered throughout the omnibus bill include:

- The National Children’s Study to track the health of 100,000 infants from birth to age 21 will get an increase of $42 million, to $111 million. NIH officials had said the $3 billion study is too expensive to continue (*Science*, 9 February 2007, p. 751). Congress also required “all investigators funded by the NIH” to submit final peer-reviewed manuscripts of papers accepted for publication to NIH’s PubMed Central for release on the Internet “no later than 12 months after the official date of publication.”
- NASA was given $40 million for future earth science missions, $60 million for the Space Interferometry Mission—$38.4 million more than it had requested—and $5 million to determine the next outer-planet destination. It will have $42 million to develop a robotic lunar lander, a mission that NASA had dropped to accommodate construction of its new rocket. Legislators also allocated $13.5 million more for microgravity life and physical sciences.
- Applied energy research at DOE may be the biggest winner. The department’s Energy Efficiency and Renewable Energy budget will rise by $282 million in 2008, to $1.7 billion, although $180 million of the increase will go to research and demonstration projects earmarked by legislators. The added program money will launch a $55 million project at the National Renewable Energy Laboratory in Golden, Colorado, to connect renewable energy systems such as intermittent wind power or plug-in hybrid cars to the U.S. electrical grid system. Legislators also added $40 million to the president’s $79 million request for research on carbon sequestration. DOE’s Advanced Scientific Computing Research program will get $354 million, $14 million more than requested.

–JEFFREY MERVIS

With reporting by Eli Kintisch, Andrew Lawler, and Eliot Marshall.

Published by AAAS

GENETICS

The Elusive ALS Genes

The disease that killed baseball legend Lou Gehrig has largely refused to reveal its secrets. In amyotrophic lateral sclerosis (ALS), motor neuron death causes irreversible wasting of skeletal muscles, but the underpinnings of this lethal condition remain elusive, particularly to geneticists.

In 1993, researchers identified mutations in the copper-zinc superoxide dismutase gene responsible for about 20% to 25% of the rare familial form of the disease, and other genes contributing to familial ALS have since been found. Yet the sporadic, or noninherited, form of ALS, making up at least 90% of cases, resists efforts to isolate genetic risk factors. In the past few years, ALS researchers intensified their hunt. After screening about 35 genes that could affect motor neurons, they tentatively linked several to sporadic ALS, including one that encodes a detoxifying enzyme.

But the hottest new tool in genetics, the whole-genome association (WGA) study, has added nothing but confusion to the gene hunt. Since August, three ALS teams have unveiled results from WGA studies. None of them has highlighted genes already under suspicion. Adding to the mystery, each WGA study tabs a different ALS gene. “Each time these things aren’t replicating, we have to ask ourselves why,” says Ammar Al-Chalabi, an ALS researcher at King’s College London.

WGA studies have soared in popularity as they’ve found genes associated with diseases such as type 2 diabetes and multiple sclerosis (*Science*, 11 May 2007, p. 820). Researchers scan patients’ DNA for variants called single-nucleotide polymorphisms (SNPs) and then compare the results to those from a healthy control group. SNPs appearing more frequently in patients will often point to a nearby gene that confers risk.

The ALS gene hunts using this method may be struggling because the disease is actually a spectrum of conditions. Many rare mutations could predispose to different ALS subtypes, making genes difficult to find in a WGA study lumping everyone together.

And the sheer thoroughness of whole-genome scans may be producing false leads for ALS scientists. Geneticists test a patient’s DNA for half a million or more SNPs, and these enormous numbers magnify the possibility of getting an association at random. “When you roll the dice 555,000 times, … by sheer chance alone, SNPs are going to show up with a significant *P* value,” says ALS researcher Bryan Traynor of the National Institute of Mental Health in Bethesda, Maryland. “They’re not genuinely associated with ALS, but they’ve shown up because of luck.” Statistical methods can correct for this, but they can obscure real associations and false positives alike.

The first WGA study for ALS, by Traynor’s group, actually found no SNPs significantly associated with the disease, although its power was limited by having fewer than 300 cases. Still, it “showed that there was no major gene that had a huge effect within ALS,” says Traynor.

Now three positive WGA studies have been published and at least two more have been submitted to journals, each of them finding different ALS genes. In the 23 August 2007 issue of the *New England Journal of Medicine*, a group from the nonprofit Translational Genomics Research Institute in Phoenix, Arizona, flagged a SNP near the obscure gene *FLJ10986*. In this study of 1152 patients, the odds of carriers of the SNP having ALS were, compared to noncarriers, 1.35 to 1, suggesting a minor contribution to the disease. In the October 2007 issue of *The Lancet Neurology*, a Dutch group reported that the inositol 1,4,5-triphosphate receptor 2 (*ITPR2*) gene was associated with ALS in three European populations. But when the same Dutch team expanded its analysis by including the patients whom Traynor surveyed and using a different methodology, *ITPR2* did not make the cutoff for significance. Instead, the Dutch team reported online 16 December in *Nature Genetics* an association for the dipeptidyl-peptidase 6 (*DPP6*) gene. In each case, the identified genes only subtly increased the odds of developing ALS.

Whole-Genome Association Studies in ALS

Lead Institution	Gene Identified	Month Published
National Institutes of Health	None	April 2007
Translational Genome Research Institute	*FLJ10986*	August 2007
University Medical Center Utrecht, the Netherlands	*ITPR2*	October 2007
University Medical Center Utrecht	*DPP6*	December 2007
King’s College London, U.K.	Undisclosed	Submitted
Harvard University	Undisclosed	Submitted
Northwestern University	Unknown	In progress
National Institutes of Health	Unknown	In progress

The *ITPR2* finding was plausible because *ITPR2* triggers release of calcium within neurons, and excess calcium can cause motor neuron death. A *DPP6* role in ALS is harder to fathom, but finding the association across four separate countries makes the Dutch researchers confident it’s genuine.

Still, the group has already embarked on studies to validate *ITPR2* and *DPP6* as ALS susceptibility genes. In the meantime, say others, these genes and others should be viewed with skepticism. “I would like to have at least one or two additional replications,” says Guy Rouleau, a neurologist at the University of Montreal in Canada. “And then I’ll think it’s *possible*.”

Before the WGA studies started to roll out, a promising ALS gene candidate was the one encoding the enzyme paraoxonase 1 (PON1). Last year, Polish and American groups reported that PON1 was associated with sporadic ALS, and this year Australian and Irish groups also found a link. “It’s only a weak signal, but it is seen every time it’s looked for,” says Al-Chalabi.

PON1 belongs to a family of enzymes that detoxify a wide variety of chemicals, including many insecticides and herbicides. If the ALS connection holds up, analyzing the effect of PON1 mutations on the enzyme’s targets could point to specific toxins or environmental exposures causing the disease. “That’s the dream,” says ALS researcher Robert Brown of Harvard Medical School in Boston.

But, frustratingly, PON1 did not emerge in any of the WGA studies. Brown suspects that only very large WGA efforts are likely to work for ALS, in which many genes probably interact with the environment.

The ALS Association is now organizing a study combining WGA data; most of the ALS groups have signed on. “In the end, it’s going to require a concerted effort by the whole ALS community … coming up with hopefully a credible answer that everyone believes,” says Al-Chalabi.

–KEN GARBER

Ken Garber is a freelance writer in Ann Arbor, Michigan.

Published by AAAS

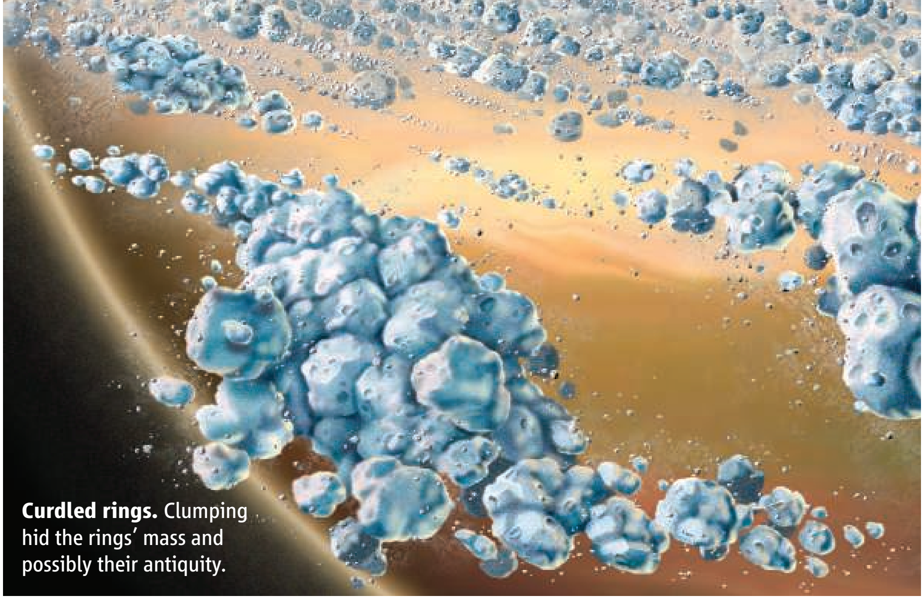

Curdled rings. Clumping hid the rings' mass and possibly their antiquity.

PLANETARY SCIENCE

Saturn's Rings Look Ancient Again

SAN FRANCISCO, CALIFORNIA—Saturn's rings, like any aging beauty, are keeping their age mysterious. Before the first spacecraft reached Saturn, planetary scientists assumed its rings formed along with the planet 4.5 billion years ago. But the Voyager spacecraft flying by in the early 1980s sent back evidence that the rings could be just a few hundred million years old. Now, the still-orbiting Cassini spacecraft is getting a longer look and finding signs of old age. "Right now, we still don't know whether it's old or new," concludes ring specialist Joseph Burns of Cornell University. But if the rings are indeed old, some researchers think they see ways that the rings make themselves look forever young.

The latest sign of the rings' antiquity is a tendency to put on weight—at least in the eyes of planetary scientists. Last month at the fall meeting of the American Geophysical Union here, Larry W. Esposito of the University of Colorado (UC), Boulder, and colleagues discussed results from Cassini's Ultraviolet Imaging Spectrograph (UVIS). In one mode of operation, UVIS can precisely and quickly record the brightness of a star as it appears to pass behind the rings, twinkling as the meter-size particles that make up the rings block varying amounts of starlight. Voyager recorded a single such stellar occultation, which Esposito used to estimate the mass of the rings. But in the dense B ring, Cassini's occultation results have yielded at least three times the mass of Voyager's. "I hit myself on the head," said Esposito. " 'I must have made a mistake with Voyager,' I thought."

Once Cassini observed a number of occultations, the reason for the discrepancy became clear: Mass in the rings is clumped, not spread uniformly. As a result, starlight passes through the rings mostly by way of nearly empty gaps, and some angles offer clearer passage than others. Esposito compares it to a car's headlights viewed through a picket fence, shining brightly viewed head-on but dimly when viewed at a steep angle. Because Voyager was looking through the rings at a higher angle, it caught more starlight and underestimated the mass.

Given the new big ring mass, planetary scientists Glen Stewart, Stuart Robbins, and Joshua Colwell, all of UC, argue that the B ring, at least, could not have formed in recent eons. A moon massive enough to form the ring is unlikely to have broken up during the past 4 billion years, they argue; collisions able to do that kind of damage were much more common during the solar system's early days, when lots of big lingering debris was still winging around.

Even if Saturn's rings formed long ago, Esposito sees reasons they might appear young. The ice in the rings' particles seems too pure to have spent eons accumulating dark, dirty meteoritic material, and moonlets in the rings are too small to have survived that much time under cometary bombardment. But a larger mass of ring ice could have diluted the pollution, Esposito argues, and the moonlets might be recycling themselves—breaking up and reassembling by agglomeration.

Researchers are comfortable with a heftier B ring but not necessarily with Esposito's take on the implications. "There's a bunch of caveats in all of this," says ring dynamicist and Cassini camera principal investigator Carolyn Porco of the Space Science Institute in Boulder, Colorado. "Very little in this area is definite. Each part of the rings may have a different age." The rings—like scientists' understanding of them—may be a work in progress.

–RICHARD A. KERR

CREDITS (TOP TO BOTTOM): NASA/JPL/UNIVERSITY OF COLORADO; PHOTOS.COM

SCIENCESCOPE

Looking Ahead to 2008:

- The National Institutes of Health's new **Human Microbiome Project** will begin a $115 million, 5-year effort to sequence 600 genomes of organisms that call humans home.

- **Astrobiology** advocates hope to use a new report from the U.S. National Academies praising efforts by NASA's Ames Research Center in Mountain View, California, to restore funding cuts by NASA in programs to study life in extreme environments and the possibility of life outside of Earth.

- China's **megascience projects** continue: A 4-year, $70 million program on seismology will start up this year. A $25 million effort to examine the causes and effects of space weather will come to a close, with oceanography and material science efforts pending.

- Scientists and educators hope to stave off efforts by proponents of **intelligent design** to influence a revision of classroom science standards next month in Texas.

- This year, the **Access to Medicine Foundation** in the Netherlands will start ranking drug companies based on how well they help poor people.

- New assessments of **coral reefs** by the Global Coral Reef Monitoring Network are at the printers. This month's report on Caribbean reefs after bleaching and hurricanes will be followed in July by a look at reefs in trouble throughout the world.

- Expect a very rough draft of the **Neandertal genome** by the end of the year, along with published analyses of gorilla, orangutan, and platypus genomes.

- The **International Linear Collider** project, which has taken several heavy hits in recent months, is hoping that the U.S. Department of Energy will pony up its share of the $1.5 million for the project's formal design effort despite a severe tightening of 2008 funding by Congress.

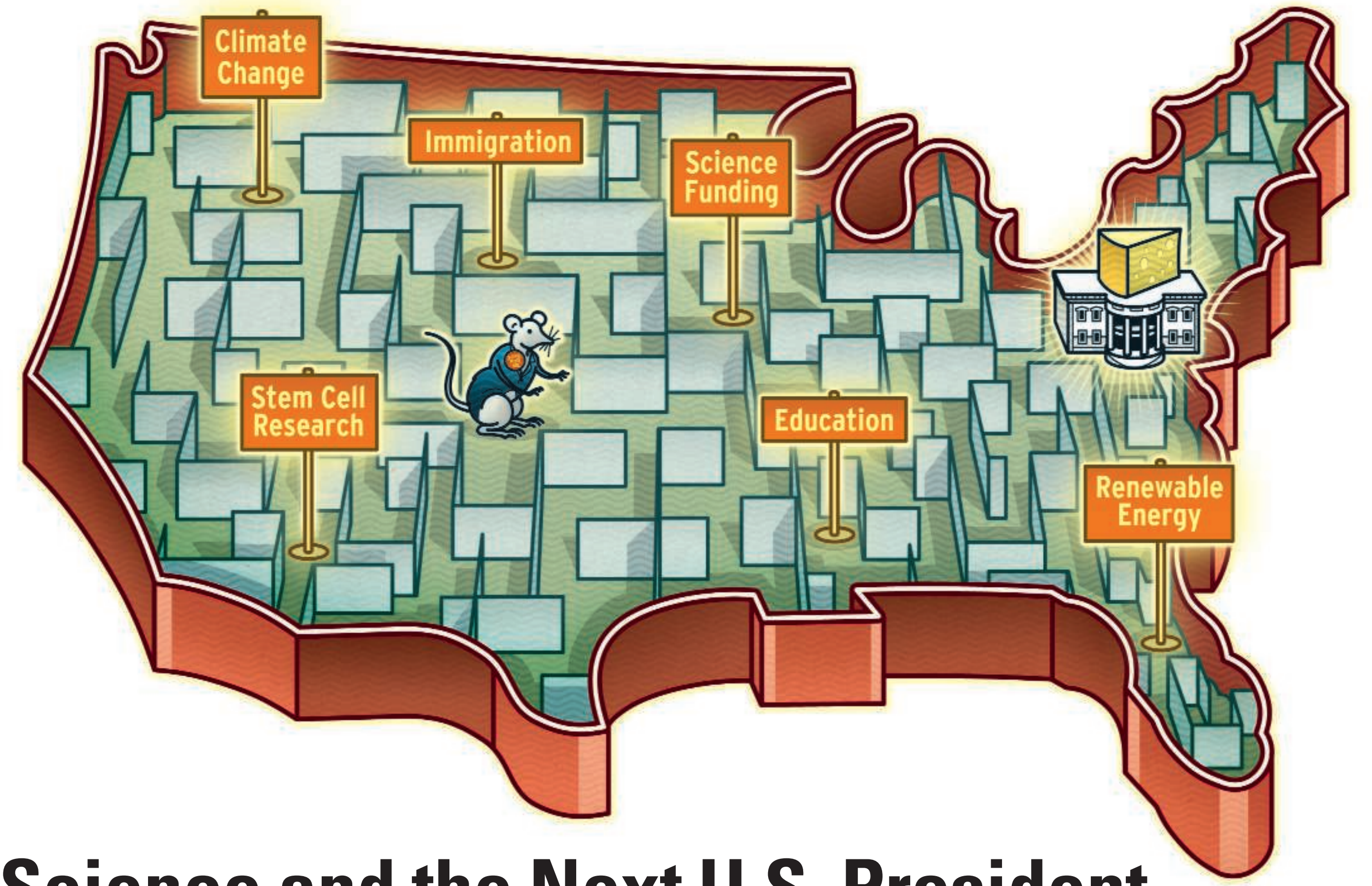

Science and the Next U.S. President

How do the candidates view science? Sometimes it's hard to tell from the campaign trail, but they have offered opinions on topics from evolution to global warming

Many factors can make or break a U.S. presidential candidate in the 2008 race for his or her party's nomination. The ability to raise millions of dollars is key, as are positions on megaissues such as the Iraq war, immigration, and taxes. Voters also want to know if a candidate can be trusted to do the right thing in a crunch. Science and scientific issues? So far, with the exception of global warming, they are not getting much play.

"It's pretty hard to find a candidate from either party who is gung ho for science," laments Representative Vernon Ehlers (R–MI), one of two Ph.D. physicists in Congress and an indefatigable promoter of science and technology. (As a supporter of Mitt Romney, whose father was governor of Ehlers's home state of Michigan back in the 1960s, Ehlers will be trying to pump science and technology into his campaign.)

But just because science isn't on the front burner in this year's seemingly interminable election campaign, that doesn't mean the community should tune out. The candidates are addressing issues, from climate change to how the next Administration should manage science, that will affect researchers next year—and for decades to come. Differences have emerged on embryonic stem cell research, on the urgency of combating climate change, and even on the teaching of evolution.

What are they saying on the stump, and how would they govern? This special report tries to answer those questions by examining the leading contenders among the Democrats and the Republicans, in alphabetical order, based on recent polls identifying those with a plausible shot at their respective nominations. (We've also provided basic information on the rest of the field.) Although none of the campaigns afforded us direct access to the candidates themselves—a telling indicator of the importance of science in the campaign, perhaps—we've talked to some of their advisers, as well as to colleagues, friends and foes alike, who are familiar with their careers.

By the time you read this, some of the candidates may have surged, and others may have slumped. However, the issues seem likely to remain relevant no matter who becomes the 44th president of the United States.

–JEFFREY MERVIS

CREDIT: PETER HOEY

Published by AAAS

DEMOCRAT

HILLARY CLINTON

Home State: **New York** Web site: **hillaryclinton.com**
Current Job: **U.S. Senator** Age: **60**

HILLARY CLINTON’S SPEECH AT THE CARNEGIE INSTITUTION of Washington on 4 October, the 50th anniversary of the launch of Sputnik, was the most detailed examination of science policy that any presidential candidate has offered to date. That’s not surprising, however, given the extensive network of former advisers to her husband that the Democratic front-runner has tapped.

Their voices could be heard in Clinton’s emphasis on innovation to drive economic growth, a bottom line that is as much a creature of the 1990s as grunge music. And the senator from New York linked her call for Americans to better “compete and innovate” in science to a post-Sputnik plea by President Dwight Eisenhower for “heroism, sacrifice, and accomplishment when the chips are down.”

But campaign adviser Thomas Kalil, formerly a technology official in the Clinton Administration and now an administrator at the University of California, Berkeley, insists that the candidate’s science platform is not stuck in the past. “2008 is not 1992,” he says. “There are a new set of challenges.”

Those new challenges include reducing the country’s dependence on foreign oil, responding to climate change, and reversing what Clinton calls the Bush Administration’s “assault on science.” To address the first two, Clinton has proposed a $50 billion research and deployment fund for green energy that she’d pay for by increasing federal taxes and royalties on oil companies. She would also establish a national energy council to oversee federal climate and greentech research and deployment programs. Both steps, she says, would help achieve the goal of an 80% reduction in carbon emissions from 1990 levels by 2050 and use tax credits, regulations, and carbon caps to create “5 million new jobs in clean energy over the next decade.” Last month, as a member of the Senate Environment and Public Works Committee, she voted for a bill almost as aggressive that passed along party lines, although the panel failed to adopt several amendments she offered (*Science*, 14 December, p. 1708).

To end what she calls President George W. Bush’s “open season on open inquiry,” the 60-year-old lawyer and former first lady says that her science adviser would report directly to her rather than be “filtered through political advisers.” Government advisory committees must not be hamstrung by political considerations, she adds, which she insists has happened repeatedly since Bush took office. In her Carnegie speech, she also promised an executive order that would “ban political appointees from altering or removing scientific conclusions in government publications without any legitimate basis … and prohibit unwarranted suppression of public statements by government scientists.”

But science policy expert Roger Pielke Jr. of the University of Colorado, Boulder, says her efforts to stop political meddling are poorly defined and won’t work. “What is ‘legitimate’ and ‘unwarranted’?” he asks. “As written, [the proposal] is a political Rorschach test.”

Clinton Administration–era official Ellis Mottur helped the campaign prepare her package of proposals, and Kalil and former White House science officials Neal Lane and Henry Kelly, who is now head of the Federation of American Scientists, were among a crew of unpaid advisers who offered input. Mottur says that he expects “the science-technology issues will come more to the fore in the general election.”

In the meantime, Clinton has called for another doubling of the $30-billion-a-year National Institutes of Health budget during the next decade, the preservation of the NASA team involved in the shuttle program even as the agency shifts to new exploration missions, and the augmentation of NASA’s earth science and aeronautics programs. But finding the money won’t be any easier than mustering the political will to tax energy companies, Pielke predicts. “Good luck finding room in the R&D budget for all of that,” he says.

However, supporting good research isn’t just about money, says physicist David Moncton, director of the Nuclear Reactor Laboratory at the Massachusetts Institute of Technology and a former administrator at two national laboratories. Just as important as any budget, says Moncton, who is not advising the campaign, are “competent individuals managing [science policy].” And Moncton thinks “that might be more likely to happen with a Hillary Clinton [presidency].

–ELI KINTISCH

CREDIT: STEPHANIE KUYKENDAL/CORBIS

Information on Other Candidates in the Race:

DEMOCRATS JOE BIDEN, CHRIS DODD, MIKE GRAVEL, DENNIS KUCINICH >> **27**
REPUBLICANS DUNCAN HUNTER, ALAN KEYES, RON PAUL >> **29**

JOHN EDWARDS MADE A FORTUNE AS A PERSONAL-INJURY lawyer in the 1980s and was John Kerry's vice president on the unsuccessful Democratic presidential ticket in 2004. But this year, he is campaigning as a populist and a Washington outsider.

The son of mill workers, Edwards pounds away at the "big, powerful interests," the "corrupt," and the "very greedy" in his standard stump speech. The 54-year-old former North Carolina senator (1998–2004) wants to make sweeping changes, some of which would affect research. He would end what he calls the "antiscience" practices of George W. Bush's Administration—such as "censoring research and slanting policy on climate change, on air pollution, on stem cell research." And he would increase science funding. Despite such promises, however, biomedical researchers who remember the malpractice lawsuits that Edwards championed 2 decades ago—some of which were based on questionable science—are wary.

If Edwards actually does move into the White House, he says his own presidential science adviser would have more clout than the current one and would play "a central role as an assistant to the president." To protect scientific integrity, Edwards would "eliminate political litmus tests for government scientists" and forbid political appointees "from overriding agencies' scientific findings unless the chief White House science adviser concludes they are erroneous."

Edwards's agenda for improving the U.S. economy includes a mixture of very specific projects and broad promises. For example, he advocates a low-cost "universal Internet" for rural communities and more research on autism and fragile X syndrome, a genetic cause of mental impairment. He favors federal funding of human embryonic stem cell research, including nuclear DNA transfer. He wants to create a universal, federally backed health system. And his spokesperson, Audrey Waters, says he supports budget increases "substantially better than the pace of inflation" for the

REPUBLICAN

RUDOLPH GIULIANI

Home State: **New York** Web site: **joinrudy2008.com**
Most Recent Job: **Founder and Executive, Giuliani Partners** Age: **63**

SPEAKING "IN THE MOST HUMBLE WAY POSSIBLE," RUDY Giuliani disclosed on the campaign stump in Iowa last summer that "I'm very good at doing the impossible. I am." Indeed, he's made a career of slaying dragons, including winning the convictions of prominent Wall Street and organized crime figures as a federal prosecutor in the 1980s and overseeing a huge drop in New York City's crime rate as its mayor from 1993 to 2001.

So what does this 63-year-old dragon slayer make of science? That's hard to determine because his campaign successfully discouraged key advisers from speaking to *Science* about specific issues. But his public career suggests that Giuliani is a pragmatist with a quick grasp of issues, a lover of statistics, and a firm believer that most tasks can be done better by private institutions than by government.

On social issues, Giuliani stands out among the Republicans for what he has said about abortion: With reservations, he would let the woman decide what to do. On a linked topic, research on human embryonic stem cells, he said in May that "as long as we're not creating life in order to destroy it—as long as we're not having human cloning … I would support [federal funding]." David Carmel, a biotech executive and member of the board of the New York Stem Cell Foundation, made the case for embryonic stem cell research in a private debate last fall that the candidate staged to explore both sides of the issue. Based on Giuliani's questions, Carmel says he believes Giuliani, if elected, would reduce federal restrictions.

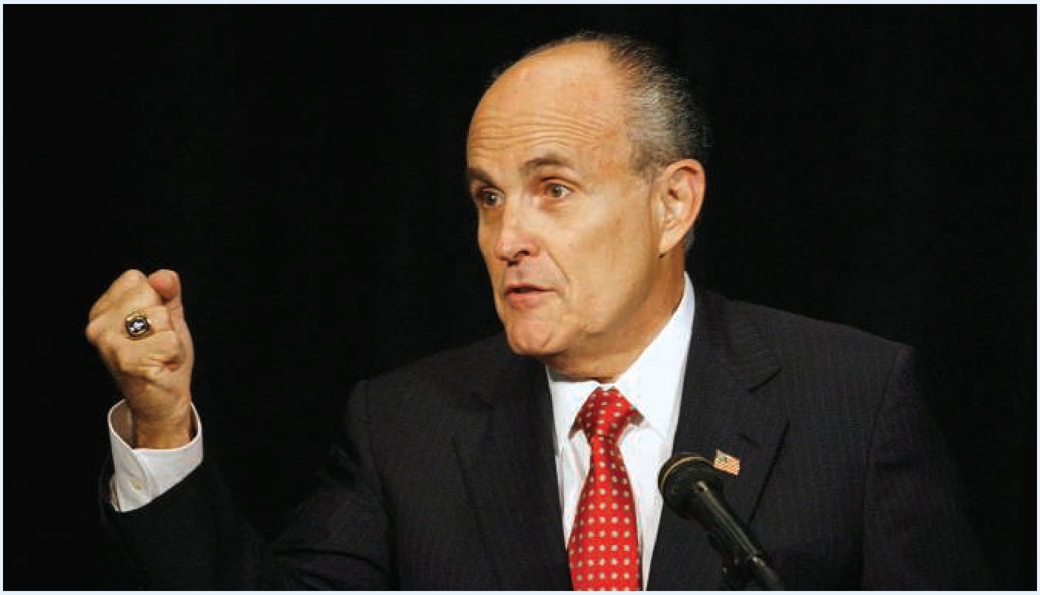

CREDITS (TOP TO BOTTOM): BRIAN SNYDER/REUTERS; KEVIN LAMARQUE/REUTERS

National Institutes of Health (NIH) and the National Science Foundation.

DEMOCRAT

JOHN EDWARDS

Home State: **North Carolina** Web site: **johnedwards.com**
Most Recent Job: **Consultant, Fortress Investment Group** Age: **54**

On environmental policy, Edwards has won the "enthusiastic endorsement" of Friends of the Earth Action, the nonprofit group's political arm. That support is based in part on his proposal to cut greenhouse gas emissions by 80% by 2050, using a cap-and-trade system to auction off permits as a regulatory incentive. Edwards says he would take at least $10 billion a year from that auction and another $3 billion from other sources to invest in a trust fund for new technologies. It would develop solar, wind, and "cellulose-based biofuel" projects.

The environmentalists are also pleased with what Edwards would not do. He opposes any expansion of nuclear power, the candidate explained in a recent debate, because it is "extremely costly … and we don't have a safe way to dispose of the nuclear waste." Liquefied coal is out, too, he says, because "the last thing we need is another carbon-based fuel."

Yet among scientists, Edwards "carries some baggage," says Peter Agre, a Nobel Prize–winning biochemist now at Johns Hopkins University in Baltimore, Maryland. Although Edwards is a "good man," says Agre, "I know people who would never vote for him" because of the way he and other lawyers pursued and won multimillion-dollar medical malpractice awards representing children born with cerebral palsy.

In a 1985 case, for example, Edwards addressed the jury in the voice of a brain-damaged child, describing from within the womb how she waited for a doctor to perform a cesarean section as a fetal heart monitor signaled her distress. The doctor was accused of waiting too long; the jury awarded $6.5 million. Many such suits were "fueled by bad science," says neurologist Karin Nelson of NIH, who concedes she has not reviewed the specific cases that Edwards handled. She says that the same type of cerebral palsy litigation has now spread to Europe—to the detriment of children's health, she believes. Nelson sat on a panel of the American College of Obstetricians and Gynecologists that in 2003 found that most cases of cerebral palsy are not caused at birth.

Asked today about Edwards's courtroom tactics, his staff points to statements from his vice presidential campaign. Speaking then about his legal team, Edwards claimed that "we would take months investigating" any brain-injury case before deciding whether to accept it. And he said he only litigated those that "were merited."

—JOCELYN KAISER AND ELIOT MARSHALL

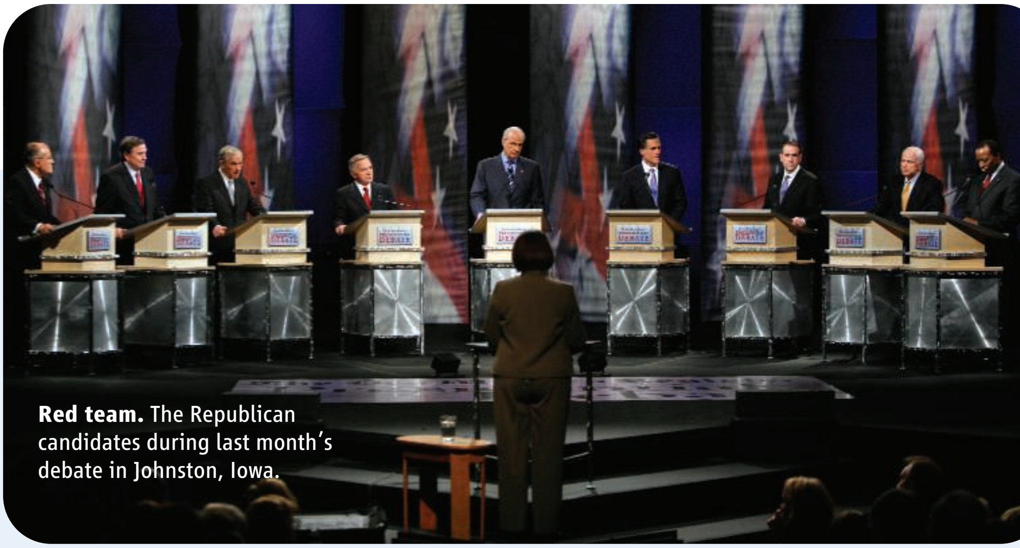

Red team. The Republican candidates during last month's debate in Johnston, Iowa.

CREDIT: CHARLIE NEIBERGALL/AP

Giuliani's record as mayor and author add few clues about his outlook on science. Rodney Nichols, former president of the New York Academy of Sciences (NYAS), gives him high marks for his interest in two city-backed projects involving science and somewhat lower marks for follow-through. Nichols recalls how the mayor agreed to host an NYAS award to honor scientific excellence, even though it "would not win [him] votes." At the same time, Nichols says that "not much came" of a panel on how to bring biotech companies into the city, as the mayor lost interest once local medical institutions began to jockey for concessions.

In his 2002 book *Leadership*, Giuliani wrote, "I loved learning biology" as a premedical student at Manhattan College. But in the end, he says that he chose law school and politics because "I liked ideas better than science." New York City invested heavily in crime statistics—a system called CompStat—to help command a burgeoning police force. The model has been copied in many cities, and Giuliani has proposed clones for other tasks, which he calls JobStat, SchoolStat, EnergyStat, and HealthStat.

The technical issue that proved most controversial for Giuliani this fall, in fact, involved his use of health data. An ad in New Hampshire claimed that people diagnosed with prostate cancer (as he was in 2000) in the United Kingdom are more likely to die of their disease because of its system of "socialized medicine" than their U.S. counterparts. The ad cited survival rates of 82% for the United States and 44% for Britain. This provoked a flurry of criticism. A spokesperson for Giuliani revealed that the candidate found the data in the journal of the Manhattan Institute for Policy Research, a conservative think tank to which he has close ties.

Experts say it's easy to misread the numbers. Recent data from the U.S. National Cancer Institute and an international survey called Eurocare indicate that the 5-year survival rates are about 77% for Britain and 98% for the United States. What this shows, according to biostatistician Donald Berry of the M. D. Anderson Cancer Center in Houston, Texas, is that U.S. doctors screen and diagnose more patients, finding prostate cancer in people not at risk of dying from it, and that "there is no credible evidence that screening decreases prostate cancer mortality." The Giuliani campaign has said it won't stop using the original ad data.

Giuliani's campaign has skated lightly over most issues with scientific and technological components. On energy, for example, he would boost all domestic energy sources, emphasizing coal, nuclear power, ethanol (with a goal of 20% more output), and renewable sources such as windmills, but he has not spelled out how this would work. Likewise, his pledges to "promote science and mathematics through technical certification or an associate degree" and "expand the number of H-1B visas for skilled foreign workers" come with few details. The League of Conservation Voters reports that Giuliani has "no articulated position" on most of the environmental issues it tracks. Giuliani has said, "I do believe there's global warming," but he has not spelled out his response to the problem.

—ELIOT MARSHALL

Published by AAAS

THE FIRST TIME MIKE HUCKABEE WAS ASKED IN A national candidates' debate if he believed in evolution, he raised his hand to say that he didn't accept the theory. The second time, Huckabee initially ducked the question and instead replied, "I'm not planning on writing the curriculum for an 8th grade science book."

Scientists in Arkansas who know Huckabee from his decade as governor say the response is consistent with his approach to many social issues: Take a strong stance but don't impose your views on others. The former president of the Arkansas Baptist State Convention holds many staunchly conservative positions, including support for displaying the Ten Commandments in public schools and opposition to the use of embryonic stem cells for research. But when it comes time to act, Huckabee has often veered toward the center of the political road.

As chief executive of this largely rural state from 1996 to January 2007, Huckabee persuaded a Democratic-led legislature to expand health coverage for poor children and raise taxes to improve schools and roads and unsuccessfully campaigned for teenage immigrants who did not have proof of citizenship to receive college vouchers after graduating from high school. Those positions were anathema to many of his constituents and a pleasant surprise to others. "He really was much less radical and ideological than we all expected," says Rita Sklar, executive director of the ACLU of Arkansas in Little Rock. He also supported a bond program to help improve infrastructure at universities.

That centrism is being tested now that Huckabee is on a national stage. Seeking to expand his base among evangelicals, for example, he has promised to fight for constitutional amendments that would ban abortion and gay marriage.

REPUBLICAN

JOHN McCAIN

Home State: **Arizona** Web site: **johnmccain.com**
Current Job: **U.S. Senator** Age: **71**

JOHN MCCAIN DOESN'T HAVE ANY SCIENTIFIC TRAINING OR expertise. But he trusts the experts. They've told him that global warming is the most urgent issue facing the world, and that makes climate change one of the three issues—along with immigration and the Iraq war—that he's emphasizing in his presidential campaign.

The 71-year-old retired Navy pilot turned Arizona politician discovered the issue during his previous, unsuccessful run for the White House in 2000, says his economic adviser, Douglas Holtz-Eakin, a former director of the Congressional Budget Office. It's popular lore that the candidate woke up to the issue when confronted by a Dartmouth College student dressed as a penguin at an event that year in New Hampshire. In fact, says Holtz-Eakin, McCain got the message "again and again" during the campaign.

McCain used his position on the Senate Commerce Committee, which he chaired from 2003 to 2005, to focus attention on the subject and has led congressional delegations to both poles to witness its impact. "He's probably more knowledgeable [about it] than all the other candidates," says Timothy Profeta, a former staffer for Senator Joseph Lieberman (I–CT) who now runs Duke University's Nicholas Institute for Environmental Policy Solutions.

McCain equates environmentalism with national security. And although he has been a staunch supporter of President George W. Bush's stance on the Iraq war, his views on climate change have triggered some sharp exchanges with Bush Administration officials. In 2002, he declared that White House science adviser John Marburger's comments on global warming, which many scientists saw as overly cautious, had "no credibility" in light of the growing severity of the problem. In a 2005 hearing, he accused Vice Admiral Conrad Lautenbacher, head of the National Oceanic and Atmospheric Administration, of having a "complete lack of concern about future generations of Americans who are affected by climate change." He has also called the president's approach to global warming "disgraceful." Last month, McCain tasted his first legislative victory on the issue, as Democrats on the Senate Environment and Public Works Committee approved a bill designed to reduce greenhouse gas emissions using a system that caps and trades emissions allowances that he and Lieberman first proposed in 2003.

John Raidt, a former Commerce Committee staffer and now one of McCain's closest advisers, says McCain "understands the limits of his own understanding; … he trusts the experts." One of these is R. James Woolsey, former chief of the CIA under President Bill Clinton, who has briefed McCain on issues relating to energy independence. Woolsey teasingly calls McCain a "very quick learner in spite of his record at the Naval Academy"—where he ranked fifth from the bottom of his class.

McCain, who has served 26 years in Congress, also listened to the scientific experts in the stem cell debate. Although he opposes abortion, he voted for a bill to expand President George W. Bush's policy on research with human embryonic stem cells. However, he draws the line at human nuclear transfer, or research cloning, arguing that there is no ethical difference between cloning for research and cloning for reproduction.

Most nonclimate science issues are far down on McCain's list of priorities.

CREDIT: CARLOS BARRIA/REUTERS

REPUBLICAN

MIKE HUCKABEE

Home State: **Arkansas** Web site: **mikehuckabee.com**
Most Recent Job: **Governor** Age: **52**

One issue dear to his heart has been the promotion of healthy living. When the Arkansas legislature rejected his proposal to use millions of dollars in tobacco-settlement funds for health care and medical research, he exercised his right as chief executive to call for a referendum, which passed handily. That effort only intensified after he was diagnosed with type 2 diabetes and shed 110 pounds.

"He would certainly be a friend" of the National Institutes of Health as president, says G. Richard Smith, who helped with the referendum and now directs the psychiatric research institute at the University of Arkansas for Medical Sciences. On the campaign trail, Huckabee has talked about funding disease-prevention efforts along the lines of the indoor smoking ban he signed into law while governor.

In a presidential debate and in a television interview, Huckabee sidestepped questions about whether human actions are behind climate change, but he supported a 2006 statement by the National Governors Association calling for more climate change research. "Our responsibility to God means that we have to be good stewards of this Earth," he said in a May debate. That attitude, say environmental advocates, is a marked shift for someone who, as governor, declined to take sides in a court battle with Oklahoma about pollution in the shared Illinois River and once referred to environmentalists as "wackos."

Although he won four statewide races, Huckabee never created the reservoir of political goodwill enjoyed by his predecessor once removed, Bill Clinton, especially among members of his own party. (The two men hail from the same small town of Hope, Arkansas.) Jeremy Hutchinson, a Republican and former assistant minority leader in the legislature, notes that Huckabee rarely socialized with or lobbied state lawmakers, unlike the famously charismatic former president. "With Clinton, even if you didn't agree with him, you liked him," says Hutchinson. Huckabee also has a short fuse, say several Arkansans inside and outside politics. "He was very thin-skinned and could be pretty vindictive," says Ernest Dumas, a newspaper columnist from Little Rock who was subjected to a 5-minute televised tirade from the governor for his past criticism of Huckabee's highway program.

Jay Barth, a political scientist at Hendrix College in Conway who has written about Huckabee's career, says Huckabee owes his success to a conservative ideology, a winning personality, and media savvy. Huckabee is "very talented [and] never made a lot of political mistakes," says Barth. "Arkansans never loved him the way they loved other politicians, [but] they never hated him," either.

–JENNIFER COUZIN

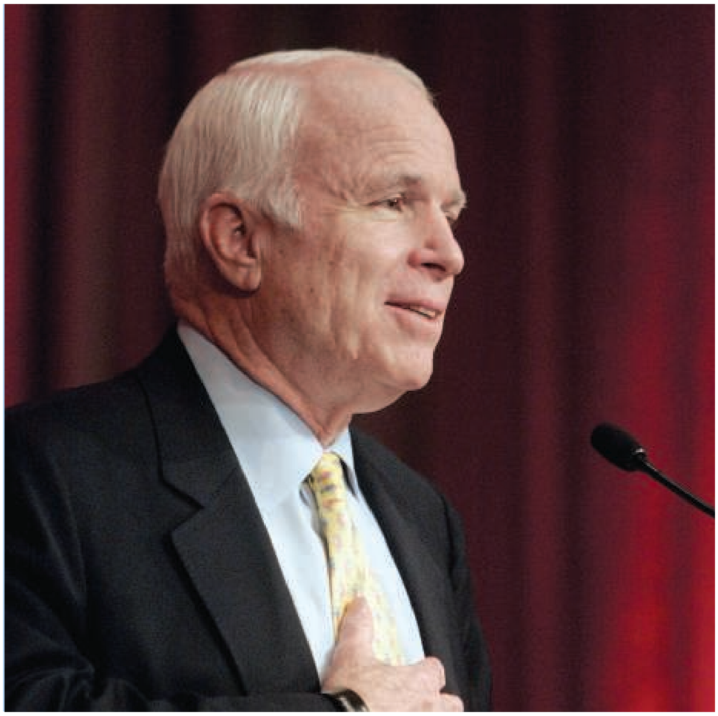

A free-trade advocate, he has sponsored a bill to restrict taxes on Internet use. He also wants to make better use of cyberspace to advance the cause of freedom in the tradition of Radio Free Europe. In keeping with his stance on immigration, he has also been involved in expanding H-1B visas for foreign science graduate students studying in the United States.

Sometimes the interests of science take a back seat to those of his constituents. He's supported an amendment to the Native American Graves Protection and Repatriation Act that could make it easier to turn over ancient human remains that are unrelated to existing American Indians to tribal representatives, a step that researchers worry will make the remains off limits. And McCain has waffled on the teaching of evolution. In 2005, he told the *Arizona Daily Star* that "there's nothing wrong with teaching different schools of thought [on] … how the world was created." But the next year, he opined that creationism should "probably not" be taught in science classes.

–CONSTANCE HOLDEN

CREDITS (TOP TO BOTTOM): MARK DUNCAN/AP; M. SPENCER GREEN/AP; JERRY S. MENDOZA/AP; ALAN DIAZ/AP; GARY MALERBA/AP

OTHER DEMOCRATS IN THE RACE

DEMOCRAT

Joe Biden

Home State: **Delaware**
Current Job: **U.S. Senator**
Web site: **joebiden.com**
Age: **65**

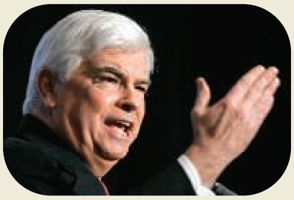

DEMOCRAT

Chris Dodd

Home State: **Connecticut**
Current Job: **U.S. Senator**
Web site: **chrisdodd.com**
Age: **63**

DEMOCRAT

Mike Gravel

Home State: **Alaska**
Current Job: **Political Activist**
Web site: **gravel2008.us**
Age: **77**

DEMOCRAT

Dennis Kucinich

Home State: **Ohio**
Current Job: **U.S. Representative**
Web site: **dennis4president.com**
Age: **61**

Published by AAAS

SPEAKING LAST SUMMER TO A CONVENTION OF BLOGGERS IN Chicago, Barack Obama accused the Bush Administration of ignoring or distorting data to shape its decisions on science-related issues. He promised the audience that his policies would be based on "evidence and facts." Political rhetoric? Perhaps. But some scientists who have seen the first-term U.S. Democratic senator in action say that's how he operated as a community activist in Chicago and as an Illinois state legislator.

DEMOCRAT

BARACK OBAMA

Home State: **Illinois** Web site: **barackobama.com**
Current Job: **U.S. Senator** Age: **46**

Eric Whitaker, a research administrator at the University of Chicago and former director of the Illinois Department of Public Health, points to a 2004 proposal before the state legislature to offer free flu shots to everyone without health insurance during a shortage of the vaccine. Obama, then chair of the Health and Human Services Committee in the state senate, pressed Whitaker and others on their advice that the shots be limited to high-risk groups. "He pushes you to defend your data," says Whitaker. In the end, Obama was convinced by their argument that vaccinating everybody would be economically unwise and bucked the majority in voting against the proposal.

Deborah Burnet, a pediatrician at the University of Chicago who studies the connection between obesity and diabetes, says Obama displayed the same evidence-based philosophy whenever she invited the Harvard Law School grad and community organizer to lecture her class on racial disparities in health. The 30-something Obama would urge her students to think about "how to use scientific inquiry to make intelligent public policy," says Burnet. She says she was so inspired by his message that students should apply "insights from scientifically collected evidence" to real-world problems that she began a program to help low-income residents make better nutritional choices.

Obama's campaign sets out a number of lofty science policy goals that might be difficult to achieve in that real world, however. He'd like to double federal spending on basic research and help more Americans get on the Web by broadening Internet access. He also wants to spend $18 billion on education initiatives covering everything from early childhood learning and precollege math and science instruction to attracting more minority students into science and engineering. Ironically, he'd pay for it in part by delaying NASA's program to return to the moon and explore Mars—a project that would employ thousands of scientists and engineers.

Like the other Democratic contenders, Obama has made global warming an important part of his campaign. He supports a market-based carbon-trading system to cut carbon emissions to 80% below 1990 levels by 2050 and wants to invest $150 billion to develop biofuels. But he's also suffered some political bumps and scrapes along the way to that position.

Last year, for example, Obama introduced a bill to subsidize the conversion of coal to liquid fuel, arguing that it would make the United States less dependent on foreign oil. But environmentalists saw it as a sop to the multibillion-dollar coal industry in his home state. Obama then backtracked,

DEMOCRAT

BILL RICHARDSON

Home State: **New Mexico** Web site: **richardsonforpresident.com**
Current Job: **Governor** Age: **60**

AS NEW MEXICO'S NEW GOVERNOR, BILL RICHARDSON enlisted experts from in-state Los Alamos National Laboratory to help him with technical issues. Barely a year later, however, they had been fired, Donald Trump–style. Richardson felt that the Department of Energy's (DOE's) weapons lab was dragging its feet on cleaning up long-standing environmental problems, and when a top lab official suggested one day that budget cuts might force the lab to recall its environmental adviser, it was the last straw. "We weren't going to be blackmailed," recalls Ned Farquhar, a former staffer now serving as senior adviser to the campaign on energy and climate.

A year later, a new set of advisers from Los Alamos was in place, and Richardson had reached a deal with the lab on a cleanup schedule. "It was pretty rigorous. I don't think the state budged very much," notes physicist Dennis Erickson, on detail as science adviser, who remembers being given 24 hours to clean out his desk. Despite having a year's work go down the drain, Erickson doesn't disagree with what the governor did. "I have nothing but good feelings toward him," says Erickson, now retired and a contributor to Richardson's presidential campaign.

Supporters say the incident demonstrates that the 60-year-old Hispanic politician is a principled manager, a tough negotiator, and someone who doesn't see a conflict between national security and the environment. But some wonder if it is also the portrait of someone who acts precipitously, punishing critics and putting principles above results.

CREDIT: GERALD HERBERT/AP

saying he would support liquefying coal only if the net carbon dioxide emissions from producing and burning the fuel were 20% lower than levels generated by petroleum-based fuels.

Observers say the awkward shuffle reflects Obama's relative inexperience in national politics. "It was naïve of him to think that he could side with the coal industry to please voters in his home state and not land in a frying pan on the national stage," says Frank O'Donnell of Clean Air Watch, a Washington, D.C.–based nonprofit. Nonetheless, O'Donnell says, the senator's green credentials are still pretty solid.

Since winning his U.S. Senate seat in 2004, Obama has continued to track health policy issues. He has proposed or supported legislation to promote embryonic stem cell research, increase research on avian influenza, and develop microbicides to protect women from HIV/AIDS. The measures suggest that Obama has retained his strong interest in applying science to public health challenges. For academic health centers, says Burnet, that means "getting the translational component going." **–YUDHIJIT BHATTACHARJEE**

Reelected easily in 2006, Richardson has promised voters that he will shake up the Washington establishment. But he's hardly a fresh face. After earning a bachelor's and a master's degree (in public policy) from Tufts University, Richardson spent nearly 30 years working for the federal government, first as a Democratic staffer, then as a seven-term congressman, and finally, as U.N. ambassador and energy secretary in the second Clinton Administration.

The most striking part of his résumé is his extensive, hands-on negotiations with regimes in North Korea, Iraq, and Sudan for the release of U.S. prisoners and other human-rights issues. Richardson has also taken a very aggressive stance on climate change, including calls for a 90% reduction in U.S. greenhouse gas emissions by 2050 through a cap-and-trade system, a 50% cut in oil consumption by 2020, greater reliance on renewable energy sources by utility companies, and federal subsidies to promote plug-in hybrid cars. "There is no free market when it comes to greenhouse gas emissions," says Farquhar. "We need rules and boundaries."

To help meet those goals, Richardson has proposed a $10 billion to $15 billion trust fund to support new energy technologies, replenished by the fruits of successful investments. But Farquhar says it's not a honey pot for academic researchers, as the fund would pursue a more product-oriented approach than the Advanced Research Projects Agency–Energy created last summer. Farquhar says Richardson also plans to "reconfigure" DOE to deal with the twin challenges of energy independence and global warming, possibly shifting DOE's ethanol program to the agriculture department and giving the Environmental Protection Agency a bigger role in climate change.

The lack of specifics is characteristic of someone who, in the words of one former aide, "has more ideas than time to implement them." That's equally true for his education platform. His response to the president's signature No Child Left Behind program to improve elementary and secondary schools is characteristically blunt: "Scrap it." But when asked what would replace the annual testing regimen and penalties for schools that don't make the grade, his answer is a call for a national summit to work out the details. His promise to "hire 100,000 new science and math teachers [and] create 250 math, science, and innovation academies" likewise ignores the fact that state and local authorities, not the federal government, hire teachers and run schools.

Despite repeated campaign statements about the importance of innovation, Richardson isn't above embracing his own scientific illiteracy as a way to identify with the average voter. In his new book on energy, *Leading by Example*, Richardson asserts that more people would use energy-saving technologies, including light-emitting diodes, if they were given simpler names. "Does anyone on Earth know what a diode is?" he writes. "Probably someone at the two national labs in New Mexico, but not me! And probably not you."

–JEFFREY MERVIS

OTHER REPUBLICANS IN THE RACE

REPUBLICAN

Duncan Hunter

Home State: **California**
Current Job: **U.S. Representative**
Web site: **gohunter08.com**
Age: **59**

REPUBLICAN

Alan Keyes

Home State: **Maryland**
Current Job: **Political Commentator**
Web site: **alankeyes.com**
Age: **57**

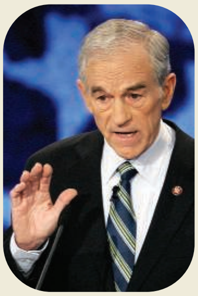

REPUBLICAN

Ron Paul

Home State: **Texas**
Current Job: **U.S. Representative**
Web site: **ronpaul2008.com**
Age: **72**

CREDITS (TOP TO BOTTOM): SETH WENIG/AP; PABLO MARTINEZ MONSIVAIS/AP; CHARLIE NEIBERGALL/AP; CHRIS O'MEARA/AP

REPUBLICAN

MITT ROMNEY

Home State: **Massachusetts** Web site: **mittromney.com**
Most Recent Job: **Governor** Age: **60**

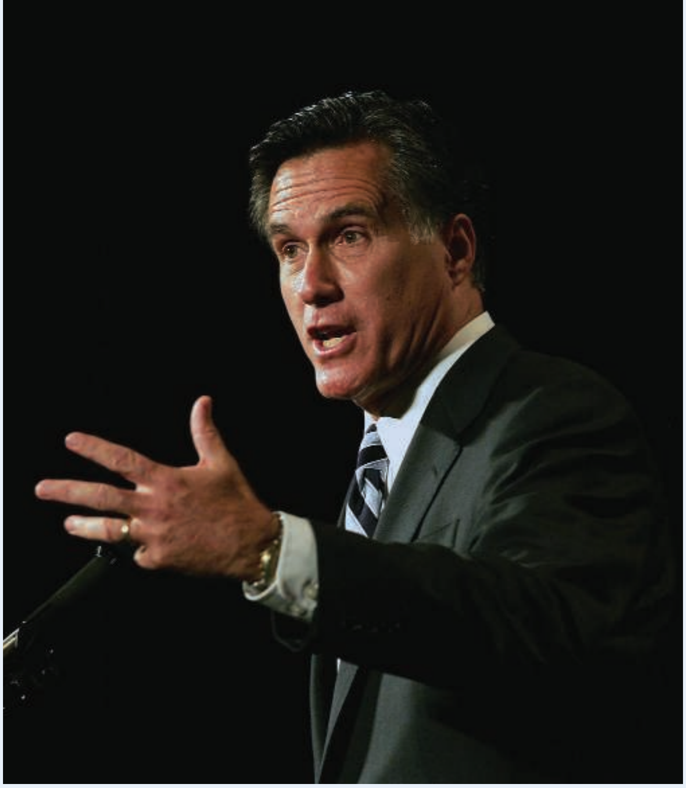

LAST MONTH, AS MITT ROMNEY CAMPAIGNED IN IOWA, HE laced his stump speeches with references to his opposition to embryonic stem (ES) cell research and abortion and his doubts about the role of humans in global warming. All those positions, plus a declaration that his Mormon faith would not dictate any decisions he might make as president, were aimed at wooing conservative Christian voters in the state.

That focus is a far cry from 5 years ago, when the 60-year-old businessman campaigned successfully to become governor of the high-tech state of Massachusetts. The new chief executive wowed biotechnology leaders and university administrators with his aggressive and no-nonsense talk about unleashing the power of research. "We were impressed by his willingness to talk about the importance of research universities in the state and national economies," says Paul Parravano, co-director of government and community relations at the Massachusetts Institute of Technology (MIT) in Cambridge. "For a lot of people here, this was fresh and important." As a venture capitalist with an MBA from Harvard University, Romney "understands the role of places like MIT and was very supportive," says another university official.

During his first years as governor, researchers say, Romney talked the talk, co-chairing a national summit on innovation and telling the Massachusetts Biotechnology Council that "we want to make sure we are at absolutely the front edge" of stem cell research. He promised he would work to provide "the same kind of opportunities that you would find in any other state in America." And he walked the walk. He launched an effort to lure more high-tech talent into the state and joined with seven other Northeastern states on a regional plan to reduce carbon dioxide emissions at power plants—the first collective U.S. effort to control greenhouse gases. He also consistently opposed efforts to introduce the teaching of intelligent design in the classroom.

IN 2000, WHEN HOUSE REPUBLICANS WANTED TO PULL the plug on the $1.4 billion Spallation Neutron Source (SNS) being built at the Department of Energy's Oak Ridge National Laboratory in Tennessee, the state's congressional delegation went to bat for the project. Fred Thompson, then one of the two Republican senators from Tennessee, was "extremely helpful" in assigning staff to work the issue, recalls physicist David Moncton, then head of the SNS project.

But Moncton, now a professor at the Massachusetts Institute of Technology, remembers something else about his interaction with the senator on SNS, which staved off the threat and opened last year. "The issue [for Thompson] was this billion-dollar project was happening in Tennessee," says Moncton. "There was no discussion of how intrinsically interested he was in science." Rick Borchelt, a longtime Democratic aide and former spokesperson for the Department of Energy lab, concurs. "He's pretty much a cipher on science and technology," says Borchelt.

The 65-year-old Tennessee native has played the president—as well as a military officer and a hard-nosed district attorney—during a long television and film career. He's also been a lawyer, lobbyist, and talk-show host after coming to Washington in 1973 as a Republican staffer during the Watergate hearings. Since jumping into the race for president last summer, he has rarely addressed science issues. But Norman J. Ornstein of the American Enterprise Institute in Washington, D.C., who worked with Thompson when he chaired what was then called the Government Affairs Committee, credits him with being "knowledgeable and insightful" on the often thorny issues that came before the panel. "I found him to be quite engaged on issues he cared about," says Ornstein. "But he was not a guy who stuck around if he didn't need to."

CREDITS (TOP TO BOTTOM): SCOTT OLSON/GETTY IMAGES; JASON REED/REUTERS

His 2-year honeymoon with the research community ended abruptly in 2005, however, just as Romney's presidential campaign was getting started. The governor abruptly backed out of the regional emissions plan, citing its cost to consumers. He vetoed a bill passed by the Massachusetts legislature to allow ES cell research, citing his ethical concerns. Research advocates say that they never were able to sit down with the governor to discuss the bill, which was a major concern for many industry and university biologists in the state. "We were never able to engage," says one supporter who requested anonymity. "This was an eye opener; he was changing his stripes."

Even so, one of the strongest advocates for science in Congress, Representative Vernon Ehlers (R–MI), calls Romney "the best choice for any scientist or engineer." The former physicist and longtime member of the House Science Committee praises the candidate as bright and unburdened by ideology, noting that "he appreciates the benefits of science." Ehlers, who knew Romney's late father, a former governor of Michigan, says that he is heading up a science advisory committee for the candidate.

Ehlers told *Science* that he expects Romney's list of priorities to include, in particular, increased funding for math and science education and, more generally, higher spending on research of all kinds. But he speculates that Romney "may choose not to be vocal" on global warming, although Ehlers himself supports sharp reductions in carbon dioxide emissions. In a July 2007 issue of *Foreign Affairs*, Romney calls for "a bold, far-reaching research initiative—an energy revolution—that will be our generation's equivalent of the Manhattan Project or the mission to the moon." But he adds that "scientists still debate how much human activity impacts the environment."

Romney can speak knowledgeably about some science issues on the campaign trail. He supports raising the cap on the number of H-1B visas so that more foreigners with high-tech skills can work in the United States. And this fall, he pledged to "substantially increase funding" for basic research related to energy efficiency and production. But as the primaries kick into high gear, expect Romney to put his focus more on hot-button social issues than the cooler high-tech matters that occupied him as governor of the Bay State.

–ANDREW LAWLER

Blue team. The Democratic contenders at an August debate in Des Moines, Iowa.

CREDIT: GETTY IMAGES

REPUBLICAN

FRED THOMPSON

Home State: **Tennessee** Web site: **fred08.com**
Current Job: **Actor and Attorney** Age: **65**

Some of Thompson's recent positions have not endeared him to researchers. Within a few hours of reading about a method of genetically reprogramming skin cells into what appear to be embryoniclike stem cells, he rushed out a statement lauding the discovery. "Today's announcement is just one more indication that our current policy in relying only on adult cells is working," he said on 20 November. Thompson ranked the achievement as the latest addition in "73 breakthroughs for adult and cord blood research" that he said have paved the way for new treatments for several diseases.

That tally comes from the Family Research Council, a conservative advocacy group in Washington, D.C. Many scientists regard the analysis, by the council's David Prentice, as seriously flawed, and even Prentice says the list did not imply that those breakthroughs had led to available treatments. "[The list] not only misrepresents existing adult stem cell treatments, but also frequently distorts the nature and content of the references he cites," wrote Steven Teitelbaum, former president of the Federation of American Societies for Experimental Biology in Bethesda, Maryland, in a letter published in *Science* (28 July 2006, p. 439). "Fred Thompson is misinformed," Teitelbaum says about the candidate's latest pronouncement.

Thompson has also climbed out on a limb in discussing climate change. "While we don't know for certain how or why climate change is occurring, it makes sense to take reasonable steps to reduce CO_2 emissions without harming our economy," notes an issues statement from the campaign. In March, Thompson jokingly told a radio audience that "quite a few planets in our solar system seem to be heating up a bit. This has led some people, not necessarily scientists, to wonder if Mars and Jupiter, nonsignatories to the Kyoto Treaty, are actually inhabited by alien SUV-driving industrialists."

Gavin Schmidt, a climate modeler at NASA's Goddard Institute for Space Studies in New York City, calls the statement "ridiculous" and says it's based on the faulty idea of a recent warming of the sun. "We've been measuring the sun['s temperature] for 30 years—it's not doing anything," Schmidt notes.

Campaign staffers declined repeated requests from *Science* to detail Thompson's views on science and technology issues. And last month, at an Iowa debate in which each Republican candidate was asked whether climate change was real and caused by human activities, Thompson chose to go for a punch line rather than inform his audience. First he declined to give a yes-or-no answer. Then, after one long-shot candidate gave a rambling response that seemed to ignore the question, Thompson passed again. "I agree with Alan Keyes's position on climate change," he cracked to wide laughter from the audience.

–ELI KINTISCH AND BENJAMIN LESTER

Published by AAAS

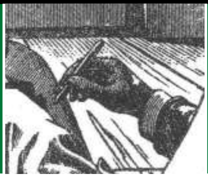

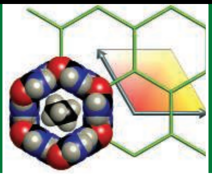

LETTERS

edited by Jennifer Sills

In Search of Peer Reviewers

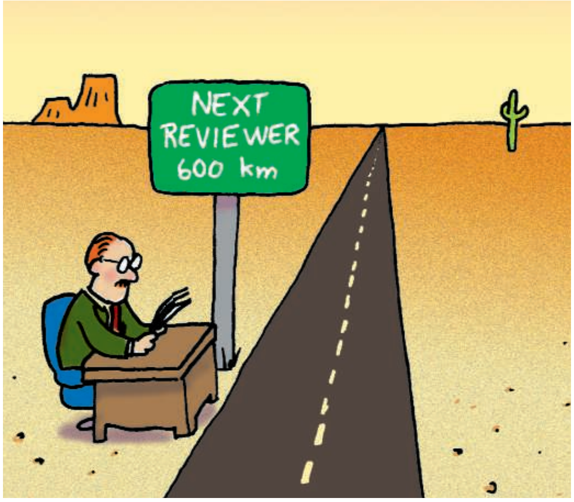

AS A PAST EDITOR OF *MARINE MAMMAL SCIENCE* and a present associate editor of the *Journal of Mammalogy*, I have had great difficulty in lining up reviewers. Sometimes it takes 8 or 10 tries to find someone who will agree to review a paper. The typical excuse is "I'm too busy."

First I try the people who have published the most relevant and recent papers on the topic in question. Then I move down the range of choices. The temptation, and sometimes the need, is to turn to potential reviewers in less-related fields or those who are not so "busy" (i.e., are not producing much themselves). This inevitably leads to less-knowledgeable reviewers and often reviews of lesser quality, which of course complicates the editor's job and sometimes enrages the authors.

If an average acceptance rate of 50% is assumed, and if each paper needs at least two reviews, then each paper published represents at least four reviews. Following this logic, if you publish three or four papers a year, you should be doing at least 12 to 16 reviews. Anything less means that you are sloughing off the work to others who are perhaps less knowledgeable and capable than you in your specialty, and you should not be upset when someone reviewing a paper of yours "doesn't have a clue."

Doing a fair share of peer reviews should be a recognized and expected part of the job for scientific professionals; it should be written into the job descriptions of salaried scientists and be considered in evaluating junior faculty for tenure. The caution should be "Publish and review, or perish."

WILLIAM F. PERRIN

Southwest Fisheries Science Center, NOAA Fisheries, La Jolla, CA 92037, USA, and Scripps Institution of Oceanography, University of California San Diego, La Jolla, CA 92037, USA. E-mail: william.perrin@noaa.gov

A Peer Review How-To

AS A MEMBER OF THREE EDITORIAL BOARDS, author of 90-some scientific papers, and reviewer of over 900 manuscripts in the past 30 years, I have seen my share of scientific reviews. Reviews have become increasingly critical and demanding. This trend has doubtless contributed to high standards, but carried too far it can become counterproductive and frustrating for authors, editors, and reviewers alike.

A reviewer's chief responsibility is to advise the editors on whether a manuscript with suggested revisions would be acceptable for publication. Reviewers should highlight a paper's strengths and weaknesses, but they need not delineate strengths in very weak papers nor stress minor weaknesses in strong papers. Reviews should be prompt and thorough and should avoid sharp language and invective.

Reviewers make two common mistakes. The first mistake is to reflexively demand that more be done. Do not require experiments beyond the scope of the paper, unless the scope is too narrow. Avoid demanding that further work apply new techniques and approaches, unless the approaches and techniques used are insufficient to support the conclusions. There is no need to require more tests of conclusions that have been demonstrated beyond reasonable doubt, and conversely, authors need not exclude every possible explanation for their results. Suggest an additional experiment, further analysis, or altered interpretation, but do not make publication contingent on these changes. If the conclusions cannot stand without additional work or if the evidence does not distinguish between reasonably likely alternatives, recommend that the editor reject the manuscript.

The second mistake often made by reviewers is failing to consider all of the journal's goals and requirements, including standards and guidelines stated in the editorial policy and gleaned from its articles. Do not reject a manuscript simply because its ideas are not original, if it offers the first strong evidence for an old but important idea. Do not reject a paper with a brilliant new idea simply because the evidence was not as comprehensive as could be imagined. Do not reject a paper simply because it is not of the highest significance, if it is beautifully executed and offers fresh ideas with strong evidence. Seek a balance among criteria in making a recommendation.

Finally, step back from your own scientific prejudices in order to judge each paper on its merits and in the context of the journal that has solicited your advice.

ROBERT S. ZUCKER

Department of Molecular and Cell Biology, University of California, Berkeley, CA 94720, USA.

CREDIT: JOE SUTLIFF

Published by AAAS

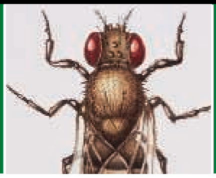

Y power

42

Assessing biofuels

43

Climate Change Goals: Where to Begin?

COLIN CHALLEN'S EDITORIAL "PLAYING CLIMATE change poker" (20 July 2007, p. 295) has a very apt title. As a British parliamentarian who chairs the All Party Parliamentary Climate Change Group, he obviously feels very good about the impressive goals set in the recent UK Draft Climate Change Bill. But he also has the equivalent of an ace in the hole which, like any good poker player, he carefully does not show.

This ace is the use of a 1990 baseline year for calculation of the targeted 60% reduction in British CO_2 production. The year 1990 was during the period when the UK was switching away from heavy reliance on coal. This switch occurred because of the increasing production of North Sea oil and because of Prime Minister Thatcher's aversion to the then-powerful and militant coal miner's union.

The UK is not alone in trying to take advantage of the vagaries of history by using 1990 as a baseline year. Germany's recent proposal for a 50% reduction in carbon dioxide emissions, presented by Prime Minister Merkel at the G8 meeting in early June, takes advantage of the 1989 German reunification that added highly inefficient eastern German industry to their 1990 baseline.

Rather than using a baseline of 17 years ago, the all-important goal-setting process to mitigate global climate effects should start with a clear understanding of where we are now and where we want to be in the future. Global climate change is too serious to be treated as a game. It is time to turn over every player's hole cards.

BERNARD D. GOLDSTEIN

Environmental and Occupational Health, University of Pittsburgh Graduate School of Public Health, Pittsburgh, PA 15261, USA.

Response

BERNARD GOLDSTEIN HAS HIT UPON A VERY important point. It is where we want to be, not where we've been, that matters. We need to achieve a safe and sustainable concentration of greenhouse gases in the atmosphere, and we should "backcast" all our calculations from that overriding objective and not obsess about 1990 as if that year had some magical quality.

Taking a baseline year does have one important quality: It provides an absolute that prevents the relativism of those politicians, notably in the administrations of the United States and China, of merely seeking to reduce the carbon intensity per unit of GDP. That is a recipe for emissions growth.

COLIN CHALLEN

All Party Parliamentary Climate Change Group, House of Commons, London SW1A 0AA, UK.

Beyond Bed Nets

DESPITE THE NOBLE EFFORTS OF ECONOMIST Jeffrey Sachs to address the malaria problems of Africa by supplying bed nets to 80% of the sleeping sites in the sub-Sahara ("Battling over bed nets," News Focus, 26 October 2007, p. 556), he might benefit from words written over 20 years ago by parasitologist J. D. Gillet: "The behaviour of the pathogens responsible for tropical disease and the behaviour of the hosts other than man are both studied in great detail, but the behaviour of man, the third component in these cycles of transmission, is for the most part totally and inexplicably disregarded" (*1*). Carefully monitored studies have shown that bed nets can be very effective against malaria (*2*), but will communities be able to maintain the 70 to 80% coverage level needed to have a dramatic effect on disease transmission? Condoms serve as an analogous strategy in the prevention of AIDS; they are less penetrable to HIV than bed nets are to mosquitoes, and yet AIDS continues to spread. The behavior of man may once again be the missing factor in our calculations. We need bed nets, but what we need more is a long-term partnership with Africans that includes education, land reform, and the mutual development of local anti-malaria strategies.

THOMAS F. MCCUTCHAN

Laboratory of Malaria and Vector Research, National Institutes of Health, Bethesda, MD 20892, USA.

References

1. J. D. Gillet, *Trans. R. Soc. Trop. Med. Hyg*. **79**, 12 (1985).
2. C. Curtis, *Trends Parasitol*. **21**, 504 (2005).

Letters to the Editor

Letters (~300 words) discuss material published in *Science* in the previous 3 months or issues of general interest. They can be submitted through the Web (www.submit2science.org) or by regular mail (1200 New York Ave., NW, Washington, DC 20005, USA). Letters are not acknowledged upon receipt, nor are authors generally consulted before publication. Whether published in full or in part, letters are subject to editing for clarity and space.

TECHNICAL COMMENT ABSTRACTS

COMMENT ON "Protein Sequences from Mastodon and *Tyrannosaurus rex* Revealed by Mass Spectrometry"

Mike Buckley, Angela Walker, Simon Y. W. Ho, Yue Yang, Colin Smith, Peter Ashton, Jane Thomas Oates, Enrico Cappellini, Hannah Koon, Kirsty Penkman, Ben Elsworth, Dave Ashford, Caroline Solazzo, Phillip Andrews, John Strahler, Beth Shapiro, Peggy Ostrom, Hasand Gandhi, Webb Miller, Brian Raney, Maria Ines Zylber, M. Thomas P. Gilbert, Richard V. Prigodich, Michael Ryan, Kenneth F. Rijsdijk, Anwar Janoo, Matthew J. Collins

We used authentication tests developed for ancient DNA to evaluate claims by Asara *et al*. (Reports, 13 April 2007, p. 280) of collagen peptide sequences recovered from mastodon and *Tyrannosaurus rex* fossils. Although the mastodon samples pass these tests, absence of amino acid composition data, lack of evidence for peptide deamidation, and association of α1(I) collagen sequences with amphibians rather than birds suggest that *T. rex* does not.

Full text at www.sciencemag.org/cgi/content/full/319/5859/33c

RESPONSE TO COMMENT ON "Protein Sequences from Mastodon and *Tyrannosaurus rex* Revealed by Mass Spectrometry"

John M. Asara and Mary H. Schweitzer

We sequenced six endogenous collagen peptides from *Tyrannosaurus rex* bone fragments using mass spectrometry. Five sequences match birds, but only two match amphibians, supporting dinosaur-bird relationships. Buckley *et al*. reinterpret and misinterpret our data and question sequence authenticity, but they used a suboptimal phylogenetic algorithm to analyze only a subset of reported sequences and they suggest analyses that are less sensitive and less specific than mass spectrometry. We disagree and use data to explain.

Full text at
www.sciencemag.org/cgi/content/full/319/5859/33d

Published by AAAS

Comment on "Protein Sequences from Mastodon and *Tyrannosaurus rex* Revealed by Mass Spectrometry"

Mike Buckley,[1] Angela Walker,[2] Simon Y. W. Ho,[3] Yue Yang,[1] Colin Smith,[4] Peter Ashton,[1] Jane Thomas Oates,[1] Enrico Cappellini,[1] Hannah Koon,[1] Kirsty Penkman,[1] Ben Elsworth,[1] Dave Ashford,[1] Caroline Solazzo,[1] Phillip Andrews,[2] John Strahler,[2] Beth Shapiro,[6] Peggy Ostrom,[5] Hasand Gandhi,[5] Webb Miller,[6] Brian Raney,[7] Maria Ines Zylber,[8] M. Thomas P. Gilbert,[9] Richard V. Prigodich,[10] Michael Ryan,[11] Kenneth F. Rijsdijk,[12] Anwar Janoo,[13] Matthew J. Collins[1]*

We used authentication tests developed for ancient DNA to evaluate claims by Asara *et al*. (Reports, 13 April 2007, p. 280) of collagen peptide sequences recovered from mastodon and *Tyrannosaurus rex* fossils. Although the mastodon samples pass these tests, absence of amino acid composition data, lack of evidence for peptide deamidation, and association of α1(I) collagen sequences with amphibians rather than birds suggest that *T. rex* does not.

Early reports of DNA preservation in multimillion-year-old bones (i.e., from dinosaurs) have been largely dismissed (*1*, *2*) (table S1), but reports of protein recovery are persistent [see (*3*) for review]. Most of these studies used secondary methods of detection, but Asara *et al*. (*2*) recently reported the direct identification of protein sequences, arguably the gold standard for molecular palaeontology, from fossil bones of an extinct mastodon and *Tyrannosaurus rex*. After initial optimism generated by reports of dinosaur DNA, there has been increasing awareness of the problems and pitfalls that bedevil analysis of ancient samples (*1*), leading to a series of recommendations for future analysis (*1*, *4*). As yet, there are no equivalent standards for fossil protein, so here we apply the recommended tests for DNA (*4*) to the authentication of the reported mastodon and *T. rex* protein sequences (*2*) (Table 1).

First, the likelihood of collagen survival needs to be considered. The extremely hierarchical structure of collagen results in unusual, catastrophic degradation (*5*) as a consequence of fibril collapse. The rate of collagen degradation in bone is slow because the mineral "locks" the components of the matrix together, preventing helical expansion, which is a prerequisite of fibril collapse (*6*). The packing that stabilizes collagen fibrils (*6*) also increases the temperature sensitivity of degradation (E_a 173 kJ mol^{-1}) (Fig. 1). Collagen decomposition would be much faster in the *T. rex* buried in the then-megathermal (>20°C) (*7*) environment of the Hell Creek formation [collagen half-life ($T_{1/2}$) = ~ 2 thousand years (ky] than it would have been in the mastodon lying within the Doeden Gravel Beds (present-day mean temperature, 7.5°C; collagen $T_{1/2}$ = 130 ky) (Fig. 1).

This risk of contamination also needs to be evaluated. Collagen is an ideal molecular target for this assessment because the protein has a highly characteristic motif that is also sufficiently variable to enable meaningful comparison between distant taxa if enough sequence is obtained (Fig. 2). Compared with ancient DNA amplification, contamination by collagen is inherently less likely. Furthermore, because the bones sampled in (*2*) were excavated by the

Table 1. Key questions to ask about ancient biomolecular investigations [adapted from (*4*)].

Test	Sample	Pass	Observation
Do the age, environmental history, and preservation of the sample suggest collagen survival?	Mastodon, 300 to 600 ky old	Yes	Collagen $T_{1/2}$ at 7.5°C = 130 ky
	T. rex, 65 million years old	No	Collagen $T_{1/2}$ at 20°C = 2 ky
Do the biomolecular and/or macromolecular preservation of the sample, the molecular target, the innate nature of the sample, and its handling history suggest that contamination is a risk?	Biomolecular preservation	?	Range of evidence presented (*8*) but no amino acid compositional data
	Macromolecular preservation	Yes	Macromolecular preservation is not the equivalent of biomolecular preservation (*9*)
	Molecular target	Yes	
	Handling history	Yes?	Large (2.5 g) samples increase risk of contamination?
Do the data suggest that the sequence is authentic, rather than the result of damage and contamination?	Mastodon and *T. rex*	No	Errors in interpretation of spectra [see table S1 and (*13*)]? Damage-induced errors in sequence
Do the results make sense, and are there enough data to make the study useful and/or to support the conclusions?	Mastodon	Yes	Weak affinity to mammals
	T. rex	No	Affinity of α1(I) peptides to amphibians, not birds or reptiles

---

[1] BioArch, Departments of Biology, Archaeology, Chemistry and Technology Facility, University of York, Post Office Box 373, York YO10 5YW, UK. [2] Department of Biological Chemistry, University of Michigan Medical School, Ann Arbor, MI 48109–0404, USA. [3] Evolutionary Biology Group, Department of Zoology, University of Oxford, OX1 3PS, UK. [4] Department of Human Evolution, Max Planck Institute for Evolutionary Anthropology, Deutscher Platz 6, D-04103, Leipzig, Germany. [5] Department of Zoology, Michigan State University, East Lansing, MI 48824, USA. [6] Department of Biology, Pennsylvania State University, University Park, PA 16802, USA. [7] Center for Biomolecular Science and Engineering, University of California–Santa Cruz, CA 95064, USA. [8] Department of Parasitology, Kuvin Center, Hebrew University of Jerusalem, Israel. [9] Biological Institute, University of Copenhagen, Universitetsparken 15, 2100 Copenhagen, Denmark. [10] Chemistry Department, Trinity College, 300 Summit Street, Hartford, CT 06106, USA. [11] Cleveland Museum of Natural History, 1 Wade Oval Drive, University Circle, Cleveland, OH 44106, USA. [12] National Museum of Natural History "Naturalis," P.O. Box 9517, 2300 RA Leiden, Netherlands. [13] National Heritage Trust Fund Mauritius, Mauritius Institute, La Chaussée Street Port Louis, Mauritius.

*To whom correspondence should be addressed. E-mail: mc80@york.ac.uk

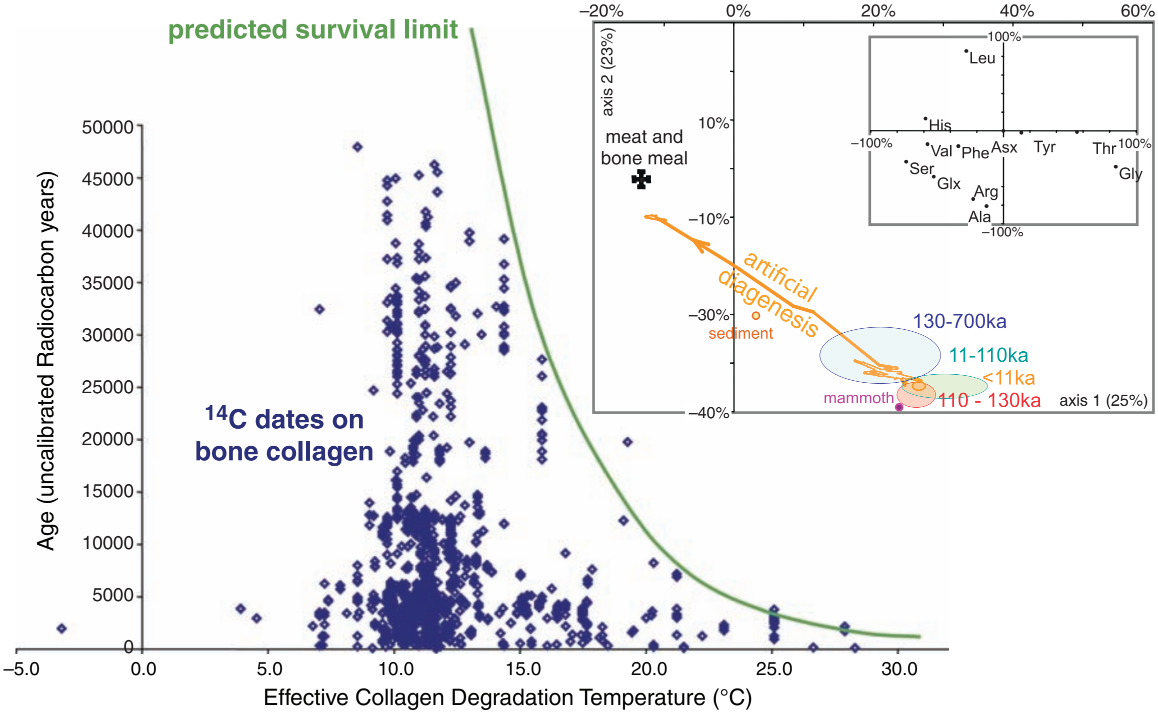

Fig. 1. Plot of radiocarbon age versus estimated effective collagen degradation temperature for radiocarbon-dated bones from laboratory databases (principally Oxford and Groningen). The line represents the expected calendar age at which 1% of the original collagen remains following a zero-order reaction; almost no bone collagen survives beyond this predicted limit. (**Inset**) The 99% confidence intervals of amino acid compositions by first two principal component analyses (48% of total variance) for bones from NW Europe aged <11 ky ($n = 324$), 11 to 110 ky ($n = 210$), 110 to 130 ky ($n = 26$), and 130 to 700 ky ($n = 31$). Pliocene samples are not plotted, as their composition ($n = 8$) is highly variable and yields of amino acids are low. The orange line indicates a compositional trend observed when compact bone is heated for 32 days at 95°C, which reduces collagen to 1% of the initial concentration [each inflection represents a separate analysis; $n = 32$)]. The composition becomes more similar to mixed tissue samples (meat and bone meal; $n = 32$), principally due to the depletion of Gly. An amino acid profile for mammoth is consistent with collagen, unlike the associated sediment sample [data from (*11*)].

authors, obvious contamination sources such as animal glue (used in conservation) can be excluded. However, concentrating protein from the large amounts of bone used (2.5 g) may have heightened the risk of extraneous proteins entering the sample during extraction, although there have been no systematic studies of this phenomenon. Independent extraction and analyses would have strengthened claims for the authenticity of the origin of the peptides (and potentially ameliorated the original problems of data interpretation) (*4*).

The remarkable soft-tissue preservation of the investigated *T. rex* specimen (MOR 1125) has been documented (*8*). However, microscopic preservation does not equate with molecular preservation (*9*). Immunohistochemistry provides support for collagen preservation, but Asara *et al.* (*2*) presented no data regarding inhibition assays with collagen from different species or cross-reactivity with likely contaminants [e.g., fungi (*10*)]. Curiously, no amino acid compositional analysis was conducted [see (*11*)], although immonium ions were identified by time-of-flight secondary ion mass spectrometry. In our experience, collagen-like amino acid profiles have been obtained in all bones from which we could obtain collagen sequence (Fig. 1, inset).

Regarding the proof of sequence authenticity, the spectra reported by Asara *et al.* (*12*) are inconsistent with some of the sequence assignments (*13*) (table S1). A common diagenetic modification, deamidation, not considered in (*2*), may shed light on authenticity. The facile succinimide-mediated deamidation (*14*) of asparagine occurred at N$_{229}$G and N$_{1156}$G in ostrich peptides (Ost 4 and Ost5) (see table S1 for nomenclature), presumably during sample preparation. Direct hydrolytic deamidation is slower (*14*), and an expectation of elevated levels of such products is reasonable for old samples. We agree with the most recent interpretation (*13*) of the spectrum illustrated in Fig. 2B as α1(I) G$_{362}$SEGPEGVR$_{370}$, the deamidated (Q→E$_{367}$) form of the sequence found in most mammals (*12*). By way of contrast, none of the three glutamine residues in the reported *T. rex* peptides are deamidated (table S1). Only time will tell if Q→E is a useful marker for authentically old collagen, but from the evidence presented, the mastodon sequence looks more diagenetically altered than *T. rex*.

The unusual, fragmented nature of the reported *T. rex* sequence does not make it amenable to standard, model-based phylogenetic analysis. Instead, we examined the phylogenetic signal of the α1(I) fragments of mastodon and *T. rex* using Neighbor-Net analysis and uncorrected genetic distances. Using the sequences reported in (*13*), both the *T. rex* and mastodon signal display an affinity with amphibians (Fig. 2A). Our reinterpretation of the spectra (*12*) changes the affinity of mastodon but not of *T. rex* (Fig. 2B). In addition to the α1(I) peptides used in the Neighbor-Net analysis, Asara *et al.* reported two other peptides from *T. rex* (*13*); we question the interpretation of the α1(II) spectra (identical to frog) but not the α2(I) spectra (identical to chicken).

We require more data to be convinced of the authenticity of the *T. rex* collagen sequences reported by Asara *et al.* Nevertheless, the handful of spectra reported for the temperate Pleistocene mastodon fail neither phylogenetic nor diagenetic tests, thus highlighting the potential of protein mass spectrometry to bridge the present gulf in our understanding between the fate of archaeological and fossil proteins. To avoid past mistakes of ancient DNA research (*1*), we recommend that future fossil protein claims be considered in light of tests for authenticity such as those presented here.

Reference and Notes

1. E. Willerslev, A. Cooper, *Proc. R. Soc. London. B. Biol. Sci.* **272**, 3 (2005).
2. J. M. Asara, M. H. Schweitzer, L. M. Freimark, M. Phillips, L. C. Cantley, *Science* **316**, 280 (2007).
3. M. H. Schweitzer, *Palaeontologia Electronica* **5**, editorial 2 (2003); http://palaeo-electronica.org/2002_2/r_and_p.pdf
4. M. T. P. Gilbert, H.-J. Bandelt, M. Hofreiter, I. Barnes, *Trends Ecol. Evol.* **20**, 541 (2005).
5. M. J. Collins, M. S. Riley, A. M. Child, G. Turner-Walker, *J. Archaeol. Sci.* **22**, 175 (1995).
6. C. A. Miles, M. Ghelashvili, *Biophys. J.* **76**, 3243 (1999).
7. K. R. Johnson, D. J. Nichols, J. H. Hartman, *The Hell Creek Formation and the Cretaceous-Tertiary Boundary in the Northern Great Plains: Geological Society of America Special Paper* **361**, 503–510 (2002).
8. M. H. Schweitzer *et al.*, *Science* **316**, 277 (2007).
9. N. S. Gupta, D. E. G. Briggs, R. D. Pancost, *J. Geol. Soc. London* **163**, 897 (2006).
10. P. Sepulveda *et al.*, *Infect. Immun.* **63**, 2173 (1995).

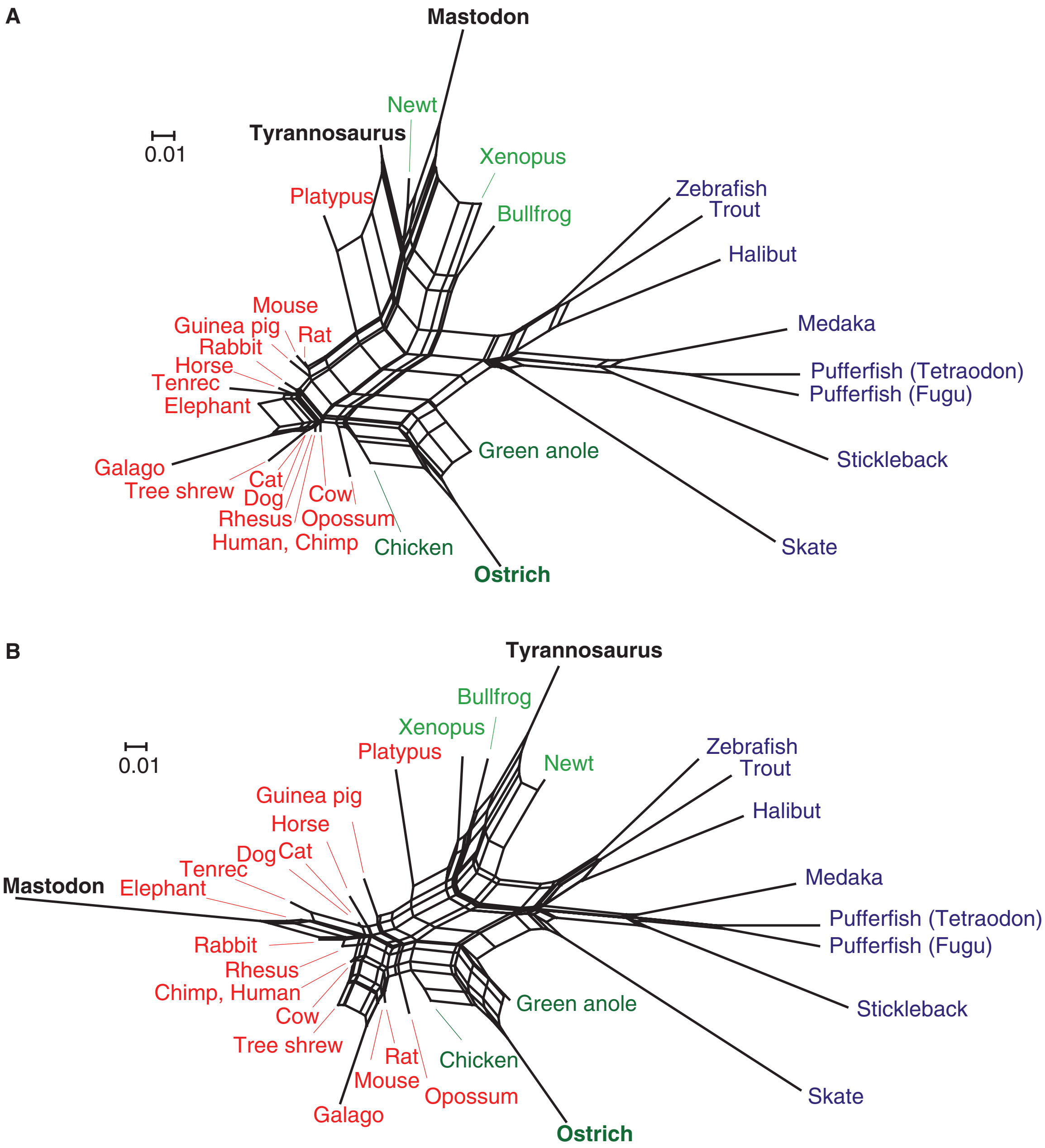

Fig. 2. Phylogenetic networks of α1(I) sequences using Neighbor-Net analysis (**A**) with the most recent Asara *et al*. assignments (*13*) and (**B**) after our reinterpretation of the mass spectrometric data (*12*). *T. rex* does not group with bird/reptile using either set of sequence alignments. More sequence is required for a full, model-based phylogenetic analysis.

11. M. Schweitzer, C. L. Hill, J. M. Asara, W. S. Lane, S. H. Pincus, *J. Mol. Evol.* **55**, 696 (2002).
12. See supporting material on *Science* Online.
13. J. M. Asara *et al.*, *Science* **317**, 1324 (2007).
14. N. E. Robinson *et al.*, *J. Pept. Res.* **63**, 426 (2004).
15. This work was supported by NSF (EAR-0309467), National Environment Research Council (NE511148, GR9/01656), National Center for Research Resources (P41-18627), European Commission (MEST-CT-2004-007909, MEST-CT-2005-020601), Wellcome Trust Bioarchaeology Fellowships (K.P. and H.K.) Analytical Chemistry Trust Fund, the Royal Society of Chemistry Analytical Division, Engineering and Physical Sciences Research Council, and the Michigan Proteome Consortium.

Supporting Online Material
www.sciencemag.org/cgi/content/full/319/5859/33c/DC1
SOM Text
Table S1
References

26 June 2007; accepted 20 November 2007
10.1126/science.1147046

Response to Comment on "Protein Sequences from Mastodon and *Tyrannosaurus rex* Revealed by Mass Spectrometry"

John M. Asara[1,2]* and Mary H. Schweitzer[3,4]

We sequenced six endogenous collagen peptides from *Tyrannosaurus rex* bone fragments using mass spectrometry. Five sequences match birds, but only two match amphibians, supporting dinosaur-bird relationships. Buckley *et al.* reinterpret and misinterpret our data and question sequence authenticity, but they used a suboptimal phylogenetic algorithm to analyze only a subset of reported sequences and they suggest analyses that are less sensitive and less specific than mass spectrometry. We disagree and use data to explain.

Buckley *et al.* (*1*) use authentication tests developed for ancient DNA to question the authenticity of peptide sequences we obtained from an exceptionally well-preserved 68-million-year-old *Tyrannosaurus rex* fossil (*2*, *3*). We disagree with their assessment for the reasons explained below. We first wish to point out that Table 1 lists the six high-confidence peptide sequences for the exceptionally well-preserved 68-million-year-old *T. rex* fossil (MOR 1125) acquired by tandem mass spectrometry (MS/MS) (*3*). All future phylogenetic analyses or critiques should be performed using these sequences.

Turning to the issue of collagen survival brought up by Buckley *et al.* (*1*), the preservational state of *T. rex* specimen MOR 1125 was described previously (*4*) and showed unexpected retention of soft tissue and cellular structures. Its burial under approximately 1000 m^3 of semiconsolidated sandstone limited its exposure to modern environmental influences (water, light, and air), contributing to the retention of endogenous protein identified first by immunochemical assays, then by ion trap mass spectrometry (*2*, *3*). Sequences were derived from multiple extractions conducted over about 1.5 years. It has been reported that cross-linking (i.e., packing) of collagen molecules increases their thermal stability, which contrasts with statements in (*1*) and which, in combination with association to bone mineral, contributes to the longevity of the molecule (*5*). Combined with supporting data, including in situ immunochemistry and enzyme-linked immunosorbent assays, atomic force microscopy, in situ time-of-flight secondary ion mass spectrometry, and various microscopic analyses (*6*), the sequence data suggest a reevaluation of theories in the Buckley *et al*. comment regarding protein longevity and preservation.

Regarding the issue of contamination risk, we showed that endogenous protein fragments derived from dinosaur bone extracts were in low/sub femtomole amounts (*2*) from milligrams of extract. Because of these low concentrations, contamination from soil bacteria and human keratin (common in most samples from dust, skin, and hair) were present. Contamination with these common sources would make bulk amino acid analysis (AAA) data meaningless, as AAA is not protein sequence specific to address the source of the amino acids. We were able to sequence the keratin and bacterial peptides separately from collagen using microcapillary liquid chromatography (LC) MS/MS. Collagen type I, concentrated in bone, is not a common source of protein contamination, as Buckley *et al*. note. Not all *T. rex* peptides are consistent with a common organism, so multiple separate contamination events are required to support the Buckley *et al*. argument for contamination as a source. This is not supported by our consistently negative controls. Furthermore, the sequences shown in Table 1 do not support links to amphibians, and amphibians are neither native to nor present at Hell Creek, nor have they ever been present in either of the labs where analysis was performed. Bone from amphibians or related organisms are not a logical source of modern contamination. Given that we observed not only gross morphological preservation but also apparent preservation of other characteristics such as elasticity and banding, in situ localization of collagen antibodies to tissues with negative controls, and collagen-consistent sequence data consistent with birds, the most parsimonious explanation is that the material is endogenous. To challenge this hypothesis requires data that support alternative hypotheses internally consistent for all data presented, not a small subset of data as in the comment by Buckley *et al*. (*1*).

Buckley *et al*. conduct a phylogenetic analysis on a small subset of sequence data that we produced but that they inappropriately reinterpret. They included only four sequences for mastodon and six for ostrich, whereas we published 78 for mastodon and 93 for ostrich (*3*). Buckley *et al*. claim that several spectra cannot be interpreted, although the fragmentation patterns and signal-to-noise-ratios are of interpretable quality. They included only five of the six peptides that we identified in *T. rex* extracts. Specifically, they chose to omit the collagen type I peptide sequence GLPGESGAVGPAGPIGSR from the α2 chain, without clear justification for doing so. This omission is important, because it is a unique match to chicken (birds). They use a single neighbor-joining algorithm to generate a phylogenetic hypothesis of protein source and do not

Table 1. Clarified 68-million-year-old *T. rex* collagen peptide sequences. Hydroxylation sites are noted with an asterisk (*) immediately following the modified residue. Single-letter abbreviations for the amino acid residues are as follows: A, Ala; C, Cys; D, Asp; E, Glu; F, Phe; G, Gly; H, His; I, Ile; K, Lys; L, Leu; M, Met; N, Asn; P, Pro; Q, Gln; R, Arg; S, Ser; T, Thr; V, Val; W, Trp; and Y, Tyr.

Peptide sequence	Protein	Organism identity
GATGAP*GIAGAP*GFP*GAR	Collagen α1t1	Identical to chicken and frog (amphibians)
GSAGPP*GATGFP*GAAGR	Collagen α1t1	Identical to multiple mammals, including chicken (no amphibian identity)
GVQGPP*GPQGPR	Collagen α1t1	Identical to chicken and opossum (no amphibian identity)
GLPGESGAVGPAGPIGSR	Collagen α2t1	Identical to chicken only (no amphibian identity)
GVVGLP*GQR	Collagen α1t1	Identical to multiple organisms, including chicken and newt (amphibians)
GAPGPQGPSGAP*GPK	Collagen α1t1	Unique *T. rex* sequence (no amphibian or bird identity)

---

[1] Division of Signal Transduction, Beth Israel Deaconess Medical Center, Boston, MA 02115, USA. [2] Department of Pathology, Harvard Medical School, Boston, MA 02115, USA. [3] Department of Marine, Earth, and Atmospheric Sciences, North Carolina State University, Raleigh, NC 27695, USA. [4] North Carolina Museum of Natural Sciences, Raleigh, NC 27601, USA.

*To whom correspondence should be addressed. E-mail: jasara@bidmc.harvard.edu

validate their hypothesis with other algorithms. It is commonly agreed by evolutionary biologists that the preferred practice is to use multiple methods to generate phylogenetic hypotheses and then look for agreement. For example, use of Bayesian analysis, parsimony, and likelihood in addition to neighbor-joining are important to validate the results from a single algorithm (*7*). Use of all of our data would make it impossible to group *T. rex* with amphibians. The sequence clustering of the majority of the dinosaur sequences (five of six) with birds (chicken) and not amphibians (only two of six) based on our data invalidates the phylogenetic conclusions proposed by Buckley *et al*. and upholds our original conclusions that birds are the closest living organisms to dinosaurs among all organisms for which collagen sequence data are available. We agree that only six high-confidence collagen-derived peptides recovered from *T. rex* may not be enough to generate robustly supported phylogenetic trees; however, the amino acid sequences of the peptides are sufficient to identify the source protein, collagen type I, and to assess dinosaur peptide sequence similarity/identity to other organisms using BLAST analysis. Future phylogenetic analyses using all of our data, in addition to new protein sequence data for critical taxa (birds and reptiles), are needed to make an accurate assessment of *T. rex* evolutionary placement.

Buckley *et al.* make five challenges to our report of endogenous collagen protein within dinosaur bone: (i) Although no standards for replication and authentication of protein data currently exist for ancient protein data, we did not apply standards currently recommended for DNA studies. (ii) We did not have our extractions conducted in multiple labs. (iii) We did not perform inhibition studies in immunohistochemical assays using multiple taxa. (iv) No standard amino acid analyses were conducted. (v) We did not account for common deamidation modifications. Our responses to these criticisms are as follows.

First, as Buckley *et al*. observe, no standards exist for ancient protein analyses. Because we are not enzymatically amplifying molecules, we are unlikely to observe exogenous contaminants in our many analyses, including localization of antibody-antigen complexes and collagen-consistent amino acid residues to the samples. No collagen signal above background was observed in multiple controls conducted in tandem in any of these diverse assays. Second, few labs exist that are dedicated to ancient protein analyses, and labs routinely capable of performing these assays generally conduct similar analyses on modern protein samples; hence, induction of modern contaminating molecules are much more likely from nondedicated protein labs. In addition, very little proteinaceous material was available for analysis, and this diminished over the course of our analyses as the material responded to modern environmental conditions. However, provided that the amount of sequenceable material is sufficient, we intend to send future samples to other labs for verification. The choice between potentially acquiring more sequences versus the risk of sending the extract to another lab for confirmation was obvious. Third, although we did not conduct multitaxon inhibition studies, we did perform these inhibition assays using bird collagen, which is more relevant and appropriate and has the strongest inhibition capacity for antibodies to bird collagen used in this study. Fourth, concentrations of proteinaceous material were insufficient to conduct amino acid analysis. Bulk amino acid analyses do not contribute enough useful information (in terms of assigning resulting signal to source protein). However, we were able to localize amino acids consistent with collagen to dinosaur tissues only and not to embedding material or analytical mounting materials. Controls, including those conducted on surrounding sandstones, undertaken in tandem with samples for each assay, were consistently negative (*6*). Fifth, we note that all instances of glutamic acid (E) and aspartic acid (D) that occur in sequences are not the result of deamidation events but may be the result of translations from genomic coding sequence. The ion trap mass spectrometer used in the study, although extremely sensitive, is capable of relatively low resolution and low mass accuracy, so these modification events were difficult to detect, though possibly present. Analysis of other fossil specimens using our newly acquired ultrahigh-resolution and mass accuracy Orbitrap mass spectrometer clearly show deamidation events. It is difficult to distinguish between posttranslational modifications and diagenetic deamidation because rates of occurrences of these modifications under natural conditions have not been well studied and because the *T. rex* and mastodon sequences were not analyzed before fossilization. Because deamidation occurs on freshly prepared proteins in our lab at levels similar to many "fossilized" proteins, we question whether deamidation is a particularly useful marker for age.

We continue our analyses of MOR 1125 and other dinosaur specimens not only to verify our original results but also to demonstrate preservation and molecular recovery in other specimens. We also continue to develop new, more sensitive, and more accurate methodologies using new instrumentation. We presented our analytical data as a first step in understanding protein preservation and evolutionary comparisons for extinct taxa. Although more sequence data from multimillion-year-old ancient fossils is a primary goal, the small sampling of data that we have shown demonstrates the possibility of obtaining multimillion-year-old sequences using mass spectrometry. Our papers provide a baseline methodology for determining sequences from ancient samples while pushing the limits of state-of-the-art instrumental sensitivity. Further work, based on experience and experimental data, will contribute to establishing standards for analyzing ancient protein samples.

References and Notes

1. M. Buckley *et al*., *Science* **319**, 33 (2008); www.sciencemag.org/cgi/content/full/319/5859/33c.
2. J. M. Asara, M. H. Schweitzer, L. M. Freimark, M. Phillips, L. C. Cantley, *Science* **316**, 280 (2007).
3. J. M. Asara *et al*., *Science* **317**, 1324 (2007).
4. M. H. Schweitzer, J. L. Wittmeyer, J. R. Horner, J. K. Toporski, *Science* **307**, 1952 (2005).
5. C. A. Miles, M. Ghelashvili, *Biophys. J.* **76**, 3243 (1999).
6. M. H. Schweitzer *et al*., *Science* **316**, 277 (2007).
7. J. J. Wiens, *Syst. Biol.* **52**, 528 (2003).

8. We thank C. L. Organ, L. M. Freimark, M. Phillips, L. C. Cantley, and J. R. Horner for helpful discussions.

10 July 2007; accepted 30 November 2007
10.1126/science.1147364

HISTORY OF SCIENCE

The Fertile Banks of the Thames

Nicholas S. Popper

The modern image of Elizabethan London evokes a shadowy haunt of swashbuckling courtiers and starchy black-clad Puritans. It does not conjure, for most, gentlemen comparing exotic floral specimens received from friends in Holland or aldermen crowding into public spaces to hear lectures on navigational and surveying instruments. Deborah Harkness's engaging *The Jewel House: Elizabethan London and the Scientific Revolution* makes clear that in Elizabeth's London there lurked a vibrant, sizable (if loose-knit) community of enthusiastic interrogators and manipulators of the natural world.

In a series of case studies, Harkness (a historian at the University of Southern California) examines evolving communities of Elizabethan students of nature. The themes of competition and collaboration, print culture and manuscript networks, useful knowledge, and a cosmopolitan and urban sensibility unite impeccably researched episodes, such as the breach of social codes perpetrated by famed herbalist John Gerard against Lime Street's naturalists. The City hummed with boasting practitioners brandishing imported naturalia and even more exotic knowledge. Individuals established niches within this market by maintaining the potency of their peculiar expertise—or discrediting rivals, as the Barber-Surgeons' Company hectored Paracelsian quack Valentine Russwurin into oblivion. Urban practitioners cohered to learn and disseminate the skills individuals claimed. Such literacies included numeracy for those interested in newfangled instruments and the ability to pitch projects to, or evaluate them for, the overmatched Principal Secretary, William Cecil, as he attempted to administer Elizabethan "Big Science."

The last chapters demonstrate how individuals relied on specific practices—observation, reading, recording, conversation, and, above all, experimentation—to accumulate and certify natural knowledge. For example, King's Bench prisoner Clement Draper amassed notebooks in which excerpted recipes from borrowed books shared the page with accounts of his conversations with visitors and fellow inmates concerning alchemical and medical preparations. Harkness masterfully interweaves tales that exemplify the citywide admiration of technological skill. For instance, the merchant Emmanuel Lucar inscribed praise on his wife Elizabeth's funerary monument for her ability in "algorism, or accounts," while King's Bench prisoner Thomas Seafold produced an elixir by baking mercury and human excrement for several days—likely to the dismay of Draper and other inmates.

The Jewel House
Elizabethan London and the Scientific Revolution
by Deborah E. Harkness
Yale University Press, New Haven, CT, 2007.
371 pp. $32.50.
ISBN 9780300111965.

To Harkness, Hugh Plat represents the pinnacle of urban sensibility, the ability to evaluate and negotiate profitably the communities and literacies teeming throughout the City. Plat was a London native who published accounts of experiments designed to evaluate natural knowledge extracted from local charlatans, foreign tradesmen, and high-born courtiers. He was concerned less with natural philosophy than with useful practical knowledge and the messy labor of experiment. Nor did he strive to impose order upon the knowledge he accumulated; rather he circulated it widely as a disorderly mass. Plat's work, Harkness argues, faithfully represented the realities of the city's brimming empirical culture—utilitarian, decentralized, even democratic.

Harkness contrasts Plat's work with the

The reviewer is at the Department of History, 129 Dickinson Hall, Princeton University, Princeton, NJ 08544–1017, USA. E-mail: npopper@princeton.edu

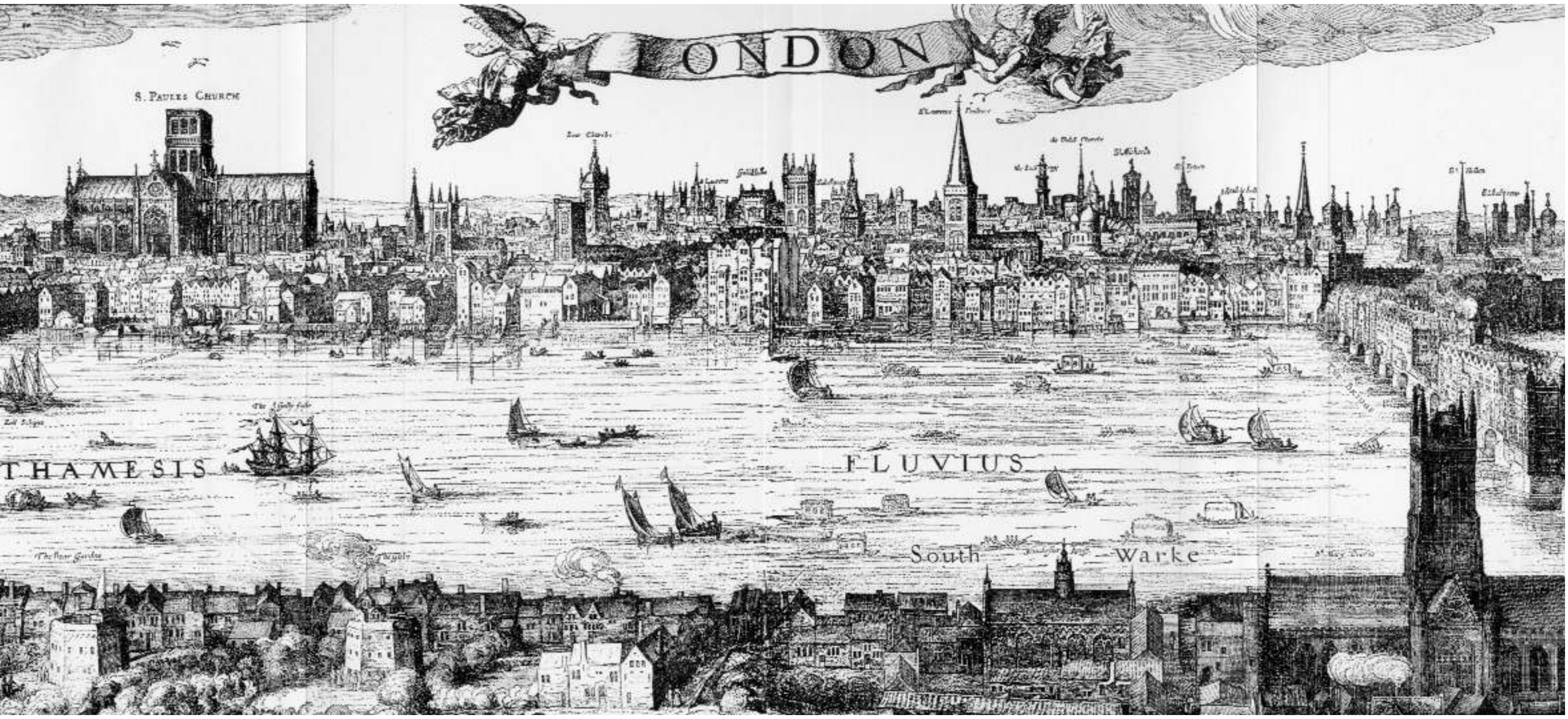

CREDIT: COURTESY ALISON STONES/UNIVERSITY OF PITTSBURGH

Second-hand view? Claes van Visscher, the Dutch printmaker who drew this well-known panorama of 1616, is believed to have never visited London.

London sanitized in Francis Bacon's utopian *New Atlantis*. As she rightly points out, when Bacon advocated empirical methods of producing knowledge, he obliquely praised the methods deployed by his City contemporaries. But Bacon combated what he perceived as a vulgar basis for producing this knowledge by devising a hierarchical institution, "Salomon's House," in which gentlemen-philosophers directed the banausic motions of uncomprehending manual laborers. Bacon's idealization concealed the ubiquity of those practices he purported to invent; in the early years of the Restoration, Royal Society members seeking to link reliable natural philosophical experiment and antirepublicanism saw Bacon's vision as the foremost precedent. Thus was destroyed the memory of Elizabethan science.

This argument will undoubtedly gain purchase among historians of early modern science. Harkness extends the half-century-long trend in studying the social and cultural factors supporting the scientific revolution by adumbrating a community of practitioners hidden in the shadows cast by the methodologies of previous scholars. Science thrived, she makes clear, in the daily lives of Elizabethan Londoners. It was not invested with the philosophical basis that Bacon and others would later grant it, but for her, as for her subjects, science is embodied by specific labor and practices for producing knowledge, not by its philosophical justifications.

An unsympathetic reader might argue that Harkness describes a sophisticated craft community that awaited only a philosophical visionary to create the category of science. This would ignore her impressive documentation of the community's size and its successful integration of disparate London inhabitants. But Harkness does underemphasize how London became a crucible for empirical knowledge. The community was fertilized by the expertise that asylum-seeking French and Dutch Calvinists transported across the Channel. Whether science, as she defines it, existed in their native communities is never considered, neither is the unwelcome implication that it came late to London. Nor does Harkness discuss the relationship between science and the religion of these technology transmitters. The autonomy of the City, and the specificity of its urban sensibility, demand further attention. Elizabethan noblemen and gentry increasingly attended the universities, and many moved to London already trained in the critical faculties Harkness prizes in Plat. Lastly, the author depicts the City as disorganized, yet egalitarian—a borderless, harmonious space in which elites and ordinary people freely shared precious knowledge. Nonetheless, she acknowledges the pervasive influence of Westminster. All manner of practitioners petitioned Elizabeth for prized royal patents or, at the very least, occasional patronage. Harkness's urban sensibility seems an incomplete explanation for the seamless cohesion of these strands in the City.

This caveat does not detract from the value of Harkness's work. Urban spaces that fostered the development and spread of scientific practices should be examined in its wake. The myth of Baconian exceptionalism will further erode, and, perhaps most important, the importance of practices to the category of science will increasingly be subject to detailed scrutiny.

10.1126/science.1151459

ARTS AND NEUROSCIENCE

Connecting Blazons and Neurons

Caroline A. Jones

The modern dream of bringing science to art takes many forms. One nurtures the hope of finally confirming the intuitions of our artists by anchoring perception in molecule and synapse. Another seeks to reveal the "secrets" of art to be simple tricks manipulating human perceptual systems. But perhaps the most powerful is the urge to analyze (and celebrate, in the great humanist tradition) the way that art brings cognition into the person-making place of culture.

Echo Objects
The Cognitive Work of Images
by Barbara Maria Stafford
University of Chicago Press, Chicago, 2007.
307 pp. $45, £27.
ISBN 9780226770512.

The aspiration to unify science and art is modern, because their separation is itself a product of modern professionalization. Here it is significant that the word scientist was a back-formation from the word artist, proposed in the 1830s by a member of the British Association for the Advancement of Science intent on distinguishing the two domains of knowledge production (*1*). Philosophy, mother of them both, can be blamed for seeding the eventual division, since Aristotle already divided the mind into *aisthetá kai noetá*—"felt" versus "thought" (a division Kant deemed "quite famous"). We could argue today about whether an empirical science or a sensual art would recognize itself as felt, or whether an increasingly conceptual art or model-driven science would claim itself as thought. But there can be no doubt that it is hard to bring the two domains together. What Barbara Maria Stafford hopes to reclaim in *Echo Objects: The Cognitive Work of Images*, her ambitious joyride of a book, is an essentially Aristotelian position: knowledge must be rooted in both a sensory aesthetics and a meaning-making abstraction. Her neuroscientifically savvy art history aims at this goal.

Writing as a fellow art historian, I am confident about Stafford's agenda with regard to our discipline. (She is tired of social history and poststructuralism and seeks a reintegration of the generalizable subject once posited by formal analysis and structuralism.) But she has lessons for neuroscience as well, and she pitches her book at the highest level of specialist discourse. Don't know what cognitive "binding" or "re-entry" are? What "connectionist versus modular" or "neural Darwinist" views might be? You may need, as I did, to read back issues of *Science* or seek online cognitive science resources to find out—Stafford (an emeritus professor at the University of Chicago) engages the debates at full tilt and assumes a high level of scientific knowledge.

What I do understand is that Stafford tries to give both sides of the internal (hardwired) versus external (modified by experience) debates but ultimately rejects what she brilliantly calls the "neural Platonism" of those who see the brain as a hardwired set of computational switches with preset neurons reading "straight," "curved," "diagonal," etc. Her view in favor of connectionism (where behavior emerges from the activity of interconnected networks) over modularity (where dedicated modules perform specific neural functions) is obviously inflected by art history's remanent humanism, but she nonetheless dislikes what she suggests is a fuzzy culturalist bias, quoting anthropologist David Lewis-Williams's conclusion that "not every facet of every culture is unique and nongeneralizable" (*2*). That is, her book holds that the capacity for thinking through symbols, patterns, and iconic forms lies deep in the structure of the brain, and art reveals much about these cognitive operations. The statements of evolutionary connectionists would seem to come closest to Stafford's views—e.g., Raffaele Calabretta and Domenico Parisi comment: "For connectionism mind is not

---

The reviewer is in the Architecture Department, Massachusetts Institute of Technology, Cambridge, MA 02139, USA. E-mail: cajones@mit.edu

symbol manipulation and is not a computational system but is the global result of the many interactions taking place in a network of neurons" (*3*). The fact that such claims emerge from models, produced from "an artificial neural network [that] consists entirely of quantitative processes in which physico-chemical causes produce physico-chemical effects" (*3*) suggests that it is such abstracting procedures that best resonate with Stafford's art historical and analytical bent.

In other words, much of cognitive science must conduct itself through maps, models, and metaphors—and so does art. This simple symmetry gives Stafford permission to pursue her integrative cause, despite the daunting complexity of the science involved. She fearlessly recommends that scientists take heed of Enlightenment worthies in their freewheeling theories of the mind's function: "The complexity of the eighteenth-century inquiry forms a useful historical antidote to the downward slide of reductionism that haunts those branches of contemporary neuroscience investigating cortical geometries and brain modularity." Similarly,

> If the neurosciences are rightly reminding the humanities of the deep biological embeddedness of imitation and the existence of a common echoic code, then the humanities have something to say about observing as well as grasping a shared situation. … The humanities can deepen scientific inquiry by demonstrating that it sometimes requires a lifetime to come not just face-to-face, but in touch with certain gestures. This is not because the actions are deceitful but because they are either so veiled or, conversely, so blindingly clear, that they cannot be immediately assimilated.

Art exemplifies an interconnected hive-mind of durational, learned comprehension over a hard-wired monad of instant perception. Its slowness and its demands that we go beyond the "good gestalt" fantasies of the early 20th century give depth and complexity to any facile claims that "mirror neurons" and "mimesis" are somehow the same thing. This insistence on informed, "effortful vision" is the book's greatest gift, although at times this message gets confused by the sheer excitement with which Stafford attempts to manipulate cognitive theory. Some of the author's conjunctions are forced: As if the neuroscientific metaphor of the blazon could be seen to take actual form in the heraldic emblem. Or as if the finger-drumming schoolgirls in artist Victor Alimpiev's marvelous video could really be imagined to be "instinctual … within a collective," producing a "spontaneous outburst of sound-copying" rather than artfully fulfilling the directions of the man behind the camera. In addition, some of the science here doesn't seem quite right. "[S]ummary forms" such as the triangle are not likely to "bypass focal attention to strike the amygdala directly," unless the author means an amygdaloid "unconscious" response to a stimulus scanned through peripheral vision. "Striking" suggests the very foveal focus she means to avoid. Moreover, amygdaloid emotions likely modulate attentiveness only after stimulation from the optic system, although that might "appear" to bypass attention itself.

But these quibbles should not detract from a heroic book that inlays biology and culture within each other like the blazons, intarsia, and emblems that Stafford writes about so well. *Echo Objects* challenges scientists to leap to more engaging conclusions, by offering them access to the tools of visual analysis, close reading, and reception theories that art history has honed for over a century. It challenges those who work with culture even more, by speculating dramatically that the long history of "affective knowledge" in art (and the empathetic human response to representations of all kinds) may indeed have something to do with those mirror neurons—although exactly what and how needs far more research (*4*).

The larger message of Stafford's intense, propulsive prose is unassailable. If we are to get much further in the great puzzle of "binding" (*5*)—how the perception of an image, the will to act on intention, or the forging of consciousness is assembled from the tens of thousands of neurons firing at any one moment in time—then there needs to be action on all fronts. We need to work together, spinning interdisciplinary guide wires across the "corpus callosum" that still divides the two cultures of science and art.

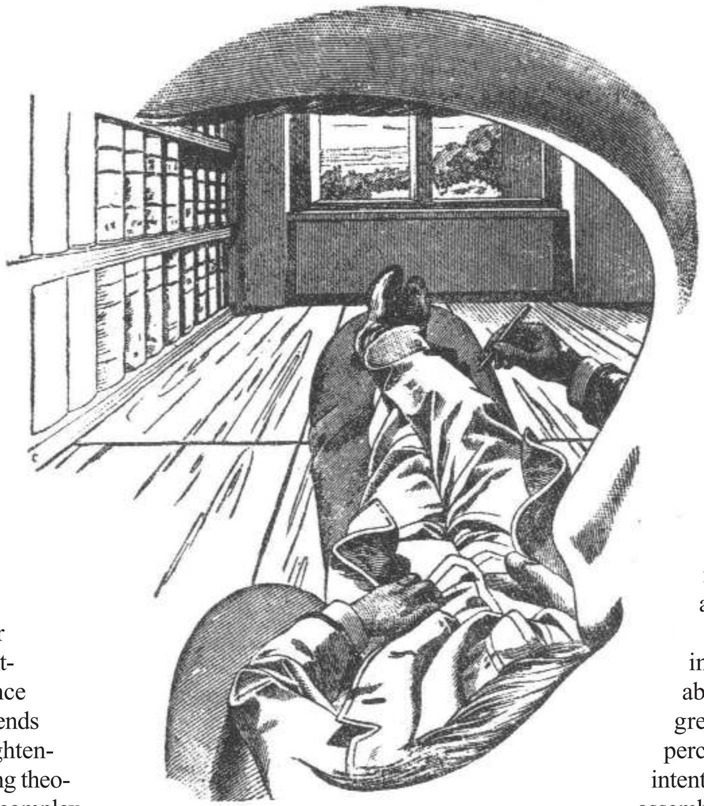

Field of vision. When in 1886 Ernst Mach published this drawing as figure 1 in his *Beiträge zur Analyse der Empfindungen* (*7*), he wrote of "mental symbols" and "sensations." The uniquely embodied nature of perception is difficult to capture in our notational and representational schemes, as the drawing attests, but Stafford claims neuroscience has revealed the deep neural order in much visual art.

CREDIT: ERNST MACH (7)

References and Notes

1. C. A. Jones, P. L. Galison, in *Picturing Science, Producing Art*, C. A. Jones, P. L. Galison, Eds. (Routledge, New York, 1998), pp. 1–21.
2. D. Lewis-Williams, D. Pearce, *Inside the Neolithic Mind: Consciousness, Cosmos and the Realm of the Gods* (Thames and Hudson, London, 2005).
3. R. Calabretta, D. Parisi, in *Modularity: Understanding the Development and Evolution of Complex Natural Systems*, W. Callebaut, D. Rasskin-Gutman, Eds. (MIT Press, Cambridge, MA, 2005), pp. 309–330; http://gral.ip.rm.cnr.it/rcalabretta/tedarwin/Altenberg.pdf.
4. Why do we cry or laugh at merely reading a representation (rather than seeing one)? Can a phone conversation about a stiff neck induce a mimic condition in the listener? The cognitive pathways induced by mimesis are far more complex than any account based on perceptual mirror neurons alone.
5. "The mammalian visual system contains a variety of cortical regions specialized to respond to different features such as shape, color, and object motion, and no single region has superordinate control. This poses the so-called 'binding problem': How do these functionally segregated regions coordinate their activities in order to associate features belonging to individual objects and distinguish among different objects?" (*6*).
6. A. K. Seth, J. L. McKinstry, G. M. Edelman, J. L. Krichmar, "Visual binding, reentry, and neuronal synchrony in a physically situated brain-based device"; available at http://cogprints.org/3353/.
7. E. Mach, *Contributions to the Analysis of the Sensations*, C. M. Williams, Transl. (Open Court, Chicago, 1897).

10.1126/science.1152256

SCIENCE AND GOVERNMENT

Revolutionizing China's Environmental Protection

China's growth has created severe environmental problems that will require fundamental changes in China's administrative system and its model of economic development.

Jianguo Liu[1]* and Jared Diamond[2]

China's economic growth in the past three decades has been the fastest among major nations, with an almost 10% annual increase in gross domestic product (GDP) (see figure, right). However, its environmental degradation has also accelerated, and its environmental sustainability index is near the bottom among the countries of the world (*1*).

Environmental crises in China have ranged from algal blooms, chemical spills, and droughts to flash floods and sandstorms. Two-thirds of China's 656 cities (with 390 million people) suffer shortages of water for domestic and industrial use, and pollution aggravates that water scarcity. China has 16 of the world's 20 cities with the worst air pollution. These environmental problems cause health suffering, economic losses, and social conflicts (*2, 3*). For instance, China's State Environmental Protection Administration (SEPA) reported that pollution in 2005 alone cost more than U.S.$200 billion (~10% of GDP). Although global effects of other countries' pollution increase these problems in China, China's environmental woes in turn affect the rest of the world (*2*). For instance, China's CO_2 emissions from fuel combustion have been increasing rapidly (see chart, right) and CO_2 from fuel comnbustion and cement production are now the world's highest (*4*), although China's per capita contribution is still far below that of many developed countries—because China has the world's largest population.

It is commendable that China has established impressive environmental goals and has tried to protect the environment. But the forces of environmental destruction have overwhelmed protection efforts and have made many of the goals empty slogans. For example, China has invested billions of dollars in combatting water pollution in its third-largest freshwater lake, Taihu Lake. Yet it simultaneously permitted hundreds of factories to undo that investment by pouring pollutants into the lake, resulting in algal blooms and lack of water for millions of people.

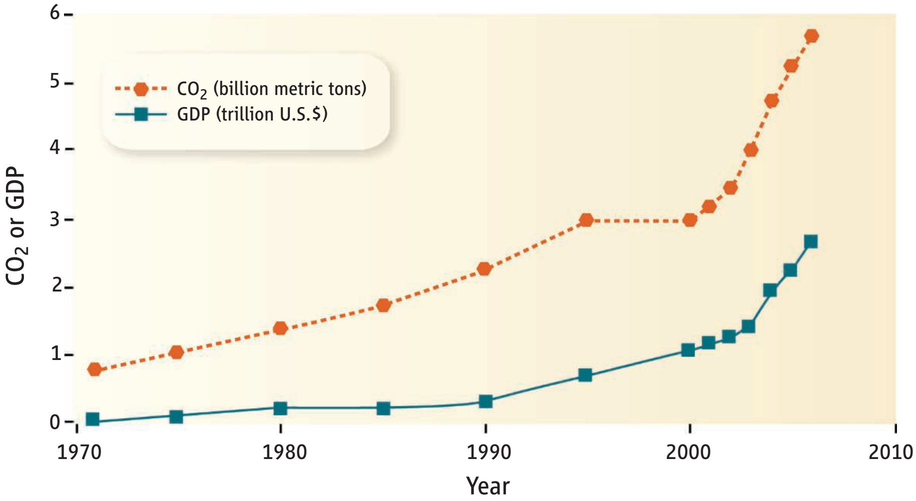

China's growth in gross domestic product (GDP) and CO_2 emissions from fuel combustion (*4*–*6*, *13*).

China has once again proclaimed a goal of turning the tide of environmental degradation (*7*) with its 11th Five-Year Plan (2006–10), but it also aims to continue fast growth in its GDP (*8*). Heavily polluting factories still rise rapidly. Although specific solutions to many specific environmental problems have been proposed, a key unanswered question is how to achieve fundamental improvement. We suggest a reform of China's administrative system and a change in its model of economic development.

Reforming the Administrative System

Economic performance is still China's main or sole criterion for selecting and promoting government leaders (e.g., provincial governors and mayors), although 2 years ago the central government called for incorporating environmental performance into the process. Ironically, when environmental disasters occur, environmental protection agencies often bear the blame. For example, after the chemical spill in the Songhua River in 2005, the director of SEPA was sacked. If China's government does not weight environmental performance equal to economic performance in selecting officials, environmental degradation will continue.

Although more than 100 environmental laws and regulations exist in China, they are often ignored by local government leaders. The maximum fines allowed for environmental violations are so small that polluting enterprises prefer paying the fines to adopting environmentally friendly technologies. Because environmental protection agencies lack the money, staff, and power to override local leaders and to shut down polluters, many environmental regulations are not enforced. China has the world's largest foreign reserve (U.S.$1.4 trillion), but its budget for environmental protection is only a small fraction of that in the U.S.A. China currently has three times the United States' population, but SEPA has only one-eighth of the employees of the U.S. Environmental Protection Agency.

Establishing a new, high-level, authoritative national organization that coordinates all relevant ministries and agencies for economic development and environmental protection could reduce conflicts among them. Consolidating ministries and agencies for protecting different components of the environment (e.g., air, forest, land, and water) could also strengthen the effectiveness of China's environmental protection.

Changing the Development Model

Rapid growth in GDP has been China's main goal during the past three decades. The domi-

---

[1] Center for Systems Integration and Sustainability, Department of Fisheries and Wildlife, Michigan State University, East Lansing, MI 48823, USA; and Guest Professor, State Key Lab of Urban and Regional Ecology, Chinese Academy of Sciences, Beijing, China, and Fudan University, Shanghai, China. [2] Geography Department, University of California at Los Angeles, Los Angeles, CA 90095, USA.

*Author for correspondence, E-mail: jliu@panda.msu.edu

nant development model has been inefficient resource use and high pollution to achieve high GDP. As do many other countries, China overstates its GDP, because it fails to subtract economic and other costs of environmental degradation. In fact, the environment is often put on the wrong side of the balance sheet when calculating GDP; polluting the environment and cleaning up the mess are both considered to be contributing to GDP, rather than subtracting from it.

To more accurately measure the country's growth, China decided to develop Green GDP in March 2004. For Green GDP, the economic costs of environmental impact and ecological destruction are subtracted from traditional GDP. With collaboration between SEPA and the National Bureau of Statistics (NBS), China released its first report on Green GDP (2004) in November 2005 (*9*). Even though the report vastly underestimated air and water pollution costs, those estimated costs (U.S.$64 billion, or ~3% of GDP in 2004) still shocked many government officials.

Unfortunately, SEPA's and NBS's marriage to produce joint reports on Green GDP has ended. Although the second annual report has been completed and SEPA hoped to release it to the public, NBS has refused to do so. NBS's stated reason is the inaccuracy of estimation methods, but it is widely believed that pressures from some government officials' concern over high economic costs played an important role.

By developing a Green GDP, China was far in advance of most other countries, including the U.S.A. It is regrettable that, when China was so close to taking a leadership role, China's NBS backed down. Although estimating Green GDP poses technical challenges, refusing to release those estimates will not help improve the evaluation methods. Stronger support for greening GDP from the State Council and the Politburo of the Communist Party (China's highest executive and decision-making bodies) may prompt NBS to release the second annual report and to continue the effort to evaluate economic losses from environmental damage.

Besides greening GDP, other measures are needed to shift China's economic development model toward high efficiency and low pollution. Those measures range from investment in environmentally friendly enterprises, reform of land ownership, loans with low interest rates to those enterprises, taxes on polluting enterprises, and eco-compensation (payments to those protecting environmentally sensitive areas) to green insurance (insurance companies cover the cost of environmental damage and push for better environmental protection) (*10*). Developing more environmentally friendly technologies for domestic use and export would increase employment and economic efficiency while reducing environmental damage.

Changing the development model requires changes in attitudes toward the environment. Many people still hope that the path followed by developed countries (pollute first, control later) will work for China, but that hope is risky because China suffers from two new disadvantages: Natural resources are more limited today (*11*), and fewer countries accept pollution transfers. Even if pollution can be controlled later, we foresee that many plant and animal species that provide essential ecosystem services to humans (e.g., the wild rice variety that helped revolutionize rice production) will become extinct. Furthermore, environmental impacts on human health and socioeconomic well-being will be much greater, as China's population is now much larger than the populations of developed countries when they suffered severe air and water pollution.

Environmental protection should be treated as an integral part of sustainable economic development. Because humans and the environment are coupled systems (*12*), there are complex interactions and feedback between humans and the environment, and negative impacts may not show up until decades later. For example, the 1998 flash floods that affected 240 million people are now recognized to have been the result of long-term deforestation and soil erosion (*2*).

Concluding Remarks and Outlook

Although it will not be easy to make these fundamental changes, there is hope that they can happen. Environmental catastrophes have awakened some government officials and the public. For instance, the 1998 floods (*2*) stimulated large-scale conservation programs (e.g., natural forest conservation and grain-to-green programs) (*12*), the 2005 chemical spill in northeast China prompted examination of locations of major chemical plants, and the 2007 algal blooms led to closure of many polluting factories along lakes. Environmental issues will also be topics of many high-level meetings such as the upcoming 2008 National People's Congress.

Environmental awareness has been increasing among China's populace. The public demands the right to speak out about environmental issues and to be engaged in environmental actions. Text messages via mobile phones and the Internet have proved to be effective new tools for China's environmentalists. Within a few days in May 2007, a million text messages were sent to residents and officials to protest a planned U.S.$1.4 billion chemical plant near the center of Xiamen City. This first-time use of massive text messaging for environmental protection forced the city government to halt the plant construction.

China's environmental revolution can also benefit from developed countries. Although those countries have exacerbated many of China's environmental problems, they have also been increasingly providing environmentally friendly technologies, investing in clean energy industries, and helping China raise pollutant emission standards. Much more can and should be done. With 590,000 foreign firms invested in China, these firms and their countries have the leverage and responsibility to help China in its efforts to become a green nation.

References and Notes

1. Yale Center for Environmental Law and Policy, Center for International Earth Science Information Network, World Economic Forum, *Environmental Performance Measurement Project* (ESI at Yale Univ., New Haven, CT, 2006); www.yale.edu/esi/.
2. J. Liu, J. Diamond, *Nature* **435**, 1179 (2005).
3. World Bank, State Environmental Protection Administration of China, *Cost of Pollution in China* (Washington, DC, 2007).
4. Netherlands Environmental Assessment Agency (MNP), "Global CO_2 emissions" (MNP, Bilthoven, 2007); www.mnp.nl/en/dossiers/Climatechange/moreinfo/Chinanowno1inCO2emissionsUSAinsecondposition.html.
5. National Bureau of Statistics of China, *China Statistical Yearbook 2004* [in Chinese] (China Statistical Press, Beijing, 2004).
6. International Energy Agency, *CO_2 Emissions from Fuel Combustion* (Organization for Economic Cooperation and Development, Paris, 2006).
7. SEPA, *China's 11th Five-Year Plan for Environmental Protection* [in Chinese] (SEPA, Beijing, 2006); www.sepa.gov.cn/plan/hjgh/sywgh/.
8. National Development and Reform Commission of China (NDRC), *The Outline of the 11th Five-Year Plan for National Economic and Social Development* [in Chinese] (NDRC, Beijing, 2006); http://ghs.ndrc.gov.cn/15ghgy/t20060526_70573.htm.
9. Chinese Academy for Environmental Planning, State Environmental Protection Administration, *China Green National Accounting Study Report 2004* (2006); http://english.sepa.gov.cn/zwxx/xwfb/200609/t20060908_92580.htm.
10. Q. Chen, J. Liu, Q. Xu, "Yue Pan: Environmental economic policies are a foundation of the scientific outlook on development" [in Chinese], 10 September 2007; www.caep.org.cn/ReadNews.asp?NewsID=1129.
11. Millennium Ecosystem Assessment (MA), *Ecosystems and Human Well-Being: Synthesis Report* (Island Press, Washington, DC, 2005).
12. J. Liu *et al.*, *Science* **317**, 1513 (2007).
13. Additional references are available as supporting material on *Science* Online.
14. We thank Z. Ouyang and two anonymous reviewers for their constructive comments on an earlier draft. Funding was provided by the NSF (0216450 and 0709717), Michigan State University, and National Natural Science Foundation of China (30428028).

Supporting Online Material
www.sciencemag.org/cgi/content/full/319/5859/37/DC1

10.1126/science.1150416

NEUROSCIENCE

Rules of Plasticity

Ongoing sensory experience may improve performance through a signaling mechanism that strengthens synapses beyond their initial potential.

Michael Brecht and Dietmar Schmitz

A fundamental feature of the mammalian central nervous system is the ability of connections (synapses) between neurons to undergo long-lasting changes in strength—so-called synaptic plasticity. Theses changes depend on neuronal activity, and in this context, processes such as long-term potentiation and long-term depression—enhanced and weakened neuronal communication, respectively—have been extensively investigated (*1*). The most studied form of synaptic plasticity is that found in the hippocampus, a brain region important for learning and memory. Although mechanistic analysis of synaptic plasticity has been productive, establishing its link to memory-guided behavior has proven difficult (*2*). On page 101 in this issue, Clem *et al.* identify strengthening of synapses in the mouse brain that may underlie sensory-dependent learning (*3*) and show that episodes of synaptic plasticity, or metaplasticity (*4*), may be related to experience-related learning.

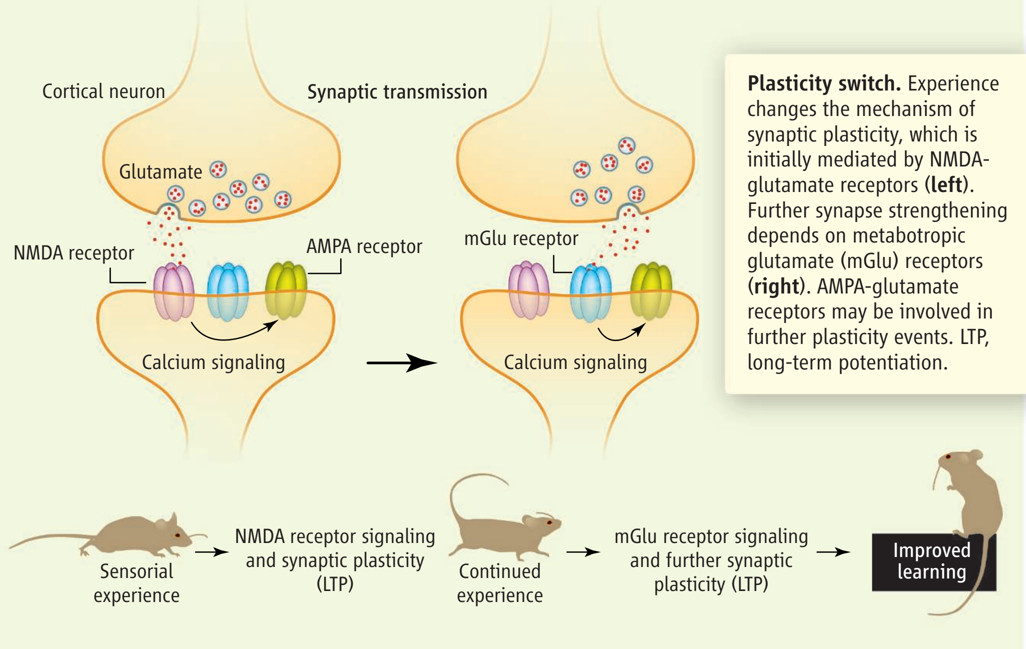

Plasticity switch. Experience changes the mechanism of synaptic plasticity, which is initially mediated by NMDA-glutamate receptors (**left**). Further synapse strengthening depends on metabotropic glutamate (mGlu) receptors (**right**). AMPA-glutamate receptors may be involved in further plasticity events. LTP, long-term potentiation.

The difficulty in linking synaptic plasticity to behavior arises from trying to identify synaptic sites in the distributed neural networks of the mammalian brain that are strengthened or weakened by specific experience. In addition, many classic paradigms that induce synaptic plasticity depend on stimulation patterns that are not physiologically plausible. Even if valid conditions are used, it is still hard to show that results gleaned from brain slice preparations underlie experience-dependent changes in behavior.

A promising model system for exploring whether synaptic modifications represent experience in the mammalian brain is the rodent barrel cortex (*5*, *6*), where sensory inputs from each whisker are transmitted to a specific neuronal cell cluster, shaped like a barrel, in the brain's cortex. Whisker displacement conveys tactile information, and a neuron within a given "barrel" will send signals to its connected neurons when the whisker that the barrel represents is deflected. Fast, experience-dependent changes in synaptic strength can be induced in the barrel cortex by simply removing all but one whisker from the animal's face. Following this manipulation, Clem *et al.* use elegant genetic techniques to visualize which cortical barrel neurons corresponds to the spared whisker.

Clem *et al.* observed that trimming all but one whisker initiates long-term potentiation of synapses between the corresponding barrel neurons, a process that requires activation of receptors for the neurotransmitter glutamate [*N*-methyl-D-aspartate (NMDA)] present at the synapse (see the figure). It has often been found that long-term potentiation can reach "saturation," wherein a synapse cannot undergo additional strengthening. This has raised the question of how further learning can occur, and the authors make some interesting observations on this issue. After a single-whisker experience, NMDA receptors opposed further potentiation in the synapses of corresponding neurons. However, pharmacologically blocking NMDA receptors restored potentiation through the activation of metabotropic glutamate receptors in the synapse. This demonstrates that ongoing experience (in this case, continued stimulation of a whisker) can extend synaptic potentiation, and thus, plasticity.

Finally, Clem *et al.* link extended synaptic potentiation with enhanced learning. Blocking NMDA receptors improved the acquisition of a whisker-dependent conditioning task in animals that had previously undergone a single-whisker experience. Thus, association learning follows the rules that govern the induction of long-term potentiation and synaptic strengthening in vitro.

What is the relation between the mechanisms of synaptic plasticity dictated by the NMDA receptor and metabotropic glutamate receptor? Do they share a common signaling pathway? Glutamate receptor activation increases the intracellular calcium concentration in the postsynaptic neuron, which affects further downstream signaling events and signal propagation between neurons. The finding by Clem *et al.* that induced long-term potentiation provokes the insertion of new glutamate receptors (AMPA receptors) into the synaptic membrane introduces another source for calcium entry and may thereby alter the threshold for any subsequent plasticity event. This might become evident only with different proto-

---

The authors are at the Bernstein Center for Computational Neuroscience, Humboldt-University Berlin, 10115 Berlin, Germany. D. Schmitz is also at Neuroscience Research Center of the Charité, Universitätsmedizin Berlin, 10117 Berlin, Germany. E-mail: michael.brecht@bccn-berlin.de

CREDIT: ADAPTED BY P. HUEY/SCIENCE

cols that induce long-term potentiation.

The distinct phases of experience-dependent synaptic strengthening reported by Clem *et al.* may correspond to behaviorally distinct stages of memory formation. In humans, temporally close training sessions on conflicting motor tasks lead to interference that is not observed when training occurs days apart (*7*). It is unclear if such findings are related to those of Clem *et al.*, but analyzing the relation between synaptic plasticity and experience should provide insights about the ability of synapses to change as circumstances require as well as higher-order forms of plasticity.

References

1. R. C. Malenka, M. F. Bear, *Neuron* **44**, 5 (2004).
2. S. J. Martin, P. D. Grimwood, R. G. Morris, *Annu. Rev. Neurosci*. **23**, 649 (2000).
3. R. L. Clem, T. Celikel, A. L. Barth, *Science* **319**, 101 (2008).
4. W. C. Abraham, W. P. Tate, *Prog. Neurobiol*. **52**, 303 (1997).
5. K. Fox, *Neuroscience* **111**, 799 (2002).
6. D. E. Feldman, M. Brecht, *Science* **310**, 810 (2005).
7. R. Shadmehr, T. Brashers-Krug, *J. Neurosci*. **17**, 409 (1997).

10.1126/science.1153231

CHEMISTRY

Beyond Born-Oppenheimer

A combined experimental and theoretical study sheds light on the intricate effects that can occur during chemical reactions.

Joel M. Bowman

According to the Born-Oppenheimer approximation, electrons move so much faster than atomic nuclei in atoms and molecules that their motions can be treated separately in quantum mechanical simulations. This approximation is used widely in theoretical and computational chemistry and in biomolecular modeling, where it underpins the concept and calculation of potential energy surfaces of molecules and chemical reactions. However, the approximation of separating electronic and nuclear motion can break down and lead to coupling of potential energy surfaces. This is especially relevant in chemical reactions, where even small non–Born-Oppenheimer (also called "nonadiabatic") couplings can have important consequences (*1*). On page 72 of this issue, Garand *et al.* (*2*) study these effects with photodetachment spectroscopy, a powerful experimental technique that can probe regions of a potential energy surface largely inaccessible by other spectroscopic methods (*3*).

Various physical effects can contribute to a breakdown of the Born-Oppenheimer approximation; among these, spin-orbit coupling is perhaps the most pervasive. This coupling describes the interaction between the electron's spin and its orbital motion around the nuclei of a molecule. This interaction can be described qualitatively by classical electrodynamics, but for a correct description, relativistic effects must be taken into account, because the velocity of the electron approaches the speed of light (*4*).

It is this type of non–Born-Oppenheimer coupling that is the focus of the paper by Garand *et al*. The authors report a beautiful joint experimental-theoretical study of nonadiabatic effects in the light-induced detachment of an electron from ClH_2^- and ClD_2^-.

In the experiment, an electron from ClH_2^- (or ClD_2^-) is detached by a fixed-frequency laser (see the figure). The resulting kinetic energy distribution of the detached electron is measured at high resolution. The peaks in this distribution correspond to the discrete quantized energies of vibrational states of ClH_2 and Cl^*H_2 (or ClD_2 and Cl^*D_2). Using very high-level quantum calculations, the authors show that these vibrational states are due to a shallow well in the potential energy surface describing the $Cl + H_2$ reaction (termed a "prereactive" van der Waals well) and also to a shallow van der Waals well in the potential energy surface of the nonreactive $Cl^* + H_2$ potential energy surface. Only some of these states are truly bound, whereas others are "quasi-bound," that is, they have a finite lifetime before decaying to form H_2 and either Cl or—with smaller probability—spin-orbit excited Cl*.

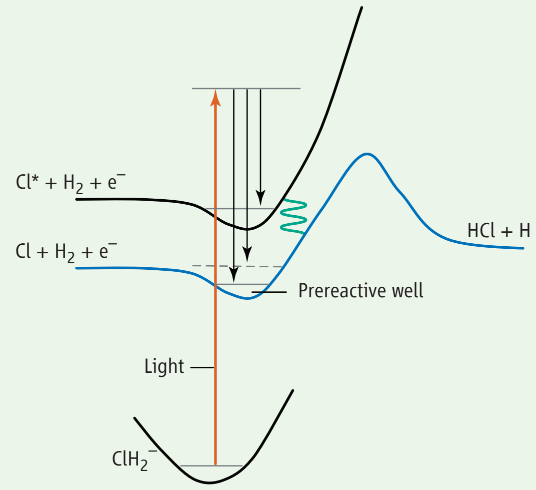

Interpretation of the experiment of Garand *et al.* Light of fixed energy ejects an electron from the stable negative ion ClH_2^-. The peaks in the electron kinetic energy distribution correspond to the energies of bound and quasi-bound states of the prereactive van der Waals wells of the $Cl + H_2$ and $Cl^* + H_2$ potentials. The middle potential (blue curve) describes the chemical reaction $Cl + H_2 \rightarrow HCl + H$. These neutral potentials are coupled by a nonadiabatic spin-orbit interaction (green wavy line). When Garand *et al.* included this interaction in their calculations, they achieved better agreement with the experiment than when the interaction was omitted.

The peak positions calculated from theory based on the Born-Oppenheimer approximation are in good agreement with experiment (within ~10 cm^{-1}). However, the level of agreement improves by about an order of magnitude when nonadiabatic effects that couple the potential surfaces are included in the calculations. This high level of agreement is also a testament to the accuracy of the potential energy surfaces and couplings used in the calculations (*5*).

The report by Garand *et al.* takes on added importance in view of a controversy that exists between theory (*6*) and experiment (*7*) on the importance of nonadiabatic effects in the reaction $Cl/Cl^* + H_2 \rightarrow HCl + H$ (*8*). As the figure shows, the interaction between Cl* and H_2 is highly repulsive and—in the absence of a nonadiabatic "hop" to the reactive lower potential—cannot lead to the products HCl + H. However, if such a "hop" were to occur, the energy difference between Cl and Cl* (10.5 kJ/mol, roughly half the reaction barrier of the lower potential) would be converted into kinetic energy on the reactive $Cl + H_2$ potential, thus increasing the probability for reaction.

Theoretical simulations of this process predict that the reactivity of Cl* will be small but significant at

---

The author is in the Department of Chemistry, Emory University, Atlanta, GA 30322, USA. E-mail: jmbowma@emory.edu

low collision energies and negligible at higher energies. Experiment finds the opposite. This disagreement stands in contrast to results reported recently for the sibling reaction F/F* + $D_2 \rightarrow$ DF + D, where theory and experiment both find a small but significant effect at low collision energies and a negligible effect at higher energies (*9*).

The probability for a nonadiabatic, spin-orbit "hop" depends on both the energy difference between the two spin-orbit potentials (illustrated in the figure for Cl/Cl* + H_2) and the magnitude of the spin-orbit coupling energy. If the two become comparable or if the latter exceeds the former, the "hop" probability increases. The report by Garand *et al.* provides new information on the likelihood of this nonadiabatic "hop" and validates the reliability of theoretical simulations.

Significant non–Born-Oppenheimer spin-orbit effects have also been reported for the reaction of S/S* with H_2 (*10, 11*). As the collaborative work by Garand *et al.* shows, such non–Born-Oppenheimer effects continue to be assessed most effectively by joint theoretical-experimental research. The excellent agreement between theory and their experiment suggests that the reaction of Cl* with H_2 is currently reproduced better by theory than experiment. New molecular beam experiments should resolve the disagreement.

References

1. A. W. Jasper, S. Nangia, C. Zhu, D. G. Truhlar, *Acc. Chem. Res*. **39**, 99 (2006).
2. E. Garand, J. Zhou, D. E. Manolopoulos, M. H. Alexander, D. M. Neumark, *Science* **319**, 72 (2008).
3. D. M. Neumark, *Phys. Chem. Chem. Phys.* **7**, 433 (2005).
4. L. D. Landau, E. M. Lifshitz, *Quantum Mechanics*, (Pergamon, Oxford, ed. 3, 1976), pp. 265–269.
5. G. Capecchi, H. J. Werner, *Phys. Chem. Chem. Phys.* **6**, 4975 (2004).
6. M. H. Alexander, G. Capecchi, H. J. Werner, *Science* **296**, 715 (2002).
7. F. Dong, S. H. Lee, K. Liu, *J. Chem. Phys.* **115**, 1197 (2001).
8. D. E. Manolopoulos, *Science* **296**, 664 (2002).
9. L. Che *et al.*, *Science* **317**, 1061 (2007).
10. B. Maiti, G. C. Schatz, G. Lendvay, *J. Phys. Chem. A* **108**, 8772 (2004).
11. T. -S Chu, K-L. Han, G. C. Schatz, *J. Phys. Chem. A* **111**, 8286 (2007).

10.1126/science.1152504

CHEMISTRY

A Phase Transition Hidden in Higher Dimensions

A molecular solid can change from one structure to another in a way that can only be described properly using four-dimensional space.

Philip Coppens

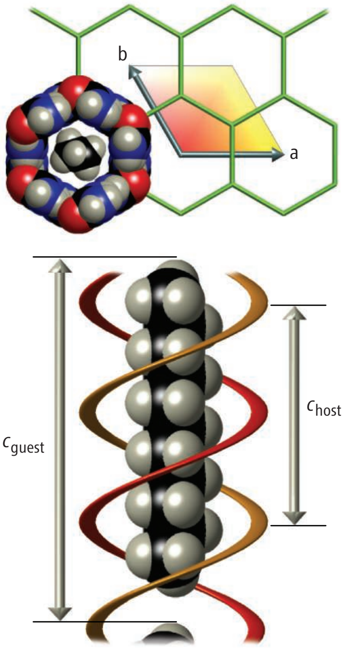

Superspace structure. (**Top**) The structure of urea-nonadecane viewed along the column direction (*c* axis). The hexagons represent the host (urea structure). (**Bottom**) View perpendicular to the columns. The hydrogen-bonded urea molecules are represented by the helices. The orientation of the guest molecules is that of the low-temperature structure; a small distortion of the hexagons that occurs on cooling through the transition at 149 K is not shown. Red, oxygen atoms; black, carbon; gray, hydrogen. Toudic *et al*. discovered a phase transition that essentially affects the interaction between the two structures coexisting in the solid rather than the individual structures. [Adapted from (*6*)]

Our knowledge of the molecular solid state has greatly increased in recent years, driven by improvements in x-ray structure determination. Solids containing several different molecular components are especially interesting to chemists and materials scientists. Such supramolecular crystalline solids exhibit an almost infinite variety, which can be exploited by synthesis of novel materials with desirable properties (*1*–*3*). In addition, these solids can also form inert molecular frameworks with cavities in which chemical reactions can be studied (*4*).

When two different types of molecules, A and B, co-crystallize and the A-A and B-B interactions are strong, two parallel structures may occur in a single crystal, each with its own periodicity (i.e., distance over which the structure repeats) (*5*). However, because the two structures are intertwined, they are not fully independent, each being modulated by the interactions between the A and B molecules (that is, the periodicity of one is imposed on the other). On page 69, Toudic *et al*. report an unprecedented new type of phase transition in which the periodicity of the interaction changes but each of the component structures retains it original repeat (*6*).

In the *n*-alkane-urea solid studied by Toudic *et al*., the linear alkane molecules are embedded in a columnar matrix of hydrogen-bonded urea molecules that form a honeycomb-like network with a channel diameter of about 5.5 Å (see the figure, top panel) (*7*). Because the length depends on the number of carbon atoms in the alkane, the repeat along the channel direction (the *c* direction in this case) in general differs from that of the urea matrix and is described by a "misfit" parameter, which is the ratio of the two repeats, c_{host} and c_{guest} (see the figure, bottom panel). When the misfit parameter does not correspond to the ratio of two simple integers, the structure is said to be incommensurate. In this case, the crystal as a whole is no longer periodic.

The periodicity can be recovered, however, by a mathematical construction using a virtual superspace of 3 + *i* dimensions, where *i* ($\leq$3) is the number of directions in which the two components have different periodicities (*5*, *8*). Thus, for a column structure as exists in the *n*-nonadecane/urea crystals studied by Toudic *et al.* with a periodicity different in the columnar direction for the urea (host) and nonadecane (guest) columns, the proper superspace has four dimensions. As a result, accounting for all the features in the diffraction pattern of such a composite intergrowth structure requires four indices, with the usual Miller indices *h*, *k*, *l* replaced by the set *h*, *k*, *l*, *m*. Miller indices are the conventional way to denote the planes and directions in a crystal lattice, and thus the reflections caused by these planes; when new peaks appear that cannot be explained by the usual set, additional indices are needed.

The author is in the Department of Chemistry, State University of New York at Buffalo, Buffalo, NY, 14260–3000, USA. E-mail: coppens@buffalo.edu

When the *c* axis is the column axis, as is the case for nonadecane/urea, the average structure of the urea (the A component), without the imposed modulation, is described by the *hkl*0 reflections, and the average structure of the alkane (the B component) by the *hk*0*m* reflections, whereas the remaining *hklm* reflections are due exclusively to the mutual interaction between the two lattices. This implies that lattice A imposes a distortion on lattice B with the A periodicity, and vice versa.

At temperatures above 149 K, all nonadecane columns in the crystal distort in an identical way. However, below this temperature, the extra *hklm* reflections that appear in the diffraction pattern show that the relative modulation of the host and guest lattices alternates from channel to channel in the *a*-axis direction (see the figure, top panel), even though the periodicity of the average structures of the host and the guest in this direction does not change, as indicated by the absence of additional *hkl*0 and *hk*0*m* reflections. This does not rule out small structural changes in the mean structures, but if they occur they must have the same periodicity perpendicular to the column direction as at temperatures above the transition; otherwise, extra reflections would occur. This is most unusual, and below a second transition at 129 K those extra reflections indeed appear, indicating that the changed repeat of the distortion now also occurs in the mean structures. Such a transition, which only affects the mutual interaction, can only be described properly in superspace, even though the physical reality is obviously three-dimensional.

The *n*-alkanes are not the only species that can be encapsulated in the urea framework (*9*–*12*), and many other multicomponent composite structures are known, including minerals, extended inorganic structures, and other organic and organometallic solids (*5*, *8*, *13*, *14*). Can the hidden phase transition be reproduced in other incommensurate materials? How do the electronic, spectroscopic, magnetic, ferroelastic, and transport properties of this type of material change when such a “hidden” intermediate phase is formed? Obviously, a great deal of work is needed to answer such questions, but the recent tremendous advances in our understanding of the organic solid state and its applications warrant further work that may reveal important new properties.

References

1. J. L. Atwood, L. J. Barbour, A. Jerga, *Science* **296**, 2367 (2002).
2. J. L. Atwood, L. J. Barbour, A. Jerga, B. L. Schottel, *Science* **298**, 1000 (2002).
3. N. L. Rosi *et al.*, *Science* **300**, 1127 (2003).
4. S.-L. Zheng, M. Messerschmidt, P. Coppens, *Chem. Comm.* 2735 (2007).
5. A. Janner, T. Janssen, *Acta Cryst.* **A36**, 408 (1980).
6. B. Toudic *et al.*, *Science* **319**, 69 (2008).
7. R. Forst, H. Jagodzinski, H. Boysen, F. Frey, *Acta Cryst.* **B43**, 187 (1987).
8. P. Coppens, *Acta Cryst*. **B51**, 402 (1995).
9. M. D. Hollingsworth *et al.*, *Angew. Chem. Int. Ed.* **41**, 965 (2002).
10. M. D. Hollingsworth, M. E. Brown, A. C. Hillier, B. D. Santarsiero, J. D. Chaney, *Science* **273**, 1355 (1996).
11. M. D. Hollingsworth *et al.*, *J. Am. Chem. Soc*. **121**, 9732 (1999).
12. K. D. M. Harris, *Supramolecular Chem.* **19**, 47 (2007).
13. S. Van Smaalen, *Crystallogr. Rev*. **4**, 79 (1995).
14. E. Makovicky, B. G. Hyde, in *Struct. Bonding* **46**, 101 (1981).

10.1126/science.1153272

GENETICS

Functionally Degenerate—Y Not So?

The Y chromosome of the common fruit fly has few functional genes but regulates the expression of hundreds of autosomal and X-linked genes.

William R. Rice and Urban Friberg

Genetic and theoretical studies of Y chromosomes have led to the conclusion that they evolve to become functionally degenerate. For example, in the fruit fly *Drosophila melanogaster*, a century of genetic research on its Y chromosome indicates that it codes for few traits besides a small number of male fertility factors (*1*). On page 91 of this issue (*2*), Lemos *et al*. change this perception of functional paucity by showing that the Y chromosome of *D. melanogaster* regulates the activity of hundreds of genes harbored on other chromosomes.

The theoretical rationale for the evolution of a degenerate Y chromosome is based on its lack of recombination, the process by which corresponding DNA segments are exchanged between homologous chromosomes, thus producing new genetic combinations. When a primitive Y chromosome stops recombining, the efficiency of natural selection drops substantially because selection cannot act independently on different Y-linked mutations. This slows the accumulation of beneficial mutations and speeds that of mildly deleterious ones. As a consequence, the fitness of a Y-linked gene wanes relative to its X-linked homolog, and it can ultimately become silenced by persistent accumulation of deleterious mutations—a result made possible because of redundancy to its X-linked homolog. Gene silencing can also be selectively favored when a Y-linked null mutation (one that results in the absence of a gene product) increases fitness because it does not interfere with the expression of its fitter X-linked homolog.

Lemos *et al*. now challenge this evolutionary view of a continually decaying Y chromosome. The authors collected Y chromosomes from *D. melanogaster* spanning different latitudes and subspecies across Africa and North America so as to maximize functional polymorphism, and then substituted each one for

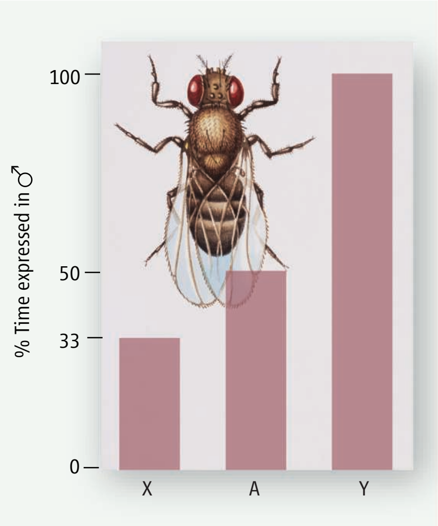

Gene expression in males. A mutation in *D. melanogaster* that influences gene expression in males experiences selection in the male fly most often when it is Y-linked (Y), least often when X-linked (X), and at an intermediate level when located on the autosomes (A).

IMAGE CREDIT: LIZZIE HARPER/PHOTO RESEARCHERS INC.

The authors are in the Department of Ecology, Evolution, and Marine Biology, University of California, Santa Barbara, CA 93106, USA. E-mail: rice@lifesci.ucsb.edu; friberg@lifesci.ucsb.edu

Published by AAAS

the Y chromosome in a single fly strain (ensuring an otherwise common genetic background). They then screened a nearly genome-wide set of genes and looked for differences in gene expression in response to the substituted Y chromosome. Because of high statistical error rates when thousands of genes are scored simultaneously, it is difficult to estimate the exact number of affected genes, but the estimates are surprisingly high, ranging from around 100 up to about 1000 (*D. melanogaster* is estimated to have ~13,000 genes).

Lemos *et al*. also detected several coherent patterns among the Y-regulated genes. The Y chromosome influences the expression of genes that are more strongly expressed in males. Genes regulated by the Y chromosome are also more strongly influenced by environmental stress (heat shock), and many are associated with sperm development. Genes that influence the mitochondria are also overrepresented in the pool of genes regulated by the Y chromosome. In addition, affected genes are more evolutionarily dynamic in terms of polymorphisms for gene expression within the species, and more diverged from a closely related congener (*Drosophila simulans*).

It is now well established that a large proportion of the genome is expressed at different levels in males and females in many organisms (*3*), and the patterns found by Lemos *et al*. fit well with what would be expected for Y-linked regulatory genes. Whereas the Y chromosome spends every generation in males, the X chromosome and autosomes alternate between the sexes across generations. A mutation favoring males that is located on the X chromosome or autosomes can therefore only accumulate when selection in females is concordant, absent, or not too strongly discordant (*4*). However, this restriction is removed for Y-linked mutations because there can be no counterselection in females. Even when a mutation results in a phenotype that is exclusive to males, it will have an advantage if Y-linked because, unlike the X chromosome and autosomes, the Y chromosome is expressed (and hence selected) in males every generation (see the figure). The Y chromosome therefore represents a favorable platform for mutations that improve male gene expression.

As many Y-linked genes have degenerated, should we expect the Y chromosome to inevitably be lost altogether? Not necessarily. As the number of functional genes on the Y chromosome declines, the efficacy of natural selection increases on the remaining genes. Decay of the Y chromosome therefore slows down over time and can ultimately stop altogether. The fitness advantage of a highly degenerated Y chromosome is illustrated by *Drosophila afinis* in which the Y chromosome is not required for fertility. In this species, males with no Y chromosome (XO) sire 25 to 38% fewer offspring when competing with XY males (*5*). The study by Lemos *et al*. provides a mechanism for the large fitness advantage of XY males, even when vital fertility factors are absent on the Y chromosome: The Y chromosome has evolved to become a major regulator of gene expression in males.

If the Y chromosome is such a strong regulator of genes in males, then why have past studies found so few Y-linked traits in humans and flies? The Y chromosome may have evolved to modulate rather than turn on or turn off gene expression. Its effects may therefore be continuous rather than discrete and thus more difficult to detect than the more distinct phenotypes associated with loss-of-function mutations. As the power of quantitative trait locus analysis increases, the phenotypic manifestations of the genes regulated by the Y chromosome discovered by Lemos *et al*. may become more apparent.

The next stage in understanding the newly discovered regulatory powers of the *Drosophila* Y chromosome will be to characterize the genetic mechanism(s) underlying their influence. It will also be interesting to see, in flies and other species, whether genomic components that are only transmitted through the matriline (mitochondria and cytoplasmic endosymbionts) have evolved to strongly influence gene expression in females. The study by Lemos *et al.* further suggests that it will be important to test whether the human Y chromosome also has evolved to become a regulatory giant.

References and Notes

1. D. L. Lindsley, G. G. Zimm, *The Genome of* Drosophila melanogaster (Academic Press, San Diego, CA, 1992).
2. B. Lemos, L. O. Araripe, D. L. Hartl, *Science* **319**, 91 (2008).
3. H. Ellegren, J. Parsch, *Nat. Rev. Genet.* **8**, 689 (2007).
4. W. R. Rice, *Evolution* **38**, 735 (1984).
5. R. A. Voelker, K. Kojima, *Evolution* **26**, 560 (1972).
6. Supported by a grant from the Wenner-Gren Foundation and by NSF grant DEB-0128780.

10.1126/science.1153482

ENVIRONMENTAL SCIENCE

How Green Are Biofuels?

Jörn P. W. Scharlemann and William F. Laurance

Many biofuels are associated with lower greenhouse-gas emissions but have greater aggregate environmental costs than gasoline.

Global warming and escalating petroleum costs are creating an urgent need to find ecologically friendly fuels. Biofuels—such as ethanol from corn (maize) and sugarcane—have been increasingly heralded as a possible savior (*1, 2*). But others have argued that biofuels will consume vast swaths of farmland and native habitats, drive up food prices, and result in little reduction in greenhouse-gas emissions (*3–5*). An innovative study by Zah *et al.* (*6*), commissioned by the Swiss government, could help to resolve this debate by providing a detailed assessment of the environmental costs and benefits of different transport biofuels.

To date, most efforts to evaluate different biofuel crops have focused on their merits for reducing greenhouse-gas emissions or fossil fuel use. Some studies suggest that corn-derived ethanol in the United States (*7*) and Europe (*8*) consumes more energy than it produces; others suggest a modest net benefit (*2*). Relative to petroleum, nearly all biofuels diminish greenhouse-gas emissions, although crops such as switchgrass easily outperform corn and soy (*9*). Such comparisons are sensitive to assumptions about local growing conditions and crop by-products, but even more important, their focus on greenhouse gases and energy use is too narrow.

The arguments that support one biofuel crop over another can easily change when one considers their full environmental effects. A key factor affecting biofuel efficacy is whether native ecosystems are destroyed to produce the biofuels. For example, regardless of how effective sugarcane is for producing ethanol, its benefits quickly diminish if carbon-rich tropical forests are being razed to make the sugarcane fields, thereby causing vast greenhouse-gas emission increases (*4*). Such comparisons become even more lopsided if the full environmental benefits of tropical forests—for example, for biodiversity

The authors are at the Smithsonian Tropical Research Institute, Apartado 0843-03092, Balboa, Ancón, Panama. E-mail: jscharlemann@gmail.com; laurancew@si.edu

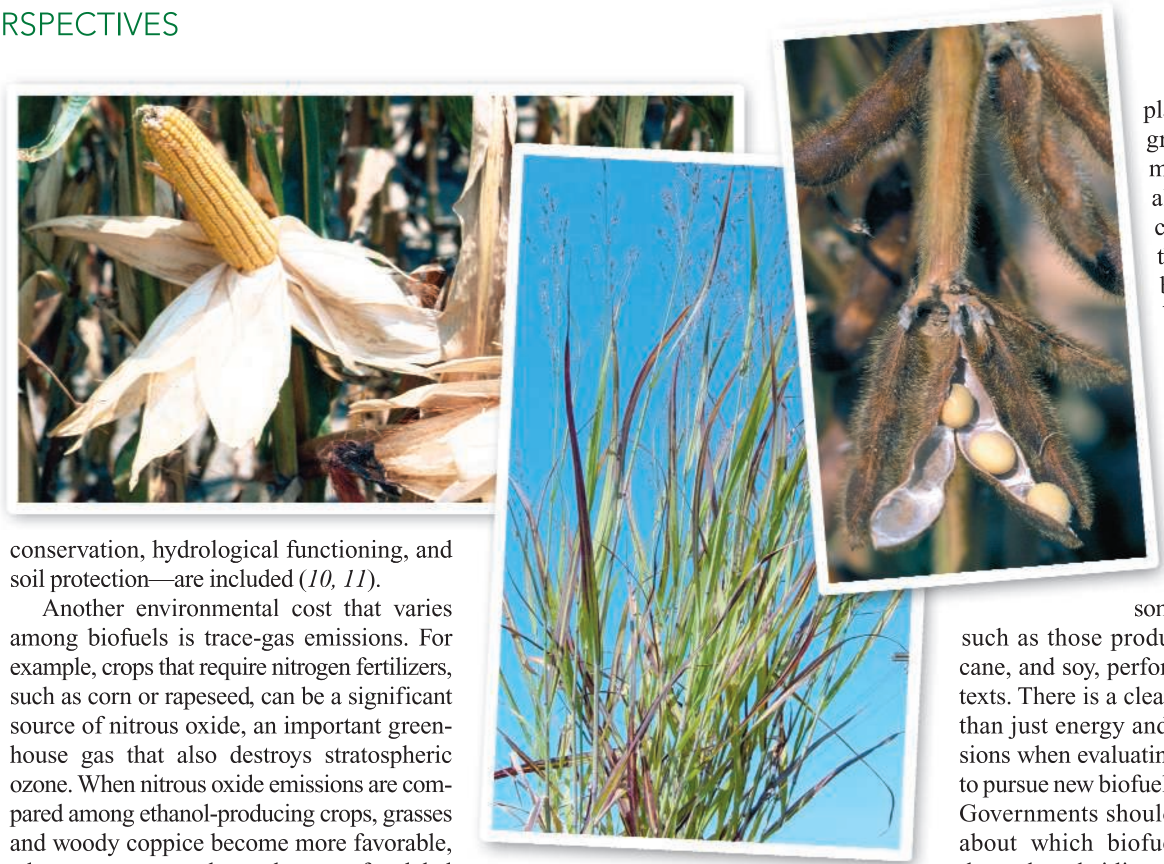

Emissions versus other impacts. Although most biofuels reduce greenhouse gas emissions relative to gasoline, many, including soy (**top right**) and corn (**top left**), do not fare well in terms of other environmental impacts (*6*). Second-generation biofuels produced from non-food plants such as switchgrass (**bottom**) may perform better in environmental terms.

CREDIT: (SOYBEANS) SCOTT BAUER/USDA AGRICULTURAL RESEARCH SERVICE, BUGWOOD.ORG; (CORN) DEWEY LEE/UNIVERSITY OF GEORGIA, BUGWOOD.ORG; (SWITCHGRASS) RICHARD OLD/XID SERVICES, INC., BUGWOOD.ORG

conservation, hydrological functioning, and soil protection—are included (*10, 11*).

Another environmental cost that varies among biofuels is trace-gas emissions. For example, crops that require nitrogen fertilizers, such as corn or rapeseed, can be a significant source of nitrous oxide, an important greenhouse gas that also destroys stratospheric ozone. When nitrous oxide emissions are compared among ethanol-producing crops, grasses and woody coppice become more favorable, whereas corn or canola may be worse for global warming than simply burning fossil fuels (*3*).

In the debate about different biofuels, one can easily be overwhelmed by the "apples and oranges" problem: Each biofuel has certain benefits and potential costs, and there is no common currency for comparing them. This is where Zah *et al.* have broken new ground by devising a conceptual scheme to evaluate different biofuels using just two criteria: greenhouse-gas emissions and overall environmental impact.

The authors compare gasoline, diesel, and natural gas with 26 different biofuels produced from a wide range of "crops." They assess the total environmental impact of each fuel by aggregating natural resource depletion and damage to human health and ecosystems into a single indicator, using two different methods (*12*). The second key criterion for each fuel is its greenhouse-gas emissions relative to gasoline.

The findings of Zah *et al.* are striking *(13*). Most (21 out of 26) biofuels reduce greenhouse-gas emissions by more than 30% relative to gasoline. But nearly half (12 out of 26) of the biofuels—including the economically most important ones, namely U.S. corn ethanol, Brazilian sugarcane ethanol and soy diesel, and Malaysian palm-oil diesel—have greater aggregate environmental costs than do fossil fuels (see the figure, top panels). Biofuels that fare best are those produced from residual products, such as biowaste or recycled cooking oil, as well as ethanol from grass or wood. The findings highlight the enormous differences in costs and benefits among different biofuels.

Despite its apparent advantages, the scheme of Zah *et al.* is not perfect. Collapsing disparate environmental costs into a single number is risky, although it is reassuring that the two different methods used yielded similar results. A bigger worry is that their analyses fail to capture the potentially important indirect effects of different biofuels. For example, U.S. government subsidies to encourage corn-based ethanol production are prompting many American farmers to shift from growing soy to growing corn. This is helping to drive up global soy prices, which in turn amplifies economic incentives to destroy Amazonian forests and Brazilian tropical savannas for soy production (*14*). Furthermore, Zah *et al.* rely on relatively old (2004) data sets and fail to consider the social consequences of large-scale biofuel production, especially rising food cost.

Zah *et al.* excluded from their analysis so-called second-generation biofuels, such as those made from the breakdown of plant cellulose or lignin, because of insufficient data. Such biofuels could be produced from nonfood plants—such as prairie grasses or trees grown on marginal land (*15*), or algae cultivated in aquaculture (*16*)— reducing the use of food crops for biofuels (see the figure, bottom panel). Some second-generation biofuels appear particularly promising in terms of their benefits and costs for biofuel production (*5*).

Not all biofuels are beneficial when their full environmental impacts are assessed; some of the most important, such as those produced from corn, sugarcane, and soy, perform poorly in many contexts. There is a clear need to consider more than just energy and greenhouse-gas emissions when evaluating different biofuels and to pursue new biofuel crops and technologies. Governments should be far more selective about which biofuel crops they support through subsidies and tax benefits. For example, multibillion-dollar subsidies for U.S. corn production appear to be a perverse incentive from a rational cost-benefit perspective.

References and Notes

1. S. Pacala, R. Sokolow, *Science* **305**, 968 (2004).
2. A. E. Farrell *et al.*, *Science* **311**, 506 (2006).
3. P. J. Crutzen, A. R. Moiser, K. A. Smith, W. Winiwarter, *Atmos. Chem. Phys. Discuss*. **7**, 11191 (2007).
4. R. Righelato, D. V. Spracklen, *Science* **317**, 902 (2007).
5. J. Hill, E. Nelson, D. Tilman, S. Polasky, D. Tiffany, *Proc. Nat. Acad. Sci. U.S.A.* **103**, 11206 (2006).
6. R. Zah *et al.*, *Ökobilanz von Energieprodukten: Ökologische Bewertung von Biotreibstoffen* (Empa, St. Gallen, Switzerland, 2007).
7. D. Pimentel, T. Patzek, G. Cecil, *Rev. Environ. Contam. Toxicol.* **189**, 25 (2007).
8. S. Ulgiati, *Crit. Rev. Plant Sci*. **20**, 71 (2001).
9. P. R. Adler, S. J. Del Grosso, W. J. Parton, *Ecol. Appl*. **17**, 675 (2007).
10. G. Bala *et al.*, *Proc. Nat. Acad. Sci. U.S.A.* **104**, 6550 (2007).
11. W. F. Laurance, *Biol. Conserv*. **91**, 109 (1999).
12. The authors use Swiss environmental impact points, which measure how much the environmental impacts exceed legal limits (see www.esu-services.ch/download/Frischknecht-2006-EcologicalScarcity-Paper.pdf) and the European Eco-indicator, which quantifies damage to human health and ecosystems (see www.pre.nl/eco-indicator99/default.htm).
13. A figure summarizing the findings of (*6*) is available as supporting material on *Science* Online.
14. W. F. Laurance, *Science* **318**, 1721 (2007).
15. D. Tilman, J. Hill, C. Lehman, *Science* **314**, 1598 (2006).
16. A. Melis, T. Happe, *Plant Physiol.* **127**, 740 (2001).

Supporting Online Material

www.sciencemag.org/cgi/content/full/319/5859/43/DC1
Fig. S1
Reference

10.1126/science.1153103

RETROSPECTIVE

Seymour Benzer (1921–2007)

The adventurous spirit of a molecular geneticist launched an era of behavioral genetic studies, all on the wings of a fruit fly.

Yuh-Nung Jan and Lily Jan

Francis Crick once said of Seymour Benzer's role in pioneering the field of neurogenetics, "If he hadn't done it, no one else could have done it." This so aptly describes one of the great biologists of our time. Seymour Benzer died on 30 November 2007 at the age of 86. He was creatively and consistently engaged at a very high level in his beloved science for 65 years, all the while having fun.

Seymour was born in the south Bronx of New York City in 1921, the son of Jewish immigrants who took up the garment trade. He grew up in Brooklyn and was the first in his family to attend college. His scientific career began as a physics graduate student at Purdue University, where his work on semiconductors contributed to developing the first transistors. Upon receiving his Ph.D. in 1947, he was immediately hired as an assistant professor in physics at Purdue.

But inspired by Erwin Schrödinger's book *What Is Life?*, in which the physicist pondered the physical nature of the gene and a "code" of life, Seymour's interest shifted to biology. In the summer of 1948, he enrolled in a course on bacteriophage at Cold Spring Harbor Laboratory, organized by biophysicist Max Delbrück. He went on to study these bacterial viruses with Delbrück at the California Institute of Technology (Caltech), and then with Andre Lwoff, Francois Jacob, and Jacques Monod at the Pasteur Institute, becoming increasingly excited about the nature of the gene. In 1953, he returned to Purdue shortly after James Watson and Francis Crick discovered the double-helix structure of DNA. There, he made his first seminal discovery that a gene is not a single indivisible unit or "mathematical point," as presumed in classical genetics, but a linear segment that could break within the gene, allowing gene parts to be swapped between chromosome pairs. He developed an extraordinarily sensitive and simple assay to detect DNA recombination events within the phage *rII* gene, and produced the first fine map of a gene, showing that a single pair of nucleotide bases is the unit of recombination. He had closed the gap between classical genetics and DNA structure.

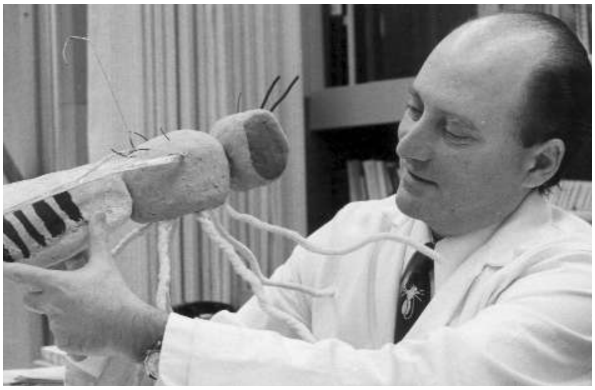

CREDIT: COURTESY OF THE ARCHIVES, CALIFORNIA INSTITUTE OF TECHNOLOGY

It was Seymour's fascination with the different personalities of his two daughters, despite being raised in the same environment, which triggered his next shift in research. He wanted to understand the connections among genes, the brain, and behavior, and in 1965, he took a sabbatical in Roger Sperry's lab at Caltech to find the proper experimental system. With the help of geneticist Edward Lewis, he settled on *Drosophila melanogaster*, and with this common fruit fly, launched the field of neurogenetics.

Seymour joined the Caltech faculty in 1967 and stayed there for the rest of his life. That year he published a remarkable paper describing a simple and elegant assay to isolate single-gene mutants defective in phototactic behavior. Over the following decade, Seymour encouraged an "anything goes" spirit in his laboratory: Ronald Konopka isolated the first mutants of the *period* gene, the beginning of understanding circadian rhythms on a molecular genetic level; Duncan Byers identified *dunce*, the first learning mutant in an organism; Jeffrey Hall's analysis of the *fruitless* mutant led the field to a major regulator of mating behavior; the isolation of the *sevenless* mutant by William Harris, together with the work on *Drosophila* eye development by Donald Ready, marked a crucial starting point for understanding cell fate specification by induction; and our own electrophysiological studies of *Shaker* mutants led to the first cloning of a potassium channel. Those studies have had a substantial impact on several areas of neurobiology, and Seymour was happy for former students and postdoctoral fellows to carry on their research passions beyond the boundaries of his laboratory.

Seymour returned to his problem-seeking mode in the 1990s and broke new ground by studying life span, nociception, and neural degeneration in *Drosophila*. He published 36 papers in his last decade (1997–2007), more than what he published in any previous decade. The papers published late in his life are some of his most interesting.

It was Seymour's enormous credential that drew students into seemingly (and wildly) improbable research programs. Perhaps less appreciated is that he provided a sanctuary for those interested in what might have been considered "fringe science" at the time. Neuroscientists in general were skeptical of the relevance of fly studies then, but a very high regard for Seymour provided the benefit of the doubt. One of us was very doubtful of Seymour's suggestion to seek support from the Scottish Rite Schizophrenia Foundation for postdoctoral work on the fly and was astonished that they funded the work. Later, a prominent neuroscientist who had reviewed the proposal revealed that although he didn't believe a word of it, he suspected things would be all right under Seymour's mentorship.

Seymour received most of the major awards and prizes in biology, with one glaring omission. It is a pity that the Nobel committee missed the opportunity to honor Seymour for his enormous and lasting contributions. No matter, his legacy will endure.

Seymour was an inspiring, generous, and benevolent mentor. Many of his former students have continued to flourish. He had the good fortune of having had two wonderful marriages, to Dotty until she passed away and then to Carol Miller, and having raised five children successfully. He was great fun to be around for his wit and adventurous spirit. For just about any city in the world, if you asked him, he would have taken out a tiny notebook and happily told you which restaurants to go to and what dishes to order. In typical Benzer style, he approached the things in life he loved with excitement and boundless curiosity. A giant in science and a wonderful human being, Seymour will be sorely missed.

10.1126/science.1154050

The authors are in the Howard Hughes Medical Institute, Departments of Physiology, Biochemistry, and Biophysics, University of California, San Francisco, CA 94143, USA. E-mail: yuhnung.jan@ucsf.edu; lily.jan@ucsf.edu

INTRODUCTION

Warp and Woof

WITH ALL RESPECT TO THE POET DYLAN THOMAS, WHO DEPICTED THE MOONLESS sky as “starless and bible-black,” a clear night is actually ablaze with specks of light. For a long time, we thought those isolated stars were the whole story. But researchers now realize that they are embedded in a filamentary structure of matter both dark and visible, called the cosmic web. In this issue, a News feature and three Perspectives bring us up to date on just what we know about the cosmic web and what we still want to know.

For starters, Adrian Cho (p. 47) surveys the many techniques astronomers are using to trace the web. Their goal is both simple and ambitious: to map everything they can see. Their tools include large-scale surveys of galaxies and galactic clusters, which probe the interplay of dark matter and dark energy; weak gravitational lensing, which detects matter by analyzing how it affects passing light; and techniques for viewing the universe through microwaves and other radiation outside the usual optical and infrared wavelengths. To make real progress, however, theorists must clear up some fundamental mysteries about how galaxies form and evolve.

As Ibata and Lewis explain (p. 50), the cosmic web shows up in our own galactic backyard. Galaxies are distributed not randomly but along the tendrils of the cosmic web, yet this pattern can only be explained by large amounts of connective dark matter. “Just like Swift’s big fleas and little fleas,” the authors write, these structures should occur at all distance scales, including within the Milky Way. Astronomers have marshaled a large observational effort to understand the web at various scales, but how do they make sense of the data?

This is where advances in modeling and theory can help. Faucher-Giguère *et al.* (p. 52) discuss supercomputer simulations that have enhanced our understanding of where the cosmic web came from. Tiny fluctuations in the very early universe have grown over billions of years into the massive cosmological structures we see today. The distribution of galaxies predicted by computer models has been dramatically confirmed by observational surveys, but much more needs to be done. New simulation techniques will have to provide higher resolution while modeling the cosmic web over immense distances.

These questions connect at the smallest scales too, as Nicastro *et al.* describe (p. 55). The exact nature of the dark matter that makes up 95% of the cosmic web remains baffling, but things aren’t much better for the remaining 5% that we can see. These are the baryons—protons and neutrons—that make up ordinary matter, yet we can account for only about half of the baryon mass predicted by the standard cosmological model. The missing baryons might be lurking in the cosmic web, and perhaps we could detect the warm-hot intergalactic matter, or WHIM, that could be their signature. Detecting these WHIMsical filaments will require both closer analysis of existing data and future observational missions.

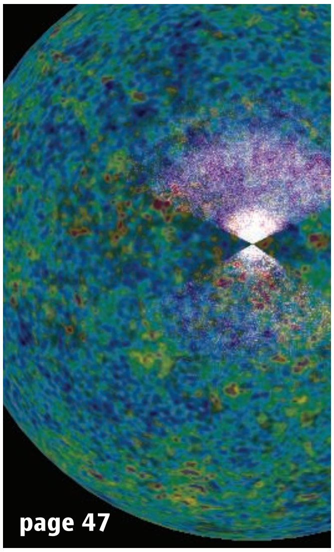

Astronomers and physicists have given us a good picture of how the elaborate filigree of matter in the cosmic web arose from the whispering echoes of the Big Bang, and the view is stunning. Their continuing efforts to map the cosmic web should begin to nail down the nature of the missing matter, whether dark or light, and tell us more about how the universe came to be and how it is evolving.

–DAVID VOSS AND ROBERT COONTZ

Cosmic Web

CONTENTS

News

Perspectives

Science

CREDIT: MARK SUBBARAO/ADLER PLANETARIUM & UNIVERSITY OF CHICAGO

NEWS

Untangling the Celestial Strings

In an effort that weaves together astronomy, astrophysics, and cosmology, scientists are mapping the filamentary framework that gives shape to the cosmos

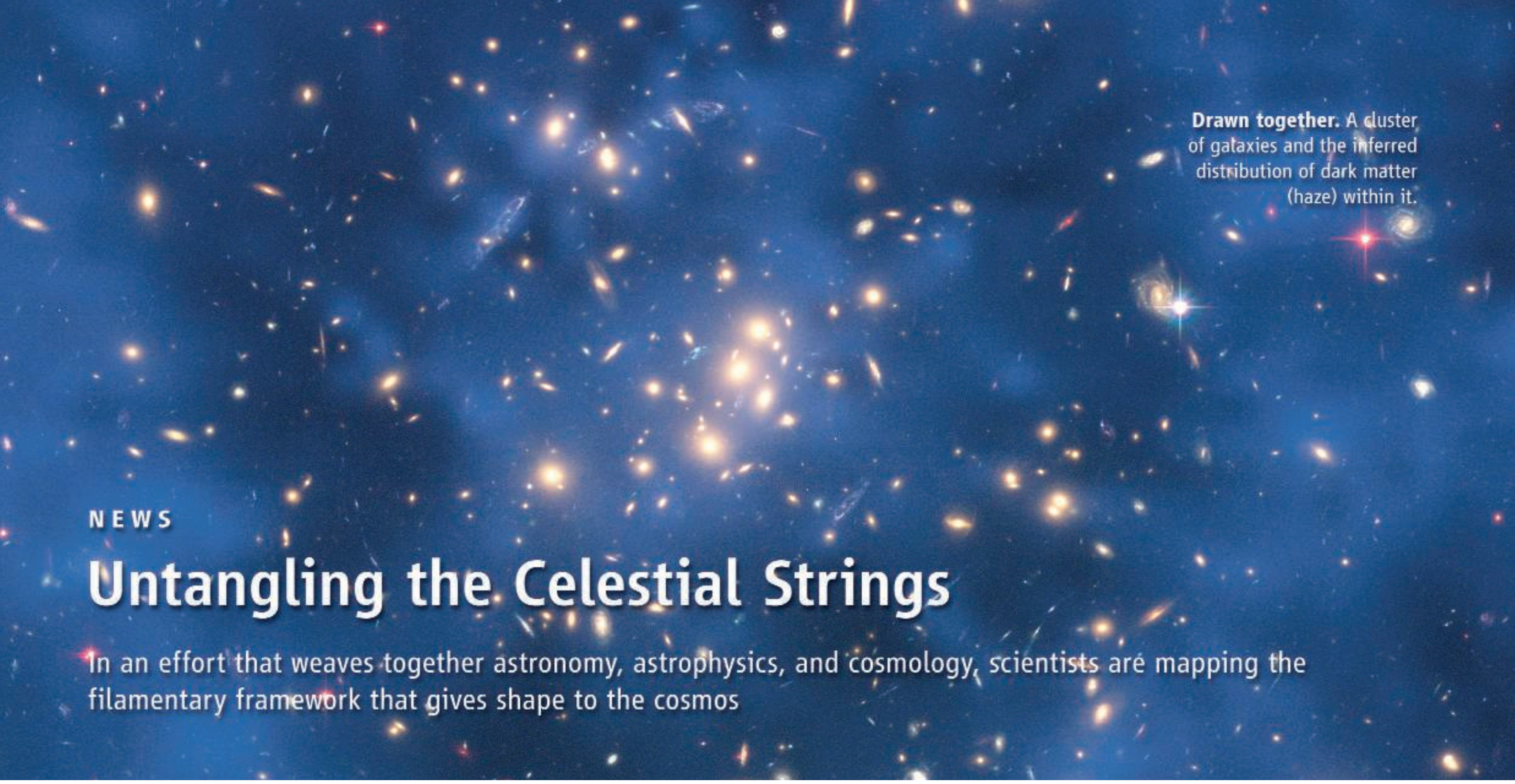

Drawn together. A cluster of galaxies and the inferred distribution of dark matter (haze) within it.

CREDIT: NASA, ESA, M. J. JEE AND H. FORD (JOHNS HOPKINS UNIVERSITY)

CHICAGO, ILLINOIS—All the universe is a tangled web, and all the stars and galaxies its captives. Fans of the Bard may groan, but that doggerel nicely sums up scientists' understanding of the cosmos. Unraveling that "cosmic web" presents astronomers, astrophysicists, and cosmologists with their next great challenge.

The web is the framework on which the universe is built. It consists primarily of "dark matter," mysterious stuff that makes up 85% of the matter in the universe but has revealed itself only through its gravity. Enormous filaments and blobs of the stuff condensed as the universe matured. Within them nestle the galaxies and their stars, creating streams of light stretching between inky voids. Even-stranger dark energy pervades everything, stretching space and affecting the evolution of the web.

That's the big picture. Now, scientists are turning to the details. What are the properties of dark matter and dark energy? Precisely how is the web organized? Exactly how do galaxies form in it? The web spans size scales from individual galaxies to the breadth of the observable universe. In its evolution, it traces the complexity we see today back through time to the big bang. And it bridges the conceptual divide between the reductive theories of cosmology and the rich and varied astrophysics of galaxies and clusters.

"To me, the really exciting part of astronomy and astrophysics in the next 15 years is how to interpret the light that we see in terms of the web of dark matter," says Howard Yee, an astronomer at the University of Toronto in Canada and one of 106 researchers who met here last month* to discuss efforts largely aimed at mapping out the cosmic web. "We don't know how to say, 'Here [in the web], a galaxy will show up at a certain time and with a certain size.' "

The drive to trace the cosmic web is changing the practice of astronomy. Researchers are turning to the galaxies with renewed interest, says Michael Gladders, an astronomer at the University of Chicago. Only now, they are analyzing them en masse. "We're going to see a resurgence of what you might consider classical astronomy—looking at distinct objects at optical and infrared wavelengths—except millions of them at a time," Gladders says.

A recipe for the universe

Ten years ago, most theorists agreed that dark matter had to exist, as its gravity appears to hold the galaxies together. Then three observations in quick succession helped cosmologists nail down a precise list of ingredients for the cosmos.

In 1998, two teams used the light from exploding stars called type Ia supernovae to measure the expansion of the universe. To their surprise, they found that instead of slowing as expected, it's speeding up as though driven by dark energy (*Science*, 27 February 1998, p. 1298).

Meanwhile, astronomers were beginning huge surveys of the galaxies. Scientists used the 3.9-meter Anglo-Australian Telescope on Mount Worrat in New South Wales, Australia, to measure the three-dimensional (3D) positions of 221,000 galaxies as part of the 2dF Galaxy Redshift Survey, which ran from 1997 to 2002. Others with the Sloan Digital Sky Survey, which began in 1998, have used a 2.5-meter telescope at Apache Point, New Mexico, to pinpoint 800,000 galaxies. The results of the surveys can help theorists probe the interplay between dark matter, whose gravity pulls galaxies together, and dark energy, which pushes them apart.

Then in 2003, NASA's Wilkinson Microwave Anisotropy Probe (WMAP) spacecraft mapped the afterglow of the big bang, the cosmic microwave background (CMB), to produce, in essence, the universe's baby picture. The universe supposedly sprang into existence infinitely dense and hot and immediately doubled its size 100 times over. After about 10^{-32} seconds of such "inflation," the expansion slowed, and 400,000 years later, the universe cooled enough to allow free-flying protons and electrons to form hydrogen atoms. That transformation freed light trapped by the particles, which has since stretched into microwaves and cooled to 2.725 kelvin.

(As light travels through the expanding universe, it is stretched, or "redshifted," to longer wavelengths. Scientist use redshift to mark cosmic history. Light whose wavelength has increased 200% has a redshift of 2 and was emitted when the universe was one-third its current size—about 10 billion years ago.)

The CMB is not exactly uniform. Inflation magnified infinitesimal quantum fluctua-

---

* Cosmic Cartography: Mapping the Universe from the Big Bang to the Present, 3–6 December.

Published by AAAS

tions in the newborn universe, which eventually seeded the filaments in the cosmic web. The fluctuations also caused the temperature of the CMB to vary across the sky by about 0.001%. Analyzing the temperature ripples, and throwing in supernova and galaxy-cluster data, WMAP researchers found that, bizarrely, the universe consists of 73% dark energy, 23% dark matter, and 4% ordinary matter and is precisely 13.7 billion years old (*Science*, 19 December 2003, p. 2038).

"The CMB is a great gift because the fluctuations are big enough to measure but small enough to be easily understood," says Gary Hinshaw, a cosmologist at NASA's Goddard Space Flight Center in Greenbelt, Maryland. "You can read the parameters right off the spectrum" of ripples. But plenty of questions remain, says cosmologist Edward "Rocky" Kolb of the University of Chicago. "The rough picture works," he says, "but the details of how galaxies form, how they interact, and whether mergers and acquisitions [of galaxies] are important still need to be worked out."

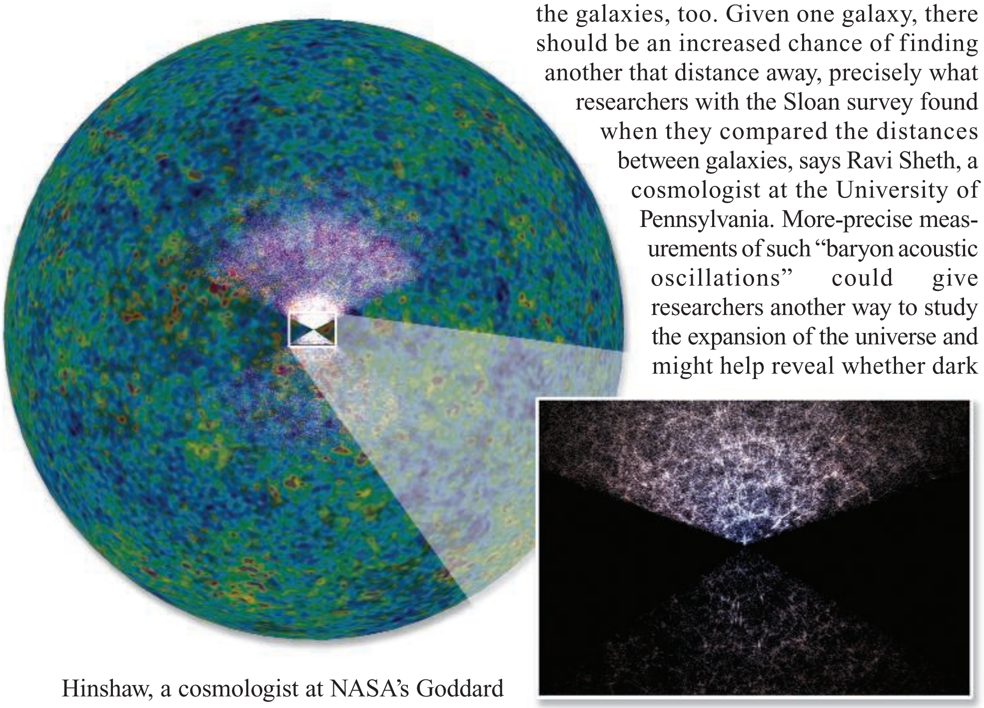

The fishbowl. The cosmic microwave background shown as a sphere with the galaxies surveyed by the Sloan Digital Sky Survey positioned inside it.

Filling in the fishbowl

Scientists hope to trace the web from near to far, from the present into the past. Humans have glimpsed the oldest light, the CMB, which appears to emanate from near the periphery of the observable universe 46.5 billion light-years away. (Everything farther away is rushing away so fast that its light will never reach us.) We've also started to explore the nearby cosmic web. So we're a bit like fish in a murky bowl that see the smudgy glass and the castle next to them. What's in between remains to be discovered.

Primarily, researchers are charting the galaxies, which lie within the dark-matter strands. In 2005, they forged a link between the ripples in the distribution of the galaxies and those in the CMB. Before atoms formed and as matter settled into the primordial fluctuations, protons pushed against light, sending tsunami-like sound waves zipping through space. Leaving their imprint on the CMB, the waves traveled about 100 kiloparsecs—326,000 light-years—before atoms formed.

Stretched 1000-fold by the expansion of the universe, that length scale should show up in the galaxies, too. Given one galaxy, there should be an increased chance of finding another that distance away, precisely what researchers with the Sloan survey found when they compared the distances between galaxies, says Ravi Sheth, a cosmologist at the University of Pennsylvania. More-precise measurements of such "baryon acoustic oscillations" could give researchers another way to study the expansion of the universe and might help reveal whether dark energy is part of space itself or is something flowing through it.

Scientists are also probing the web by counting clusters of galaxies, which form when individual galaxies fall into gargantuan clumps of dark matter. The size and number of the swarms reveal the distribution of dark matter. At the same time, the stretching effects of dark energy slow the formation of jumbo agglomerations. So simply tallying the abundance of clusters of different sizes at different redshifts promises to reveal properties of both weird substances, says Toronto's Yee.

Moreover, clusters are relatively easy to spot with optical and infrared telescopes, he says. That's because the galaxies in them tend to be old and filled with red giant stars, all of which emit light of essentially the same color. So by looking at the colors of the galaxies, astronomers can immediately tell which ones belong to the same cluster and what the cluster's redshift is. Using this technique, Yee and colleagues with the Red-Sequence Cluster Survey, which uses the Canada-France-Hawaii Telescope atop Mauna Kea in Hawaii, have been scanning 1000 square degrees of sky and have cataloged 20,000 clusters.

Researchers are striving to "see" the dark-matter filaments by observing how their gravity bends light from more distant galaxies and skews their images. Known as weak gravitational lensing, the technique allows scientists to detect dark-matter blobs directly, without looking at the stars or galaxies in them, says Gary Bernstein, a cosmologist at the University of Pennsylvania.

Because of weak lensing, the galaxies ever-so-slightly tend to line up, like fish in a school. Researchers first observed the effect in 2000, and last year, Richard Massey, an astronomer at the California Institute of Technology in Pasadena, and colleagues took a big step further. Using images of half a million galaxies from NASA's Hubble Space Telescope, they compared the lensing of galaxies at three different distances to crudely map a bit of the 3D web, as they reported in the 18 January 2007 issue of *Nature*. Ultimately, researchers hope to perform such 3D studies over huge swaths of the sky, Bernstein says.

Looking with other eyes

Staring at galaxies with optical and infrared telescopes is not the only way to study the cosmic web. For example, radio astronomers can join the hunt for galaxy clusters by looking for pimple-like spots in the CMB. Those spots arise because of a bit of physics called the Sunyaev-Zel'dovich effect. Microwave photons from the CMB crash into the electrons in hot, ionized gas within galaxy clusters, explains Matt Dobbs, an astrophysicist at McGill University in Montreal, Canada. The collisions change the microwaves' energy, creating the telltale distortion. Because the effect does not depend on the cluster's own light, it should help to reveal fainter, more distant clusters, Dobbs says.

So far, most studies have probed the Sunyaev-Zel'dovich effect in clusters already found some other way. But the Sunyaev-Zel'dovich Array, a collection of eight 3.5-meter radio dishes in Owens Valley, California, is scanning 6 square degrees of sky in a blind search for new clusters. And the 6-meter Atacama Cosmology Telescope in Chile

CREDITS: MARK SUBBARAO/ADLER PLANETARIUM AND UNIVERSITY OF CHICAGO

and the 10-meter South Pole Telescope will scan 200 and 4000 square degrees of sky, respectively, which should reveal thousands of clusters.

Researchers needn't look only at galaxies. Most ordinary matter resides not in stars and galaxies but in huge clouds of neutral and ionized gas. Astronomers can detect neutral hydrogen by looking toward celestial beacons called quasars. Whenever a quasar's light passes through atomic hydrogen, some of it will be absorbed, creating a dip, or absorption line, in its spectrum. The wavelength of the dip reveals the cloud's redshift, the width of the dip reveals its temperature, and the depth of the dip reveals the amount of gas in the cloud, explains astronomer Michael Rauch of the Observatories of the Carnegie Institution of Washington in Pasadena, California. By studying many quasars, researchers hope to map out the distribution of gas in the web.

Scientists might be able to go even a step further in time. Atomic hydrogen emits radio waves of a distinct wavelength, 21 centimeters, when the proton in the atom flips. Researchers hope to exploit that radiation to detect the distribution of hydrogen back when the universe was less than a billion years old, when the first stars were forming. To do that, however, they'll need an observatory such as the proposed Square Kilometer Array, a collection of hundreds of radio dishes that astronomers propose to build in South Africa or Australia sometime in the next decade.

Our lumpy neighborhood

Galaxies form in the web's smaller knots, and scientists are striving to determine how they swirl into existence. That's important because in galaxies, the dark-matter-dominated picture blurs. "It seems to work well on the large scales," says Kathryn Johnston, an astrophysicist at Columbia University. "Where there seem to be some problems is on the small scales." For example, simulations predict that the Milky Way should be surrounded by many more small satellite galaxies than astronomers have seen (*Science*, 3 August, p. 594).

Theorists know so little about galaxy formation that in their cosmological simulations, they let the dark matter evolve by itself and "paint" the galaxies onto the clumps and strands at the end. To fill the voids in their understanding, scientists are studying our own galaxy. "The Milky Way is the only galaxy for which we can hope to get three-dimensional data about the positions and velocities" of individual stars, says Heidi Newberg, an astrophysicist at Rensselaer Polytechnic University in Troy, New York.

Crash of the Titans. The Milky Way formed through collisions like this one between distant spirals.

CREDIT: NASA AND THE HUBBLE HERITAGE TEAM (STSCI)

Most of the Milky Way's stars lie in its thin disk. But that disk resides in a fatter blob of dark matter known as a halo. Scientists once thought that the halo was smooth and that the stars in it were evenly distributed. In the past decade, that picture has changed thanks largely to star studies made by the Sloan survey. "As we keep looking deeper at the data, we keep seeing more and more lumps and things," Newberg says. "There are big lumps, little lumps, smeared-across-the-sky lumps. It's just lumps everywhere."

The halo seems to have been produced exclusively through the mergers of smaller galaxies, Newberg says. As the smaller galaxies fall in, the Milky Way's gravity tears them into sinuous "tidal streams," such as the Sagittarius stream, which arches over the disk. By measuring the positions and velocities of stars, researchers can determine, statistically, which ones belong to which stream. And they may be able to make clearer connections by comparing the stars' chemical content, Johnston said at the meeting.

Mapped out?

Ultimately, the cosmic web may bridge the divide between cosmology on one hand and astronomy and astrophysics on the other. Cosmologists seek to reduce the universe to its most basic ingredients and rules. Astronomers and astrophysicists study the myriad objects in the heavens and try to explain how they work and whether they are related to one another. In principle, the cosmic web ties the two types of work together. Whether it will in practice remains to be seen, says Chicago's Kolb. "Ten or 20 years from now, we may look back and say it had that unifying effect," he says. "But we're too close to it now" to know if that will be the case.

Nevertheless, interest in the web is helping to change the craft of astronomy, fueling the drive to ever-larger surveys. For example, even as the Sloan survey continues, researchers with the Dark Energy Survey plan to use the 4-meter Blanco Telescope at the Cerro Tololo Inter-American Observatory in Chile to observe 5000 square degrees of sky and pinpoint 200 million galaxies. The first Pan-STARRS telescope on Mauna Kea will survey 3/4 of the sky—30,000 square degress—starting this year. And researchers have proposed an 8.4-meter behemoth known as the Large Synoptic Survey Telescope that would use a 3-gigapixel camera to image 10 square degrees of the sky at a time and fix the positions and redshift of 3 billion galaxies starting in 2014.

Many embrace the bigger-is-better approach. "You're compelled to do this by the science," says Steven Myers, an astronomer at the National Radio Astronomy Observatory in Socorro, New Mexico. "I'm very enthusiastic for the new age of great survey projects."

Surveys are growing so large that some researchers are beginning to talk of spotting all the 100 billion bright galaxies in the observable universe. The cosmos will always provide new mysteries, says Timothy McKay, an astrophysicist at the University of Michigan, Ann Arbor, who works on both the Sloan survey and the Dark Energy Survey, but researchers should eventually chart all of its large features. "We should look forward to a future in which the universe we can observe will be observed," he says. "This cosmos incognita will be mapped out in our lifetimes."

Researchers won't run out of galaxies to observe for a while, however. In the meantime, they've got plenty to do as they try to weave a deeper understanding of the cosmos one conceptual thread at a time.

–ADRIAN CHO

PERSPECTIVE

The Cosmic Web in Our Own Backyard

Rodrigo A. Ibata[1] **and Geraint F. Lewis**[2]

On the largest scales, matter is strung out on an intricate pattern known as the cosmic web. The tendrils of this web should reach right into our own cosmic backyard, lacing the Galactic halo with lumps of dark matter. The search for these lumps, lit up by stars that formed within them, is a major astronomical endeavor, although it has failed to find the huge expected population. Is this a dark matter crisis, or does it provide clues to the complexities of gas physics in the early universe? New technologies in the coming decade will reveal the answer.

The universe is seen to be awash with billions of galaxies, some larger and many smaller than our own Milky Way. A census of the galaxies, however, reveals a startling property of our universe: Galaxies are not dotted randomly throughout the cosmos but are generally concentrated in groups or clusters, which are themselves connected by a multitude of filaments known as the cosmic web. At first sight, this observation stands in stark contrast to our knowledge of the state of the early universe, which was remarkably smooth, as inferred from the almost-uniform temperature of the cosmic microwave background over the sky (*1*, *2*). This background radiation also reveals the seeds of galaxy formation, possessing tiny inhomogeneities that grew under the influence of gravity into the universe we see around us today. In recent years, it has become clear that the filamentary distribution of the galaxies can only be explained by requiring the presence of vast quantities of unseen material enveloping galaxies (*3*). Indeed, this dark matter is by far the dominant mass in the universe, and all visible material, such as stars and gas, essentially only goes along for the ride.

To explain the large-scale distribution of galaxies in the sky, dark matter must be "collisionless," meaning that two pure dark matter entities would pass through each other like ghostly bodies, feeling only the mutual gravitational tug, with an absence of any material contact. This, of course, means that, whatever shapes the dark matter is inclined to take, these will only depend on the physics of gravity, which on the scale of galaxies is approximated well by Newton's law of gravitational forces. Using these physical principles in a cosmological setting to predict the evolution of structure from an initially homogenous starting point early in the universe, computer simulations have shown that the natural outcome is the growth of roughly spherical dark matter "halos" (*4*), as well as the development of tenuous filaments connecting them (*5*). A fascinating aspect of Newton's law of gravity is that it makes no mention of any special distance scale over which gravity should work, and this means that, if additional forces such as gas and radiation pressure can be ignored, the structure of the dark matter on the scales of clusters of galaxies will be similar to the structure of the dark matter on the scales of the smallest of galaxies (*6*) (nearly a factor of a billion lower in mass).

This is precisely what is seen in numerical models of the growth of cosmological structure, with massive halos of dark matter playing host to a multitude of smaller halos and filaments, and, just like Swift's big fleas and little fleas, this hierarchical structure must continue on all scales (*7*), from clusters of galaxies, to the dark matter halos of galaxies like our own Milky Way, and down to the subcomponents of these galaxies. Testing the veracity of this prediction, that the cosmic web has strands that wind their way into our Galaxy (Fig. 1), has been the focus of a substantial observational effort by several research teams around the world.

The nearby filaments connect our Local Group of galaxies to the large-scale cosmic web, and computer models reveal that these filaments should channel a steady rain of pristine

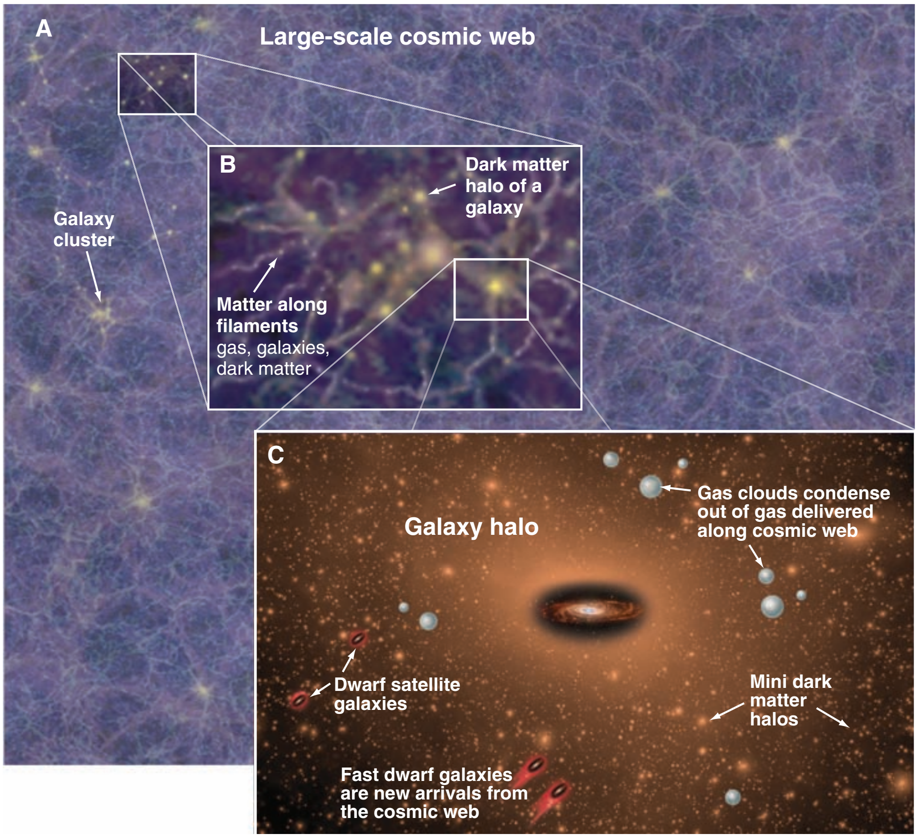

Fig. 1. Schematic diagram showing the position of a typical galaxy within the cosmic web. (**A**) On the very largest scales, clusters of galaxies are linked up by filaments of dark matter. (**B**) Within the filaments we find the dark matter halos of numerous galaxies, as well as very tenuous reservoirs of gas. (**C**) Zooming into halo of a galaxy like the Milky Way, theory predicts that the structure of the halo should be homologous to that of a cluster of galaxies, possessing a vast swarm of smaller subhaloes. Some of these subhaloes may be populated by stars (in which case we detect a dwarf satellite galaxy) and others may contain only gas, whereas the majority may be purely composed of dark matter and hence invisible.

---

[1] Observatoire Astronomique de Strasbourg, 11, rue de l'Université, 67000 Strasbourg, France. [2] Institute of Astronomy, School of Physics, A29, University of Sydney, NSW 2006, Australia.

dwarf galaxies, comprising stars and dark matter, into the local environment. Because they fall in from large distances and accelerate over a large fraction of the age of the universe, those dwarf galaxies that are in the process of arriving today can be expected to exhibit very large speeds, and this is precisely what has been detected recently with two new high-speed galaxies in the vicinity of Andromeda, And XII (*8*) and And XIV (*9*); these are probably among the newest arrivals to the Local Group of galaxies.

Gas is also conveyed into galaxies along the filaments, but because of pressure forces this is rapidly slowed down, first shock heating and then condensing into clouds that fall into the center of the gravitational well and contribute to the buildup of the gaseous disk component of galaxies. For several decades, we have known that clouds of atomic hydrogen, known as high-velocity clouds, surround the Milky Way, and beautiful radio observations of the Andromeda galaxy (*10*) have recently shown a similarly rich distribution of cold gaseous structures raining down upon that galaxy. Hence, both large galaxies within the Local Group appear to be continually accreting gas fed to them from the cosmic web.

But what is the future of the recently accreted dwarf galaxies? Some may pass straight through the Local Group, but orbits of others will be degraded over time through the process of dynamical friction, eventually bringing them into the powerful tidal fields of the massive galaxies. Once a dwarf has strayed too close, these tidal forces act to steadily shred it, ripping off stars and gas to form extensive tidal streams of stars that envelope the galaxy. Two prominent examples, the Sagittarius and the Monoceros streams (*11*, *12*), are visible within the Milky Way, with the Giant Stellar Stream (Fig. 2) dominating the halo of Andromeda (*13*). Many smaller, fainter streams, allowing us to get an accurate picture of the current rate of assimilation of stars into these galaxies, accompany these debris tails. Clearly, the process of galaxy formation for both the Milky Way and Andromeda galaxies is still under way, with the break-up of these dwarf galaxies directly contributing to the stellar populations in the galactic disk and halo, all ultimately fed by the cosmic web.

Although observations confirm the drizzle of new material into the Local Group and ultimately onto galaxies, from our computer models we also expect a large population of small dark matter halos to accompany the Milky Way and Andromeda. But what do surveys of our own backyard actually reveal? Although some dwarf satellite galaxies have been known since time immemorial (the Large and Small Magellanic Clouds were known to ancient inhabitants of the Southern Hemisphere), recent discoveries from the Sloan Digital Sky Survey (*14*) show that the Milky Way does indeed play host to a much larger population of small dwarf galaxies than previously known, with the puniest of these having masses that range down to a millionth of that of our own Galaxy (*15*). The work of our own team using the giant, wide-field camera of the Canada-France-Hawaii Telescope (Fig. 2) indicates that a similar population is also present around our nearest large neighbor, the Andromeda galaxy (*16*).

However, a major problem remains; the dark matter paradigm predicts that a myriad of dark matter halos, literally thousands of them, should be seen orbiting these giant galaxies, many more than the 20 or so dwarf galaxies that are actually observed (*17*). So, where are the missing galaxies? This question has been the root of substantial argument, with many experts suggesting that the dark matter halos are there but are not visible because star formation was extinguished early in the history of these tiny galaxies (*18*). Although astronomers are now examining more novel approaches, such as gravitational lensing, to search for small-scale dark matter halos that are truly dark, some have suggested that perhaps they are just not there. This would have far-reaching consequences for fundamental physics because our favored dark matter model would need to be reexamined.

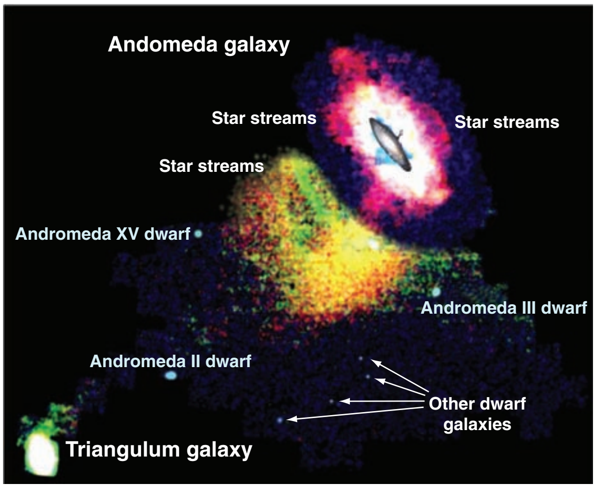

Fig. 2. Stellar structures detected between the Andromeda and Triangulum galaxies, two neighboring galaxies to our own, which are separated by about 700,000 light years. Andromeda, which is a classical spiral galaxy similar to our own Milky Way, has a disklike main body, but at large distances we detect numerous satellite galaxies and star streams. The star streams are the remnants of ancient satellites that have been destroyed by the powerful gravitational tides of Andromeda.

Although the number of dark matter halos may not meet our theoretical expectations, studying our local dwarf galaxy population can provide important clues to the origins of the Milky Way and the Local Group of galaxies. Given that our best model of galaxy formation predicts that the Milky Way grew over time through the assimilation of such dwarf galaxies, the existence of the Sagittarius dwarf galaxy, with its accompanying stellar stream that is depositing stars into the halo of the Milky Way, demonstrates that this formation mechanism is at least partially true. Nevertheless, there are problems with this scenario: Recent detailed chemical analyses indicate that the dwarfs we see around us today could not be the basic building blocks from which the majority of the Milky Way was constructed because they have a different distribution of chemical elements (*19*). However, in this picture, the surviving dwarf galaxies possess unusual properties compared with those of the bulk of the original population, being on average both more distant and less massive than those that were assimilated in the formation of the Galaxy. Proponents of the hierarchical formation picture assert that this selection bias may account for the difference in chemical makeup of the remaining dwarfs compared with that observed in the halo of the Milky Way (*20*). What is needed to settle this issue is a detailed study of remnants of ancient accreted galaxies to compare to “normal” stars; the difficulty is identifying bona fide remnants.

It is now clear that the Milky Way and the entire Local Group are dynamically evolving entities, greatly influenced by the cosmic web; can we guess where the breakthroughs in the study of this lie? We know that the tidal debris from a disrupted satellite galaxy will take a long time to disperse, and hence galaxies should be riddled with the fossil evidence of past accretion events (*21*). The steadily growing field of galactic archaeology uses kinematic and chemical fingerprinting, determining the precise chemical makeup of the star, to search for groups with a common origin (*22*); stars that are born together, either within the Galaxy or brought in through accretion, will possess many common properties. We are patiently awaiting the arrival of massive multifiber systems, especially the proposed Wide Field Multi-Object Spectrograph (WFMOS) on an 8-m-class telescope, to provide the massive data sets to begin to disentangle the complex accretion history and dynamical mixing of large galaxies.

Probably the most important contribution to this field will come from the GAIA experiment. Starting in 2011, this cornerstone project of the European Space Agency will map and measure the motions of over a billion stars in our Galaxy with precision orders of magnitude greater than what is currently possible. Coupled with the detailed chemical analysis provided by WFMOS, we will, for the first time, be able to reunite the long-dispersed stars from ancient accretion events, completely dissecting the Milky Way and laying bare its history. We will then be able to directly determine to what extent the Galaxy was built from dwarf galaxies that fell in through the local cosmic web.

What are the future challenges in understanding our local cosmology? Clearly, we are entering the age where near-field archaeologists will be awash with observational data, and we will be faced with the kinematics of a billion stars and detailed chemistry of several million stars not only in the Milky Way but also within our nearest neighbors. The resulting data challenges are substantial, and novel data-mining techniques will be required to cross-match the kinematic and chemical fingerprints to uncover stellar siblings. But how are the results of this to be interpreted? Again, astronomers will have to rely on the power of numerical simulations to examine in detail the growth of the Milky Way through the continual accretion of dwarf galaxies. However, it is important to remember that a galaxy like our own Milky Way contains roughly 200 billion individual stars, embedded within a much more massive dark matter halo, and as of yet no computer can track the complex gravitational interplay between these many bodies. Hence, our current simulations, where a single particle will represent roughly 10 to 100 thousand stars, present us with an exceedingly crude, sledgehammer view of the subtleties of galaxy formation, and we will need a revolution in computer power before we truly understand the origins of the Milky Way galaxy and its relation to the cosmic web.

References

1. G. Smoot *et al*., *Astrophys. J.* **396**, L1 (1992).
2. D. Spergel *et al*., *Astrophys. J.* **170** (suppl.), 377 (2007).
3. V. Springel *et al*., *Nature* **435**, 629 (2005).
4. J. Navarro, C. Frenk, S. White, *Astrophys. J.* **490**, 493 (1997).
5. A. Klypin, S. Shandarin, *Mon. Not. R. Astron. Soc.* **204**, 891 (1983).
6. B. Moore *et al*., *Phys. Rev. D* **64**, 063508 (2001).
7. J. Diemand, B. Moore, J. Stadel, *Nature* **433**, 389 (2005).
8. S. Chapman *et al*., *Astrophys. J.* **662**, L79 (2007).
9. S. Majewski *et al*., *Astrophys. J.* **670**, L9 (2007).
10. R. Braun, D. Thilker, *Astron. Astrophys.* **417**, 421 (2004).
11. R. Ibata, G. Lewis, M. Irwin, E. Totten, T. Quinn, *Astrophys. J.* **551**, 294 (2001).
12. B. Yanny *et al*., *Astrophys. J.* **540**, 825 (2000).
13. R. Ibata, M. Irwin, G. Lewis, A. Ferguson, N. Tanvir, *Nature* **412**, 49 (2001).
14. V. Belokurov *et al*., *Astrophys. J.* **654**, 897 (2007).
15. B. Willman *et al*., *Astrophys. J.* **626**, 85 (2005).
16. N. Martin *et al*., *Mon. Not. R. Astron. Soc.* **371**, 1983 (2006).
17. A. Klypin, A. Kravtsov, O. Valenzuela, F. Prada, *Astrophys. J.* **522**, 82 (1999).
18. J. Bullock, A. Kravtsov, D. Weinberg, *Astrophys. J.* **539**, 517 (2000).
19. K. Venn *et al*., *Astron. J.* **128**, 1177 (2004).
20. L. Sales, J. Navarro, M. Abadi, M. Steinmetz, *Mon. Not. R. Astron. Soc.* **379**, 1464 (2007).
21. K. Johnston, L. Hernquist, M. Bolte, *Astrophys. J.* **465**, 278 (1996).
22. K. Freeman, J. Bland-Hawthorn, *Annu. Rev. Astron. Astrophys.* **40**, 487 (2002).

10.1126/science.1152008

PERSPECTIVE

Numerical Simulations Unravel the Cosmic Web

Claude-André Faucher-Giguère,* Adam Lidz, Lars Hernquist

The universe is permeated by a network of filaments, sheets, and knots collectively forming a "cosmic web." The discovery of the cosmic web, especially through its signature of absorption of light from distant sources by neutral hydrogen in the intervening intergalactic medium, exemplifies the interplay between theory and experiment that drives science and is one of the great examples in which numerical simulations have played a key and decisive role. We recount the milestones in our understanding of cosmic structure; summarize its impact on astronomy, cosmology, and physics; and look ahead by outlining the challenges faced as we prepare to probe the cosmic web at new wavelengths.

Cosmologists envision a universe made up of filaments, knots, and sheets reminiscent of pancakes (1), dubbed the "cosmic web" by Bond and collaborators (2). This picture of the cosmos—now well entrenched even in popular culture—is, however, much more than mere fantasy. Indeed, it is one of the best-established results of cosmological research and underpins much of our contemporary understanding of large-scale structure and galaxy formation.

After Schmidt's spectroscopic observations of a distant quasar (a fantastically bright point source located at a cosmological distance, later understood to be powered by a supermassive black hole accreting from its host galaxy) in 1965 (3), Gunn and Peterson (4) and (independently) Scheuer (5) and Shklovski (6) pointed out that the spectra of distant quasars should show absorption by neutral hydrogen along the line of sight blueward of their Lyman-α (Lyα) emission line. Refining this calculation, Bahcall and Salpeter (7) argued that the clumpy intergalactic gas should give rise to a collection of discrete absorption lines, termed the "Lyα forest." The following year, observers, particularly Lynds and co-workers (8), indeed saw those lines.

Their exact nature, however, gave rise to a more extended and heated debate. Were the lines—then poorly resolved—really of cosmological origin, or were they instead associated with the quasars themselves? The extreme conditions needed for quasar ejecta to produce the Lyα forest (9), the random redshift distribution of the absorption lines (10), as well as the association of metal-rich systems with intervening galaxies (11), eventually left no doubt that most of the Lyα clouds are in fact cosmological.

Inspired by research on the interstellar medium, the Lyα absorbers were originally envisioned as dense, cool clouds confined by pressure within a hotter, tenuous intercloud background (12, 13). However, this model raised questions of its own, namely, how did the clouds form in the first place? Ultimately, the model simply failed to account for the observed distribution of neutral hydrogen column densities, and other confinement mechanisms involving gravity were also found unsatisfactory.

The key breakthrough in elucidating the nature of the Lyα forest came as astrophysicists tried to understand the formation of structure in the universe. In our current model of structure formation, tiny fluctuations in the primordial plasma grew through the gravitational instability, eventually forming a cosmic network of knots, filaments, and sheets. Because gravity is a purely attractive force, regions of slightly higher density in the early universe accrete matter from their surroundings and grow more overdense with time. As the universe evolves, the cosmic web sharpens: Underdense regions, known as voids, empty material onto the filaments, and this material subsequently flows into overdense knots (Fig. 1). On large scales, where gas pressure can be neglected, intergalactic neutral hydrogen should trace this web.

What if, then, the Lyα forest were simply a representation of the cosmic density field? This was a far-reaching question transcending intergalactic clouds, for its answer not only would provide a powerful test of structure formation

---

Department of Astronomy, Harvard University, 60 Garden Street, Cambridge, MA 02138, USA.

*To whom correspondence should be addressed. E-mail: cgiguere@cfa.harvard.edu

models but also would potentially leave us with a new and exquisitely detailed astrophysical and cosmological probe.

After promising analytical calculations, particularly by Rees (*14*), suggested that absorption by gas confined in dark matter "mini-halos" could account for the basic properties of the Lyα forest, two major developments in the 1990s allowed astrophysicists to tackle the question with unprecedented precision: the advent of high-resolution spectrographs and numerical cosmological simulations. The new High Resolution Echelle Spectrometer (HIRES) spectrograph installed at the Keck Observatories on Mauna Kea, Hawaii, provided quasar spectra with fully resolved Lyα forests. At about the same time, the Cosmic Background Explorer (COBE) satellite had recently detected small anisotropies, subsequently mapped in sharp detail by the Wilkinson Microwave Anisotropy Probe (*15*), imprinted on the cosmic microwave background when the universe was only 400,000 years old (*16*). The COBE observations fueled efforts to model the growth of structure in the universe. Did the minuscule fluctuations in the very early universe observed by COBE actually evolve into the rich structure observed by astronomers? After advances in computer algorithms and technology, first-principles simulations traced the hydrodynamic evolution of cosmic structures from initial conditions motivated by the cosmic microwave background down to the current epoch [see discussion and references in (*17*)]. Zel'dovich did anticipate the cosmic network of filaments, knots, and sheets seen in the simulations. However, the detailed simulations turned the model into a quantitative one, with predictions worthy of comparison against the exacting data now available. Assuming that the Lyα forest originated from absorption by intervening neutral hydrogen, it was then straightforward to produce mock spectra, which could be tested directly against the actual observations (Fig. 2).

The results of these analyses showed that the simulations were exactly right. In particular, the calculations of (*18*, *19*) demonstrated correspondence between observations and theory over nearly eight orders of magnitude in the strength of the absorbing structures, at the time an unprecedented achievement in numerical cosmology. The level of agreement has only improved over the past decade as simulations and observations have been refined and as our knowledge of the underlying cosmological model has become firmer. The conclusion appears inescapable: The primordial fluctuations seen in the cosmic microwave background did grow by five orders of magnitude over billions of years, precisely as calculated, to form the observed cosmic web.

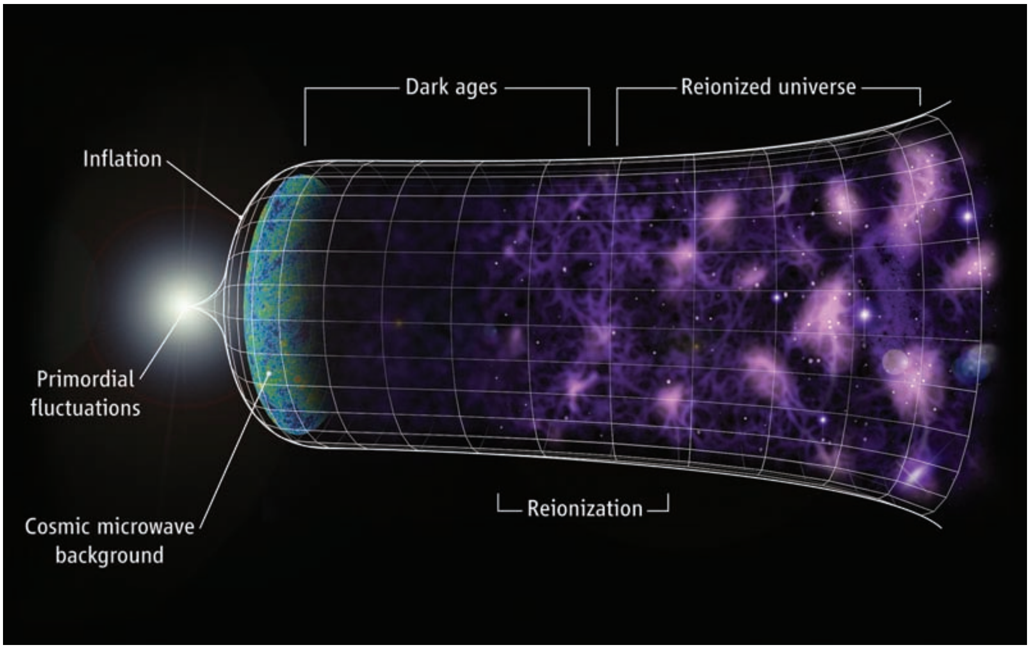

Fig. 1. View of the expanding universe illustrating the evolving cosmic web. Primordial fluctuations of quantum mechanical origin are stretched by an early superluminal phase of expansion known as "inflation." Four hundred thousand years after the Big Bang, these fluctuations imprint tiny anisotropies in the cosmic microwave background as electrons and protons combine to form neutral hydrogen. As the universe continues to expand, these fluctuations grow through the gravitational instability, eventually giving rise to the first stars and galaxies, whose radiation reionizes the intergalactic medium, thereby ending the cosmological "dark ages." The cosmic web sharpens as the universe becomes more mature and becomes visible in the Lyα forest and in the spatial distribution of galaxies.

The discovery of the cosmic web in the Lyα forest has had a broad and profound impact beyond confirming the gravitational instability paradigm for structure formation and explaining the basic properties of the intergalactic medium in a cosmological context. In current hierarchical models of structure formation, condensed objects such as galaxies are thought to form in the denser clumps of the cosmic web. The same numerical simulations that were so successful in explaining quasar absorption systems can thus be used to theoretically calculate the spatial distribution of galaxies, another prediction that can be put to stringent test by observations, and indeed has been vindicated by galaxy surveys. The intergalactic medium probed by current observations is almost fully ionized, owing to the ultraviolet radiation field from star-forming galaxies and the super-massive black holes powering quasars. The imprint of the cosmic web in the Lyα forest, arising from the small residual fraction of neutral gas, thus also traces the cosmic radiation content, providing a unique record of the cosmic history of star formation and black hole growth (*20*).

Observations of the cosmic web have reached beyond astrophysics and into fundamental physics as well. In the paradigm of structure formation that the Lyα forest has been instrumental in establishing, the cosmic web is nothing but an evolved snapshot of the tiny primordial fluctuations produced at the very beginning, in an epoch of "inflation" during which the universe expanded by more than 25 orders of magnitude in size. By measuring the detailed properties of the cosmic web, we can constrain the properties of inflation itself and the physical mechanisms driving it (*21*, *22*). In addition, an overwhelming number of lines of evidence, including galactic rotation curves, the velocity dispersions of galaxy clusters, and gravitational lensing, indicate that the cosmic matter budget is dominated by invisible "dark matter."

Owing to its lack of nongravitational interactions with the rest of the universe, however, the nature of dark matter remains largely a mystery. The leading dark matter candidate is an exotic particle, never yet observed in Earth-bound laboratories, generically referred to as a "weakly interacting massive particle," or WIMP. Observations of large-scale structure through galaxy surveys first ruled out the neutrino as a candidate for "hot" dark matter (*23*), leading to the present cold dark matter paradigm, and are now putting severe upper limits on the neutrino's mass (*24*). The Lyα forest, being more sensitive to smaller scales on

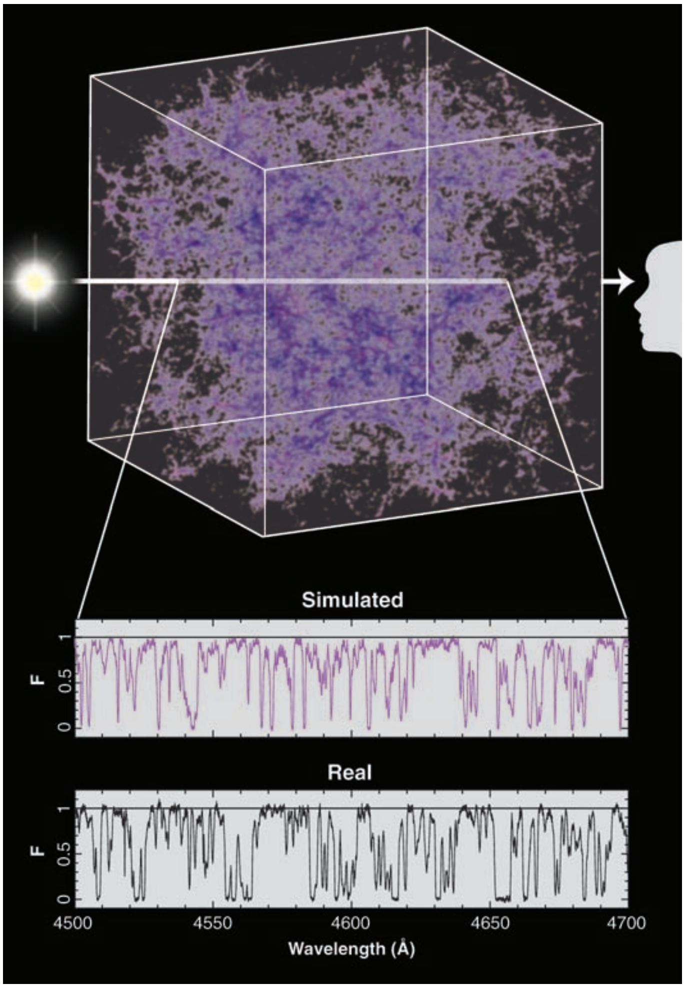

Fig. 2. Illustration of the Lyα forest. An observer looks at a distant quasar. Neutral hydrogen tracing the cosmic web produces absorption features, collectively known as the Lyα forest, in the quasar spectrum. The figure shows a line of sight through a cosmological simulation, with the resulting mock Lyα forest compared to the spectrum of an actual quasar, known as Q1422, and located at redshift $z = 3.6$ (spectrum courtesy of M. Rauch, Observatories of the Carnegie Institution of Washington, Pasadena, CA, and W. Sargent, California Institute of Technology, Pasadena, CA). The similarity between the mock and actual spectra is remarkable, unambiguously elucidating the nature of the Lyα forest as the imprint of cosmological fluctuations. Each spectrum has been normalized by its continuum level.

the order of 1 megaparsec, currently provides the most rigorous constraints on intermediate models of "warm," more massive, dark matter (*25*, *26*).

The bulk of research on cosmic structure, in particular from the Lyα forest and galaxy surveys, has thus far focused on observations in the optical part of the electromagnetic spectrum. Astronomy, however, is an increasingly multiwavelength endeavor, and the study of the cosmic web is poised to follow this trend as new frontiers are explored. Accordingly, new opportunities for novel theoretical calculations and observational discoveries abound.

One of the most exciting frontiers of contemporary cosmology is the early universe, when the first stars and galaxies formed and illuminated their surroundings. During this epoch of "reionization," electrons were unbound from hydrogen atoms (which had combined to become neutral at the time the anisotropies were imprinted in the cosmic microwave background) by ultraviolet radiation, which had begun filling intergalactic space. Neutral hydrogen before and during reionization can potentially be observed through its emission of 21-cm radio radiation. Several low-frequency observatories—such as the Murchison Widefield Array (MWA) in Western Australia, the Low Frequency Array (LOFAR) in the Netherlands and, ultimately, the Square Kilometer Array (SKA)—are being planned, constructed, or entering service to detect this redshifted emission. Simultaneously, ever more powerful infrared telescopes are attempting to discover the first sources of light directly. This is in fact a primary scientific goal of the James Webb Space Telescope, the Hubble Space Telescope's successor scheduled for launch in 2013, as well as of very large ground-based observatories.

New windows are also now opening on the lower-redshift universe. A new ultraviolet spectrograph, the Cosmic Origins Spectrograph (COS), will be installed aboard Hubble during its 2008 servicing mission and will provide a direct and detailed probe of the cosmic distribution of helium at intermediate redshifts. Because more energetic photons are required to doubly ionize helium, it is thought to have been fully ionized later than hydrogen, near the peak of quasar activity. The study of helium reionization thus promises to become a powerful probe of quasar activity and its feedback on the intergalactic medium in the very near future.

At still lower redshifts, the nonlinear growth of cosmic structure shocks the intergalactic medium, heating it to temperatures up to 10^7 K (*27*, *28*). The high temperatures in the local "warm-hot intergalactic medium," or WHIM, imply that yet heavier elements are ionized and hence that higher-energy wavelengths, including x-rays, are the probes of choice for this physical regime.

Each of these observations is, however, accompanied by theoretical challenges. The epochs of hydrogen and helium reionization involve nonequilibrium radiative transfer phenomena, which are only beginning to be included in cosmological simulations. Simulations must evolve large regions of the universe to overcome cosmic variance and capture the large scales of reionization, yet high resolution is needed to resolve the sources and sinks of radiation, as well as the clumpiness of the gas. At the present time, approximations are used to treat the problem with available computational resources and explore the important effects without resorting to prohibitive, fully self-consistent radiation hydrodynamics (*29*, *30*). Feedback processes such as galactic winds and metal enrichment are only crudely, if at all, included and may be particularly important to understand the low-redshift high-energy absorption. Moreover, star and galaxy formation and quasar activity are often modeled using prescriptions, which, albeit physically motivated, do not offer the satisfaction of ab initio calculations.

As the rich array of new and diverse observations promises a wealth of surprises, will the theoreticians be clever enough to provide results with true predictive power for the multiwavelength cosmic web?

References and Notes

1. Y. B. Zel'Dovich, *Astron. Astrophys.* **5**, 84 (1970).
2. J. R. Bond, L. Kofman, D. Pogosyan, *Nature* **380**, 603 (1996).
3. M. Schmidt, *Astrophys. J.* **141**, 1295 (1965).
4. J. E. Gunn, B. A. Peterson, *Astrophys. J.* **142**, 1633 (1965).
5. P. A. G. Scheuer, *Nature* **207**, 963 (1965).
6. I. S. Shklovskii, *Sov. Astron.* **8**, 638 (1965).
7. J. N. Bahcall, E. E. Salpeter, *Astrophys. J.* **142**, 1677 (1965).
8. E. M. Burbidge, C. R. Lynds, G. R. Burbidge, *Astrophys. J.* **144**, 447 (1966).
9. P. Goldreich, W. Sargent, *Comments Astrophys.* **6**, 133 (1976).
10. J. N. Bahcall, P. J. E. Peebles, *Astrophys. J.* **156**, L7 (1969).
11. J. Bergeron, *Astron. Astrophys.* **155**, L8 (1986).
12. W. L. W. Sargent, P. J. Young, A. Boksenberg, D. Tytler, *Astrophys. J. Suppl.* **42**, 41 (1980).
13. J. P. Ostriker, S. Ikeuchi, *Astrophys. J.* **268**, L63 (1983).
14. M. J. Rees, *Mon. Not. R. Astron. Soc.* **218**, 25P (1986).
15. D. N. Spergel *et al.*, *Astrophys. J. Suppl.* **148**, 175 (2003).
16. G. F. Smoot *et al.*, *Astrophys. J.* **396**, L1 (1992).
17. M. Rauch, *Annu. Rev. Astron. Astrophys.* **36**, 267 (1998).
18. L. Hernquist, N. Katz, D. H. Weinberg, J. Miralda-Escude, *Astrophys. J.* **457**, L51 (1996).
19. N. Katz, D. H. Weinberg, L. Hernquist, J. Miralda-Escude, *Astrophys. J.* **457**, L57 (1996).

20. M. Rauch *et al.*, *Astrophys. J.* **489**, 7 (1997).
21. R. A. C. Croft, D. H. Weinberg, N. Katz, L. Hernquist, *Astrophys. J.* **495**, 44 (1998).
22. P. McDonald *et al.*, *Astrophys. J.* **635**, 761 (2005).
23. S. D. M. White, C. S. Frenk, M. Davis, *Astrophys. J.* **274**, L1 (1983).
24. U. Seljak, A. Slosar, P. McDonald, *J. Cosmol. Astropart. Phys.* **10**, 14 (2006).
25. M. Viel, J. Lesgourgues, M. G. Haehnelt, S. Matarrese, A. Riotto, *Phys. Rev. Lett.* **97**, 071301 (2006).
26. U. Seljak, A. Makarov, P. McDonald, H. Trac, *Phys. Rev. Lett.* **97**, 191303 (2006).
27. R. Cen, J. P. Ostriker, *Astrophys. J.* **514**, 1 (1999).
28. R. Davé *et al.*, *Astrophys. J.* **552**, 473 (2001).
29. M. McQuinn *et al.*, *Mon. Not. R. Astron. Soc.* **377**, 1043 (2007).
30. O. Zahn *et al.*, *Astrophys. J.* **654**, 12 (2007).

10.1126/science.1151476

PERSPECTIVE

Missing Baryons and the Warm-Hot Intergalactic Medium

Fabrizio Nicastro,[1,2] **Smita Mathur,**[3] **Martin Elvis**[1]

Stars and gas in galaxies, hot intracluster medium, and intergalactic photo-ionized gas make up at most half of the baryons that are expected to be present in the universe. The majority of baryons are still missing and are expected to be hidden in a web of warm-hot intergalactic medium. This matter was shock-heated during the collapse of density perturbations that led to the formation of the relaxed structures that we see today. Finding the missing baryons and thereby producing a complete inventory of possibly the only detectable component of the energy-mass budget of the universe is crucial to validate or invalidate our standard cosmological model.

Despite recent progress in cosmology in assaying the energy and mass budget of the universe, very little is still known about the nature and origin of most of its constituents. Within the framework of our standard cosmological model (SCM) (*1*, *2*), most (95%) of the universe (or Ω, the mass density of the universe divided by the critical density required to close the universe) is composed primarily of "dark" energy (70%) and "dark" matter (25%), both dubbed "dark" as a reflection of our inability to directly detect and identify them. Less well known is that the situation is only marginally better for the universe's remaining 5% of detectable matter.

As baryons—the protons and atomic nuclei that constitute the ordinary matter of which stars, planets, and ourselves are made—this remaining matter should, in principle, be in a form that we can detect and measure in its physical state. We know from absorption line spectroscopy of distant quasars that clouds of baryons were present in the early universe about 10 billion years ago (redshift $z \cong 2$) (*3*, *4*)), in the form of photo-ionized diffuse intergalactic gas, accounting for at least three-quarters of the total baryon mass in the universe as inferred by both cosmic microwave background anisotropies (*1*, *2*) and "big-bang nucleosynthesis" predictions when combined with observed light-element ratios at $z > 2$ (*5*) ($\Omega_b > 3.5\%$, i.e., >73% of the estimated baryon mass in the universe). However, these clouds of photo-ionized intergalactic gas became more and more sparse as time moved toward the present and structures (galaxies, galaxy groups, and clusters) started to be assembled. Only a small fraction of the baryons that were present in the intergalactic medium at $z > 2$ are now found in stars, cold or warm interstellar matter, hot intracluster gas, and residual photo-ionized intergalactic medium. Today we can account for less than 50% of the baryon mass predicted by the SCM, implying that at least 50% of the baryons are now "missing" (*6*, *7*) (Fig. 1).

The leading theory of cosmological structure formation (known as Λ-CDM; or, cold dark matter models including dark energy, designated by the cosmological constant Λ) predicts that, as the universe evolves toward the present and density perturbation grows to form structures, baryons in the diffuse intergalactic medium accelerate toward the sites of structure formation under the growing influence of gravity and go through shocks that heat them to temperatures of millions of kelvin. These "missing baryons" may have become difficult to detect by being concentrated in a filamentary web of tenuous (baryon density

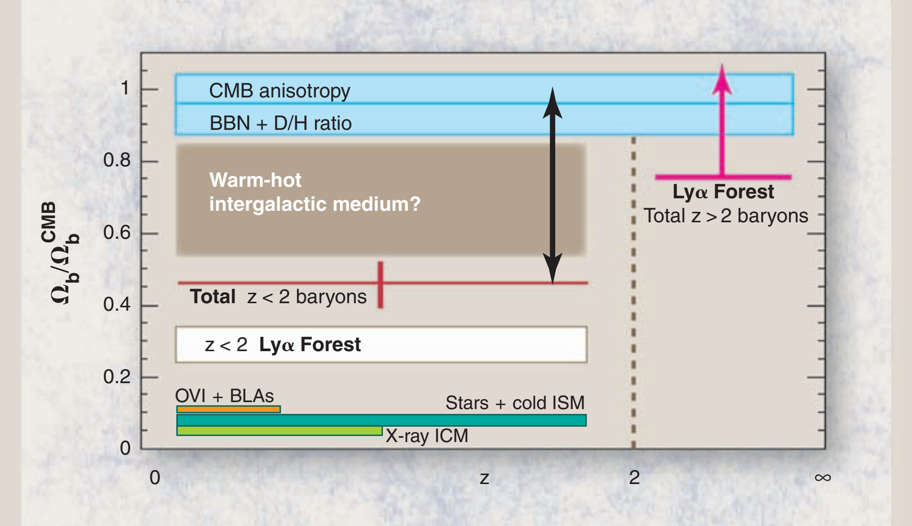

Fig. 1. Baryon density in the universe, at all redshifts, normalized to the cosmological mass density of baryons derived from cosmic microwave background (CMB) anisotropy measurements. Two completely independent measures, based on anisotropies of the CMB, on one hand, and on observations of the deuterium-to-hydrogen (D/H) ratio combined with big bang nucleosynthesis (BBN) models, on the other, nicely converge toward a total cosmological mass density of baryons in the universe of ~4.5% (cyan shaded rectangle). At redshifts $z > 2$, nearly all the expected baryons are found in the Lyα forest (magenta lower limit; the measure is a lower limit due to uncertainties in the ionization correction). At $z \leq 2$, however, adding up the baryons observed in stars and cold interstellar medium (ISM) in galaxies, residual low-*z* Lyα forest, OVI and BLA absorbers, and x-ray hot gas in clusters of galaxies accounts for less than half of the expected cosmological mass density of baryons in the universe (red point). The rest of the baryons still elude detection, and hence are "missing baryons." A theoretical solution to this problem has been relatively recently offered by hydrodynamical simulations for the formation of structures in the universe.

---

[1] Harvard-Smithsonian Center for Astrophysics, Cambridge, MA 02138, USA. [2] Osservatorio Astronomico di Roma–Istituto Nazionale di Astrofísica, Rome I-00040, Italy. [3] Ohio State University, Columbus, OH 43210, USA.

*To whom correspondence should be addressed. E-mail: fnicastro@cfa.harvard.edu

$n_b \cong 10^{-6}$ to 10^{-5} cm^{-3}, corresponding to overdensities of $\delta = n_b/\langle n_b \rangle \cong 5$ to 50, compared with the average baryon density in the universe $\langle n_b \rangle = 2 \times 10^{-7}$ cm^{-3}) warm-hot intergalactic medium (WHIM) that has been continuously shock-heated during the process of structure formation [e.g., (*8*)]. This matter is hot (10^5 to 10^7 K) and is so highly ionized that it can only absorb or emit far-ultraviolet (FUV) and soft x-ray photons, primarily at lines of highly ionized (Li-like, He-like, or H-like) C, O, Ne, and Fe [e.g., (*9*)].

If identifying the mysterious dark energy and dark matter is challenging, then the problem of missing baryons is more acute. One could even argue that baryons represent the only directly detectable component of the predicted mass-energy budget of the universe [e.g., (*10*, *11*)]. Moreover, determining the physical conditions, metal (heavy element) content, dynamics, and kinematics of these baryons, as a function of cosmic time, gives us a unique set of tools to study the evolution of large-scale structure (LSS) in the universe and the feedback mechanisms of gas ejected from galaxies and quasars onto LSS in the framework of such models [e.g., (*12*)].

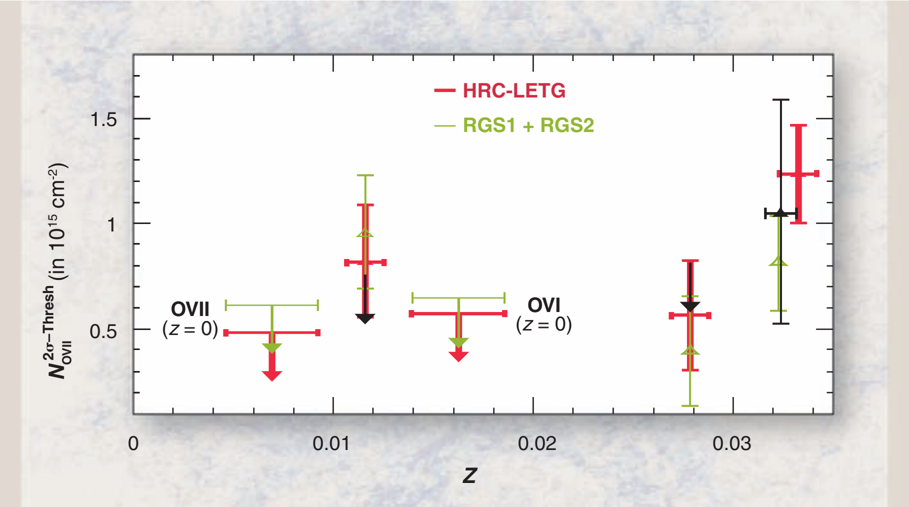

Fig. 2. Measurements (with associated 1σ errors) and 2σ upper limits of OVII column densities from $z = 0$ to $z = 0.03$ (the redshift of Mkn 421), as derived from the Chandra LETG (red symbols) spectrum of Mkn 421 (*14*, *15*) and our (green symbols) and Rasmussen *et al.*'s (*17*) (black symbols) analyses of the XMM-*Newton* RGS spectrum of Mkn 421. The two bins at $z = 0$ to 0.004 and $z = 0.020$ to 0.024 contain absorption lines both in the LETG and RGS spectra, noncontroversially identified as $z = 0$ OVII and OVI transitions, and are not shown in this figure. In Rasmussen *et al.*, analysis of the RGS spectrum, the upper limits at $z = 0.011$ and $z = 0.027$ (black arrows) are fully consistent with the Chandra measurements within their 1σ statistical errors (red points). Moreover, in our analysis of the RGS spectrum of Mkn 421, we actually detect absorption lines at these two positions (green points at $z = 0.011$ and $z = 0.027$), with intensities consistent with those of the lines detected in the Chandra spectrum of Mkn 421.

This program of tracking the cosmic baryons can only be carried out by exploiting the synergies between multiwavelength observational approaches and theoretical computations: High-resolution x-ray and UV spectroscopy measures (i) relative and absolute metal content, (ii) ionization correction, and so (iii) mass of the WHIM filaments; optical and infrared multifilter photometry and spectroscopy measure the galaxy density around WHIM filaments, and so map dark-matter concentrations in the universe. These observations can then be used to feed and hence refine new simulations, to study and address the fundamental problem of feedback between virialized structures and the surrounding diffuse intergalactic medium. All this has only relatively recently become possible thanks to the advent of sufficiently high-resolution x-ray and UV optics {Chandra and Hubble Space Telescope (HST) and spectrometers [gratings on Chandra, HST, XMM-*Newton* (XMM, X-ray Multimirror Mission)] plus the Far Ultraviolet Spectroscopic Explorer (FUSE)}, on one hand, and the rapidly increasing power of today's computational resources (such as high-resolution hydrodynamical simulations, refined and extended atomic-data computations, nonequilibrium postshock ionization modeling), on the other.

Because of the extreme low density (1 to 10 particles per cubic meter) and relatively small size (1 to 10 Mpc) of the WHIM filaments, the intensity of the signal expected from the WHIM observables (either in emission or in absorption) is low, both in the UV and in the x-ray band. This makes the search for the missing baryons particularly challenging.

Direct detection of the emission signal from the WHIM requires ideally large field of view and effective area imager-spectrometers, a combination that is not yet available. The most promising observational strategy with current instrumentation is to search for the WHIM in absorption (as discrete absorption lines) in the UV and x-ray spectra of bright, intrinsically featureless, background astrophysical sources.

At WHIM temperatures, the dominant ions of oxygen (the most abundant metal in gas with solar-like composition) are OVII (≅80% of oxygen in the entire WHIM temperature range) and OVI (≅20% of oxygen at the low end of the WHIM temperature distribution). The strongest transitions from these ions are the OVI $1s^2 2s \rightarrow 1s^2 2p$ doublet at 1031.9 and 1037.6 Å (UV) and the OVII Kα resonant at 21.6 Å (x-rays). The key to the detectability of an absorption line is the transition contrast, i.e., the ratio between the line wavelength and its equivalent width (EW), compared with the spectrometer resolving power. The line transition contrast expected from the WHIM is similar in the UV and the x-ray band: $[1031.9/\mathrm{EW}(\mathrm{OVI}\lambda_{1031.9})] \geq 1500$ to 15,000 versus $[21.6/\mathrm{EW}(\mathrm{OVII}\lambda_{21.6})] \geq 2700$ to 27,000. However, although the resolving power of the current UV spectrometers is similar to or better than the OVI transition contrast, in the x-ray band the situation is worse. Consequently, despite the dominant distribution of OVII expected in the WHIM (tracking 70 to 80% of the WHIM mass) compared to OVI, the search for the WHIM, so far, has been much more fruitful in the UV than in the x-ray band [e.g. (*7*, *13*)].

Hydrodynamical simulations for the formation of LSS in the universe [e.g., (*8*)] successfully reproduce the measured number of OVI absorbers per unit redshift interval with EW larger than a given threshold (*7*, *9*). Danforth and Shull (*7*) estimated the contribution of the WHIM baryons detectable through OVI absorption down to an OVI column density of $N_{OVI} > 10^{13.4}$ cm^{-2} (i.e., the low-temperature end of the WHIM mass distribution) to Ω, and found that it is, at most, only 10% of the missing baryons ($\Omega_{OVI} = 0.22\%$).

An alternative, and complementary, way of searching for the missing mass in the local universe is to look for hydrogen absorption in the form of broad Lyα absorbers (BLAs). At WHIM temperatures most of the H is ionized, but the residual HI (neutral hydrogen) can still imprint Lyman series absorption onto the UV spectra of background objects; these absorption lines must therefore be broad (with widths given by Doppler parameter $b \geq 42$ km s^{-1}, for temperatures $\log T \geq 5$). Richter and collaborators (*13*) analyzed HST spectra from the lines of sight to four bright active galactic nuclei (AGN) and found that the fraction of Ω detectable through BLAs down to $N_{HI}/b > 10^{11.3}$ cm^{-2} km^{-1} s is $\Omega_{BLAs} = 0.27\%$, similar to the contribution to Ω detectable through OVI absorbers, and again only ~10% of the missing baryons. These studies prove not only that both BLAs and OVI absorbers can be considered potential good tracers of the WHIM, but also that the WHIM itself has mostly likely been already detected through these two transitions in the UV band. However, owing to the high temperature of the WHIM, only a relatively small fraction of the WHIM distribution can be probed by BLAs and OVI absorbers; the vast majority (70 to 80%) of the missing mass remains to be found via the x-ray band.

Owing to the observational difficulty of making these measurements, they are controversial. The statistically strongest evidence to date comes from a Chandra LETG (low-energy transmission grating spectrometer) spectrum of the nearby ($z = 0.03$) blazar Mkn 421 that shows a number of absorption lines, some identified with two different intervening WHIM systems at $z = 0.011$ and $z = 0.027$ (*14*, *15*) at significances of 3.5σ and 4.9σ, respectively. However, analysis of a better signal-to-noise (S/N), but poorer spectral resolution, XMM-*Newton* reflection grating spectrometer (RGS) spectrum of Mkn 421 does not show some of these absorption lines (*16–18*). We note (*16*), however, that both sets of observations are consistent within observational errors (Fig. 2). Further observations are thus required to definitely confirm or rule out the proposed WHIM detections along this line of sight.

Deep WHIM studies require both the UV and the x-ray bands. The x-ray band is crucial to detect the WHIM systems and derive an accurate ionization correction. The UV band is vital to measure the associated amount of HI and hence the baryonic mass in each system, which otherwise depends on the ratio of heavier elements to hydrogen (the "abundances"). The full potentiality of UV WHIM studies will be available only after the Shuttle Servicing Mission 4 has restored spectral capabilities to the HST; the new COS UV spectrograph will provide spectra of accurately selected bright x-ray targets with a S/N ratio sufficient to detect BLAs. In the x-ray band, the situation is far more challenging because future instruments are some way off. Current observational facilities should first be exploited to their limits.

According to theory, the chances of finding a WHIM filament along a random line of sight in the universe increases with (i) the crossed path length between the observer and the beacon used to obtain x-ray images of the intervening space, and (ii) the inverse of the baryon column density in the filament: The larger the amount of baryons in the filament, the lower the probability of finding one. Observationally, instead, the chances of detecting such systems increase with the square root of (i) the detector throughput (the effective area A_{eff}), (ii) the spectrometer resolving power ($R = \lambda/\Delta\lambda$), and (iii) the amount of dedicated observing time (Δt); for a given instrument, A_{eff} and R are fixed parameters, and only the observation exposure Δt can be chosen.

It can be shown that detection of the WHIM is within the reach of current instrumentation, but it requires very long observations, on the order of several million seconds. Hydrodynamical simulations predict (*9*) a 95.5% chance of finding at least one OVII WHIM system with a column density $N_{\mathrm{OVII}} \geq 8 \times 10^{14}\ \mathrm{cm}^{-2}$ along any random line of sight between $z = 0$ to 0.3. This probability increases to 99.7% when N_{OVII} is less than half this value. For background targets with a quiescent soft x-ray flux of ≥ 1 mCrab (of which there are few), ~2 to 3 Ms and ~10 Ms are required, with either the LETG or the RGSs, to become sensitive, at a statistical significance ≥3σ, to $N_{\mathrm{OVII}} = 8 \times 10^{14}\ \mathrm{cm}^{-2}$ and $N_{\mathrm{OVII}} = 4 \times 10^{14}\ \mathrm{cm}^{-2}$, respectively. Combined LETG and RGS exposures of up to ~10 Ms, therefore, would certainly allow us to either detect the WHIM or to disprove models.

Deep WHIM studies, however, await future missions. Constellation-X (*19*) [and to a similar extent XEUS (*20*) or any of the several proposed mission concepts dedicated to WHIM studies, e.g., Pharos (*21*) or Edge (*22*)] will allow us to study ~60 different lines of sight toward all the available extragalactic targets at $z \geq 0.3$ and with quiescent soft x-ray flux ≥ 0.2 mCrab, with average exposures of ≤100 ks each. Lowering the flux threshold by a factor of only 2 (from 0.2 to 0.1 mCrab) would more than double the number of available targets, and hence the number of lines of sight, requiring only twice as deep exposures per line of sight.

Alternative baryon reservoirs had been proposed before hydrodynamical simulations, run in the framework of a Λ-CDM universe, became available, which include, for example, large amounts of cold molecular gas around galaxies (*23*) or tenuous intragroup hot gas [e.g., (*7*)]. However, these scenarios clash with the outcome of Λ-CDM simulations, which all agree in predicting the WHIM as the main reservoir of baryons in the local universe. In the next decade, we will be in a position to trace all the WHIM baryons in the universe and so either see whether the missing baryon problem still holds or validate theoretical predictions and the SCM.

References and Notes

1. C. L. Bennett *et al.*, *Astrophys. J.* **148** (suppl.), 1 (2003).
2. D. N. Spergel *et al.*, *Astrophys. J.* **148** (suppl.), 175 (2003).
3. M. Rauch, *Annu. Rev. Astron. Astrophys.* **36**, 267 (1998).
4. D. Kirkman *et al.*, *Astrophys. J.* **149** (suppl.), 1 (2003).
5. D. H. Weinberg, *Astrophys. J.* **490**, 564 (1997).
6. M. Fukugita, http://arxiv.org/abs/astro-ph/0312517v1 (2003).
7. C. W. Danforth, M. J. Shull, *Astrophys. J.* **624**, 555 (2005).
8. R. Cen, J. P. Ostriker, *Astrophys. J.* **650**, 560 (2006).
9. R. Cen, T. Fang, *Astrophys. J.* **650**, 573 (2006).
10. S. D. M. White, http://arxiv.org/abs/0704.2291v1. (2007).
11. A. Albrecht, http://arxiv.org/abs/0710.0867 (2007).
12. J. T. Stocke *et al.*, *Astrophys. J.* **641**, 217 (2006).
13. P. Richter *et al.*, *Astron. Astrophys.* **445**, 827 (2006).
14. F. Nicastro *et al.*, *Nature* **433**, 495 (2005).
15. F. Nicastro *et al.*, *Astrophys. J.* **629**, 700 (2005).
16. R. Williams *et al.*, *Astrophys. J.* **642**, L95 (2006).
17. J. Rasmussen *et al.*, *Astrophys. J.* **656**, 129 (2007).
18. J. Kaastra *et al.*, *Astrophys. J.* **652**, 189 (2006).
19. http://constellation.gsfc.nasa.gov/index.html.
20. www.rssd.esa.int/index.php?project=xeus.
21. M. Elvis *et al.*, http://arxiv.org/abs/astro-ph/0303444. (2003).
22. L. Piro *et al.*, *Proc. SPIE* **6266**, 62660K (2006).
23. D. Pfenniger, F. Combes, *Astron. Astrophys.* **285**, 94 (1994).

24. F.N. acknowledges support from NASA Long-Term Space Astrophysics grant NNG04GD49G.

10.1126/science.1151400

Rarity of Males in Pea Aphids Results in Mutational Decay

Jennifer A. Brisson* and Sergey V. Nuzhdin†

The pea aphid, *Acyrthosiphon pisum*, has a complex life cycle that alternates seasonally between asexual and sexual reproduction (*1*). During the spring and summer months, *A. pisum* reproduces parthenogenetically, producing clonal daughters for 10 to 20 generations. Fall temperatures and photoperiods induce the production of sexual females and males (*2*), which mate to produce overwintering eggs that hatch into asexual females [Supporting Online Material (SOM) text].

Asexual females dominate the life cycle because of their short generation time, high fecundity, and longer seasonal presence. We hypothesized that males experience relaxed selection, resulting in accelerated evolution of male-biased genes relative to asexual female–biased genes.

In a previous study, whole-body asexual female and male RNA was hybridized on an *A. pisum* cDNA microarray representing ~10% of the genome (1734 unique genes) (*3*). We identified significantly different transcript accumulation between sexes via *t* test with a false discovery rate (FDR) < 0.05 and at least a twofold change in expression, yielding 107 asexual female–biased, 127 male-biased, and 95 sex-neutral genes (SOM text).

We identified orthologs of *A. pisum* genes in Genbank from the green peach aphid, *Myzus persicae* [in the same tribe as *A. pisum* (Macrosiphini)], and the cotton-melon aphid, *Aphis gossypii* [in the same subfamily but a different tribe (Aphidini)] (*4*). When comparing *A. pisum* and *M. persicae* orthologs, we found no differences between asexual female-biased and neutral nonsynonymous (K_a) and synonymous (K_s) rates of evolution, nor between their ratios (K_a/K_s). However, both K_a and K_a/K_s were significantly larger (Mann-Whitney U test, $P < 0.002$, all comparisons) in male-biased genes compared with those of asexual female–biased and neutral genes (Fig. 1). Male-biased genes also were more divergent, relative to neutral and female-specific genes, in comparisons of *A. pisum* with *A. gossypii* with K_a and K_a/K_s significantly larger (P = 0.016, 0.001 and 0.026, 0.002, respectively). We found no evidence for codon bias (table S1), and it is unknown what proportion of these genes is X-linked versus autosomal.

Transcript accumulation level and sex specificity on K_a/K_s values were examined because genes with high levels of transcript accumulation evolve slower than genes with low transcript accumulation (*5*). Two-way analysis of variance (ANOVA) with expression level and sex bias established significance of both terms (mean square = 0.1365, F = 25.45, $P <$ 0.0001 and mean square = 0.6535, F = 121.86, $P <$ 0.0001; respectively). Thus, although weakly expressed genes evolve faster than genes with higher transcript levels, the effect of sex is much stronger.

This accelerated rate of male-biased gene evolution is consistent with both positive and relaxed selection. In some species, accelerated evolution of male-biased genes is influenced by positive selection on reproductive proteins (*6*). This may be true in *A. pisum*, but it is not likely the case for the genes examined here. Because the microarray was constructed from expressed sequence tags (ESTs) from asexual female cDNA libraries, we did not assay exclusively male-specific transcripts and probably underestimated the overall rate of acceleration of evolution of male-biased genes.

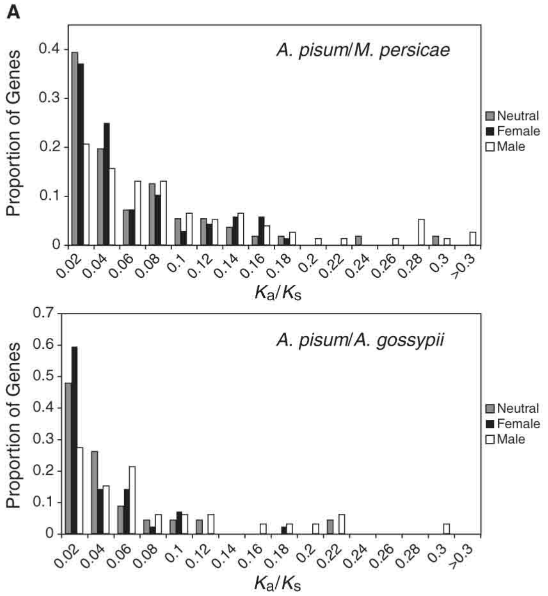

B

Parameter	Male-biased genes	Asexual female-biased genes	Neutral genes
	M. persicae		
N	77	67	56
K_a	0.023	0.015	0.012
K_s	0.262	0.231	0.245
K_a/K_s	0.091	0.047	0.050
	A. gossypii		
N	33	42	23
K_a	0.032	0.010	0.012
K_s	0.416	0.330	0.371
K_a/K_s	0.071	0.029	0.036

Fig. 1. (**A**) Distribution of K_a/K_s values for each class of gene and each species comparison. (**B**) Evolutionary rates for genes with sex-biased or sex-neutral expression in comparisons of *A. pisum* to *M. persicae* and *A. gossypii*.

To distinguish between relaxed and positive selection, we sequenced 14 female- and 13 male-biased genes from 12 geographically disparate *A. pisum* clones and noted nonsynonymous and synonymous changes (table S2, averaging ~10 individuals per locus). Despite low coding region diversity, we found significantly more nonsynonymous changes in male-biased genes (five versus zero; Fisher's exact test, P = 0.05). We also observed an excess of nonsynonymous changes in male-biased genes between *A. pisum* and *M. persicae* homologs ($P <$ 0.001, table S3) consistent with the K_a/K_s comparisons, and the numbers of nonsynonymous changes were consistent between interspecific and intraspecific data sets (P = 0.30 and 0.26 for asexual female–biased and male-biased genes, respectively). The excess of nonsynonymous coding changes and consistency between interspecific and intraspecific patterns support relaxed, rather than positive, selection on male-biased genes in *A. pisum*.

Our data show that the dominance of the life cycle by parthenogenetic females can result in the mutational decay of male-biased genes. Whereas asexual female–biased genes are under constant selection, male-biased genes experience selection at most once per year (SOM text). Sexual selection may further reduce the effective population size of males, resulting in the fixation of weakly deleterious mutations (*7*). If relaxed selection alone is sufficient to produce accelerated male-biased gene evolution, we predict a similar pattern of decay in sexual female–biased genes. We conclude that the variation in genes related to males and asexual females are different in species combining sexual and asexual reproduction. These findings suggest new prospects for the role of sexual versus asexual reproduction in the adaptability of species to various environmental conditions.

References and Notes

1. N. A. Moran, *Annu. Rev. Entomol.* **37**, 321 (1992).
2. S. Via, *Entomol. Exp. Appl.* **65**, 119 (1992).
3. J. A. Brisson, G. K. Davis, D. L. Stern, *Evol. Dev.* **9**, 338 (2007).
4. C. D. Von Dohlen, C. A. Rowe, O. E. Heie, *Mol. Phylogenet. Evol.* **38**, 316 (2006).
5. S. Subramanian, S. Kumar, *Genetics* **168**, 373 (2004).
6. A. Civetta, R. S. Singh, *Genome* **42**, 1033 (1999).
7. W. G. Hill, A. Robertson, *Genet. Res.* **8**, 269 (1966).
8. J.A.B. is supported by an National Research Service Award postdoctoral fellowship from the NIH, and S.V.N. is supported by NSF and NIH. Thanks to G. Davis and D. Stern for sharing unpublished data, P. Hui for laboratory assistance, and C. Braendle and T. Leonardo for aphid samples.

Supporting Online Material

www.sciencemag.org/cgi/content/full/319/5859/58/DC1
Materials and Methods
SOM Text
Tables S1 to S8
References

17 July 2007; accepted 23 October 2007
10.1126/science.1147919

Section of Ecology and Evolution, University of California, Davis, CA 95616, USA.

*To whom correspondence should be addressed. E-mail: jabrisson@ucdavis.edu

†Present address: University of Southern California, Los Angeles, CA 90089, USA.

Physiological Sex Predicts Hybrid Sterility Regardless of Genotype

John H. Malone* and P. Michalak†

Haldane's rule states that the heterogametic sex (ZW or XY) suffers the most negative effects of interspecific hybridization and has been observed across taxa, including fruit flies, butterflies, birds, and mammals (*1*, *2*). The ubiquity of Haldane's rule implies that common systems isolate and maintain distinct biological species, and the mechanisms underlying Haldane's rule have been identified (*2*), although exceptions to this rule have been documented.

Female *Xenopus* frogs have heterogametic sex chromosomes (ZW), whereas males are homogametic (ZZ). In over 100 crosses across more than 20 species, males are sterile and females are fertile (*3*), opposite the prediction of Haldane's rule for sterility. Dominance effects, in which deleterious alleles are fully expressed in the heterogametic sex, explains Haldane's rule in organisms with ZW sex determination (i.e., birds and butterflies). However, dominance cannot explain male sterility in hybrid *Xenopus* because in the heterogametic sex, in this case females, Z-linked recessive alleles should cause hybrid dysfunction and, yet, hybrid females are fertile.

The faster-male evolution hypothesis suggests that either (i) spermatogenesis is sensitive to perturbations occurring in hybrids and/or (ii) sexual selection on male-specific genes drives them to evolve faster than female-specific genes, leading to hybrid male defects (*4*, *5*). We hypothesized that the faster-male hypothesis explains why females are fertile in *Xenopus*. We created sex-reversed *Xenopus laevis* × *X. mueller* hybrids, dissecting sex chromosome effects from physiological sex effects, resulting in Z_LZ_M genetic males (subscripts denote the origin of chromosomes from either *X. laevis* or *X. mueller* that are phenotypically female and Z_LW_M genetic females that are phenotypically male.

Sex-reversed hybrid females did not differ in the number of fertilized eggs and the proportion of eggs that hatched into tadpoles relative to normal hybrid females. Nor were there differences in the number of eggs laid during mating (Fig. 1A). Both normal and sex-reversed hybrid males failed to fertilize any eggs. Conspecific males fertilize females in vivo in 100% of crosses with a fertilization rate of 62 to 63%. Normal hybrid males are completely sterile and have a dramatically lower abundance of sperm compared to conspecifics (*6*). These results demonstrate that sex-reversed hybrid males and sex-reversed hybrid females have the same phenotype as normal hybrid individuals, despite their inverse genetic background. Hierarchical clusterings of microarray gene expression profiles (Fig. 1B) support that sex reversal is phenotypically complete, because we detected no evidence of differential expression between normal and sex-reversed females and males. These results suggest that the W chromosome in *Xenopus* bears few, if any, genes expressed in adult gonads and consists mainly of loci controlling the developmental regulation of physiological sex.

A

		% Eggs Fertilized and Dividing			% Fertilized Eggs that Hatched into Tadpoles			Total Number of Eggs Deposited		
Phenotype	Genotype	Mean	SD	N	Mean	SD	N	Mean	SD	N
Phenotypic Females	ZW	0.52	0.27	8	0.51	0.34	6	2088.7	1390.9	7
	ZZ	0.52	0.28	9	0.56	0.29	8	1388.3	1151.5	9
ANOVA (ZW vs. ZZ)		$F_{1,15}$=0.0004; P=0.995			$F_{1,12}$=0.1013; P=0.756			$F_{1,14}$=1.22; P=0.289		
Phenotypic Males	ZW	0	-	3	-			-		
	ZZ	0	-	15	-			-		

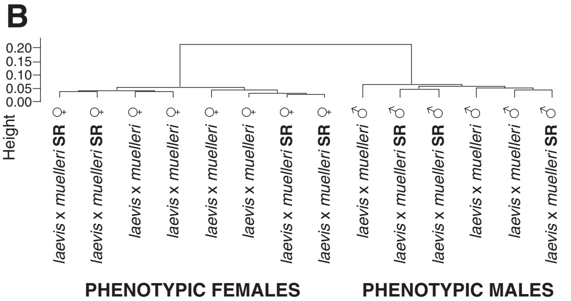

Fig. 1. (**A**) Fertility of crossed ZW and ZZ individuals of the same phenotypic sex. SD indicates standard deviation; *N*, sample size. (**B**) Hierarchical clustering of gene expression data for normal and sex-reversed hybrids of *X. laevis* × *X. muelleri*. FDR-corrected moderated *t* tests reveal no difference in gene expression between normal and sex-reversed females and normal and sex-reversed males. ♀, normal female (ZW); ♂, normal male (ZZ); SR ♀, sex-reversed female (ZZ); and SR ♂, sex-reversed male (ZW).

These results support the faster male evolution hypothesis. First, fertility and expression profiles matched both normal and sex-reversed individuals. Hybrid males, both normal and sex-reversed, were sterile, whereas both types of hybrid females were fertile. Physiological maleness appears to be the most important predictor of sterility, rather than chromosomal background, and implies that gene dosage effects (*7*) do not affect normal oogenesis and spermatogenesis. Given these results, it is difficult to determine whether sterility results from the sensitivity of spermatogenesis and/or sexual selection on male-specific genes because both genetic backgrounds yielded the same phenotype. However, more genes have been identified in testis compared with ovary in both *X. laevis* and *X. muelleri*, suggesting that spermatogenesis is more easily perturbed than oogenesis in hybrids. Interestingly, gene expression differences between species were more pronounced for female-specific genes compared with male-specific genes (*8*), suggesting that changes in expression of female-specific genes occur faster than in male-specific genes. This suggests that male sterility is not due to selection or divergence of male-specific genes. Overall, evidence suggests that spermatogenesis is sensitive to gene expression, perhaps because of the more numerous genes involved, and is easily perturbed in a hybrid genetic background. The role of female gene expression divergence and our data suggest that organisms with ZW sex determination differ in how they produce patterns of postzygotic reproductive isolation.

References and Notes

1. J. B. S. Haldane, *J. Genet.* **12**, 101 (1922).
2. J. A. Coyne, H. A. Orr, *Speciation* (Sinauer, Sunderland, MA, 2004), pp. 283–319.
3. H. R. Kobel, in *The Biology of Xenopus*, R. C. Tinsley, H. R. Kobel, Eds. (Clarendon, Oxford, 1996), pp. 391–401.
4. C.-I. Wu, A. W. Davis, *Am. Nat.* **142**, 187 (1993).
5. C.-I. Wu, N. A. Johnson, M. F. Palopli, *Trends Ecol. Evol.* **11**, 281 (1996).
6. J. H. Malone, T. H. Chrzanowski, P. Michalak, *PLoS ONE* **2**, e781 (2007).
7. Y. Zhang, B. Oliver, *Curr. Opin. Genet. Dev.* **17**, 113 (2007).
8. J. H. Malone, D. L. Hawkins Jr., P. Michalak, *J. Mol. Evol.* **63**, 427 (2006).
9. This work was conducted following the protocols of the University of Texas–Arlington Animal Care Committee (protocol no. A05.001). We thank R. C. Tinsley for donating *X. muelleri*; M. Ito for W chromosome marker primer sequences; and J. Malcom, D. C. Forsdyke, and anonymous reviewers for comments. Funded by an NSF Dissertation Improvement Grant (DEB-0508882) and a Texas Academy of Science Student Research Grant to J.H.M. and a SPRING Research and Nanotechnology Transfer Program Strategic Partnership for Research in Nanotechnology Grant (26-0201-31) to P.M. Microarray data have been deposited in Gene Expression Omnibus, accession GSE9507.

Supporting Online Material

www.sciencemag.org/cgi/content/full/319/5859/59/DC1
Materials and Methods
Figs. S1 and S2
References

23 July 2007; accepted 6 November 2007
10.1126/science.1148231

Department of Biology, University of Texas at Arlington, Box 19498, Arlington, TX 76019, USA.

*Present address: Laboratory of Cellular and Developmental Biology, National Institute of Diabetes and Digestive and Kidney Diseases, National Institutes of Health, Department of Health and Human Services, Building 50, Room 3314, Bethesda, MD 20892, USA.

†To whom correspondence should be addressed. E-mail: michalak@uta.edu

Reduced North Atlantic Deep Water Coeval with the Glacial Lake Agassiz Freshwater Outburst

Helga (Kikki) Flesche Kleiven,[1,3]* Catherine Kissel,[2] Carlo Laj,[2] Ulysses S. Ninnemann,[1,3] Thomas O. Richter,[4] Elsa Cortijo[2]

An outstanding climate anomaly 8200 years before the present (B.P.) in the North Atlantic is commonly postulated to be the result of weakened overturning circulation triggered by a freshwater outburst. New stable isotopic and sedimentological records from a northwest Atlantic sediment core reveal that the most prominent Holocene anomaly in bottom-water chemistry and flow speed in the deep limb of the Atlantic overturning circulation begins at ~8.38 thousand years B.P., coeval with the catastrophic drainage of Lake Agassiz. The influence of Lower North Atlantic Deep Water was strongly reduced at our site for ~100 years after the outburst, confirming the ocean's sensitivity to freshwater forcing. The similarities between the timing and duration of the pronounced deep circulation changes and regional climate anomalies support a causal link.

An abrupt cooling event ~8200 years before the present (B.P.) [centered between 8.21 and 8.14 thousand years (ky) B.P. (*1*)] is the most extreme climatic anomaly in the Greenland ice core δ^{18}O records during the otherwise relatively quiescent Holocene period (*2*–*4*). Associated anomalies in various marine and terrestrial proxy records demonstrate that climate change at this time, although most pronounced in Greenland and around the North Atlantic, had a broad and variable expression within the Northern Hemisphere and tropics (*5*, *6*). Identifying the antecedents of such an unusually extreme and widely felt Holocene perturbation is important, particularly for predicting how climate may change, but records that can be used to test the mechanisms hypothesized to have caused the event have been elusive.

Alley *et al.* (*4*) originally postulated that this climate anomaly could have been driven by changes in ocean overturning circulation. If correct, the 8.2 ky B.P. event provides an invaluable case study for understanding both the stability of ocean overturning circulation during warm climate states and the sensitivity of the climate system to any such changes. However, because of the disparate geographic and temporal expression of the climate anomaly, it has been difficult to verify whether the ocean was involved (*6*), let alone delineate its influence. Hence, a prerequisite for any analysis of the nature of climate-ocean coupling across the 8.2 ky B.P. event is an understanding of the changes in ocean circulation at this time.

The occurrence of the outburst flood from proglacial Lake Agassiz on the southwest margin of the retreating Laurentide Ice Sheet into the North Atlantic via the Hudson Strait at 8.47 ± 0.3 ky B.P. (*7*), preceding or potentially coeval with the 8.2 ky B.P. event, supports the idea that ocean circulation may have at least changed at this time, because the freshwater outburst provides a plausible trigger for altering ocean overturning circulation. Using the estimated volume of the outburst flood [e.g., (*8*, *9*)], several model studies show that such a flood is capable of triggering ocean overturning changes that could result in climate anomalies quantitatively similar to those observed in many areas (*10*–*12*). Yet, paleoceanographic observations of deep ocean circulation changes at the time of either the outburst flood or the climate anomaly are equivocal. A number of studies have observed changes in the deep North Atlantic circulation and properties around the 8.2 ky B.P. event (*13*, *14*), but these changes are similar in magnitude to those that have occurred repeatedly during the Holocene. The question remains whether this is because no anomalously large circulation event accompanied the 8.2 ky B.P. climate anomaly or because these sediment records lack the resolution to faithfully reflect such a brief event (*15*).

As a first step in addressing this question, Ellison *et al.* (*16*) demonstrate that it is possible to resolve decadal-century scale bottom-water circulation changes in the early Holocene using suitably expanded sediment records. Using a bottom-water flow-speed proxy to reconstruct changes in Iceland-Scotland Overflow Water, Ellison *et al.* (*16*) show that one of the two major branches of the Nordic Seas overflows was reduced just after the Lake Agassiz freshwater outburst. Although detailed, their deep-water record spans only ~2000 years and thus cannot resolve whether the observed deep-water changes were anomalously large relative to others during the Holocene. In addition, given that only half of the total flux in the Nordic Seas overflows exits through the Eastern branches (*17*, *18*), it is unclear whether the integrated overflows were reduced after the freshwater outburst or whether the western (Denmark Strait) overflow simply increased in compensation, as model results suggest could happen (*19*). Hence, to assess the sensitivity of meridional overturning circulation (MOC) to the Agassiz freshwater out-

---

[1] Bjerknes Centre for Climate Research, University of Bergen, N-5007 Norway. [2] Laboratoire des Sciences du Climat et de l'Environnement, 91198 Gif-sur-Yvette, France. [3] Department of Earth Science, University of Bergen, N-5007 Norway. [4] Royal Netherlands Institute for Sea Research, 1790 AB Den Burg, Netherlands.

*To whom correspondence should be addressed. E-mail: kikki@uib.no

Fig. 1. Map of study area with the location of core MD03-2665 (57°26.56N, 48°36.60W; 3440-m water depth) marked with a red circle. The black arrows indicate the overflows and spreading pathways of deep and intermediate currents, after (*21*, *35*, *36*). The total area covered by Lake Agassiz is shaded, and the general routing of the overflow and outburst through the Hudson bay to the North Atlantic is marked with a blue arrow [modified after (*9*)].

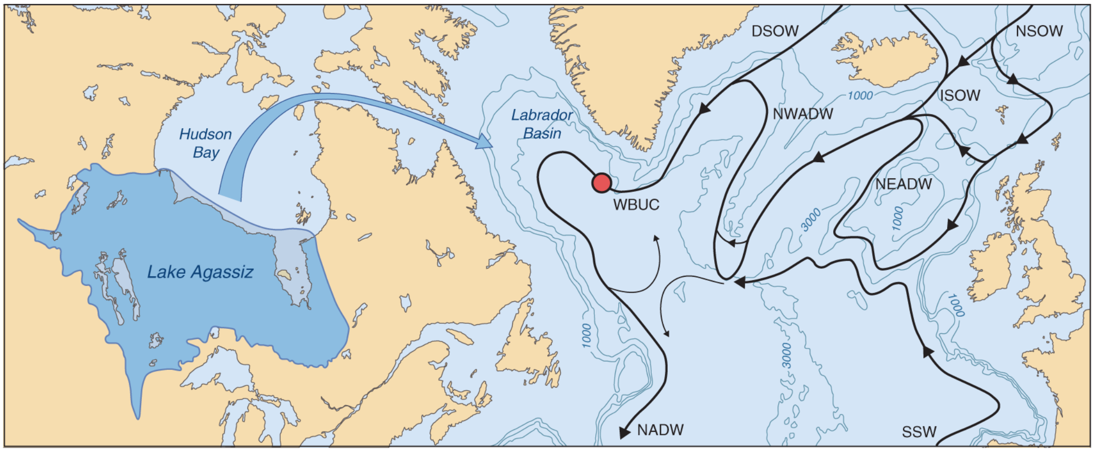

burst, a characterization of the integrated Nordic seas overflows is required.

Here, we present records of deep ocean circulation and chemical properties from Eirik Drift core MD03-2665 (57°26.56N, 48°36.60W; 3440-m water depth) (Fig. 1). This site is sensitively situated and provides the temporal fidelity to detect whether changes in deep-water properties and circulation accompanied the Lake Agassiz outburst. The Eirik Drift accumulates rapidly as a result of the influx of sediments eroded from the Denmark Strait and eastern Greenland margin suspended in Denmark Strait Overflow Water (DSOW) (*20*). DSOW combines with North West Atlantic Deep Water (NWADW) to form the Western Boundary Undercurrent (WBUC) (*21*). The seafloor at site MD03-2665 lies just below the main axis of the sediment-laden WBUC and hence preserves expanded interglacial intervals (*22*). Thus, this location is well situated to monitor changes in the past circulation and properties of newly formed Lower North Atlantic Deep Water (LNADW) along its western boundary flow path. The interval from 0 to 11 ky B.P. is dated by 24 ^{14}C accelerator mass spectrometry (AMS) dates (table S1 and figs. S3 and S4). The average sedimentation rates (90 cm/ky from 10.7 to 8.5 ky B.P., >200 cm/ky from 8.5 to 8.2 ky B.P., and 40 cm/ky thereafter) are suitable for resolving even brief circulation anomalies such as those simulated in response to the Lake Agassiz outburst (*23*).

Eirik Drift proxy records. To assess the timing, amplitude, and nature of deep-water changes during the past 10 ky, we have generated a suite of high-resolution sedimentary, geochemical, and magnetic proxy data (Fig. 2 and Supporting Online Material). The most striking feature in all of our records is the large deviation beginning at 3.45-m core depth. Our epibenthic carbon isotope record

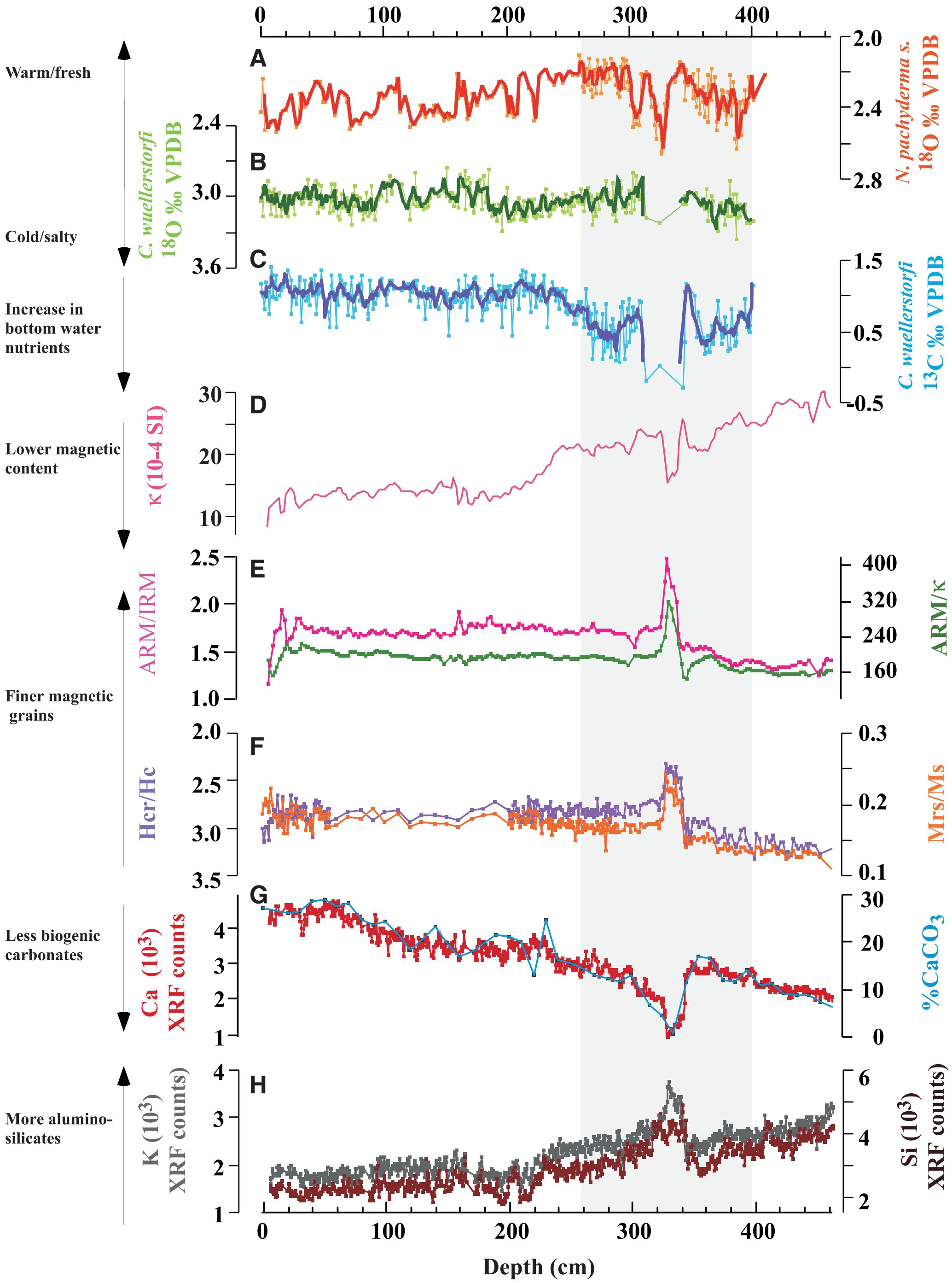

Fig. 2. Proxy records along the Holocene section of core MD03-2665 plotted versus depth. (**A**) *Neogloboquadrina pachyderma* sinistral coiling δ^{18}O‰ VPDB plotted with a 5-point running mean. (**B**) *Cibicidoides wuellerstorfi* δ^{18}O‰ VPDB plotted with a 5-point running mean. (**C**) *Cibicidoides wuellerstorfi* δ^{13}C‰ VPDB plotted with a 5-point running mean. (**D**) Low-field magnetic susceptibility. (**E**) Anhysteretic remanent magnetization/isothermal remanent magnetization (ARM/IRM) and ARM/κ ratios as proxies for magnetic grain size. (**F**) Hcr/Hc and Mrs/Ms hysteresis ratio also illustrating changes in magnetic domain states related to magnetic grain sizes. (**G**) Ca element measured every 5 mm by XRF scanning superimposed to CaCO$_3$ percentages measured at lower resolution. (**H**) Potassium (K) and silicon (Si) major elements. The shaded area highlights the study interval shown in Figs. 3 and 4 (i.e., 7300 to 9300 calendar years B.P.).

(Fig. 2C) implies a pronounced shift in the chemistry of bottom waters bathing the site: δ^{13}C decreases sharply from average Holocene values of about 1 per mil (‰) [Vienna Pee Dee belemnite (VPDB)] to below 0‰ over a few centimeters, followed by a similarly sharp recovery at ~3.15-m core depth.

Concurrently, the magnetic properties and sedimentary composition of the core also change dramatically at 3.45 m (Fig. 2, D to H). The magnetic properties indicate that magnetite is the main magnetic carrier (*S*-ratio close to unity and Curie temperature at about 570 to 580°C; see supporting online material) and that its average grain size fines abruptly in this interval, in contrast to an otherwise uniform magnetic grain size throughout the past 10 ky. In addition, the concentration in magnetic particles is reduced twofold during the episode. The two main transport vectors for magnetic particles in the North Atlantic are bottom currents carrying large amounts of magnetite-rich sediments originating from the Nordic basaltic provinces and iceberg discharges. The latter are characterized by episodic supplies of poorly sorted magnetic grains, resulting in a clear coarsening of the magnetic fraction (*24*). In addition, the amount of magnetic minerals associated with iceberg discharges is much smaller than the magnetic load transported by the main deep currents. This is true even along the main path of icebergs, where discharges are at a maximum, and also during periods when the magnetic fraction undergoes a twofold decrease, along the path of the bottom current (*25*). Therefore, at this site changes in the magnetic contents most likely illustrate changes in the passive transport of magnetic particles, i.e., changes in the strength of the DWBUC at the core depth (*26*). Thus, the sharp reduction in the number and size of magnetic grains suggests that there was a rapid decrease in bottom-current activity transporting magnetic grains to this site.

Concomitantly, major element analyses done with x-ray fluorescence (XRF) scanning show a marked drop in the Ca contents, while the aluminosilicate–derived elements K and Si increase by about 60%. $CaCO_3$ percentages abruptly decrease from 17% to 0.6%, subsequently recovering to values of about 20% after the event. These changes coincide with an apparent abrupt increase in sedimentation rates as inferred from the AMS^{14}C chronology (see Supporting Online Material). The pronounced change in bulk sediment chemical composition indicates dilution of biogenic carbonate by fine-grained terrigenous material. The coincidence in timing of this sedimentary event with the Lake Agassiz flood points toward the outburst as the source of fine material, although the lack of detrital carbonate (found in very proximal outburst sediments) may suggest that the sedimentary changes originate from other source regions or WBUC fluctuations (*27*). In all proxies, the onset of the event is very abrupt, occurring within a few centimeters, whereas the return to average Holocene values is slightly more gradual, at least in the proxies that were measured continuously. Thus, all of our proxies show a synchronous geochemical and sedimentological anomaly that is the most prominent one within the Holocene.

Deep-water changes. What could have driven such an anomalously large and abrupt change coevally in our proxies of deep-water chemistry and flow, as well as sedimentary composition? The inferred increase in bottom-water nutrients, decrease in sediment biogenic content, and weakening bottom-current activity with decrease in magnetic grain size and concentration are all consistent with a sudden and pronounced decrease of LNADW influence at the site. The lower benthic δ^{13}C values generally observed before 7.5 ky B.P. are consistent with previous suggestions that not all components of NADW were at modern strength in the early Holocene (*27*, *28*). However, it is notable that just before the extreme event, benthic foraminiferal δ^{13}C values rise to just over 1‰ versus VPDB—similar to late Holocene North Atlantic core top values (*29*)—suggesting that the site was bathed by a low-nutrient water mass isotopically similar to modern LNADW. The subsequent decrease in foraminiferal δ^{13}C of over 1‰ in just a few centimeters suggests that during the anomaly low-nutrient LNADW was replaced by a high-nutrient deep-water mass.

Because this ventilation change was accomplished very rapidly, over a few decades or less in our age model, it was most likely related to changing deep-circulation dynamics and shifting of water-mass boundaries relative to our site rather than solely caused by a gradual accumulation of nutrients related to a slowdown in ventilation. The most likely explanation is that the boundary between LNADW (high δ^{13}C) and southern source deep water (low δ^{13}C) shoaled across our core site. The fact that our benthic δ^{13}C values drop to levels equivalent to those found in Southern Ocean deep waters during the early Holocene (*30*) strongly supports this scenario. The decrease in bottom-current activity indicated by the decrease in magnetic grain size and concentration in our core is also consistent with a shoaled or decreased DWBUC and may be the equivalent of the oceanographic event recorded in other sites below the DWBUC previously dated at ~8.8 ky B.P. (*27*).

The reduced influence of low-nutrient LNADW at our site from ~8.38 to 8.27 ky B.P. suggests that a shoaling and perhaps a reduction in the MOC occurred at this time. Because our site lies near the base of the bounding topography guiding the DWBUC on its westward path, the combined Nordic Seas overflows should influence our location provided they are dense enough. Our results show that for ~100 years none of the Nordic Seas overflows produced low-nutrient deep water dense enough to mix down to 3440 m. Model studies (*31*) suggest that on decadal time scales the MOC transport is highly sensitive and linearly related to

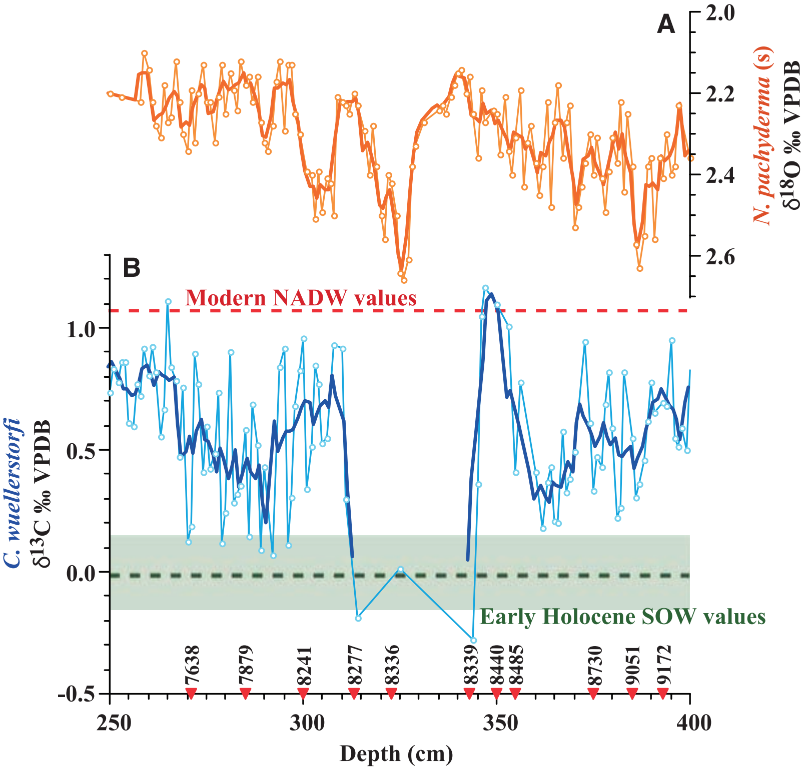

Fig. 3. (**A**) *Neogloboquadrina pachyderma* sinistral coiling δ^{18}O‰ VPDB plotted with a 5-point running mean and (**B**) *Cibicidoides wuellerstorfi* δ^{13}C‰ VPDB plotted with a 5-point running mean. Both records are plotted versus depth in the core. Typical Holocene NADW δ^{13}C values are indicated by the red dashed line (*29*); Holocene SOW δ^{13}C mean values and 1σ variance (taken from core TN057-15) are indicated by the green dashed line and the shaded bar, respectively (*30*). Position and calibrated ages of the AMS ^{14}C dated levels in this interval are indicated along the depth axes in red triangles.

the density of DSOW, the most influential water mass at our core site today. Thus, the overall vigor of MOC is likely to have decreased in tandem with the drop in overflow density, provided that such sensitivity studies apply to longer time scales. A centennial reduction in Nordic Seas overflows (the deep limb of MOC) is consistent with the observation that the northward flux of warm Atlantic water in the Nordic Seas (the upper limb of the MOC) was also reduced for ~100 years around the 8.2 ky B.P. event (*32*).

The fact that the only anomalously large disruption in the deep southward flowing branch of the MOC occurs coevally with the largest known outburst of freshwater to the North Atlantic, the Lake Agassiz outburst, supports the hypothesis that MOC is sensitive to freshwater forcing. Indeed, our inference that the density, and perhaps the flux, of the southward flowing branch of the MOC were decreased matches model predictions for the nature and timing of the deep-water response to the Lake Agassiz outburst (*23*, *33*). The rate at which the deep-water changes are accomplished in our core demonstrates that these shifts in deep-ocean circulation can occur in perhaps as little as a few decades, even in warm climate states, just as models predict [e.g., (*23*)].

Surface ocean response. Having defined the timing and duration of the deep circulation anomaly associated with the outburst, it is possible to consider more explicitly the impact of these circulation changes on climate. Our site is located near the bull's-eye of the cooling related to MOC weakening in many model experiments (*10*, *23*). If taken to solely reflect temperature, planktonic foraminiferal $\delta^{18}O$ at our site indicate a sharp near-surface cooling of ~1.5°C, but only ~15 cm after the initiation of the deep-circulation event (Fig. 3). This suggests either that there was no local cooling accompanying the initial perturbation in ocean circulation or that the influence of any cooling was offset by changes in the $\delta^{18}O$ of water at this location. Model studies suggest that the freshwater from the Agassiz outburst could indeed dampen or offset the effects of cooling on planktonic $\delta^{18}O$ (*10*), and paired planktonic Mg/Ca and $\delta^{18}O$ records suggest that this damping did occur south of Iceland during the 8.2 ky B.P. event (*34*). Another possibility is that the delay was real. Taken at face value, this offset might suggest that changes in ocean circulation are more of a prerequisite for, rather than a direct driver of, the 8.2 ky B.P. cooling event. Yet, as sedimentation rates increased dramatically at the onset of the deep-water anomaly, this depth offset may represent a time delay of only a couple of decades—and much less if the increased sedimentation rate was due to a pulsed input of sediments.

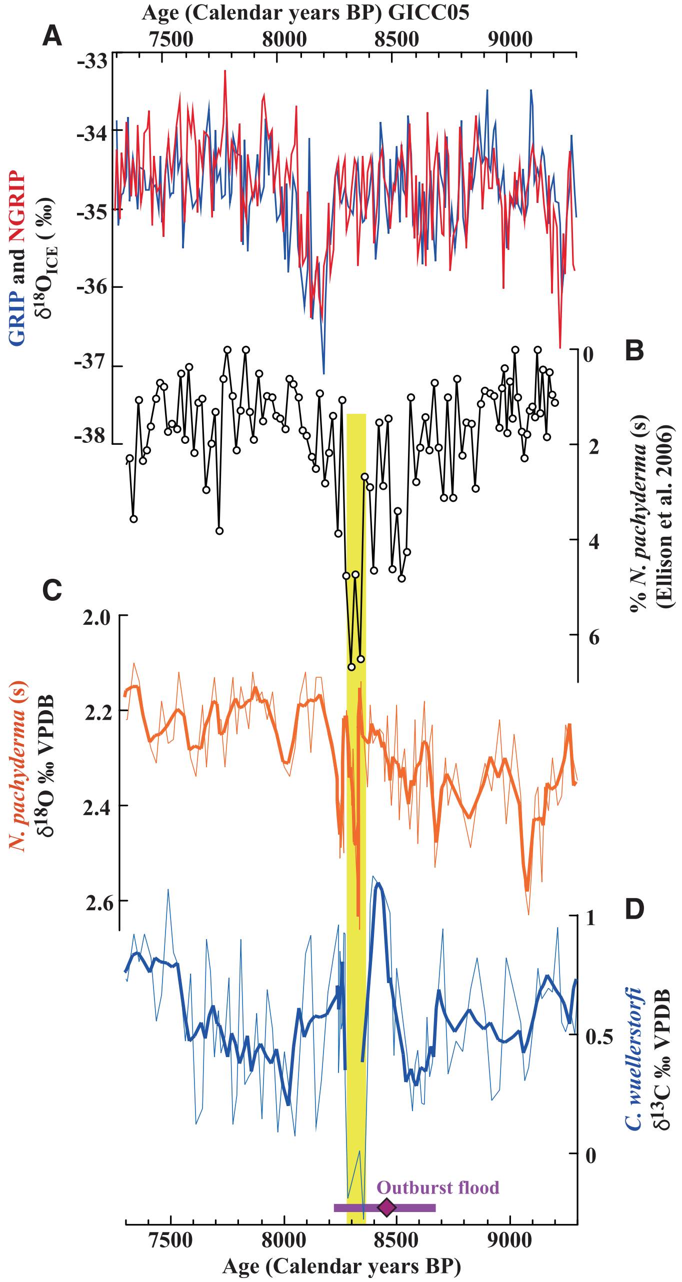

Fig. 4. Paleoceanographic records along core MD03-2665 compared with *Neogloboquadrina pachyderma* (sinistral coiling) percentage counts from core MD99-2251 and NGRIP and GRIP ice core data over the interval 7300 to 9300 calendar years B.P. (**A**) NGRIP and GRIP $\delta^{18}O_{ice}$‰ after (*37*) plotted on the ice core chronology of (*38*, *39*). (**B**) Percentage *Neogloboquadrina pachyderma* sinistral coiling after (*16*). (**C**) *Neogloboquadrina pachyderma* sinistral coiling $\delta^{18}O$‰ VPDB plotted with a 5-point running mean. (**D**) *Cibicidoides wuellerstorfi* $\delta^{13}C$‰ VPDB plotted with a 5-point running mean. The yellow vertical bar highlights the interval where LNADW influence is inferred to be absent at our site. Also shown is the age for the Lake Agassiz drainage event: 8470 years B.P. (*7*) (purple diamond), with its 1 SD uncertainties (8160 to 8740 years B.P.) denoted by a purple line. The age model used for (C) and (D) is described in the Supporting Online Material.

Despite the apparent offset in duration between the climate and deep ventilation changes co-registered in our core, two points strongly support a connection: (i) at our site, the largest surface ocean cooling (planktonic $\delta^{18}O$ increase) during the Holocene occurs during the period when NADW influence is weakest, and (ii) the magnitude of the cooling event and the nature of the deep circulation change are both similar to those modeled in response to a freshwater-induced slowdown of MOC. Furthermore, it is likely that the surface cooling associated with the deep-water changes in our core is the local equivalent of the strong but brief 8.2 ky B.P. cooling observed in circum-Atlantic records because it is coeval (within the dating uncertainties) with the anomalously large cooling observed in marine and Greenland ice core temperature proxies (Fig. 4). Seen in this way, our proxy records provide a means of delineating which parts of the compound climate signal around 8.2 ky B.P. could be related to ocean circulation changes—the weaker multicentennial cooling versus the much stronger cooling event superimposed on this, which lasted <100 years. Although Ellison *et al.* (*16*) find that the eastern branch of the Nordic Seas overflow was reduced for ~400 years after the flood outburst, our findings suggest that the perturbation in the integrated Nordic Seas overflows was much shorter (~100 years) and much more closely matches the timing and duration of the southerly advance of polar waters inferred by Ellison *et al.* (*16*) (Fig. 4). This suggests that only the brief and anomalously strong portion of the 8.2 ky B.P. cooling seen in Greenland and North Atlantic records was associated with a reduction of southward-flowing NADW (Fig. 4).

Our co-registered climate and deep-water records show other periods in which climate and circulation changed in concert. For example the second largest Holocene cooling (planktonic $\delta^{18}O$ increase) in our record, centered at ~9.1 ky B.P., is also associated with a decrease in LNADW (benthic $\delta^{13}C$) at our site (Fig. 4). However, it is clear that not every change in surface climate at our site has an accompanying change in deep circulation (and vice versa)—emphasizing even more strongly the uniqueness of the coeval extremes in climate and deep circulation that follow the Lake Agassiz flood outburst.

Wider climatic implications. Despite the complex nature of the climate record, the fact that large-scale changes in deep-ocean circulation are accomplished just as quickly in the natural world as is predicted in computer simulations [e.g., (*12*)] confirms that they were sufficiently rapid to be a plausible mechanism for driving the similarly abrupt changes seen in paleoclimate records. This observation helps to define the minimum time scale for altering ocean circulation and demonstrates that it is rapid enough to be relevant for human societies. The fact that these past ocean circulation changes are associated with the largest climate variations in the past underscores the importance of understanding the minimum freshwater forcing capable of affecting such large circulation changes—particularly given the concerns about the impact of future warming on the Greenland ice sheet.

References and Notes

1. E. R. Thomas *et al.*, *Quat. Sci. Rev.* **26**, 70 (2007).
2. S. J. Johnsen *et al.*, *Nature* **359**, 203 (1992).
3. W. Dansgaard *et al.*, *Nature* **364**, 218 (1993).
4. R. B. Alley *et al.*, *Geology* **25**, 483 (1997).
5. R. B. Alley, A. M. Ágústdóttir, *Quat. Sci. Rev.* **24**, 1123 (2005).
6. E. J. Rohling, H. Pälike, *Nature* **434**, 975 (2005).
7. D. C. Barber *et al.*, *Nature* **400**, 344 (1999).
8. D. W. Leverington, J. D. Mann, J. T. Teller, *Quat. Res.* **57**, 244 (2002).
9. J. T. Teller, D. W. Leverington, J. D. Mann, *Quat. Sci. Rev.* **21**, 879 (2002).
10. A. N. LeGrande *et al.*, *Proc. Natl. Acad. Sci. U.S.A.* **103**, 837 (2006).
11. E. Bauer, A. Ganopolski, *Paleoceanography* **19**, PA3014 (2004).
12. A. P. Wiersma, H. Renssen, *Quat. Sci. Rev.* **25**, 63 (2006).
13. I. R. Hall, G. G. Bianchi, J. R. Evans, *Quat. Sci. Rev.* **23**, 1529 (2004).
14. D. W. Oppo, J. McManus, J. D. Cullen, *Nature* **422**, 277 (2003).
15. L. D. Keigwin, J. P. Sachs, Y. Rosenthal, E. A. Boyle, *Paleoceanography* **20**, PA2003 (2005).
16. C. R. W. Ellison, M. R. Chapman, I. R. Hall, *Science* **312**, 1929 (2006).
17. B. Hansen, S. Østerhus, *Prog. Oceanogr.* **45**, 109 (2000).
18. B. Hansen, W. R. Turrell, S. Østerhus, *Nature* **411**, 927 (2001).
19. A. Biastoch, R. H. Kase, D. B. Stammer, *J. Phys. Oceanogr.* **33**, 2307 (2003).
20. C. N. Wold, *Paleoceanography* **9**, 917 (1994).
21. M. S. McCartney, *Prog. Oceanogr.* **29**, 283 (1992).
22. C. Hillaire-Marcel, A. de Vernal, G. Bilodeau, G. Wu, *Can. J. Earth Sci.* **31**, 63 (1994).
23. A. P. Wiersma, H. Renssen, H. Gosse, T. Fichefet, *Clim. Dyn.* **27**, 831 (2006).
24. C. Kissel, *C.R. Acad. Sci. Paris* **337**, 908 (2005).
25. J. S. Stoner, J. E. T. Channell, C. Hillaire-Marcel, *Paleoceanography* **11**, 309 (1996).
26. C. Kissel *et al.*, *Earth Planet. Sci. Lett.* **171**, 489 (1999).
27. C. Hillaire-Marcel, A. de Vernal, D. J. W. Piper, *Geophys. Res. Lett.* **34**, L15601 (2007).
28. C. Hillaire-Marcel, A. de Vernal, G. Bilodeau, A. J. Weaver, *Nature* **410**, 1073 (2001).
29. W. B. Curry, D. W. Oppo, *Paleoceanography* **20**, PA1017 (2005).
30. U. S. Ninnemann, C. D. Charles, *Earth Planet. Sci. Lett.* **201**, 383 (2002).
31. M. Latif *et al.*, *J. Clim.* **19**, 4631 (2006).
32. D. Klitgaard-Kristensen, H. P. Sejrup, H. Haflidason, S. Johnsen, M. Spurk, *J. Quat. Sci.* **13**, 165 (1998).
33. H. Renssen, H. Goosse, T. Fichefet, J.-M. Campin, *Geophys. Res. Lett.* **28**, 1567 (2001).
34. R. E. Came, D. W. Oppo, J. F. McManus, *Geology* **35**, 315 (2007).
35. W. J. Schmitz, M. S. McCartney, *Reviews of Geophysics* **31**, 29 (1993).
36. R. R. Dickson, J. Brown, *J. Geophys. Res.* **99**, 12319 (1994).
37. S. O. Rasmussen, B. M. Vinther, H. B. Clausen, K. K. Andersen, *Quat. Sci. Rev.* **26**, 1907 (2007).
38. S. O. Rasmussen *et al.*, *J. Geophys. Res.* **111**, D06102 (2006).
39. B. M. Vinther *et al.*, *J. Geophys. Res.* **111**, D13102 (2006).
40. We thank the Centre for Ice and Climate (especially B. Vinther, S. Johnsen, and S. Rasmussen) at the Niels Bohr Institute at University of Copenhagen, for supplying the unpublished GRIP and NGRIP data. We are also grateful for technical assistance from D.-I. Blindheim, E. Bjørseth, E. V. Galaasen, O. Hansen, and I. V. Johansen from Bjerknes Centre for Climate Research (BCCR)/University of Bergen (UoB) and C. Wandres and F. Dewilde from Laboratoire des Sciences du Climat et de l'Environnement (LSCE), Commisariat à l'Energie Atomique (CEA), Centre National de la Recherche Scientifique (CNRS), Université Versailles-Saint-Quentin (UVSQ). This work was supported by the BCCR, the UoB, and the Norwegian Research Council, and at LSCE by the CEA and CNRS through the Institut des Sciences de l'Univers, Programme National d'Etude du Climat (INSU-PNEDC-Impair) project. Additional funding was provided by the PACLIVA EU EVK2-2002-00143 and the Agence National de la Recherche, Integration des Contraintes Paléoclimatiques: Réduire les Incertitudes sur l'Evolution du Climat des Périodes Chaudes (ANR-PICC) projects. The GIFA ^{14}C dates were obtained by AMS Artemis from LMC14, National Service of INSU. We are grateful to M. Paterne (LSCE) for her help with the GIFA ^{14}C data. The ship and scientific technology for the P.I.C.A.S.S.O. cruise were provided by the Institut Polaire Paul Emile Victor (IPEV) within the framework of the International Marine Global Changes (IMAGES) program. H.F.K. and U.S.N. analyzed the planktonic and benthic stable isotope data in this study and prepared samples for the KIA AMS ^{14}C dates. E.C. was responsible for the paleoceanographic team in LSCE. C.K. and C.L. are responsible for the magnetic and $CaCO_3$ analyses reported here and C.L. was chief scientist on P.I.C.A.S.S.O. T.O.R. is responsible for the x-ray fluorescence scans.

Supporting Online Material

www.sciencemag.org/cgi/content/full/1148924/DC1
Materials and Methods
Figs. S1 to S4
Table S1
References

8 August 2007; accepted 8 November 2007
Published online 6 December 2007;
10.1126/science.1148924
Include this information when citing this paper.

The *Physcomitrella* Genome Reveals Evolutionary Insights into the Conquest of Land by Plants

Stefan A. Rensing,[1] Daniel Lang,[1] Andreas D. Zimmer,[1] Astrid Terry,[2] Asaf Salamov,[3] Harris Shapiro,[3] Tomoaki Nishiyama,[4] Pierre-François Perroud,[5] Erika A. Lindquist,[3] Yasuko Kamisugi,[6] Takako Tanahashi,[7,8] Keiko Sakakibara,[9] Tomomichi Fujita,[10] Kazuko Oishi,[11] Tadasu Shin-I,[11] Yoko Kuroki,[12] Atsushi Toyoda,[12] Yutaka Suzuki,[13] Shin-ichi Hashimoto,[14] Kazuo Yamaguchi,[4,15] Sumio Sugano,[13] Yuji Kohara,[11,16] Asao Fujiyama,[12,17,18] Aldwin Anterola,[19] Setsuyuki Aoki,[20] Neil Ashton,[21] W. Brad Barbazuk,[22] Elizabeth Barker,[21] Jeffrey L. Bennetzen,[23] Robert Blankenship,[5] Sung Hyun Cho,[5] Susan K. Dutcher,[24] Mark Estelle,[25] Jeffrey A. Fawcett,[26] Heidrun Gundlach,[27] Kousuke Hanada,[28,29] Alexander Heyl,[30] Karen A. Hicks,[31,32] Jon Hughes,[33] Martin Lohr,[34] Klaus Mayer,[27] Alexander Melkozernov,[35] Takashi Murata,[7,8] David R. Nelson,[36] Birgit Pils,[37] Michael Prigge,[25] Bernd Reiss,[31] Tanya Renner,[38] Stephane Rombauts,[26] Paul J. Rushton,[39] Anton Sanderfoot,[40] Gabriele Schween,[1] Shin-Han Shiu,[28] Kurt Stueber,[31] Frederica L. Theodoulou,[41] Hank Tu,[3] Yves Van de Peer,[26] Paul J. Verrier,[42] Elizabeth Waters,[37] Andrew Wood,[19] Lixing Yang,[23] David Cove,[5,6] Andrew C. Cuming,[6] Mitsuyasu Hasebe,[7,8,43] Susan Lucas,[2] Brent D. Mishler,[44] Ralf Reski,[1] Igor V. Grigoriev,[3] Ralph S. Quatrano,[5]* Jeffrey L. Boore[3,44,45]

We report the draft genome sequence of the model moss *Physcomitrella patens* and compare its features with those of flowering plants, from which it is separated by more than 400 million years, and unicellular aquatic algae. This comparison reveals genomic changes concomitant with the evolutionary movement to land, including a general increase in gene family complexity; loss of genes associated with aquatic environments (e.g., flagellar arms); acquisition of genes for tolerating terrestrial stresses (e.g., variation in temperature and water availability); and the development of the auxin and abscisic acid signaling pathways for coordinating multicellular growth and dehydration response. The *Physcomitrella* genome provides a resource for phylogenetic inferences about gene function and for experimental analysis of plant processes through this plant's unique facility for reverse genetics.

Here, we report the draft genome sequence of the moss *Physcomitrella patens*, the first bryophyte genome to be sequenced. The embryophytes (land plants) began to diverge about 450 million years ago (Ma). Bryophytes, comprising hornworts, mosses, and liverworts, are remnants of early diverging lineages of embryophytes and thus occupy an ideal phylogenetic position for reconstructing ancient evolutionary changes and illuminating one of the most important events in earth history—the conquest of land by plants (Fig. 1). The terrestrial environment involves variations in water availability and temperature, as well as increased exposure to radiation. Adaptation entailed dramatic changes in body plan (*1*) and modifications to cellular, physiological, and regulatory processes. Primary adaptations included enhanced osmoregulation and osmoprotection, desiccation and freezing tolerance, heat resistance, synthesis and accumulation of protective "sunscreens," and enhanced DNA repair mechanisms. Fossil evidence suggests that early land plants were structurally similar to extant bryophytes (*2*); they probably had a dominant haploid phase and were dependent on water for sexual reproduction, having motile male gametes.

The genome sequence of *P. patens* allows us to reconstruct the events of genome evolution that occurred in the colonization of land, through comparisons with the genome sequences of several angiosperms (*Arabidopsis thaliana*, *Oryza sativa*, and *Populus trichocarpa*), as well as aquatic unicellular green algae (*Ostreococcus tauri*, *Ostreococcus lucimarinus*, and *Chlamydomonas reinhardtii*).

Features of the Whole Genome

General genome properties. The draft genome sequence of *P. patens* ssp. *patens* (strain Gransden 2004) was determined by whole-genome shotgun sequencing, assembling into 480 mega–base pairs of scaffold sequence with a depth of ~8.6× (*3*, *4*); expressed sequence tag (EST) coverage of the assembly is over 98%. The sequence contains 35,938 predicted and annotated *P. patens* gene models (tables S1 to S5). Most predicted genes are supported by multiple types of evidence (table S4), and 84% of the predicted proteins appear complete. About 20% of the analyzed genes show alternative splicing (table S6), a frequency similar to that of *A. thaliana* and *O. sativa* (*5*).

Repetitive sequences and transposons. An ab initio approach detected 14,366 repetitive elements comprising 1381 families [average member number 10, length 1292 bp (table S7)]. The largest repetitive sequence is from the "AT-rich, low complexity" class (23% of the repetitive fraction), and 15 families account for over 84% of the repetitive fraction (table S8).

Long terminal repeat retrotransposons (LTR-Rs) are generally the most abundant class of transposable elements, contributing substantially to flowering plant genome size (*6*). Of the 4795 full-length LTR-Rs in *P. patens*, 46% are gypsy-like and 2% are copia-like. *P. patens* contains about three times as many full-length LTR-Rs as *A. thaliana*, but about one-third as many as *O. sativa*. The density among the three genomes is lowest in *P. patens* (fig. S1). Although about half of the *P. patens* genome consists of 157,127 LTR-Rs, only 3% exist as intact full-length elements. The remainder is made of diverged and partial remnants, often fragmented by mutual insertions (fig. S2). Nested regions are common, with 14% of LTR-Rs inserted into another LTR-R (table S9). The genome also contains 895 solo LTR-Rs, probably as a result of unequal crossing-over or DNA repair. Periodic retrotransposition activity peaks are discernible over the past 10 million years (My) (Fig. 2). Only one full-length element is inserted within a gene, which suggests strong selection against transposon insertion into genes ($P < 0.001$).

Helitrons (rolling-circle transposons) are an ancient class of transposons present in animals, fungi, and plants (*7*). Different from all eukaryotic genomes sequenced so far, the *P. patens* genome contains only a single Helitron family (table S10) with 19 members. High sequence similarity (96%) suggests that they have been active within the past 3 My. Presumably, multiple Helitron families evolved in all plant lineages, including *P. patens*, but we predict that a rapid process of DNA removal has excised all members that have not been active recently, a process that has been demonstrated in other plant genomes (*6*).

Gene and genome duplications. Gene and genome duplications are major driving forces of gene diversification and evolution (*8*). In *P. patens*, the K_s distribution plot (i.e., the frequency classes of synonymous substitutions) among paralogs shows a clear peak at around 0.5 to 0.9 (fig. S3), which suggests that a large-scale duplication, possibly involving the whole genome, has occurred. The presence of this peak confirms EST-based data (*9*). Additional evidence for a large-scale duplication comes from the identification of 77 nonoverlapping duplicated segments containing at least five paralogous gene pairs. All duplicated segments have an average K_s of 0.5 to 0.7.

Tandemly arrayed genes (TAGs) can contribute substantially to genome size. However, only ~1% of the protein-encoding genes in *P. patens* occur in tandem array, in contrast to *A. thaliana* (~16%), *O. sativa* (~14%), and *P. trichocarpa* (11%) (*10*–*12*). The majority of *P. patens* TAG clusters are made up of two genes that are not separated by an intervening gene (fig. S4). Compared with non-TAG genes, genes in TAGs are significantly shorter ($P < 0.001$) in terms of gene, coding sequence (CDS), and intron length, whereas their G/C content is significantly higher (table S11). Functional analysis of TAGs compared with paralogous non-TAG clusters reveals that photosynthesis proteins, particularly antenna proteins, are significantly ($P < 0.05$) enriched among the TAGs [section 3.6, St 58 A/B (*13*)]. Other enriched categories are glyoxylate and dicarboxylate metabolism, carbon fixation, and ribosome assembly (fig. S5). Apparently, *P. patens* has increased the genetic playground for photosynthesis and related carbon-based metabolism in its recent past.

Comparison of the K_s of *P. patens* TAGs with paralogs that were established during the large-scale genome duplication (K_s ~0.5 to 0.9) sug-

---

[1] Plant Biotechnology, Faculty of Biology, University of Freiburg, Schaenzlestrasse 1, D-79104 Freiburg, Germany. [2] U.S. Department of Energy (DOE) Joint Genome Institute and Lawrence Livermore National Laboratory, 2800 Mitchell Drive, Walnut Creek, CA 94598, USA. [3] DOE Joint Genome Institute and Lawrence Berkeley National Laboratory, 2800 Mitchell Drive, Walnut Creek, CA 94598, USA. [4] Advanced Science Research Center, Kanazawa University, 13-1 Takara-machi Kanazawa 920-0934, Japan. [5] Department of Biology, Washington University, 1 Brookings Drive, St. Louis, MO 63130–4899, USA. [6] Centre for Plant Sciences, University of Leeds, Leeds LS2 9JT, UK. [7] National Institute for Basic Biology, Okazaki 444-8585, Japan. [8] Department of Basic Biology, School of Life Science, The Graduate University for Advanced Studies, Okazaki 444-8585, Japan. [9] School of Biological Sciences, Monash University, Clayton Campus, Melbourne, VIC 3800, Australia. [10] Department of Biological Sciences, Faculty of Science, Hokkaido University, Sapporo 060-0810, Japan. [11] Genome Biology Laboratory, Center for Genetic Resource Information, National Institute of Genetics, Mishima 411-8540, Japan. [12] RIKEN Genomic Sciences Center, Kanagawa 230-0045, Japan. [13] Laboratory of Functional Genomics, Department of Medical Genome Sciences, Graduate School of Frontier Sciences, The University of Tokyo, Tokyo 108-8639, Japan. [14] Department of Molecular Preventive Medicine, School of Medicine, The University of Tokyo, Tokyo 113-8654, Japan. [15] Division of Life Science, Graduate School of Natural Science and Technology, Kanazawa University, Kanazawa 920-1192, Japan. [16] Department of Genetics, School of Life Science, The Graduate University for Advanced Studies, Mishima 411-8540, Japan. [17] National Institute of Informatics, Tokyo 101-8403, Japan. [18] Department of Informatics, School of Multidisciplinary Sciences, The Graduate University for Advanced Studies, Tokyo 101-8403, Japan. [19] Department of Plant Biology, Southern Illinois University, Carbondale, IL 62901–6509, USA. [20] Life-Science Informatics Unit, Graduate School of Information Science, Nagoya University, Furo-cho, Chikusa-ku, Nagoya 464-8601, Japan. [21] University of Regina, 3737 Wascana Parkway, Regina, SK S4S 0A2, Canada. [22] Donald Danforth Plant Science Center, 975 North Warson Road, St. Louis, MO 63132, USA. [23] Department of Genetics, Davison Life Sciences Complex, University of Georgia, Athens, GA 30602–7223, USA. [24] Department of Genetics, Washington University, 660 South Euclid Avenue, St. Louis, MO 63108, USA. [25] Department of Biology, Indiana University, 1001 East Third Street, Bloomington, IN 47405–3700, USA. [26] VIB Department of Plant Systems Biology, Ghent University, Technologie Park 927, 9052 Ghent, Belgium. [27] MIPS/IBI Institute for Bioinformatics, GSF Research Center for Environment and Health, Ingolstaedter Landstrasse 1, D-85764 Neuherberg, Germany. [28] Department of Plant Biology, 166 Plant Biology Building, Michigan State University, East Lansing, MI 48824–1312, USA. [29] RIKEN Plant Science Center, 1-7-22 Suehiro, Tsurumi, Yokohama, Kanagawa 230-0045, Japan. [30] Free University, Institute for Biology, Applied Genetics Neubau, Albrecht-Thaer-Weg 6, D-14195 Berlin, Germany. [31] Max-Planck Institute of Plant Breeding Research, Carl-von-Linne-Weg 10, D-50829 Cologne, Germany. [32] Biology Department, Kenyon College, Gambier, OH 43022, USA. [33] Pflanzenphysiologie, Justus Liebig University, Senckenbergstrasse 3, D-35390 Giessen, Germany. [34] Institute of General Botany, Johannes Gutenberg-University, D-55099 Mainz, Germany. [35] Department of Chemistry and Biochemistry, Arizona State University, Tempe, AZ 85287–1604, USA. [36] University of Tennessee-Memphis, 101 Molecular Science Building, 858 Madison Avenue, Memphis, TN 38163, USA. [37] Department of Bioinformatics, Biozentrum, Am Hubland, Würzburg University, D-97074 Würzburg, Germany. [38] Biology Department, San Diego State University, North Life Sciences Room 102, 5500 Campanile Drive, San Diego, CA 92182–4614, USA. [39] Department of Biology, Gilmer Hall, 485 McCormick Road, University of Virginia, Charlottesville, VA 22903, USA. [40] Department of Plant Biology, University of Minnesota, 250 Biological Science Center, 1445 Gortner Avenue, St. Paul, MN 55108, USA. [41] Biological Chemistry Department, Rothamsted Research, Harpenden, Hertfordshire AL5 2JQ, UK. [42] Biomathematics and Bioinformatics Department, Rothamsted Research, Harpenden, Hertfordshire AL5 2JQ, UK. [43] ERATO, Japan Science and Technology Agency, Okazaki 444-8585, Japan. [44] Department of Integrative Biology, 3060 Valley Life Sciences Building, University of California, Berkeley, CA 94720, USA. [45] Genome Project Solutions, 1024 Promenade Street, Hercules, CA 94547, USA.

*To whom correspondence should be addressed: E-mail: rsq@wustl.edu

gests that most TAGs were established recently ($K_s < 0.1$). It is noteworthy that *P. patens* TAG partners tend to be located on opposite strands (64.4%, with 36.4% in head-to-head orientation and 28.0% in tail-to-tail orientation), whereas there is a tendency (68 to 88%) for TAGs to be located on the same DNA strand in *A. thaliana*, *O. sativa* (*11*), *Caenorhabditis elegans*, *Homo sapiens*, *Mus musculus*, and *Rattus norvegicus* (*11*, *14*). Significantly fewer substitutions ($P < 0.001$) are observed within them (average $K_s = 0.59$) than in those that are located on the same strand ($K_s = 1.25$). Homologous recombination between TAGs on the same strand may have resulted in loss of such TAGs, whereas gene conversion associated with homologous recombination of TAGs on opposite strands may have resulted in reduction of sequence divergence (K_s) between those. These differences in TAG organization might be connected to the exceptional reliance on sequence similarity for DNA repair observed in *P. patens* (*15*, *16*). Alternatively, the generation and exclusion rate of TAGs on the opposite strand might have been higher than for TAGs on the same strand in the ancestor of *P. patens*.

Gene and domain family expansion patterns. Eukaryotic gene family sizes differ mainly because of different rates of gene duplication and retention, and gene content differences may reflect species-specific adaptations. Overall, lineage-specific gains among domain families occurred at a lower rate (by a factor of about three) in the *P. patens* compared with the *A. thaliana* lineage (Fig. 3A). Similarly, in comparisons with the *O. sativa* and *P. trichocarpa* lineages, gene gain rates in the *P. patens* lineage are substantially lower. Among gene families shared by both *P. patens* and *A. thaliana*, there are consistently fewer families with relatively large gains (≥6) in the *P. patens* lineage (Fig. 3B), which indicates that the gain rate differences noted in Fig. 3A are mainly due to higher retention rates of large families in the *A. thaliana* lineage. In addition, many *P. patens* gene families with higher-than-average gain rates in general also have elevated rates of gene loss (Fig. 3C).

Highly expanded gene families in the *P. patens* lineage are not necessarily highly expanded in the *A. thaliana* lineage ($r^2 = 0.33$, $P < 2 \times 10^{-16}$). Only 36 families with significantly higher-than-average gains are common to both the *P. patens* and *A. thaliana* lineages, whereas 43 are significantly expanded only in *P. patens* (Fig. 3A). Examples of parallel expansion include genes encoding protein kinases and leucine-rich–repeat proteins, as well as Apetala 2 (AP2) and Myb transcription factors. Transcription factor duplicates are retained in the *P. patens* lineage with a rate lower than those in the flowering plant lineage, yet higher than in algae (*17*); for example, the MADS-box and WRKY transcription factor families are intermediate in size compared with flowering plants and algae (table S12 and S13).

Families that significantly expanded only in the *P. patens* lineage include histidine kinases and response regulators. Both families are parts of two-component signaling networks important in plants, fungi, and bacteria. These two families are much larger in *P. patens* than those found in sequenced angiosperm genomes; their increased size suggests a more elaborate use of two-component systems in *P. patens*.

The *P. patens* genome contains genes for each of the core groups of small guanosine triphosphatases (G proteins) (fig. S6, A and B), consistent with increased complexity of vesicle trafficking machinery, not present in green algae, which suggests that such complexity was already present in

Fig. 1. Land plant evolution. Bryophytes comprise three separate lineages which, together with the vascular plants (including the flowering plants), make up the embryophytes (land plants) (*38*). These four lineages, remnants of the initial radiation of land plants in the Silurian, began to diverge from each other about 450 Ma.

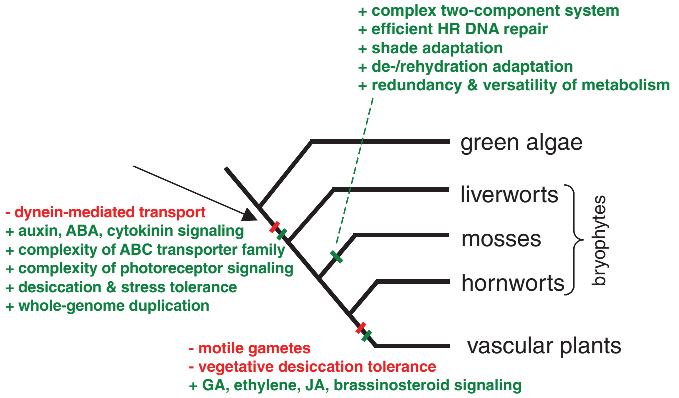

Fig. 2. Periodic cycles of LTR retrotransposon activity. *P. patens* underwent periodic cycles of LTR-R amplifications. The most recent activity peaks at an estimated 1 to 1.5 Ma, preceded by invasion events around 3, 4, and 5.5 Ma. Gypsy-like elements are younger (average 3.2, median 3.0) than copia-like elements (average 3.9, median 3.6), coinciding with an increased full-length copy number by a factor of seven. The gradual decrease between 5 to 12 Ma probably reflects element deterioration leading to loss of ability to detect these elements. Numbers found of each element are shown in parentheses.

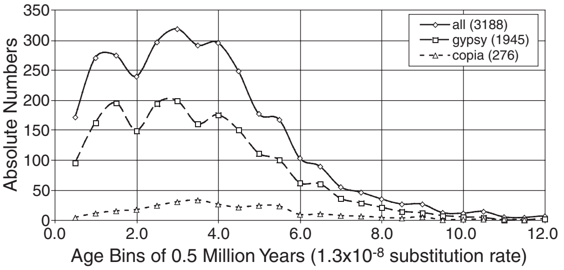

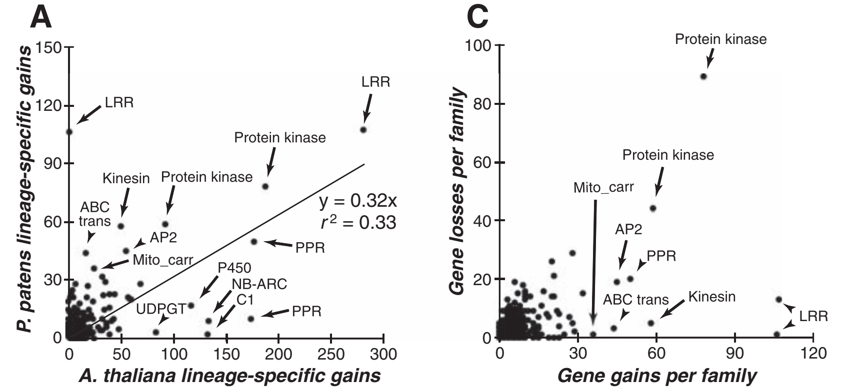

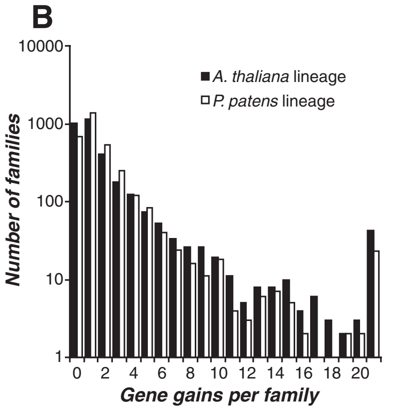

Fig. 3. Domain family expansion patterns in *P. patens.* (**A**) Gain is defined as the presence of paralogous gene copies uniquely arising in one lineage based on the results of reconciliation between gene family and species trees. Large gene families are labeled on the basis of the predominant Pfam domain names. Some domain names occur more than once since they are the predominant domains in multiple gene families. (**B**) Relations between lineage-specific gains per family and the number of families in the *A. thaliana* and *P. patens* lineage. (**C**) The relation between gain and loss among *P. patens* gene families.

the last common ancestor of land plants. *P. patens* also has a large adenosine triphosphate binding cassette (ABC) superfamily [121 members; (tables S14 and S15); St 29_ABDI/C/F/G, 9, 57, 110 to 113], similar in size to that in *A. thaliana* (130) and *O. sativa* (129), but larger than *O. tauri* (~50) and twice that of humans and *Drosophila melanogaster* (48 and 56, respectively). In flowering plants, most ABC-containing proteins are membrane-bound transporters for lipids, hormones, secondary metabolites, metals, and xenobiotics and control certain ion channels. The sessile habit and metabolic diversity of land plants appears to require a large repertoire of ABC proteins.

Adaptations to the Terrestrial Environment

Desiccation tolerance. Desiccation tolerance (DT) is widespread in reproductive structures of vascular plants, but vegetative DT is rare, except among bryophytes (*18*). Evolution of this trait was important in facilitating the colonization of the land, but was lost subsequently in vascular plants. DT in seeds is dependent on the phytohormone abscisic acid (ABA) to induce expression of seed-specific genes, such as late embryogenesis abundant proteins (LEAs), a group of proteins that accumulate during desiccation. *P. patens* is highly dehydration-tolerant (*19*) and contains orthologs of LEA genes and other genes expressed during the DT response in the poikilohydric moss *Tortula ruralis* (*20*) and in flowering plants (*21*).

ABA signaling also operates in the *P. patens* drought response (*21*). The genome contains putative homologs of the *A. thaliana* ABA receptors, one of which appears to have been specialized for a role in seed development, and the transcription factor ABI5, which implicates it in the regulation of ABA-mediated gene expression. Particularly interesting is ABI3, the seed-specific transcription factor of the B3 family (St 132), which, when mutated, results in the loss of desiccation-tolerance in seeds (*22*). The *P. patens* genome contains four *ABI3*-like genes, one of which (*PpABI3A*) functions to potentiate ABA responses in *P. patens* and partially complements the *A. thaliana abi3-6* mutant (*23*).

Finding these genes in *P. patens* and similar sequences in liverworts (*Riccia fluitans* and *Marchantia polymorpha*) suggests that desiccation tolerance gene networks likely originated in the last common ancestor of extant land plants.

Metabolic pathways. Cytochrome P450 enzymes that incorporate oxygen into small lipophilic compounds are represented by 250 to 350 members in genomes of flowering plants, 71 genes in *P. patens*, and 40 in *C. reinhardtii*. Specific examples of P450s lacking in *P. patens* are related to the absence and regulation of key molecules in flowering plants. One P450 required for the synthesis of gibberellic acid (CYP88) is absent, as is the enzyme needed to make *S*-lignols (CYP84) required for the accumulation of lignin. The CYP86 family includes fatty acid omega-hydroxylases involved in the formation of cutin, which prevents dehydration of plant tissues. The presence of CYP86 in *P. patens*, but not in green algae, suggests that cutin may have evolved in the ancestral land plants as an innovative mechanism to survive a terrestrial habitat.

Most enzymatic steps in carotenoid and chlorophyll biosynthetic pathways are more complex in terms of paralog frequencies in *P. patens* than in *A. thaliana* and *C. reinhardtii* (Fig. 4 and table S16). This is consistent with previous interpretations that the *P. patens* genome encodes seemingly redundant metabolic pathways and contains a network of genes for functions like phototoxic stress tolerance (*9*). Unlike light harvesting complex (LHC) proteins, most genes (79%) of the carotenoid and chlorophyll metabolic pathways are not TAGs and were acquired during the whole-genome duplication, i.e., since the divergence from the lineage leading to flowering plants (*9*).

One striking exception is the genes involved at the branching point of siroheme and heme/chlorophyll formation (Fig. 4 and table S16). UROS and UMT are encoded by single copy genes in *P. patens* (Fig. 4), whereas conserved ancient paralogs encode UROD (St 76). These paralogs had already been acquired before the split of green algae and land plants (St 76) and probably are functionally divergent (*24*, *25*). Note that both the UROD3 (St 76) and CPX2 (St 59) subfamilies are present in algae and *P. patens*, but have been lost in flowering plants.

Signaling pathways. The phytohormones and light receptors for morphogenesis found in flowering plants are absent in the unicellular algae, but are present in *P. patens*, e.g., genes for all four classes of cytokinin signaling pathways found in flowering plants. These include at least three

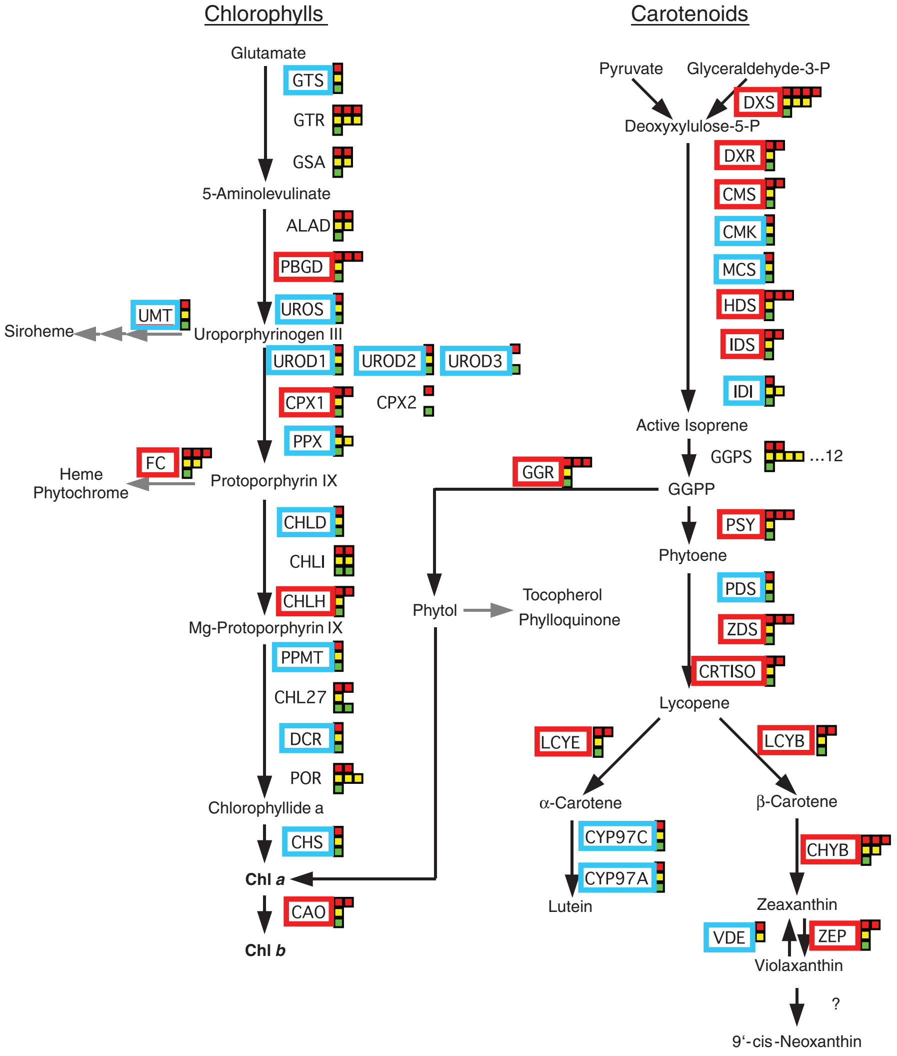

Fig. 4. Paralog frequencies in the biosynthetic pathways of chlorophylls and carotenoids in *P. patens*, *A. thaliana*, and *C. reinhardtii.* Denoted are products that accumulate to significant amounts, major intermediates, and known enzymes of both pathways (for full names of enzymes, see table S16). Major pathways are indicated by black arrows; branch-points leading to the formation of related compounds (italicized) are indicated by gray arrows. For each reaction, colored squares symbolize the number of (iso-) enzymes in *P. patens* (red), *A. thaliana* (yellow), and *C. reinhardtii* (green). Enzymes for which *P. patens* has more paralogs than *A. thaliana* and *C. reinhardtii* are boxed in red, those encoded by unique genes in *P. patens* are boxed in blue.

cytokinin receptors, two of which have been confirmed by EST evidence, which make *P. patens* the earliest diverging species that contains genes for all members of the cytokinin signal transduction pathway known today.

Ten gene families implicated in auxin homeostasis and signaling have been analyzed [(table S17), St 25, 33_A/B, 41, 45, 71, 73_7, 77, 85, 88, 89]. The *C. reinhardtii*, *O. lucimarinus*, and *O. tauri* genomes do not encode these, but the *P. patens* genome encodes members of each family [although, on the basis of phylogenies of the GH3 and ILL proteins, St 71 and 85, *P. patens* might not conjugate IAA to alanine, leucine, aspartic acid, or glutamic acid consistent with empirical data (*26*)]. Angiosperms dedicate a larger proportion of their genomes to auxin signaling; only one (AUX1/LAX; St 41) of the 10 families has as many members as angiosperm genomes. On the basis of analysis of *A. thaliana* and our phylogenetic analyses, the auxin signaling pathway has undergone substantial functional diversification within vascular plants since they diverged from bryophytes.

Although no ethylene responses have been noted in mosses, the *P. patens* genome codes for six putative ETR-like ethylene receptors, at least one of which is known to bind ethylene (*27*). Two putative 1-aminocyclopropane-1-carboxylate (ACC) synthases, catalyzing a critical step in ethylene biosynthesis, were also found. Two transcription factors with strong similarity to the EIN3 ethylene signaling family are also apparent as are six N-RAMP-type (natural resistance–associated macrophage protein) channel proteins, one or more of which might be involved in ethylene signaling, similar to EIN2 in *A. thaliana*.

Protective proteins. Adaptation to land also required the evolution of proteins that protect against stresses such as variation in temperature, light, and water availability. One example of this is the expansion of the heat shock protein 70 (HSP70) family to nine cytosolic members in *P. patens* (St 24), whereas all algal genomes sequenced to date encode one single cytosolic HSP70 (*28*).

The complement of the LHC genes is significantly expanded in *P. patens* when compared with algae and vascular plants [St 58_A (table S18A)]. Although several LHC homologs were already present in the last common ancestor of all land plants, more have been retained after the whole-genome duplication in *P. patens*, and more of these genes are present in TAGs than in *A. thaliana* (table S19). Redundancy and expansion of these abundantly expressed proteins probably contributes to a robustness of the photosynthetic antenna, i.e., the capacity to deal with high light intensities. The photoprotective early light–induced proteins (ELIPs) expanded extensively in *P. patens* [St 58_B (table S18B)]. Numerous ELIP-like proteins with supposedly free radical scavenging activity may reflect adaptation to dehydration and rehydration cycles and associated avoidance of photo-oxidative damage.

DNA repair. DNA damage repair maintains genomic integrity. Double-strand breaks (DSBs) can be repaired by nonhomologous end-joining (NHEJ), but are more precisely repaired using a second copy of the sequence. The introduction of linear DNA into a cell mimics DNA damage, and mosses, uniquely among plants, but like yeast, show a strong preference for the use of a homologous sequence for the incorporation of linear DNA into the genome.

Cell-cycle control is tightly connected to DNA-damage repair (*29*). Proteins known to be involved in these processes in both vertebrates and *A. thaliana* are ATM, ATR, CHK1, CHK2, PARP1, BRCA1, BRCA2, and BARD1. Although *P. patens* encodes the first four of these, there are no homologs found of BRCA1, BRCA2, and BARD1. RAD51 and the RAD51 paralogs (RAD51B, RAD51C, RAD51D, XRCC2, and XRCC3) are important for repair that results in homologous recombination in vertebrates and in *A. thaliana*; *P. patens* encodes all but XRCC3. However, although *A. thaliana* encodes one RAD51, *P. patens* encodes two (*30*). Other genes involved in DSB repair, chromatin remodeling, and processing of recombination intermediates known from *A. thaliana* (INO80, RAD54, MRE11, RAD50, NBS1, RecQ helicases (WRN, BLM, MUS81) are also present in *P. patens*. Additionally, both plant species, but not metazoans, encode SRS2, whereas *P. patens*, like other plants, lacks RAD52. In *A. thaliana* and yeast, the KU70/KU80 complex, DNA ligase IV, and XRCC4 contribute to NHEJ. These genes are also encoded by the *P. patens* genome. In addition, both plant species, but not yeast (*31*), encode the DNA-dependent protein kinase catalytic subunit (DNA-PKcs).

In our phylogenetic analyses, *P. patens* homologs of RAD54B, as well as Centrins and CHD7, cluster with algal and metazoan homologs, whereas flowering plant homologs do not (St 12_2, 28_2, 28_7). Although RAD51 and RAD54 interact in chromatin remodeling in humans (*32*), Centrins are important for genome stability in *C. reinhardtii* (*33*) and in nucleotide excision and DSB repair in *A. thaliana* (*34*). CHD7 is a chromodomain DNA helicase, important for chromatin structure, mutation of which causes developmental aberrations in mammals (*35*).

DNA damage is repaired by multisubunit macromolecular complexes of dynamic composition and conformation (*36*). The special features of the *P. patens* genome (no BRCA1, BRCA2, and BARD1, duplicated RAD51, and phylogenetically conserved RAD54B, Centrins, and CHD7) may well reflect the specific needs of a haploid genome for genome integrity surveillance and account for the efficiency of homology-dependent DSB repair in the *P. patens* genome.

Conclusions for Land Plant Evolution

P. patens occupies a position on the evolutionary tree that, through comparisons with aquatic algae and vascular plants, allows reconstruction of evolutionary changes in genomes that are concomitant to the conquest of land. From this, we conclude that the last common ancestor of all land plants (i) lost genes associated with aquatic environments (e.g., flagellar components for gametic motility); (ii) lost dynein-mediated transport; (iii) gained signaling capacities, such as those for auxin, ABA, cytokinin, and more complex photoreception; (iv) gained tolerance for abiotic stresses, such as drought, radiation, and extremes of temperature; (v) gained more elaborate transport capabilities; and (vi) had an overall increase in gene family complexity. Some of these events may have been enabled by the opportunities for evolutionary novelty created by one or more duplications of the whole genome.

These comparisons also enable reconstruction of the genomic events that occurred after the split of vascular plants and mosses. For example, the former acquired even more elaborate signaling [e.g., through gibberellic acid (GA), jasmonic acid (JA), ethylene, and brassinosteroids], but lost vegetative dehydration tolerance and motile gametes, whereas the latter gained an elaborate use of two-component systems, efficient homology-based DNA repair, and adaptation to shade and de-/rehydration cycles, as well as a redundant and versatile metabolism. The *P. patens* genome sequence provides a resource for the study of both gene function (*37*) and evolutionary reconstruction.

References and Notes

1. S. K. Floyd, J. L. Bowman, *Int. J. Plant Sci.* **168**, 1 (2007).
2. P. R. Kenrick, P. Crane, *Nature* **389**, 33 (1997).
3. Materials and methods are available as supporting material on *Science* Online.
4. Version 1.1 of the *P. patens* genome assembly and annotation can be accessed through the JGI Genome Portal at www.jgi.doe.gov/Physcomitrella; sequences have been deposited at DDBJ/EMBL/GenBank under the project accession ABEU01000000.
5. Y.-Y. Shen *et al.*, *Nature* **443**, 823 (2006).
6. C. Vitte, J. L. Bennetzen, *Proc. Natl. Acad. Sci. U.S.A.* **103**, 17638 (2006).
7. V. V. Kapitonov, J. Jurka, *Proc. Natl. Acad. Sci. U.S.A.* **98**, 8714 (2001).
8. M. Lynch, J. S. Conery, *Science* **290**, 1151 (2000).
9. S. A. Rensing *et al.*, *BMC Evol. Biol.* **7**, 130 (2007).
10. International Rice Genome Sequencing Project, *Nature* **436**, 793 (2005).
11. C. Rizzon, L. Ponger, B. S. Gaut, *PLoS Comput Biol* **2**, e115 (2006).
12. G. A. Tuskan *et al.*, *Science* **313**, 1596 (2006).
13. St stands for supplementary tree; these can be accessed via www.cosmoss.org/bm/supplementary_trees/Rensing_et_al_2007/.
14. C. Semple, K. H. Wolfe, *J. Mol. Evol.* **48**, 555 (1999).
15. H. Puchta, *J. Exp. Bot.* **56**, 1 (2005).
16. Y. Kamisugi *et al.*, *Nucleic Acids Res.* **34**, 6205 (2006).
17. S. Richardt, D. Lang, W. Frank, R. Reski, S. A. Rensing, *Plant Physiol.* **143**, 1452 (2007).
18. M. Oliver, J. Velten, B. Mishler, *Integr. Comp. Biol.* **45**, 788 (2005).
19. W. Frank, D. Ratnadewi, R. Reski, *Planta* **220**, 384 (2005).
20. L. Saavedra *et al.*, *Plant J.* **45**, 237 (2006).
21. A. C. Cuming, S. H. Cho, Y. Kamisugi, H. Graham, R. S. Quatrano, *New Phytol.* **176**, 275 (2007).
22. J. Giraudat *et al.*, *Plant Cell* **4**, 1251 (1992).
23. H. H. Marella, Y. Sakata, R. S. Quatrano, *Plant J.* **46**, 1032 (2006).
24. G. Hu, N. Yalpani, S. P. Briggs, G. S. Gurmukh, S. Johal, *Plant Cell* **10**, 1095 (1998).
25. H. P. Mock, B. Grimm, *Plant Physiol.* **113**, 1101 (1997).
26. A. E. Sztein, J. D. Cohen, I. G. de la Fuente, T. J. Cooke, *Am. J. Bot.* **86**, 1544 (1999).
27. W. Wang *et al.*, *Plant Cell* **18**, 3429 (2006).

28. W. Wang, B. Vinocur, O. Shoseyov, A. Altman, *Trends Plant Sci.* **9**, 244 (2004).
29. P. Sung, H. Klein, *Nat. Rev. Mol. Cell Biol.* **7**, 739 (2006).
30. U. Markmann-Mulisch *et al.*, *Proc. Natl. Acad. Sci. U.S.A.* **99**, 2959 (2002).
31. J. M. Daley, P. L. Palmbos, D. Wu, T. E. Wilson, *Annu. Rev. Genet.* **39**, 431 (2005).
32. Y. Zhang *et al.*, *Nat. Struct. Mol. Biol.* **14**, 639 (2007).
33. I. Zamora, W. F. Marshall, *BMC Biol.* **3**, 15 (2005).
34. L. Liang, S. Flury, V. Kalck, B. Hohn, J. Molinier, *Plant Mol. Biol.* **61**, 345 (2006).
35. E. A. Hurd *et al.*, *Mammal Genome* **18**, 94 (2007).
36. O. Llorca, *Curr. Opin. Struct. Biol.* **17**, 215 (2007).
37. R. S. Quatrano, S. F. McDaniel, A. Khandelwal, P.-F. Perroud, D. J. Cove, *Curr. Opin. Plant Biol.* **10**, 182 (2007).
38. D. G. Kelch, A. Driskell, B. Mishler, in *Molecular Systematics of Bryophytes*, B. Goffinet, V. Hollowell, R. Magill, Eds. (Missouri Botanical Garden Press, St. Louis, MO, 2004), pp. 3–12.

39. We thank K. Zhou and S. Pitluck at DOE Joint Genome Institute (JGI) for GenBank submissions and G. Werner and his group at JGI for support of gene annotation tools. Discussions with M. Oliver and K. Fisher on desiccation tolerance are greatly appreciated. N. Lyons efficiently handled many of the administrative tasks throughout the project and the detailed preparation of the final manuscript. Part of this work was funded by German National Science Foundation (DFG) grant RE 837/10 to R.R., by a U.K. Biotechnology and Biological Sciences Research Council (BBSRC) grant (24/P11357) to A.C.C. and by grants to R.S.Q. from the NSF (IBN 0112461 and 0425749-1) and Washington University. This work was also supported by Grant-in-Aid for Scientific Research on Priority Areas from the Ministry of Education, Culture, Sports, Science and Technology of Japan (to T.T., T.F., Y. Kuroki, A.T., Y.S., S.H., K.Y., S.S., Y. Kohara, A.F., T.M., T.N., and M.H). This work was performed under the auspices of the U.S. Department of Energy's Office of Science, Biological and Environmental Research Program, and by the University of California, Lawrence Livermore National Laboratory under contract no. W-7405-Eng-48, Lawrence Berkeley National Laboratory under contract no. DE-AC02-05CH11231, and Los Alamos National Laboratory under contract no. W-7405-ENG-36.

Supporting Online Material
www.sciencemag.org/cgi/content/full/1150646/DC1
Materials and Methods
SOM Text
Figs. S1 to S8
Tables S1 to S23
References

18 September 2007; accepted 21 November 2007
Published online 13 December 2007;
10.1126/science.1150646
Include this information when citing this paper.

Hidden Degrees of Freedom in Aperiodic Materials

Bertrand Toudic,[1,2]* Pilar Garcia,[1,2] Christophe Odin,[1,2] Philippe Rabiller,[1,2] Claude Ecolivet,[1,2] Eric Collet,[1,2] Philippe Bourges,[3] Garry J. McIntyre,[4] Mark D. Hollingsworth,[5] Tomasz Breczewski[6]

Numerous crystalline materials, including those of bioorganic origin, comprise incommensurate sublattices whose mutual arrangement is described in a superspace framework exceeding three dimensions. We report direct observation by neutron diffraction of superspace symmetry breaking in a solid-solid phase transition of an incommensurate host-guest system: the channel inclusion compound of nonadecane/urea. Strikingly, this phase transition generates a unit cell doubling that concerns only the modulation of one substructure by the other—an internal variable available only in superspace. This unanticipated pathway for degrees of freedom to rearrange leads to a second phase transition, which again is controlled by the higher dimensionality of superspace. These results reveal nature's capacity to explore the increased number of phases allowed in aperiodic crystals.

Aperiodicity (*1*, *2*) plays a central role in the structure and physical properties of materials as diverse as quasi-crystals (*3*), superconductors (*4*), and zeolites (*5*). In a number of solid-state supramolecular assemblies—a class of materials ubiquitous both in nature and in the laboratory—modern diffraction methods have revealed incommensurate relations between the basic structures of the noncovalently assembled constituents. In host-guest systems, for example, aperiodicity is an essential element that controls phenomena as diverse as crystal growth (*6*), polar ordering of guests (*7*), and absorption and molecular transport (*8*). Aperiodic materials are described in the framework of a higher-dimensional space called superspace, which decomposes into two orthogonal subspaces: the usual three-dimensional physical space and an internal one (*9*, *10*). The increase in dimensionality theoretically allows many more phases (*11*, *12*); however, the role of aperiodicity in the structural changes of supramolecular assemblies has been largely ignored. In the transformations of such materials, aperiodicity resulting from different interacting length scales should play a major role, coupling structure and dynamics, in particular through the mechanism of free sliding (*13*, *14*). Here, we highlight the richness of transformations associated with the new degrees of freedom hidden in superspace, taking as an example a prototypical host-guest system of nonadecane/urea.

Supramolecular chemistry and crystal engineering enable the formation of a diverse array of aperiodic host-guest architectures in which guest molecules are confined with their own periodicity to nanochannels. Although such host structures may be held together by simple van der Waals forces (*8*), covalent bonds (*5*, *15*), or hydrogen bonds, as in the diverse structures formed by certain dipeptides (*16*), a common feature is that the host is more rigid than the guest component. This is typically the case for urea inclusion compounds, in which urea molecules are connected by hydrogen bonds to form helical ribbons, which are woven together to form a honeycomb array of linear, nonintersecting, hexagonal tunnels that contain straight-chain hydrocarbons and analogs (Fig. 1) (*17*). Guests such as nonadecane pack end to end within van der Waals contact of each other and undergo substantial torsions, librations, and translations, as well as diffusive motions or jumps about the sixfold axis of the host (*18*). For this host-guest system, the ratio of repeat lengths along the channel axis of the urea host ($\mathbf{c}_{\text{host}}$) and nonadecane guest ($\mathbf{c}_{\text{guest}}$) is not a rational number, so the crystal is said to be incommensurate.

Although the locations ($\mathbf{G}_{hkl}$) of diffraction peaks of typical three-dimensional crystals can be defined with three indices (*h*, *k*, and *l*), an additional parameter or parameters must be used to describe the diffraction patterns of aperiodic materials such as incommensurate channel inclusion compounds. In the linear tunnels of urea, $\mathbf{c}_{\text{host}}$ and $\mathbf{c}_{\text{guest}}$ are parallel, so one extra parameter is required to describe the system. Thus, for this nanotubular intergrowth structure, with its single incommensurate direction (**c**), a four-dimensional superspace description gives the positions of all of the Bragg peaks (*8*, *9*):

$$\mathbf{G}_{hklm} = h\mathbf{a}^* + k\mathbf{b}^* + l\mathbf{c}^*_{\text{host}} + m\mathbf{c}^*_{\text{guest}} \qquad (1)$$

where $\mathbf{a}^*$, $\mathbf{b}^*$, $\mathbf{c}^*_{\text{host}}$, and $\mathbf{c}^*_{\text{guest}}$ are the conventional reciprocal unit vectors, which differ

---

[1] Université de Rennes 1, Institut de Physique de Rennes (IPR), 35042 Rennes Cedex, France. [2] CNRS, UMR 6251, IPR, 263 Avenue du Général Leclerc, 35042 Rennes Cedex, France. [3] Laboratoire Léon Brillouin, CEA-CNRS, CE-Saclay, 91191 Gif-sur-Yvette, France. [4] Institut Laue-Langevin, 38042 Grenoble Cedex 9, France. [5] Department of Chemistry, Kansas State University, Manhattan, KS 66506, USA. [6] Facultad de Ciencias, Universidad del Pais Vasco, Apdo 644, Bilbao, Spain.

*To whom correspondence should be addressed. E-mail: bertrand.toudic@univ-rennes1.fr

along **c*** for host and guest sublattices. With this and other composite incommensurate crystals, the interaction between the substructures requires that the system be treated as an integral whole, even though the influence of one substructure on the other (the intermodulation) may be weak enough to maintain the mean periodicity of the two substructures (*19*). However, the collinearity of $\mathbf{c}_{\mathrm{host}}$ and $\mathbf{c}_{\mathrm{guest}}$ simplifies things greatly. As illustrated in Fig. 1C, the Bragg peaks may be separated into four distinct classes: (i) Peaks from the commensurate (**a***, **b***) plane are indexed (*h k* 0 0) and are called common Bragg peaks; (ii) host peaks reflect the mean periodicity of the host and are indexed (*h k l* 0); (iii) guest peaks reflect the mean periodicity of the guest and are indexed (*h k* 0 *m*); and (iv) satellite peaks, which characterize the intermodulation of one substructure on the other, are indexed as (*h k l m*) with *l* and *m* not equal to zero. All four classes of reflections have been reported in the diffraction patterns of alkane/urea inclusion compounds (*20*, *21*).

Structural instabilities have been studied extensively in alkane/urea crystals, and although the literature points to a homogeneous hexagonal-to-orthorhombic phase transition (*22*–*25*), such treatments cannot accommodate the role of aperiodicity in such transformations. In fact, and in contrast with traditional (periodic) materials, many more types of phase transitions may be considered in crystallographic systems requiring four or more dimensions, even when considering only the group/subgroup relations between phases. For transitions within aperiodic materials in which the unit cell dimensions increase, it is conceivable that reflections in any of the aforementioned classes could emerge. With incommensurate nanotubular structures, such as those formed by urea, each of the different classes of reflections corresponds to a different type of ordering and/or interaction.

Here, we report a high-resolution neutron diffraction (*26*) analysis of nonadecane-d$_{40}$/urea-d$_4$, a compound characterized by a misfit parameter value $\mathbf{c}_{\mathrm{host}}/\mathbf{c}_{\mathrm{guest}} \approx 0.418$ and an upper phase transition at T_{c1} = 149 K. Figure 2A shows a section of the diffraction pattern in the (**a***, **c***) plane measured slightly above the transition temperature. The striking result is the presence of superstructure satellite peaks in the absence of superstructure peaks in the basal commensurate plane. The extended reciprocal line measured below the transition temperature (at T_{c1}–10.1 K) is shown in Fig. 2C. This superstructure line contains neither common, host, nor guest Bragg peaks. According to the simplest (3 + 1)–dimensional description, the superstructure peaks may be indexed by the summation rule defined in Fig. 1C.

These observations constitute proof of a structural instability that doubles the cell exclusively for the internal variable that is available only in an *n*-dimensional space, with $n > 3$. In effect, they rule out the usual three-dimensional interpretation applied to phase transitions in this group of materials, in which a single hexagonal-to-orthorhombic transition (*22*–*24*) was most readily described in terms of a herringbone ordering of the guest molecules coupled to an antiferroelastic shearing of the host substructure (*25*). Throughout the alkane/urea series, this phase transition has been shown to exhibit a strong calorimetric signature (*27*), verifying substantial structural ordering. However, the present example shows that the long-range order parameter that governs this structural instability is inhomogeneous because it varies in space. Thus, although host-guest intermodulation was previously neglected in the discussions of such phase transitions, it appears to be the driving force in the cooperative rearrangement of these soft materials.

A major outcome of superspace symmetry breaking concerns the richness of phases accessible to this and other aperiodic materials. In addition to satellite Bragg peaks, common, host, and guest Bragg peaks appear in the superstructure line in diffraction profiles collected at temperatures below a second phase transition, which occurs at T_{c2} = 129 K (Fig. 3). Thus, at 99.3 K, all four types of superstructure Bragg peaks are present, indicating a homogeneous component to the order parameter that emerges in addition to the inhomogeneous one appearing at higher temperatures.

An obvious question concerns the physical nature of the higher-temperature phase transition in this crystal. In accord with the large calorimetric signature, previous solid-state ^{2}H nuclear magnetic resonance studies of single crystals of nonadecane-d$_{40}$/urea revealed that rapid reorientations of guest molecules about the channel axis become essentially frozen upon cooling through the transition, and that the guests furthermore become precisely oriented with their zigzag chains aligned toward the vertices of the channels (*24*). In the process of cooling through T_{c1}, the average positions of host and guest molecules are the same from channel to channel, as shown by the C-centered orthorhombic symmetry displayed by host and guest reflections (figs. S1 to S7). This absence of cell doubling for the mean structure is in stark contrast with the doubling of the real four-dimensional unit cell along the **a** axis, as signified by the emergence of the strong superstructure satellite reflections. These satellite reflections satisfy the systematic absence conditions for twofold screw axes along the orthorhombic axes, indicating that the intermodulation between host and guest substructures alternates from channel to channel. Thus, the doubling of the unit cell at the phase transition arises solely from the differences in intermodulation between adjacent channels, and signifies that the arrangement of guests and/or hosts deviates in the opposite sense from that of their neighbors in adjacent channels, even though the mean structures remain the same from channel to channel. Such an unusual way for degrees of freedom to rearrange is a natural consequence of the aperiodicity in this incommensurate system.

The occurrence of the second phase transition (Fig. 3B) is also a direct consequence of the higher dimensionality of superspace. At T_{c2}, the prior doubling of the intermodulation leads to a doubling along the **a** axis of the host and guest substructures. In that same transition, the mean structures of host and guest furthermore adopt twofold screw ar-

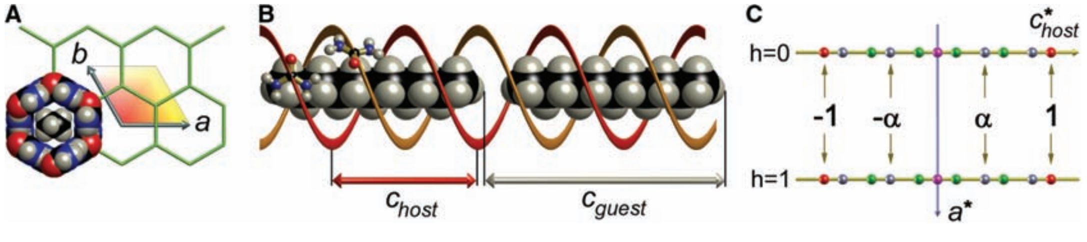

Fig. 1. Real and reciprocal images of a self-assembled aperiodic material. (**A**) Alkane/urea crystals are prototypical examples of nanotubular intergrowth compounds. The projected **ab** plane, normal to the channels, is commensurate. (**B**) Along the channel, the periodicity of the host urea subsystem is c_{host} = 1.102 nm at room temperature, whereas the guest periodicity, c_{guest}, is roughly a linear function of the number of carbon atoms in the alkane molecule. The irrational ratio, $c_{\mathrm{host}}/c_{\mathrm{guest}}$, defines a misfit parameter α. (**C**) The reciprocal image is characterized by four different types of diffraction peaks (*9*, *18*, *19*). The common Bragg peaks in purple are located at (*h*, *k*, 0, 0). The scale refers to the host periodicity, so host Bragg peaks (*h*, *k*, *l*, 0) in red are at integer positions along **c***, and guest Bragg peaks (*h*, *k*, 0, *m*) in gray are at multiple values of α (which is also equal to $c^*_{\mathrm{guest}}/c^*_{\mathrm{host}}$). Intermodulation satellite Bragg peaks, in green, are along **c*** at the summation positions (*h*, *k*, *l*, *m*) with *l* and *m* different from zero. The presence of these satellites shows that each sublattice is modulated by the periodic potential of the other one.

rangements along the orthorhombic axis in much the same way as the intermodulation does in the intermediate phase (figs. S1 to S3). Although the complete crystal structure of nonadecane/urea is currently inaccessible, further studies on other members of this class of urea inclusion compounds may reveal specific systems that will provide even more insights into the nature of these materials.

Our study highlights the increase in structural solutions upon going from three-dimensional to higher-dimensional structures. Quite unexpectedly, we have found a transition that uses only the extra variables available in four-dimensional superspace. These additional structural degrees of freedom may combine with dynamical ones to allow new properties that are essential in tuning the functionalities of nanoscale materials. In urea inclusion compounds, for example, subnanofluidity illustrated by the molecular transport of the guest molecules (*8*), selective compressibility (*28*), and a pressure-induced lock-in (*29*) were recently reported. All of these phenomena rely on the aperiodicity of the structures, which theoretically allows a displacement of one substructure with respect to the other without any restoring force (*13*). Further work concerning the structure and dynamics of materials for which aperiodicity enhances the number of degrees of freedom should be very fruitful.

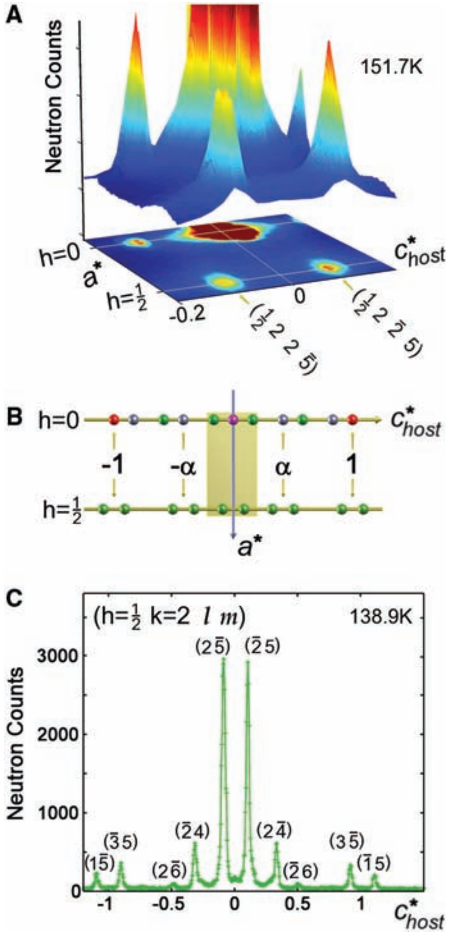

Fig. 2. Evidence of symmetry breaking in the fourth dimension of the superspace. (**A**) Neutron diffraction pattern measured in nonadecane-d$_{40}$/urea-d$_4$ at T = 151.7 K. The horizontal abscissa is indexed in host reciprocal units. The structure line, at the rear of the pattern, contains the huge common-structure Bragg peak (0, 2, 0, 0) with the neighboring satellite (0, 2, $\bar{1}$, 2). The superstructure line appears as pretransitional diffuse scattering within the undistorted high-symmetry phase. In this superstructure line (½, 2, l, m), the common (½, 2, 0, 0) superstructure scattering is absent, whereas superstructure satellites (½, 2, $\bar{2}$, 5) and (½, 2, 2, $\bar{5}$) exist. (**B**) The diagram illustrates symmetry breaking in the internal superspace below T_{c1}, where only satellite Bragg peaks (h/2, k, l, m) with l and m different from zero are present in the superstructure line. The shaded region corresponds to the reciprocal region probed in the uppermost image. (**C**) Superstructure line (½, 2, l, m), measured at 138.9 K, showing the presence of only satellites. According to the summation rule defined in Fig. 1C, the observed locations of the satellites at ±0.090 in host reciprocal units along c^* are indexed by (l, m) equal to ±($\bar{2}$, 5), at ±0.328 by ±($\bar{2}$, 4), at ±0.508 by ±($\bar{2}$, 6), at ±0.910 by ±($\bar{3}$, 5), and at ±1.090 by ±($\bar{1}$, 5).

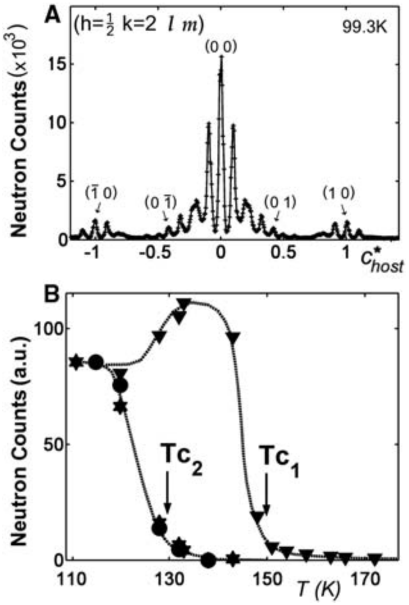

Fig. 3. Sequence of phases in superspace. (**A**) The superstructure line (½, 2, l, m) of nonadecane-d$_{40}$/urea-d$_4$ at 99.3 K reveals the existence of all four types of superstructure reflections, indicating an additional ordered phase in the superspace formalism. (**B**) Evolution of the normalized intensity of superstructure Bragg peaks with temperature. All the satellites appearing at the upper transition behave in the same manner; for clarity, only the temperature dependence of the strongest one (½, 2, 2, $\bar{5}$) is shown, represented by triangles; the common (½, 2, 0, 0) and the host (½, 2, $\bar{1}$, 0) superstructure scattering are symbolized by stars and circles, respectively. Two transition temperatures are derived, T_{c1} = 149 K and T_{c2} = 129 K. Lines are shown as visual guides.

References and Notes

1. T. Janssen, G. Chapuis, M. de Boissieu, *Aperiodic Crystals: From Modulated Phases to Quasicrystals* (Oxford Univ. Press, Oxford, 2007).
2. E. Macia, *Rep. Prog. Phys.* **69**, 397 (2006).
3. E. Abe, Y. Yan, S. J. Pennycook, *Nat. Mater.* **3**, 759 (2004).
4. P. A. Midgley, S. M. Hayden, L. Taillefer, B. Bogenberger, H. von Löhneysen, *Phys. Rev. Lett.* **70**, 678 (1993).
5. B. Smit, T. L. M. Maesen, *Nature* **374**, 42 (1995).
6. M. D. Hollingsworth, M. E. Brown, A. C. Hillier, B. D. Santarsiero, J. D. Chaney, *Science* **273**, 1355 (1996).
7. O. König, H.-B. Bürgi, T. Armbruster, J. Hulliger, T. Weber, *J. Am. Chem. Soc.* **119**, 10632 (1997).
8. J. Marti-Rujas, A. Desmedt, K. D. M. Harris, F. Guillaume, *J. Am. Chem. Soc.* **126**, 11124 (2004).
9. T. Janssen, A. Janner, A. Looijenga-Vos, P. M. de Wolf, in *International Tables for Crystallography Vol. C*, A. J. C. Wilson, Ed. (Kluwer Academic, Dordrecht, Netherlands, 1995), pp. 797–844.
10. P. Coppens, *Acta Crystallogr. B* **51**, 402 (1995).
11. A. Janner, T. Janssen, J. C. Toledano, in *Lecture Notes in Physics, vol. 201*, G. Denardo *et al.*, Eds. (Springer, Berlin, 1984), pp. 394–396.
12. S. Van Smaalen, K. D. M. Harris, *Proc. R. Soc. London Ser. A* **452**, 677 (1996).
13. T. Janssen, *J. Phys. Cond. Matter* **14**, 12411 (2002).
14. O. M. Braun, A. Vanossi, E. Tosatti, *Phys. Rev. Lett.* **95**, 026102 (2005).
15. W. Mickelson, S. Aloni, W.-Q. Han, J. Cumings, A. Zettl, *Science* **300**, 467 (2003).
16. C. H. Görbitz, *Chem. Eur. J.* **13**, 1022 (2007).
17. M. D. Hollingsworth, K. D. M. Harris, in *Comprehensive Supramolecular Chemistry*, D. D. MacNicol, R. Bishop, F. Toda, Eds. (Pergamon, Oxford, 1996), vol. 6, pp. 177–237.
18. F. Guillaume, C. Sourisseau, *J. Chem. Phys.* **93**, 3536 (1990).
19. K. D. M. Harris, J. M. Thomas, *J. Chem. Soc. Faraday Trans.* **86**, 2985 (1990).
20. R. Lefort *et al.*, *Phys. Rev. Lett.* **77**, 4027 (1996).
21. T. Weber, H. Boysen, M. Honal, F. Frey, R. B. Neder, *Z. Kristall.* **211**, 238 (1996).
22. Y. Chatani, Y. Taki, H. Tadokoro, *Acta Crystallogr. B* **33**, 309 (1977).
23. R. Forst, H. Jagodzinski, H. Boysen, F. Frey, *Acta Crystallogr. B* **46**, 70 (1990).
24. H. Le Lann *et al.*, *Phys. Rev. B* **62**, 5442 (2000).
25. R. M. Lynden-Bell, *Mol. Phys.* **79**, 313 (1993).
26. The data were collected with an incident neutron wave vector k_i = 1.55 Å^{-1} on the triple-axis spectrometer 4F1 installed on a cold neutron source at the Laboratoire Léon Brillouin in Saclay, France.
27. R. C. Pemberton, N. G. Parsonage, *Trans. Faraday Soc.* **61**, 2112 (1965).
28. L. Bourgeois, C. Ecolivet, B. Toudic, P. Bourges, T. Breczewski, *Phys. Rev. Lett.* **91**, 025504 (2003).
29. B. Toudic, F. Aubert, C. Ecolivet, P. Bourges, T. Breczewski, *Phys. Rev. Lett.* **96**, 145503 (2006).
30. We thank M. Huard and F. Guillaume for discussions. Supported by grant 43708-AC10 from the Petroleum Research Fund, administered by the American Chemical Society (M.D.H.).

Supporting Online Material

www.sciencemag.org/cgi/content/full/319/5859/69/DC1
Materials and Methods
Figs. S1 to S7

19 June 2007; accepted 19 November 2007
10.1126/science.1146745

CORRECTED 2 MAY 2008; SEE LAST PAGE

Nonadiabatic Interactions in the Cl + H_2 Reaction Probed by ClH_2^- and ClD_2^- Photoelectron Imaging

Etienne Garand,[1] Jia Zhou,[1] David E. Manolopoulos,[2]* Millard H. Alexander,[3]* Daniel M. Neumark[1,4]*

The degree of electronic and nuclear coupling in the Cl + H_2 reaction has become a vexing problem in chemical dynamics. We report slow electron velocity-map imaging (SEVI) spectra of ClH_2^- and ClD_2^-. These spectra probe the reactant valley of the neutral reaction potential energy surface, where nonadiabatic transitions responsible for reactivity of the Cl excited spin-orbit state with H_2 would occur. The SEVI spectra reveal progressions in low-frequency Cl·H_2 bending and stretching modes, and are compared to simulations with and without nonadiabatic couplings between the Cl spin-orbit states. Although nonadiabatic effects are small, their inclusion improves agreement with experiment. This comparison validates the theoretical treatment, especially of the nonadiabatic effects, in this critical region of the Cl + H_2 reaction, and suggests strongly that these effects are minor.

The Cl + H_2 → HCl + H reaction has been studied for more than a century, serving as a benchmark for the development of bimolecular reaction rate theory (*1*). It has attracted renewed attention over the past decade, as fresh theoretical and experimental results have highlighted unanticipated features of the reaction and challenged our fundamental understanding of its dynamics. In particular, a study of the Cl + HD reaction by Skouteris *et al*. (*2*) provided experimental evidence that the weak van der Waals (vdW) forces in the reactant valley have a notable effect on the branching ratio of the HCl:DCl product as a function of collision energy. These results suggest that spectroscopic study of the prereactive Cl·H_2 complex would provide new insights into how weak vdW interactions affect chemical reactivity.

Such an experiment would also shed light on an important ongoing controversy concerning the relative reactivities of ground-state Cl($^2P_{3/2}$) and excited spin-orbit state Cl*($^2P_{1/2}$), lying 882.3 cm^{-1} higher, measured in crossed molecular beam experiments by Liu and co-workers (*3*, *4*). For reactions of Cl or F with H_2, only the X($^2P_{3/2}$) state correlates adiabatically with the HX + H products in their electronic ground state. Experience shows that the Born-Oppenheimer (BO) approximation will govern chemical reactions, so that the electronically adiabatic pathway should always dominate (*5*, *6*). This is confirmed by multi–potential energy surface (PES) reactive scattering calculations on the F + H_2 (*7*) and Cl + H_2 (*8*, *9*) systems by Alexander *et al*., and, most convincingly, in a recent comparison with crossed molecular beam experiments by Yang and co-workers (*10*) on the F + D_2 system. In that comparison, the calculations were based on a highly correlated, scaled set of PESs in which the experimental exoergicity and the presumed experimental barrier height were accurately reproduced. Only at very low collision energies, where the reaction barrier quenches the BO-allowed F + D_2 reaction, did the BO-forbidden F* + D_2 reaction become comparable in relative importance. In contrast, the experiments of Liu and co-workers imply that the exact opposite is true for the Cl/Cl* + H_2 reaction: At low energy, the BO-allowed reaction dominates, but as the collision energy increases, the BO-forbidden reaction becomes increasingly important. These results can be explained only by postulating that nonadiabaticity in the Cl + H_2 reaction is qualitatively different from that in the F + H_2 reaction and in the quantum simulations of the Cl + H_2 reaction. This difference—and, in particular, the discrepancy between experiment and theory—is currently one of the major unresolved problems in chemical reaction dynamics.

With these considerations in mind, we report high-resolution photoelectron imaging spectra of ClH_2^- and ClD_2^-. This experiment spectroscopically probes the prereactive complex of the Cl + H_2 reaction, offering complementary information to Liu's reactive scattering experiments, in precisely the region where the nonadiabatic transitions responsible for the reactivity of the Cl*($^2P_{1/2}$) state are expected to occur (*7*–*9*, *11*, *12*). The experimental results are compared with two separate sets of Franck-Condon (FC) simulations in which the nonadiabatic coupling between the Capecchi-Werner ab initio PESs (*13*) is first neglected and then retained.

Photoelectron spectroscopy of anionic complexes has been used to probe the transition states of bimolecular reactions (*14*, *15*). A notable example of this transition-state spectroscopy was a study of the FH_2^- anion, whose ground-state geometry has good FC overlap with the early barrier of the F + H_2 reaction (*16*, *17*). In contrast, the Cl + H_2 reaction has a later barrier, and thus the equilibrium geometry of ClH_2^- is much closer to the reactant valley than to the transition state (Fig. 1). The ClH_2^- anion wave function has good FC overlap with the vibrational and hindered rotor states of the neutral Cl·H_2 vdW complex (*18*); with an energy resolution of 1 meV, it was predicted that several features associated with bound and resonance states of this prereactive complex could be resolved (*18*).

Photoelectron spectra of ClH_2^- and ClD_2^- obtained with a conventional negative ion time-of-flight photoelectron spectrometer have been reported (*19*). These spectra exhibited features associated with the spin-orbit splitting in the Cl·H_2 complex. However, finer structures associated with vibrations and hindered rotor motions of the complex could not be observed because of the limited resolution, around 8 to 10 meV. Recently, Osterwalder *et al*. (*20*) developed slow electron velocity-map imaging (SEVI), which combines the high collection efficiency of velocity-map

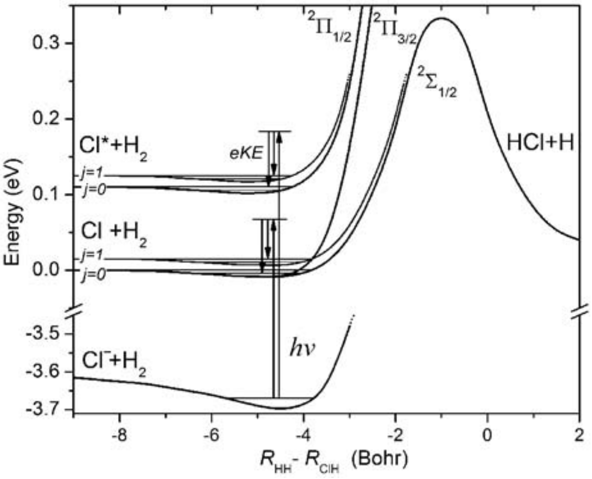

Fig. 1. Schematic view of the Cl·H_2 anionic and neutral PESs in terms of relative distance between the atoms. Photodetachment of ClH_2^- probes the shallow vdW wells in the entrance valley of the Cl + H_2 reaction, where the nonadiabatic transitions responsible for the reactivity of the Cl*($^2P_{1/2}$) state are expected to occur.

---

[1]Department of Chemistry, University of California, Berkeley, CA 94720, USA. [2]Physical and Theoretical Chemistry Laboratory, Oxford University, South Parks Road, Oxford OX1 3QZ, UK. [3]Department of Chemistry and Biochemistry and Institute for Physical Science and Technology, University of Maryland, College Park, MD 20742, USA. [4]Chemical Sciences Division, Lawrence Berkeley National Laboratory, Berkeley, CA 94720, USA.

*To whom correspondence should be addressed. E-mail: david.manolopoulos@chem.ox.ac.uk (D.E.M.); mha@umd.edu (M.H.A.); dneumark@berkeley.edu (D.M.N.)

imaging (VMI) (*21*, *22*) with the high resolution of threshold photodetachment. In this technique, mass-selected anions generated from a pulsed molecular beam are photodetached at energies slightly above threshold by means of a tunable dye laser. The resulting slow photoelectrons are extracted collinearly with the ion beam by a VMI assembly and mapped onto imaging microchannel plates coupled to a phosphor screen. High-resolution photoelectron spectra are obtained by angular integration of the inverse-Abel transformed images. All the observed transitions have similar widths in electron velocity, so the resolution scales as the square root of the electron kinetic energy. The highest resolution, up to 1 cm^{-1} for atomic anions, is obtained at wavelengths close to the threshold for a particular photodetachment transition, whereas lower-resolution spectra with wider energy windows can be measured by operating further from threshold (*23*).

Preliminary SEVI spectra (*20*) of ClD_2^- resolved more structure than was seen in the photoelectron spectra. However, by shortening the electron flight tube to minimize the effect of stray fields and using an Even-Lavie pulsed valve with a pulsed ionizer (*24*) and higher backing pressure [250 psi total, using trace CCl_4 in a 10:1 Ar:H_2(D_2) mix] to produce colder anions, we have improved on the resolution of this earlier study, finding many previously unseen features that allow for rigorous comparison with theory.

Overview SEVI spectra of ClH_2^- and ClD_2^- taken at wavelengths of 326.5 nm and 323.0 nm, respectively, are shown in Fig. 2. The $^{37}ClH_2^-$ isotopolog was chosen to avoid interference from photodetachment of $^{37}Cl^-$, which produces photoelectrons in the same energy range; for ClD_2^-, the more abundant $^{35}ClD_2^-$ was used. The SEVI spectrum of Cl^- taken at 325 nm, acquired for calibration, is shown in the bottom panel of Fig. 2 for comparison. The ClH_2^- and ClD_2^- spectra are dominated by two main features associated with the spin-orbit states of the chlorine atom. Although these features already show more structure than was seen previously, the resolution of the SEVI spectra can be improved further by tuning the detachment laser just above the threshold of the feature of interest.

This procedure yields the spectra of the two spin-orbit features of ClH_2^- and ClD_2^- in Figs. 3 and 4, respectively. These higher-resolution spectra reveal several new features. For example, in Fig. 2, the shoulder and first two peaks in the $Cl(^2P_{3/2})\cdot D_2$ band appear as five features in the top panel of Fig. 4, with the two peaks each being split into closely spaced doublets.

As shown in Fig. 1, the interaction of Cl and Cl* with H_2 ($^1\Sigma_g^+$) gives rise to three adiabatic electronic PESs, labeled $^2\Sigma_{1/2}$, $^2\Pi_{3/2}$, and $^2\Pi_{1/2}$, in linear geometries (*25*). In the adiabatic limit, only $Cl(^2P_{3/2})$ atoms that approach H_2 on the $^2\Sigma_{1/2}$ PES react to form ground-state products. Figure 1 also shows that each electronic state has bend/hindered rotor levels that correlate to various H_2 rotational levels *j* (only *j* = 0 and 1 are shown) and that each bend level has a shallow vdW well that supports very-low-frequency Cl·H_2 stretching vibrations.

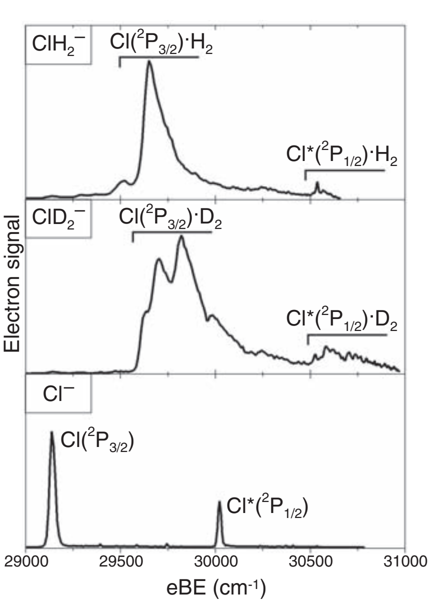

Fig. 2. Overview SEVI spectra of ClH_2^- (**top**) and ClD_2^- (**middle**) taken at wavelengths of 326.5 nm and 323 nm, respectively. The SEVI spectrum of Cl^- (**bottom**) taken at 325 nm is shown for comparison. All spectra show electron signal as a function of electron binding energy (eBE), defined as the difference between the photon energy and the measured electron kinetic energy.

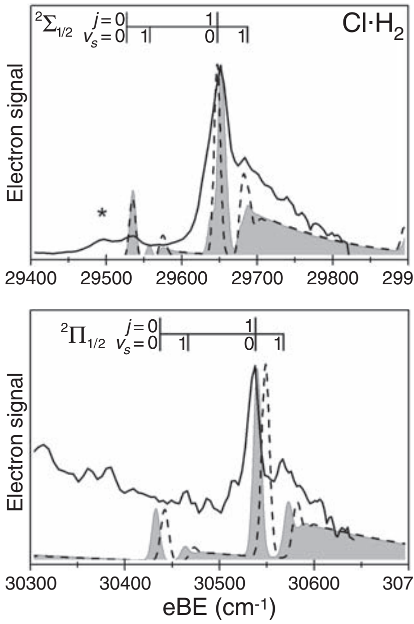

Fig. 3. High-resolution SEVI spectrum of ClH_2^- (solid line) is compared with FC simulations where the nonadiabatic interactions are neglected (dashed line) and included (gray-shaded area). Both spectra show electron signal as a function of eBE, defined as in Fig. 2. (**Top**) Average of three spectra taken between 334.5 and 335.5 nm; (**bottom**) average of three spectra taken between 326 and 326.5 nm.

The spectra in Figs. 3 and 4 can be fully assigned, on the basis of electronically adiabatic FC simulations of detachment, to the three neutral states. The dashed lines in Figs. 3 and 4 show the simulated spectra obtained using the coupled-cluster [CCSD(T)] PES of Alexander (*26*) for the anion and retaining all three electronically adiabatic PESs of Capecchi and Werner (*13*) for the neutral, as described in (*18*). None of the nonadiabatic couplings were included. The simulated spectra assume the usual ortho:para ratio of 3:1 for ClH_2 and 2:1 for ClD_2. (The rotational quantum number *j* is even for *p*-H_2 and *o*-D_2 and odd for *o*-H_2 and *p*-D_2.) Because the intensity of the experimental signal is arbitrary, the experimental and calculated intensities have been scaled to give the same maximum peak height in each panel. The theoretical spectra were also shifted slightly to match the position of the origin transition in Cl·H_2 (29,533 cm^{-1}) and Cl·D_2 (29,631 cm^{-1}). This shift was the only adjustable parameter used in the simulations.

In the top panel of Fig. 3, the observed peaks are associated with the hindered H_2(*j* = 0 and 1) rotor states of the weakly bound Cl·H_2 complex on the ground $^2\Sigma_{1/2}$ electronic PES. One quantum of excitation in the Cl·H_2 vdW stretching vibration (v_s) is also observed at 30 cm^{-1} above the (*j* = 1, v_s = 0) level. These quantum numbers can be unambiguously assigned by means of a simple adiabatic-bender analysis (*27*, *28*). Transitions to the vdW bound and resonance states associated with the $^2\Pi_{3/2}$ electronic state are predicted to have lower intensities, owing to poorer FC overlap with the anion wave function, and are buried beneath these $^2\Sigma_{1/2}$ transitions (*18*). The peak marked with an asterisk at 29,495 cm^{-1} lies 153 cm^{-1} below the (*j* = 1, v_s = 0) peak. Because this shift is close to the measured stretching vibration in the anion (*26*), we assign this peak to a hot band originating from the anion v_s = 1 state. Finally, the two features in the bottom panel of Fig. 3 are assigned to the (*j* = 1, v_s = 0) and (*j* = 1, v_s = 1) vdW bend-stretch states on the $^2\Pi_{1/2}$ excited electronic state.

The ClD_2^- spectrum exhibits similar features but with a smaller hindered rotor spacing. In the top panel of Fig. 4, the observed transitions are assigned to hindered D_2 rotor modes (*j* = 0, 1, 2) on the $^2\Sigma_{1/2}$ ground electronic state, with a 30 cm^{-1} stretching vibration resolved for the *j* = 1 and 2 levels. Similar transitions are observed on the $^2\Pi_{1/2}$ electronic state and are shown in the bottom panel of Fig. 4.

Although the electronically adiabatic simulations in Figs. 3 and 4 allow us to assign most features in the measured spectra, there are some clear differences (on the order of 10 cm^{-1}) between several of the predicted peak positions and those observed experimentally. To address these discrepancies, we performed a second set of FC simulations in which the dynamics of the neutral

Cl·H_2 complex were described by the same Hamiltonian used by Alexander *et al.* in their multi-PES quantum reactive scattering calculations for Cl + H_2 (*8*, *9*). This treatment includes four quasi-diabatic PESs as well as the spin-orbit and Coriolis coupling between the electronic-rovibrational states (*7*).

In modeling the photodetachment process, we assumed as in our adiabatic simulations that the ClH_2^- anion was sufficiently rotationally cold to be modeled by total angular momentum $J = 0$. We also exploited the Wigner threshold law for anion photodetachment (*29*, *30*), which implies that the dominant excitation pathway at sufficiently low electron kinetic energies will be the excitation of a Cl 3p electron to a continuum s orbital. Allowing for the angular momenta of the incident photon and the departing photoelectron, these assumptions lead to independent excitation of the $J = 1/2$ and $J = 3/2$ angular momentum states of Cl·H_2, corresponding to the excitation of $Cl(^2P_{1/2})\cdot H_2$ and $Cl(^2P_{3/2})\cdot H_2$, respectively.

The neutral angular momentum states $\Psi^{JM}_{\text{neutral}}$ were constructed by dressing the anion vibrational wave function ψ^{00}_{anion} with appropriate linear combinations of Wigner rotation matrix elements $D^{J*}_{MK}(\Omega)$ (to describe the rotational motion of the triatomic complex) and $Cl(^2P)$ atom electronic states $|JK\rangle$, with equal amplitudes for each of the $(2J + 1)$ projections of J on the Cl-H_2 axis, as represented by

$$\Psi^{JM}_{\text{neutral}} = \left(\frac{2J+1}{4\pi}\right)^{1/2} \sum_{K=-J}^{J} D^{J*}_{MK}(\Omega)|JK\rangle\psi^{00}_{\text{anion}} \qquad (1)$$

where K and M are the projections of J on the body- and space-frame z axes, and Ω denotes the set of Euler angles used to transform between the two frames.

The FC spectrum, given by

$$P^J(E) = \langle\Psi^{JM}_{\text{neutral}}|\delta(E - H)|\Psi^{JM}_{\text{neutral}}\rangle \qquad (2)$$

was then calculated using the time-dependent wave packet method with absorbing boundary conditions described in (*18*), but now including electrostatic, spin-orbit, and Coriolis coupling between the diabatic electronic states (*7*). The gray-shaded spectra superimposed in Figs. 3 and 4 are the predicted photoelectron spectra for normal ClH_2^- and ClD_2^- when these nonadiabatic couplings are retained.

Alexander *et al.* (*9*) have shown that the main nonadiabatic effect in the Cl + H_2 reaction is the coupling between the $^2\Sigma_{1/2}$ and $^2\Pi_{1/2}$ electronic states induced by the spin-orbit Hamiltonian. The effect of this coupling will be strongest when the splitting between the $^2\Sigma$ and $^2\Pi$ states, independent of spin-orbit coupling, is comparable to the magnitude of the spin-orbit coupling. The point at which these two are equivalent in magnitude occurs close to the bottom of the prereactive vdW well probed in this study (*9*). In addition, because all of the transitions resolved here correspond to photodetachment to the $^2\Sigma_{1/2}$ and $^2\Pi_{1/2}$ states (recall that transitions to the bend-stretch levels associated with the $^2\Pi_{3/2}$ state have poorer FC overlap with the anion), the effect of this spin-orbit coupling, if large, should be directly observable. However, it can be seen from Figs. 3 and 4 that the inclusion of nonadiabatic effects in the FC simulation induces only subtle changes in the calculated spectra.

The most noticeable difference between the two simulations is the reduction, when the nonadiabatic coupling is retained, of the splitting between the bend-stretch levels associated with the $^2\Sigma_{1/2}$ and $^2\Pi_{1/2}$ states. For example, in the ClH_2 spectra, the splitting between the $(j = 1, v_s = 0)$ levels associated with these two states is reduced from 902 to 888 cm^{-1}, in excellent agreement with the value of 887 cm^{-1} found experimentally. Similarly, in ClD_2, the spacing between the $(j = 0, v_s = 0)$ levels is reduced from 908 to 900 cm^{-1}, which exactly matches the experimental spectrum. These reductions can be explained in terms of small changes in the shapes of the adiabatic-bender potentials induced by the spin-orbit, Coriolis, and electrostatic couplings, which result in changes in the energies of the bend-stretch vdW levels in the two electronic states.

The bottom panels of Figs. 3 and 4 also show that the widths of the peaks from the two sets of simulations are comparable. The $^2\Pi_{1/2}$ states can decay by nonadiabatic coupling to the lower $^2\Sigma_{1/2}$ states, but only if nonadiabatic coupling is included. If the magnitude of nonadiabatic couplings were large, the peaks would be significantly broadened in the fully coupled calculation. This is not observed.

The effect of including the nonadiabatic coupling can be seen more clearly in the ClD_2^- spectra, which display a denser vibrational structure owing to the larger mass of the deuterium atom. In the lower $^2\Sigma_{1/2}$ state, relative to the adiabatic simulation, the hindered rotor spacing is slightly increased and the $v_s = 1$ level lies closer to the dissociative continuum. Overall, the effects of nonadiabatic coupling are small, but their incorporation into the simulations results in a noticeably better match with the high-resolution SEVI spectra.

The comparison between experimental and calculated spectra shown in Figs. 3 and 4 leads to two important conclusions regarding the Cl + H_2 reaction. First, the level of agreement of both sets of simulations with the experimental spectra validates the accuracy of the Capecchi-Werner PESs in the region of the vdW well in the reactant valley. This validation is important because the weak interactions that give rise to this well play a decisive role in determining the product branching ratio of the Cl + HD reaction (*2*). Second, our results show that the effects of non-BO couplings in the prereactive region have been correctly evaluated in the theoretical simulation, to nearly spectroscopic (1 cm^{-1}) accuracy.

The present treatment of the nonadiabatic electronic-vibrational-rotational motion of the ClH_2 system is based on the same Hamiltonian as was used in the quantum reactive scattering calculations of Alexander *et al.* (*8*). Hence, the good agreement found here tends to support the prediction of these calculations that the adiabatic Cl + H_2 reaction pathway will dominate as the collision energy increases. In principle, we expect that the sophisticated ab initio techniques used by Capecchi and Werner (*13*) for the determination of the ClH_2 PESs should be as accurate as those used for the FH_2 system, for which theory and experiment agree on the extent of nonadiabaticity (*10*). Ultimately, the disagreement between these reactive scattering calculations (*8*) and earlier experimental work (*3*, *4*) may demand a new experimental investigation of this reaction.

Finally, our results show that the SEVI technique can yield vibrationally resolved spectra of weakly bound vdW complexes. This method has considerable promise for studies of bimolecular reactions involving polyatomic reactants such as F + CH_4 and Cl + CH_4. The reactive resonances reported recently for these reactions (*31*, *32*) should be spectroscopically accessible if SEVI is used.

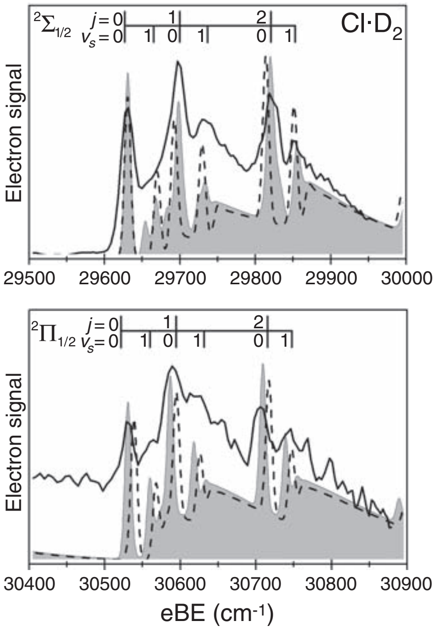

Fig. 4. High-resolution SEVI spectrum of ClD_2^- (solid line) is compared with FC simulations where the nonadiabatic interactions are neglected (dashed line) and included (gray-shaded area). Both spectra show electron signal as a function of eBE. (**Top**) Average of three spectra taken between 333 and 334 nm; (**bottom**) average of three spectra taken between 323 and 324 nm.

References

1. M. Alagia *et al.*, *Science* **273**, 1519 (1996).
2. D. Skouteris *et al.*, *Science* **286**, 1713 (1999).
3. F. Dong, S. H. Lee, K. Liu, *J. Chem. Phys.* **115**, 1197 (2001).

4. S. H. Lee, K. P. Liu, *J. Chem. Phys.* **111**, 6253 (1999).
5. P. J. Dagdigian, M. L. Campbell, *Chem. Rev.* **87**, 1 (1987).
6. R. J. Donovan, *Chem. Rev.* **70**, 489 (1970).
7. M. H. Alexander, D. E. Manolopoulos, H.-J. Werner, *J. Chem. Phys.* **113**, 11084 (2000).
8. M. H. Alexander, G. Capecchi, H.-J. Werner, *Science* **296**, 715 (2002).
9. M. H. Alexander, G. Capecchi, H.-J. Werner, *Faraday Disc.* **127**, 59 (2004).
10. L. Che *et al.*, *Science* **317**, 1061 (2007).
11. E. E. Nikitin, *Theory of Elementary Atomic and Molecular Processes in Gases* (Clarendon, Oxford, 1974).
12. V. Aquilanti, G. Grossi, *J. Chem. Phys.* **73**, 1165 (1980).
13. G. Capecchi, H.-J. Werner, *Phys. Chem. Chem. Phys.* **6**, 4975 (2004).
14. D. M. Neumark, *Phys. Chem. Chem. Phys.* **7**, 433 (2005).
15. D. M. Neumark, *J. Chem. Phys.* **125**, 132303 (2006).
16. S. E. Bradforth, D. W. Arnold, D. M. Neumark, D. E. Manolopoulos, *J. Chem. Phys.* **99**, 6345 (1993).
17. D. E. Manolopoulos *et al.*, *Science* **262**, 1852 (1993).
18. D. E. Manolopoulos, M. H. Alexander, *Phys. Chem. Chem. Phys.* **6**, 4984 (2004).
19. M. J. Ferguson, G. Meloni, H. Gomez, D. M. Neumark, *J. Chem. Phys.* **117**, 8181 (2002).
20. A. Osterwalder, M. J. Nee, J. Zhou, D. M. Neumark, *J. Chem. Phys.* **121**, 6317 (2004).
21. D. W. Chandler, P. L. Houston, *J. Chem. Phys.* **87**, 1445 (1987).
22. A. Eppink, D. H. Parker, *Rev. Sci. Instrum.* **68**, 3477 (1997).
23. J. Zhou, E. Garand, W. Eisfeld, D. M. Neumark, *J. Chem. Phys.* **127**, 034304 (2007).
24. U. Even, J. Jortner, D. Noy, N. Lavie, C. Cossart-Magos, *J. Chem. Phys.* **112**, 8068 (2000).
25. V. Aquilanti, S. Cavalli, F. Pirani, A. Volpi, D. Cappelletti, *J. Phys. Chem. A* **105**, 2401 (2001).
26. M. H. Alexander, *J. Chem. Phys.* **118**, 9637 (2003).
27. S. L. Holmgren, M. Waldman, W. Klemperer, *J. Chem. Phys.* **67**, 4414 (1977).
28. M. H. Alexander, S. Gregurick, P. J. Dagdigian, *J. Chem. Phys.* **101**, 2887 (1994).
29. R. C. Bilodeau, M. Scheer, H. K. Haugen, *Phys. Rev. Lett.* **87**, 143001 (2001).
30. E. P. Wigner, *Phys. Rev.* **73**, 1002 (1948).
31. W. Shiu, J. J. Lin, K. P. Liu, *Phys. Rev. Lett.* **92**, 103201 (2004).
32. B. Zhang, K. Liu, *J. Chem. Phys.* **122**, 101102 (2005).

17 September 2007; accepted 1 November 2007
10.1126/science.1150602

Helium and Neon Abundances and Compositions in Cometary Matter

Bernard Marty,[1] Russell L. Palma,[2,3] Robert O. Pepin,[3]* Laurent Zimmermann,[1] Dennis J. Schlutter,[3] Peter G. Burnard,[1] Andrew J. Westphal,[4] Christopher J. Snead,[4] Saša Bajt,[5] Richard H. Becker,[3] Jacob E. Simones[2]

Materials trapped and preserved in comets date from the earliest history of the solar system. Particles captured by the Stardust spacecraft from comet 81P/Wild 2 are indisputable cometary matter available for laboratory study. Here we report measurements of noble gases in Stardust material. Neon isotope ratios are within the range observed in "phase Q," a ubiquitous, primitive organic carrier of noble gases in meteorites. Helium displays ^{3}He/^{4}He ratios twice those in phase Q and in Jupiter's atmosphere. Abundances per gram are surprisingly large, suggesting implantation by ion irradiation. The gases are probably carried in high-temperature igneous grains similar to particles found in other Stardust studies. Collectively, the evidence points to gas acquisition in a hot, high ion-flux nebular environment close to the young Sun.

Comets are frozen, largely unaltered reservoirs of dust and gases present in the early solar nebula. They are likely to contain well-preserved records of the chemical, mineralogic, and isotopic character of primordial solar-system matter. On 15 January 2006, the Stardust Mission returned to Earth with a cargo of particles collected from the coma of comet 81P/Wild 2 (*1*). These not only open the door to detailed laboratory investigation of the nature of cometary matter, but will also provide chemical, mineralogic, and isotopic markers for identifying samples of comets suspected to be already present in extraterrestrial material collections [e.g., (*2*–*6*)].

Noble gases are excellent tracers of contributions from various solar-system volatile reservoirs and of physical processing of gases acquired from these reservoirs. Their elemental and isotopic compositions in primitive meteorites differ from those in the Sun, as represented by the solar wind. Planetary atmospheres display noble gas signatures distinct from both solar and meteoritic patterns. A detailed knowledge of cometary noble gas abundances and isotopic compositions, unknown before Stardust, will allow investigation of compositional links between comets, the solar nebula, primitive meteorites for which a cometary origin has been advocated (*7*, *8*), micrometeorites and interplanetary dust particles (IDPs), and the atmospheres of Earth, Mars, and Venus, where contributions of noble gases carried by comets have been proposed and debated (*9*–*11*).

The Wild 2 particles were collected by Stardust in aerogel, a porous low-density silica glass designed to decelerate an impacting grain with minimal alteration (*1*). The material analyzed in this study was extracted from the bulbous cavity wall of the capture track shown in Fig. 1A. We report results of helium and neon measurements on five subsamples of this material [Fig. 1B and fig. S1 (*12*)], carried out independently, using different extraction and analytical methods, at Centre de Recherches Pétrographiques et Géochimiques (CRPG) Nancy, France, and the University of Minnesota, Minneapolis, USA (*13*). Gases were thermally released from the five samples, two (Thera-1 and Thera-2) at CRPG by single-step laser melting and three (St-1, St-2, St-3) at Minnesota by multistep pyrolysis to ~1400°C. Evolved He and Ne abundances were not large, in some cases exceeding blank levels by factors of only 2 to 3, and so accurate assessments of aerogel and instrumental blanks were crucial. Details on blank determinations, and other discussions of materials and methods, are set out in (*12*).

The bulbous track-wall samples are mixtures of aerogel and small grains shed from the impacting particle. Gases were held very retentively in their host grains; temperatures above ~1250°C (±50°C) were required to degas He and Ne in the Minnesota step-heating procedure. Originally we thought that gases might have been liberated by flash heating of the incident particle in the upper part of its deceleration track (Fig. 1A) and trapped in melted aerogel that rapidly chilled to silica glass along the track walls. It is now clear that the ~1200° to 1250°C temperatures reached before initiation of release (*12*) are incompatible with siting in aerogel. Diffusion coefficients for He in vitreous silica (*14*) are so large at these temperatures that glassy aerogel would empty itself in ~10 s—comparable to step heating times—even if diffusion distances were comparable to the 1-mm sample dimensions (Fig. 1B and fig. S1), and much more quickly (<1 s) at the ≤100-μm scale. Observed release profiles instead point to gas siting in refractory grains. This inference is consistent with the bulb-wall mineralogy measured by x-ray absorption spectroscopy (supporting online text), indicating that the grains are composed primarily (~75% by mass) of high-temperature metal (FeNi), metal-sulfur, and metal-carbon minerals. The remaining 25% are mostly silicates together with unidentified components. A separate search for carbon compounds was carried out by infrared (IR) spectroscopy (supporting online text) to address the possibility that the gas carriers might be refractory organic materials. None were detected. However, the search covered only a small fraction of the bulb wall and adjacent aerogel, so the presence of heterogeneously distributed organics is not ruled out. We return to the issue of the nature of the gas carrier later in the paper.

---

[1] Centre de Recherches Pétrographiques et Géochimiques, Nancy Université, BP 20, 54501 Vandoeuvre-lès-Nancy Cedex, France. [2] Department of Physics and Astronomy, Minnesota State University, Mankato, MN 56001, USA. [3] School of Physics and Astronomy, University of Minnesota, Minneapolis, MN 55455, USA. [4] Space Sciences Laboratory, University of California, Berkeley, CA 94720, USA. [5] Institute of Geophysics and Planetary Physics, Lawrence Livermore National Laboratory, Livermore, CA 94550, USA.

*To whom correspondence should be addressed. E-mail: pepin001@umn.edu

ERRATUM

Post date 2 May 2008

Reports: "Nonadiabatic interactions in the Cl + H_2 reaction probed by ClH_2^- and ClD_2^- photoelectron imaging" by E. Garand *et al*. (4 January, p. 72). This research was supported by Air Force Office of Scientific Research grant F49620 03 1 0085 (D.M.N.), NSF grant CHE0413743 (M.H.A.), and Office of Naval Research grant N000140510460 (D.E.M.). E.G. thanks the Natural Science and Engineering Research Council of Canada for a postgraduate scholarship.

Neon isotopic compositions were measured in both noble gas laboratories. Extractions with enough Ne for relatively precise measurement yielded similar isotope ratios: ^{20}Ne/^{22}Ne = 10.68 ± 0.35 and 10.49 ± 0.24 together with ^{21}Ne/^{22}Ne = 0.0273 ± 0.0024 and 0.0279 ± 0.0017, measured, respectively, in St-1 at Minnesota and Thera-2 at CRPG (Table 1). Both ^{20}Ne/^{22}Ne ratios are >2.5σ above the atmospheric value of 9.80. These compositions fall within the range observed for meteoritic Ne—specifically, for Ne in "phase Q" (*15*), a minor macromolecular organic phase, ubiquitous in chondritic and achondritic meteorites, that hosts neon with ^{20}Ne/^{22}Ne ratios ranging from 10.1 to 10.7, and ^{21}Ne/^{22}Ne from a lower limit of 0.0278 to 0.0294 (Table 1). Stardust Ne lies within error in the Ne-Q data field, with the nominal ^{21}Ne/^{22}Ne ratios straddling its lower limit (Fig. 2A).

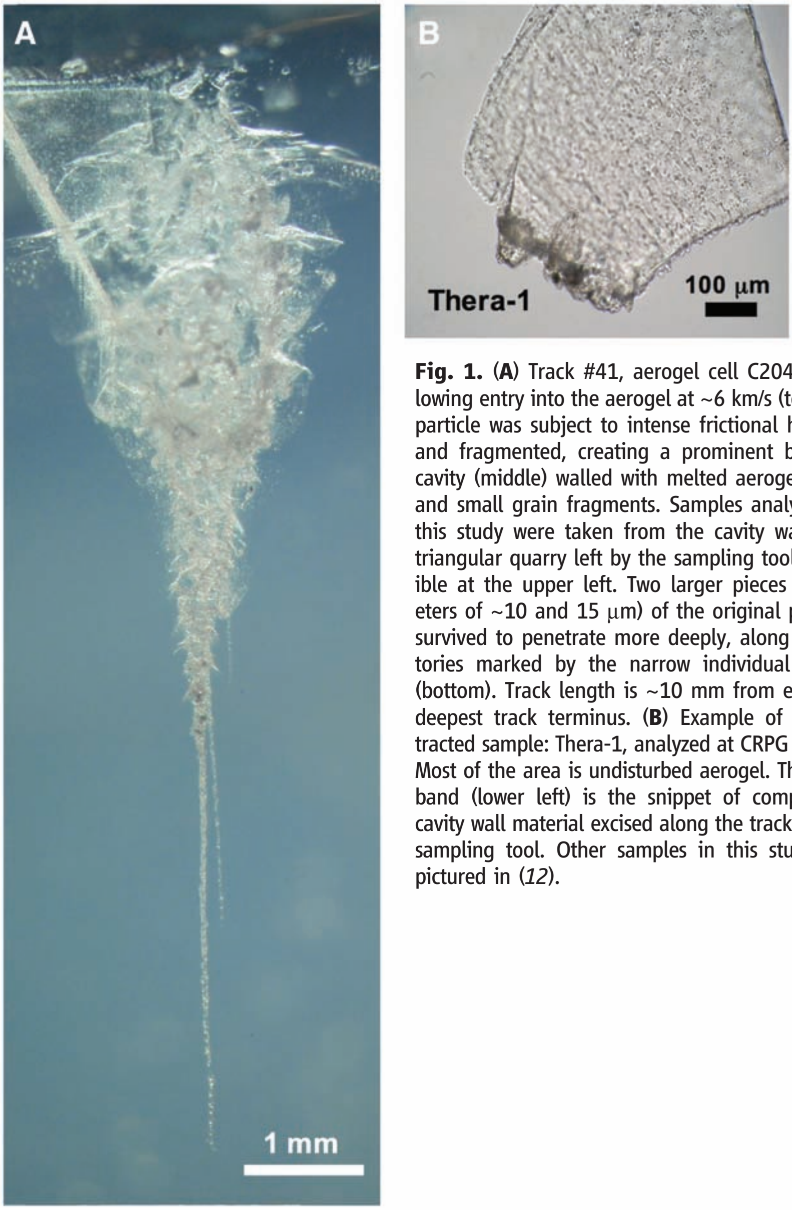

Fig. 1. (**A**) Track #41, aerogel cell C2044. Following entry into the aerogel at ~6 km/s (top) the particle was subject to intense frictional heating and fragmented, creating a prominent bulbous cavity (middle) walled with melted aerogel silica and small grain fragments. Samples analyzed in this study were taken from the cavity wall; the triangular quarry left by the sampling tool is visible at the upper left. Two larger pieces (diameters of ~10 and 15 μm) of the original particle survived to penetrate more deeply, along trajectories marked by the narrow individual tracks (bottom). Track length is ~10 mm from entry to deepest track terminus. (**B**) Example of an extracted sample: Thera-1, analyzed at CRPG Nancy. Most of the area is undisturbed aerogel. The dark band (lower left) is the snippet of compressed cavity wall material excised along the track by the sampling tool. Other samples in this study are pictured in (*12*).

Are there alternatives to a Q-Ne–like source—in particular, a source with solar composition (*16*–*18*)—that might account for the Ne isotopic distributions within the uncertainties of the present data? The ^{20}Ne/^{22}Ne ratio in Thera-1 could be consistent with a solar-wind Ne end-member (Table 1), but it is not diagnostic because its large uncertainty also overlaps the air and Q compositions. Compared to solar wind ratios, ^{21}Ne/^{22}Ne in Thera-1 is lower by ~3σ, and the two most precise determinations of ^{20}Ne/^{22}Ne are ~10σ lower (Table 1). Contemporary solar wind as a principal source of Stardust Ne is therefore ruled out, a conclusion reinforced by measured ^{3}He/^{4}He ratios that differ from those of the solar wind by >5σ (Fig. 2B). One possibility might be that the Ne composition reflects mixing of solar Ne with an air contaminant. However, the source of such a large and similar air contribution in both laboratories—constituting ~75% of the ^{20}Ne in St-1 and Thera-2 and greatly exceeding aerogel blank levels (*12*)—is not evident. Also, ^{21}Ne/^{22}Ne ratios fall to the left of the air-solar mixing line in Fig. 2A, although this is a relatively weak constraint because the deviations are only ~1σ.

Isotopic evidence that a He component resembling Q-He is also present would go far toward establishing a Q-gas source. However, as discussed next, the ^{3}He/^{4}He ratios observed in St-1 and St-2 are approximately twice the Q-He ratio. So, the light cometary noble gases, if they have a Q-affinity, appear to be distinct from the meteoritic component in this respect. Their ^{4}He/^{20}Ne elemental ratios of ~1 to 20 are also distinct, much below the ~80 to 140 range in phase Q (Table 1).

Detection of ^{3}He, which cannot derive from terrestrial contamination, is by itself firm evidence that indigenous gases are indeed present in Stardust samples. The ^{3}He/^{4}He ratio is important because in principle it can point to when comets acquired their noble gases, and from what volatile reservoir—the early protosolar nebula, a locus near the evolving Sun after the deuterium burning that elevated the level of protosolar ^{3}He, or by later implantation of solar wind radiation. Of the compositions plotted in Fig. 2B, the jovian atmospheric ratio is thought to reflect the primordial nebular (protosolar) value, "D-burning" is an estimate of ^{3}He/^{4}He in the Sun following deuterium burning, and "Solar Wind" represents measurements of the ratio in collectors of the contemporary solar wind returned by the Genesis Mission.

Table 1. Helium and neon abundances, relative abundances, and isotope ratios in Stardust particle track samples. Uncertainties are ±1σ (NM: not measured). Limits for ^{4}He and ^{3}He/^{4}He in St-3 reflect the probable presence of an anomalous ^{4}He blank contribution (*12*). Phase Q and Solar compositions are listed for comparison. Phase Q data are from (*15*). Solar (solar wind) data are averages or ranges of measurements in Genesis collector materials (*16*–*18*).

Sample	^{4}He ($\times10^{-11}$ cm^3 STP)	^{3}He/^{4}He ($\times10^{-4}$)	^{20}Ne ($\times10^{-11}$ cm^3 STP)	^{20}Ne/^{22}Ne	^{21}Ne/^{22}Ne ($\times10^{-2}$)	^{4}He/^{20}Ne
St-1*	7.27 ± 0.36	2.92 ± 0.26	5.34 ± 0.42	10.68 ± 0.35	2.73 ± 0.24	1.36 ± 0.13
St-2*	5.26 ± 0.30	2.47 ± 0.34	0.94 ± 0.14	9.0 ± 1.6	3.9 ± 1.1	5.60 ± 0.89
St-3*	<66.9 ± 2.4	>0.318 ± 0.032	1.06 ± 0.15	9.3 ± 1.6	4.2 ± 1.8	<63.1 ± 9.2
Thera-1†	53 ± 17	NM	2.47 ± 0.65	12.9 ± 3.2	2.45 ± 0.29	21.4 ± 4.9
Thera-2†	17.5 ± 3.8	NM	5.80 ± 0.43	10.49 ± 0.24	2.79 ± 0.17	3.0 ± 1.3
Phase Q		1.45 ± 0.15		10.1–10.7	2.78–2.94	110 ± 30
Solar		4.44 ± 0.10		13.90 ± 0.08	3.35 ± 0.07	520–670

*Analyzed at the University of Minnesota, USA. †Analyzed at CRPG Nancy, France.

The differences between the Q-He and observed ^{3}He/^{4}He ratios (Fig. 2B) cannot be attributed to excess ^{3}He produced by nuclear spallation during space exposure to high-energy galactic cosmic rays (GCRs). Although the abundances of ^{3}He in these samples are small (<600,000 atoms), concentrations per gram of host grains are not. The mass density of grain fragments lodged in the bulbous cavity wall, assessed by Fe fluorescence measurements, is ~350 ng/cm^{2} assuming uniform areal density, and the average area of cavity wall material in each of the five analyzed samples is ~7.3 × 10^{-4} cm^{2} (supporting online text). The average grain mass per sample is then ~0.26 ng, and the corresponding ^{3}He concentration, obtained by dividing this mass into the Table 1 abundances, is ~7.1 × 10^{-5} cm^{3} STP/g. About half of this would have to be spallogenic to elevate ^{3}He/^{4}He from Q-He to the measured ratio (Fig. 2B). Calculations (supporting online text) show that this would require the particle to reside within the upper meter of the surface, where ^{3}He production is maximum, for times exceeding the age of the solar system. In reality, abundances of spallation products in the active surface of a comet should be essentially nil; shallow zones where they might conceivably accumulate over long times have eroded away. Average sublimation erosion of the Wild 2 surface just since its 1974 appearance is estimated to be ~1 m (*19*), corresponding to ~5 m in the ~20% of the surface covered by the gas and dust jets encountered by Stardust (*20*) if these source areas were active on previous apparitions.

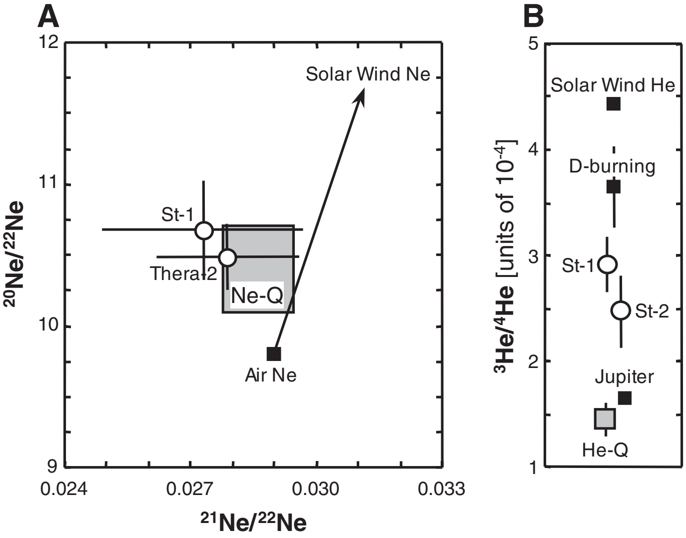

Fig. 2. (**A**) Neon isotope ratios in Ne-Q, and in Stardust samples St-1 and Thera-2 (Table 1). Ne-Q isotopic range (shaded area) is from (*15*). The solid line extending from Air-Ne defines compositions generated by mixtures of air with solar wind Ne, offscale at ^{20}Ne/^{22}Ne = 13.90 ± 0.08, ^{21}Ne/^{22}Ne = 0.0335 ± 0.0007 (*16–18*). (**B**) Helium isotope ratios in St-1 and St-2 (Table 1), compared to ^{3}He/^{4}He measured in other solar-system reservoirs: 1.45 ± 0.15 × 10^{-4} in He-Q (*15*), 1.66 ± 0.05 × 10^{-4} in Jupiter's atmosphere (*29*), 4.44 ± 0.10 × 10^{-4} in Genesis measurements of present-day solar wind (*16–18*). The ratio in the Sun following deuterium burning is estimated to be 3.65 ± 0.38 × 10^{-4} (*30*). Error bars in (A) and (B) are 1σ.

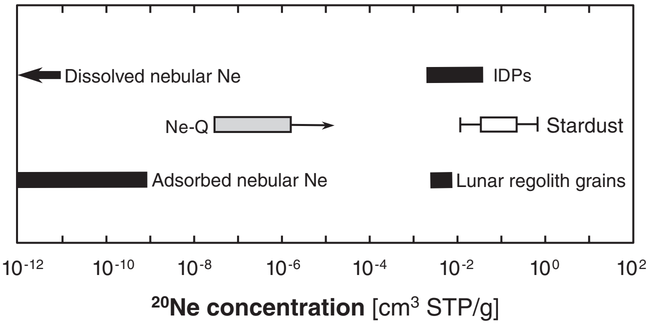

Fig. 3. Concentration ranges of ^{20}Ne in cm^{3} STP/g (1 cm^{3} STP = 2.69 × 10^{19} atoms) in the Stardust samples, the Q-Ne carrier phase (*15*), ~5- to 10-μm-diameter IDPs (*31*), and ~1- to 10-μm lunar regolith grains (*32*) irradiated by the solar wind; measured in the laboratory for adsorption on carbon black at ~20° to 400°C (*33*); and calculated for Ne dissolved in basaltic melt and partitioned into Fe crystals (there are no available data for FeS partitioning), using gas-melt distribution and iron-melt partition coefficients from (*34*) and (*35*). Stardust concentrations are from measured ^{20}Ne abundances (Table 1) and average host grain masses of 0.26 ng per sample. The plotted IDP range is for the Group 2 IDPs in (*31*), which have an average He isotope ratio consistent with implanted solar wind. Concentrations of adsorbed and dissolved Ne depend on Ne partial pressure in the ambient gas. Plotted ranges assume a total nebular pressure of 10^{-3} atm (100 Pa) close to the Sun (*36*), and a corresponding Ne partial pressure of 10^{-7} atm (*37*). The highest concentration of dissolved Ne, at ~10^{-11} cm^{3} STP/g, is for equilibrium solution into basaltic melt (*34*); the arrow points to concentrations partitioned into iron crystals, lower by a factor of ~10 at low pressure (*35*). Error bars on the Stardust range reflect a conservative estimate of a factor 3 uncertainty in calculations of concentrations.

With a degassed grain mass of ~0.26 ng, average concentrations of the principal isotopes ^{4}He and ^{20}Ne (Table 1) are ~1 and ~0.1 cm^{3} STP/g, respectively. These high values have important implications for how the Stardust samples acquired their noble gases. It is clear (Fig. 3) that equilibrium solubility of nebular Ne into melt—from which the Stardust minerals are assumed to have crystallized—is many orders of magnitude too small at calculated nebular pressures to match observed Ne concentrations. A similar shortfall is seen for physical adsorption of ambient Ne in grain-surface structures, even for a favorable case, shown here, of adsorption on finely divided carbon. In contrast, Stardust Ne concentrations are interestingly comparable to those implanted in IDPs and lunar regolith grains by solar-wind ion irradiation (Fig. 3). Among known gas acquisition mechanisms, it appears that only ion implantation could generate such high Ne (and He) loading in these mineral grains.

In the context of a possible Q-gas source for Stardust Ne, one sees in Fig. 3 that the Q-Ne abundances per gram of "carrier phase" in meteorites are lower than the Stardust Ne range by factors of ~10^{5}; the corresponding factors for He are ~10^{4}. However, this "carrier phase," a residue isolated by chemical dissolution of silicate minerals, is itself a mixture of several mineralogic and organic components. The actual hosts of Q-gases appear to be organic materials (*21*, *22*), but their masses, though much debated, are essentially unknown (*15*). It seems likely that the true Q-carriers constitute only a fraction of total residue mass, and thus the Fig. 3 concentrations are indicated as lower limits, possibly by orders of magnitude.

Where do we presently stand on interpreting these Ne and He distributions in Stardust material? There are two important issues. One is the nature of the material carrying the noble gases. We know from the high temperatures (≥1250°C) needed to release them that the host is refractory, consistent with the mineralogy of the grains lodged in the track wall that we have assumed to be the carriers. But, just on this basis, they are not the only option; organic carriers of meteoritic Q-gases also retain major fractions of their gases until heated to >1200°C (*23*). Some Stardust particle tracks are rich in carbonaceous matter (*24*), raising the possibility of an organic host. There are indications, however, that this one is not. An IR spectroscopy search of a small sample of bulb-wall material and adjacent aerogel for organics was negative, setting an upper limit of ~10 fg on average in the samples analyzed for noble gases assuming that organic materials are uniformly distributed in the track wall (supporting online text). Average ^{20}Ne and ^{4}He concentrations would then have to exceed ~3 liters/g and ~20 liters/g, respectively, if the gases were trapped in this amount of organic matter. Trapping capacities in organic compound structures could not approach these levels. A caution here, because the IR search was limited to a small fraction of the total bulb wall area, is that higher abundances of heterogeneously distributed organics could be sited elsewhere in the track and in the samples. However, a large fraction of these organics, if present, is likely to be barren of noble gases. There is evidence that many of the Stardust organic components are labile, volatilized during particle capture and diffused into aerogel adjacent to tracks (*24*). Helium and Ne released by labile carrier volatilization probably escaped on impact, because we have argued earlier, on the basis of high release temperatures, that Stardust gases are not trapped in aerogel. The most likely organic carriers are therefore those refractory enough to retain their gases during impact heating. What fraction of total organics these might constitute is unknown.

The alternative that the Stardust He and Ne are carried in FeS-Fe grains is consistent with the finding that abundant Q-gases are present in sulfide- and metal-rich separates from certain meteorites (*25*), although this study did not prove that the gases were actually sited in these phases. We have shown that the required Ne loading of such grains, while large, is not implausible (Fig. 3). Whether this is also the case for a putative organic carrier remains to be seen. Either way, however, the high noble gas concentrations reported here are unlikely to be much lower, no matter what the carrier actually is.

The second issue concerns the compositional nature of the source reservoir. Neon isotopes resemble Q-Ne, but a Q-like source for both Ne and He encounters the problems of the high ^{3}He/^{4}He and low ^{4}He/^{20}Ne ratios (Fig. 2B and Table 1). These latter ratios, however, do not necessarily reflect the elemental composition of the source reservoir. Helium thermally escapes from trapping sites more readily than Ne, so low ^{4}He/^{20}Ne could result from diffusive loss from grains during gas incorporation or over their metamorphic history. Diffusion also alters isotope ratios, with the lighter species escaping preferentially, and this led a reviewer to ask if the gases initially implanted in the grains could have been solar rather than Q-like —i.e., a direct sampling of the ancient Sun, subsequently fractionated from solar ratios (Table 1) to the observed composition by extreme diffusive losses. An alternative might be gas acquisition from an initially solar reservoir that had been fractionated by mass-dependent losses to space. Both hypotheses, however, fail a central test: Diffusion calculations (supporting online text) show that replication of the observed Ne and He isotope ratios requires the percentage of solar Ne depletion to greatly exceed that of the lighter He, an unphysical result either for diffusion from natural minerals or for Rayleigh distillation of a gaseous reservoir.

We conclude that the Stardust Ne data point more firmly to a Q-gas source than to other alternatives. The anomalously high ^{3}He/^{4}He and low ^{4}He/^{20}Ne ratios remain unexplained, although it may be possible to reconcile them with the Q-like Ne by invoking a multistage model of gas acquisition and loss (supporting online text). The presence of Q-gases would be an important clue to the antiquity of the Wild 2 gas reservoir. They have just the characteristics one would expect for a fundamental constituent of the early solar nebula. They are present in all meteorites that have been subject to the experimental procedures required to isolate their carrier phase (*15*), and ^{3}He/^{4}He in Q is close to the Jupiter atmospheric ratio (Fig. 2B), a marker for He composition in the primitive nebula.

A central question for the noble gases is where they were acquired by the comet particles. One of the surprises in samples collected from an icy object forming, and, for much of its lifetime, residing in the cold outer reaches of the solar system was the discovery that many of its constituent particles, including that in track 41, are igneous, refractory "rocklets" processed at very high temperatures, presumably close to the Sun before transport to the outer nebula and incorporation into Wild 2 (*1*, *26*–*28*). Another is the finding here of high concentrations of He and Ne that, of known gas acquisition mechanisms, only ion irradiation seems capable of explaining (Fig. 3). These observations, together with the isotopic data in Fig. 2—pointing to a source containing primitive Q-Ne, and a He composition that could reflect later addition of a solar component to diffused Q-He—suggest that Stardust grains and the carbonaceous carrier now found in meteorites sampled the same Q-gas reservoir, the grains by ion implantation in an energetic environment near the young evolving Sun.

Particles transported from hot inner zones of the solar nebula are thought to constitute ~10% of the mass of Wild 2 (*1*). The large gas concentrations reported here may therefore have important implications for the supply of comet-carried volatiles to planets if these particles are collectively characterized by similar concentrations and their mass fraction in Wild 2 is typical of comets in general. The isotope ratios and high concentrations of Ne are particularly relevant in efforts to model cometary noble gas contributions to planetary atmospheres (*9*, *10*).

References and Notes

1. D. Brownlee *et al.*, *Science* **314**, 1711 (2006).
2. S. Messenger, *Meteorit. Planet. Sci.* **37**, 1491 (2002).
3. A. O. Nier, D. J. Schlutter, *Meteoritics* **28**, 675 (1993).
4. R. O. Pepin, R. L. Palma, D. J. Schlutter, *Meteorit. Planet. Sci.* **36**, 1515 (2001).
5. R. L. Palma, R. O. Pepin, D. J. Schlutter, *Meteorit. Planet. Sci.* **40**, A120 (2005).
6. D. J. Joswiak, D. E. Brownlee, R. O. Pepin, D. J. Schlutter, in *Dust in Planetary Systems*, H. Krüger, A. Graps, Eds. (ESA Publication SP-643, 2007), pp. 141–144.
7. K. Lodders, R. Osborne, *Space Sci. Rev.* **90**, 289 (1999).
8. M. Gounelle, P. Spurny, P. A. Bland, *Meteorit. Planet. Sci.* **41**, 135 (2006).
9. T. Owen, A. Bar-Nun, I. Kleinfeld, *Nature* **358**, 43 (1992).
10. N. Dauphas, *Icarus* **165**, 326 (2003).
11. R. O. Pepin, *Earth Planet. Sci. Lett.* **252**, 1 (2006).
12. Materials and methods are available as supporting material on *Science* Online.
13. A brief report of experimental methods and noble gas data obtained at CRPG Nancy (Table 1) appeared earlier in (*27*).
14. J. E. Shelby, *Phys. Rev. B* **4**, 2681 (1971).
15. H. Busemann, H. Baur, R. Wieler, *Meteorit. Planet. Sci.* **35**, 949 (2000).
16. J. C. Mabry *et al.*, *38th Lunar Planet. Sci. Conf.* abstract 2412: CD-ROM (2007); available at www.lpi.usra.edu/publications/absearch.
17. V. S. Heber, H. Baur, D. S. Burnett, R. Wieler, *38th Lunar Planet. Sci. Conf.* abstract 1894: CD-ROM (2007); available at www.lpi.usra.edu/publications/absearch.
18. A. Grimberg, D. S. Burnett, P. Bochsler, H. Baur, R. Wieler, *Space Sci. Rev.* **130**, 293 (2007).
19. D. E. Brownlee *et al.*, *Science* **304**, 1764 (2004).
20. Z. Sekanina, D. E. Brownlee, T. E. Economou, A. J. Tuzzolino, S. F. Green, *Science* **304**, 1769 (2004).
21. U. Ott, R. Mack, S. Chang, *Geochim. Cosmochim. Acta* **45**, 1751 (1981).
22. Y. Marrocchi, S. Derenne, B. Marty, F. Robert, *Earth Planet. Sci. Lett.* **236**, 569 (2005).
23. G. R. Huss, R. S. Lewis, S. Hemkin, *Geochim. Cosmochim. Acta* **60**, 3311 (1996).
24. S. A. Sandford *et al.*, *Science* **314**, 1720 (2006).
25. H. Busemann, O. Eugster, *Meteorit. Planet. Sci.* **37**, 1865 (2002).
26. D. E. Brownlee, D. Joswiak, J. Bradley, G. Matrajt, *38th Lunar Planet. Sci. Conf.* abstract 2189: CD-ROM (2007); available at www.lpi.usra.edu/publications/absearch.
27. K. D. McKeegan *et al.*, *Science* **314**, 1724 (2006).
28. M. E. Zolensky *et al.*, *Science* **314**, 1735 (2006).
29. P. R. Mahaffy, T. M. Donahue, S. K. Atreya, T. C. Owen, H. B. Niemann, *Space Sci. Rev.* **84**, 251 (1998).
30. J. Geiss *et al.*, *Space Sci. Rev.* **110**, 307 (2004).
31. R. O. Pepin, R. L. Palma, D. J. Schlutter, *Meteorit. Planet. Sci.* **35**, 495 (2000).
32. P. Eberhardt *et al.*, in *Proc. 3rd Lunar Sci. Conf.*, D. Heymann, Ed. (MIT Press, Cambridge MA, 1972), vol. 2, pp. 1821–1856.
33. J. F. Wacker, *Geochim. Cosmochim. Acta* **53**, 1421 (1989).
34. A. Jambon, H. Weber, O. Braun, *Geochim. Cosmochim. Acta* **50**, 401 (1986).
35. J. Matsuda *et al.*, *Science* **259**, 788 (1993).
36. J. A. Wood, G. E. Morfill, in *Meteorites and the Early Solar System*, J. F. Kerridge, M. S. Matthews, Eds. (Univ. of Arizona Press, Tucson, 1988), pp. 329–347.
37. E. Anders, N. Grevesse, *Geochim. Cosmochim. Acta* **53**, 197 (1989).
38. This study was funded at Nancy by the Centre National de la Recherche Scientifique (CNRS), the Région Lorraine, and the Centre National d'Etudes Spatiales (CNES), at Minnesota by grant NAG5-11732 from the NASA Cosmochemistry Program, and at Berkeley by NASA grant NNG05GR30G. Part of this work was performed under the auspices of the U.S. Department of Energy by Lawrence Livermore National Laboratory under contract DE-AC52-07NA27344. We thank M. C. Martin [Advanced Light Source, Lawrence Berkeley National Laboratory (ALS, LBNL)] for helpful discussions. Z. Gainsforth (UC Berkeley, Space Science Laboratory), and M. Marcus and S. Fakra (ALS, LBNL), provided crucial support for the x-ray absorption near-edge structure analyses. Suggestions from three reviewers greatly improved the presentation. Encouragement from the Stardust Preliminary Examination Team, in particular from K. McKeegan and D. E. Brownlee, is gratefully acknowledged. This is CRPG contribution 1870.

Supporting Online Material

www.sciencemag.org/cgi/content/full/319/5859/75/DC1
Materials and Methods
SOM Text
Figs. S1 to S3
Table S1
References

18 July 2007; accepted 16 November 2007
10.1126/science.1148001

Temperature and Composition of Saturn's Polar Hot Spots and Hexagon

L. N. Fletcher,[1]* P. G. J. Irwin,[1] G. S. Orton,[2] N. A. Teanby,[1] R. K. Achterberg,[3] G. L. Bjoraker,[3] P. L. Read,[1] A. A. Simon-Miller,[3] C. Howett,[1] R. de Kok,[1] N. Bowles,[1] S. B. Calcutt,[1] B. Hesman,[3] F. M. Flasar[3]

Saturn's poles exhibit an unexpected symmetry in hot, cyclonic polar vortices, despite huge seasonal differences in solar flux. The cores of both vortices are depleted in phosphine gas, probably resulting from subsidence of air into the troposphere. The warm cores are present throughout the upper troposphere and stratosphere at both poles. The thermal structure associated with the marked hexagonal polar jet at 77°N has been observed for the first time. Both the warm cyclonic belt at 79°N and the cold anticyclonic zone at 75°N exhibit the hexagonal structure.

Just before the Cassini spacecraft's arrival at Saturn, infrared images from the W. M. Keck Observatories revealed a localized "hot spot," thought to be connected to the southern summer conditions, centered on the south pole in both the troposphere and stratosphere (*1*). Cassini's high orbital inclination in 2007 provided an unparalleled opportunity for the study of the localized structure of both poles under different seasonal conditions (only the summer hemisphere can be viewed by Earth-based telescopes). Contrary to expectations, new observations from the Composite Infrared Spectrometer (CIRS) (*2*) have demonstrated that Saturn's northern winter pole also featured a hot cyclonic vortex, despite having been shrouded in the darkness of polar winter since 1995, and that the cores of both polar vortices were depleted in disequilibrium chemicals. Furthermore, the north polar troposphere had a hexagon-shaped thermal region like that observed in reflected sunlight at shorter wavelengths (*3*, *4*).

Global mid-infrared (600- to 1400-cm^{-1}) radiance maps at 15.0-cm^{-1} spectral resolution were used to derive the atmospheric temperatures at altitudes in the stratosphere between 1.0 to 6.6 mbar and in the upper troposphere between 60 to 800 mbar (*5*). The same basic pattern of localized hot poles surrounded by warm belts and cool zones exists in the tropospheres of both summer and winter hemispheres (Fig. 1), despite the large seasonal differences (Fig. 2). Both polar hot spots are surrounded by cooler polar zones in the 70- to 300-mbar region that extend from the hot spot toward the warm polar belts at 79°N and 76°S. Cyclonic warm features, such as the polar belts and hot spots, are related to horizontal convergence and subsidence of tropospheric air [see the supporting online material (SOM)], whereas the cold polar zones are related to divergence of upwelling air, forming polar circulation cells that are part of a planet-wide circulation centered on strong equatorial upwelling.

Polar jets are essential features of these polar circulation cells. The maxima in the meridional temperature gradient correspond to the prograde polar jets at 77°N (*3*) and 74°S (*6*) (the equatorward side of the polar belts), observed from cloud-feature tracking, and to the jet at 87°S that has been shown to encircle the southern cyclonic hot spot (*7*). Symmetry arguments lead us to expect that the temperature gradient at 88°N might also be associated with a prograde polar jet. However, no wind measurements were available poleward of 82°N from Voyager (*8*), and the polar night currently inhibits wind measurements from Cassini at high northern latitudes. The thermal windshear equations (*8*) imply that all of the polar jets decay with altitude into the stratosphere.

The polar atmospheres also show some notable differences. The large-scale structure of the polar belts is particularly interesting, with hexagonal perturbations only evident in the northern troposphere at 79°N. Furthermore, the northern hot spot and polar zone were more closely confined in latitude to the pole than their southern counterparts. The stratospheric temperatures are asymmetric between the two hemispheres (Fig. 1) as a result of seasonal differences in radiative processes and photochemistry (*5*, *9*). At 1 mbar, the summer stratosphere exhibits a warm polar collar, with temperatures beginning to rise from 70°S (154 K) to the south pole (164 to 165 K), whereas the northern stratosphere shows no comparable warm polar collar. The warm southern collar is likely to be seasonal in nature, resulting from solar absorption by high-altitude stratospheric aerosols (*10*, *11*) and the photochemistry of methane and its daughter molecules, which are constrained within 10° to 15° of the south pole by the polar jet at 74°S. The southern collar may dissipate, and a northern warm collar may form, as the north pole moves into sunlight after the ring plane crossing of 2009, which is analogous to the seasonal dissipation of Earth's polar vortices.

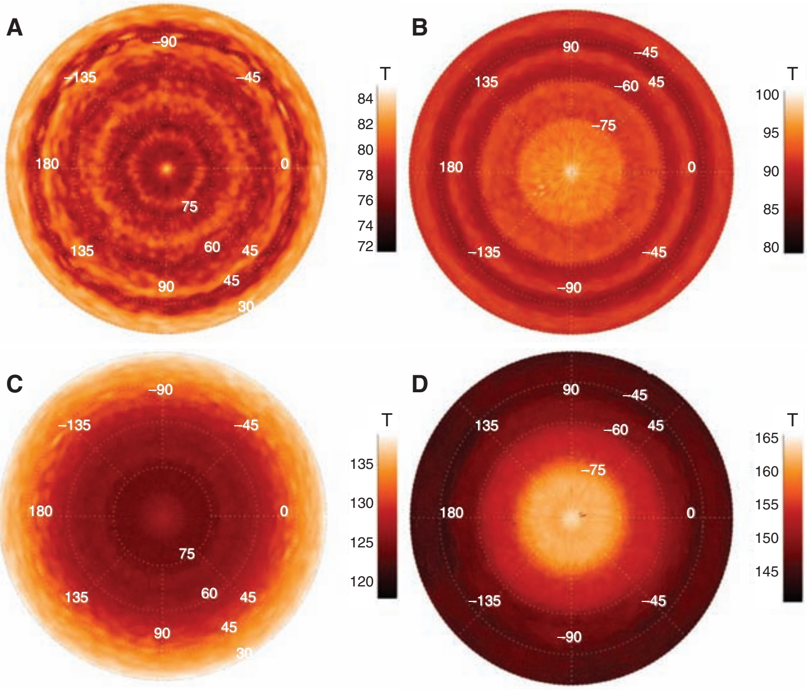

Fig. 1. Orthographic projection of Saturn's polar temperatures in the troposphere at 100 mbar (**A** and **B**) and the stratosphere at 1 mbar (**C** and **D**). The northern hemisphere is shown on the left [(A) and (C)], and the southern hemisphere is shown on the right [(B) and (D)]. Temperatures were retrieved by fitting the 600- to 680-cm^{-1} and 1250- to 1350-cm^{-1} regions of CIRS spectra at 15.0-cm^{-1} spectral resolution. The polar hot spots are clearly visible in the tropospheres, which are surrounded by warm polar belts at 79°N and 76°S, with the former showing a coherent hexagonal structure. Roughly three warm belts are shown concentric around each pole in this latitude range. The stratosphere shows a large seasonal difference in temperature and in the nature of the polar hoods but reveals similarities in the warm polar vortices.

---

[1] Atmospheric, Oceanic, and Planetary Physics, Department of Physics, University of Oxford, Clarendon Laboratory, Parks Road, Oxford OX1 3PU, UK. [2] Jet Propulsion Laboratory, California Institute of Technology, 4800 Oak Grove Drive, Pasadena, CA 91109, USA. [3] NASA/Goddard Spaceflight Center, Greenbelt, MD 20771, USA.

*To whom correspondence should be addressed. E-mail: fletcher@atm.ox.ac.uk

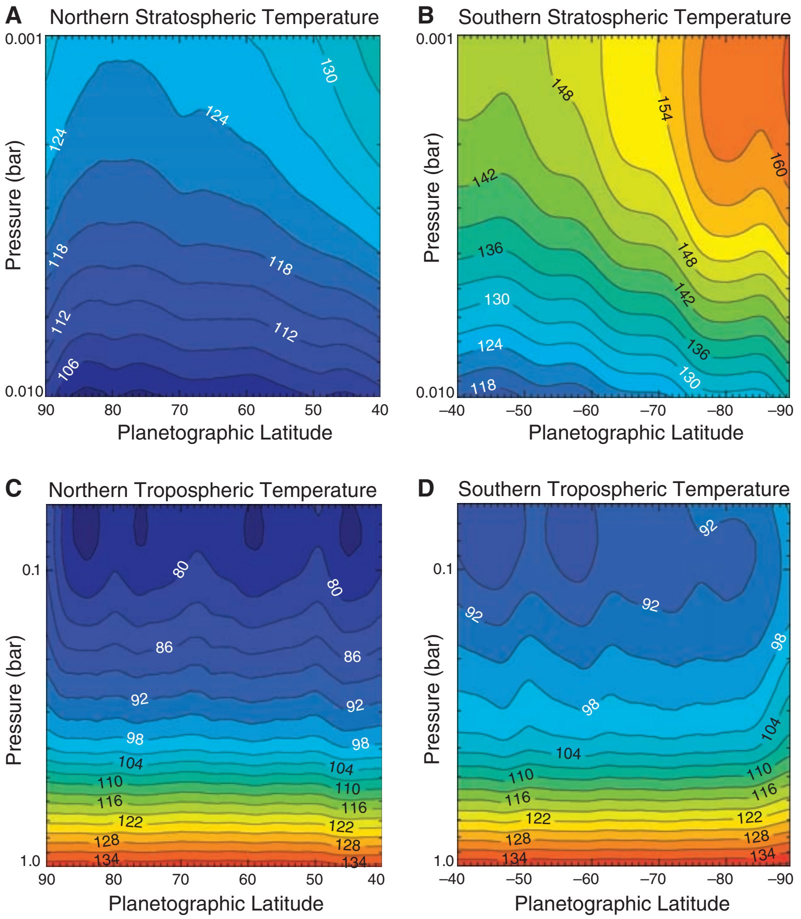

Fig. 2. Zonal mean temperatures in the stratosphere (**A** and **B**) and troposphere (**C** and **D**) for the northern [(A) and (C)] and southern [(B) and (D)] hemispheres. The hexagon coincides with the warm belt at 79°N. Temperature contrasts between belts and zones and seasonal asymmetries become less pronounced at depth in the troposphere. The stratosphere near 1 mbar demonstrates the largest asymmetry in temperature. Hot spots at both poles, surrounded by cooler polar zones, are clearly visible in each contour plot. At 160 mbar, the south polar hot spot (99 K, which is 6 K warmer than the temperature at 80°S) is 8 K warmer than the northern hot spot (91 K, which is 8 K warmer than the temperature at 84°N). The south polar zone showed less contrast because of the higher levels of solar flux, and this finding only became apparent when spectra were zonally averaged. Both tropospheric and stratospheric temperatures were retrieved simultaneously from the 600- to 680-cm^{-1} and 875- to 1400-cm^{-1} regions of 15.0-cm^{-1} resolution CIRS spectra [with PH_3 held constant (*8*)]. No temperature information was available between 6 to 60 mbar, so this region is omitted (see SOM text).

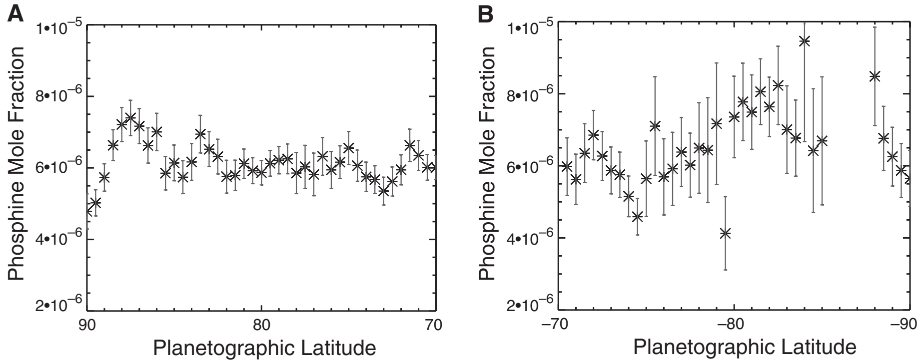

Fig. 3. The meridional distribution of PH_3, a tracer for tropospheric motion, is shown within 20° of each pole. The northern and southern hemispheres are shown in (**A**) and (**B**), respectively. Minima are present at each pole, with local maxima of around 8 ppm for the cooler polar zones surrounding each pole. Mole fractions were derived by fitting the 900- to 1200-cm^{-1} region of CIRS spectra at 2.5-cm^{-1} resolution (*8*) and are quoted for the 550-mbar level, below which the mole fraction is assumed to remain constant with depth into the lower troposphere (*12*). Error bars indicate the standard retrieval errors as described in (*12*).

Yet even in the stratosphere, a symmetry exists within the localized polar vortices observed in both the winter and summer hemispheres. Poleward of the tropospheric polar belt at 79°N, the stratospheric temperature exhibits a slow increase in temperature toward the north pole (128.5 K), which can only be explained dynamically (because radiative heating should be absent at the north pole). The presence of localized hot spots in both summer and winter environments suggests that they could be present throughout Saturn's yearly cycle.

Phosphine gas (PH_3) is a particularly important tracer for the mean overturning of the tropospheres on Jupiter and Saturn (*12*, *13*), because its vertical distribution in the upper troposphere is determined by a balance between vertical mixing below the radiative-convective boundary (400 to 600 mbar) and ultraviolet photochemical destruction at higher altitudes. Saturn's 900- to 1200-cm^{-1} spectra are better reproduced (by 1 to 2 σ) if we vary PH_3 with latitude while simultaneously retrieving temperature. When PH_3 variability is taken into account, the polar hot spots still persist to 800 mbar (the high-pressure limit of the range of CIRS altitude sensitivity). Phosphine is depleted locally at both poles [mole fractions of 5.6 ± 0.7 parts per million (ppm) at 90°S and 4.8 ± 0.5 ppm at 90°N], which implies strong local subsidence in the cores of the polar vortices (Fig. 3). The inferred polar subsidence is consistent with the depressed cloud features seen in Cassini/Imaging Science Subsystem (ISS) imaging of the south pole (*7*) and the clearing of clouds at 2 to 3 bar inferred from 5-μm imaging by Cassini/Visual and Infrared Mapping Spectrometer (VIMS) (*14*). The latitudinally varying composition within each vortex is consistent with the inhibition of lateral mixing across the polar vortex boundaries.

Conversely, there are enhancements in phosphine within both of the cool polar zones (7.4 ± 0.5 ppm at 87.5°N and signs of the abundance exceeding 8 ppm between 80° and 85°S). Visible images of the south polar zone depict a mottled cloud structure (*15*) with multiple stormlike features, which may be regions of localized anticyclonic upwelling, leading to the elevated PH_3 and lower tropospheric temperatures. The polar composition shows a symmetry between the two hemispheres that is irrespective of seasonal differences in the levels of solar flux, leading to the photochemical destruction of PH_3.

Saturn's most interesting polar asymmetry is the hexagonal shape of the cyclonic polar belt and anticyclonic zone to the north and south of the prograde jet at 77°N (*3*). Although ephemeral polygonal waves were encountered in Cassini/ISS images of the southern hemisphere (*15*), there is nothing to rival the long-lived north polar hexagon (*6*). A Lomb-Scargle periodogram (SOM text and fig. S4) was used to conduct a spatiospectral analysis to search for periodicity in the temperature field to confirm the absence of zonal thermal wave activity at the southern pole. The south polar belt at 76°S is not being perturbed into a coherent hexagonal structure in the same way as the north polar belt at 79°N, though the reason for this hemispherical asymmetry is unclear. The hexagon does not extend into the stratosphere at 1 to 6 mbar (Fig. 1).

The striated clouds comprising the northern hexagon were first observed in visible images from Voyager 2 in Saturn's northern spring of 1981 (*3*) and were observed again in northern autumn in the early 1990s from both the ground (*4*) and the Hubble Space Telescope (*16*). Cassini/CIRS and Cassini/VIMS (*14*) observed the thermal field of the hexagon during northern winter (2007), showing that the hexagon is a long-lived feature that is present throughout Saturn's yearly cycle. The 100- to 800-mbar warm hexagon coincides with the 5-μm-bright inner hexagon at 79°N, and the colder zonelike region coincides with the 5-μm-dark hexagon at 76°N, which is thought to be located at 2 to 3 bar (*14*). Upwelling on the equatorial side of the polar jet and subsidence on the poleward side might be responsible for both the warming at 100 to 800 mbar and the cloud clearing leading to the 5-μm-bright hexagon at 2 to 3 bar in VIMS images (*14*).

The persistence of the hexagon over different saturnian seasons with huge changes in solar flux suggests that the hexagon is insensitive to radiative processes. Notably, there is also an absence of any prominent vortices (Fig. 1) interacting with the hexagon at the present time. The presence of a large anticyclonic polar spot at 74.9°N (in the anticyclonic zone equatorward of the polar jet) in Voyager images (*3*, *17*) and ground-based observations (*4*, *18*) led to speculation that a pole-encircling Rossby wave was being forced by interactions between the jet and the anticyclone (*19*). Consistent with the motion equations of (*18*), a cold anticyclonic spot should occur at 115°W (Fig. 1), but the spot does not appear to be present at this time. The CIRS spatial resolution of 0.5° to 1.0° is sufficient to resolve any such features in the temperature field, unless the forcing vortex is outside of the 100- to 800-mbar range. Alternative mechanisms may be required to account for the horizontal structure of the polar belt without the need for prominent local vortices.

Finally, because the hexagon remains stationary with respect to the radio rotation period measured at the time of the Voyager encounters (*14*), it seems reasonable to assume that the mechanism creating the stationary hexagonal structure is deeply rooted in the convective lower troposphere, irrespective of whether the inferred upwelling and subsidence are restricted to a shallow weather layer above 3 to 5 bar. However, because the radio period is now known to vary with time (*20*), the relationship between the hexagon rotation and Saturn's bulk rotation inferred from the radio period is uncertain.

The existence of symmetrical polar circulation cells in both hemispheres of Saturn, despite considerable seasonal differences, with localized subsidence in a polar vortex surrounded by upwelling in cooler polar zones, suggests that these might be general features of giant-planet atmospheric motions, both in our solar system and elsewhere. Pioneer 11 showed Jupiter's poles to be slightly warmer than the equator above the cloud tops (*21*), and recent images of Neptune also demonstrate the presence of a tropospheric hot spot at the south pole (*22*). We can extend the analogy further and compare Saturn's poles to those of the terrestrial planets, such as the seasonal polar vortices of Earth and Mars, and to those of Titan; the winter stratospheric wave patterns on Earth (*23*); and Venus' warm dipolar feature (two clearings in the stratospheric clouds straddling the north and south poles) surrounded by a collar of cooler air (*24*).

References and Notes

1. G. S. Orton, P. A. Yanamandra-Fisher, *Science* **307**, 696 (2005).
2. F. M. Flasar *et al.*, *Space Sci. Rev.* **115**, 169 (2004).
3. D. A. Godfrey, *Icarus* **76**, 335 (1988).
4. A. Sánchez-Lavega, J. Lecacheux, F. Colas, P. Laques, *Science* **260**, 329 (1993).
5. L. N. Fletcher *et al.*, *Icarus* **189**, 457 (2007).
6. A. Sánchez-Lavega, S. Pérez-Hoyos, J. R. Acarreta, R. G. French, *Icarus* **160**, 216 (2002).
7. A. Sánchez-Lavega, R. Hueso, S. Pérez-Hoyos, J. F. Rojas, *Icarus* **184**, 524 (2006).
8. Materials and methods are available as supporting material on *Science* Online.
9. B. J. Conrath, J. A. Pirraglia, *Icarus* **53**, 286 (1983).
10. S. Pérez-Hoyos, A. Sánchez-Lavega, R. G. French, J. F. Rojas, *Icarus* **176**, 155 (2005).
11. E. Karkoschka, M. Tomasko, *Icarus* **179**, 195 (2005).
12. L. N. Fletcher *et al.*, *Icarus* **188**, 72 (2007).
13. P. G. J. Irwin *et al.*, *Icarus* **172**, 37 (2004).
14. K. Baines *et al.*, *Geophys. Res. Abstr.* **9**, 02109 (2007).
15. A. R. Vasavada *et al.*, *J. Geophys. Res. (Planets)* **111**, 5004 (2006).
16. J. Caldwell, X.-M. Hua, B. Turgeon, J. A. Westphal, C. D. Barnet, *Science* **260**, 326 (1993).
17. B. A. Smith *et al.*, *Science* **215**, 504 (1982).
18. A. Sánchez-Lavega *et al.*, *Icarus* **128**, 322 (1997).
19. M. Allison, D. A. Godfrey, R. F. Beebe, *Science* **247**, 1061 (1990).
20. D. A. Gurnett *et al.*, *Science* **316**, 442 (2007).
21. A. P. Ingersoll, *Science* **248**, 308 (1990).
22. G. S. Orton, T. Encrenaz, C. Leyrat, R. Puetter, A. J. Friedson, *Astron. Astrophys.* **473**, L5 (2007).
23. D. E. Venne, J. L. Stanford, *J. Atmos. Sci.* **39**, 1026 (1982).
24. F. W. Taylor *et al.*, *J. Geophys. Res.* **85**, 7963 (1980).
25. This work was carried out at the Atmospheric, Oceanic, and Planetary Physics Department at the University of Oxford. The UK authors acknowledge the support of the Science and Technology Facilities Council. We acknowledge the members of the Cassini and CIRS investigation teams involved in the building, testing, and calibration of the instrument, along with the design of imaging sequences, instrument commands, and other vital operational tasks. The authors also thank K. Baines, M. Roos-Serote, A. Aguiar, Y. H. Yamazaki, and R. Wordsworth for their helpful comments and suggestions.

Supporting Online Material

www.sciencemag.org/cgi/content/full/319/5859/79/DC1
Materials and Methods
SOM Text
Figs. S1 to S4
References

21 August 2007; accepted 19 November 2007
10.1126/science.1149514

The Avalon Explosion: Evolution of Ediacara Morphospace

Bing Shen, Lin Dong, Shuhai Xiao,* Michał Kowalewski

Ediacara fossils [575 to 542 million years ago (Ma)] represent Earth's oldest known complex macroscopic life forms, but their morphological history is poorly understood. A comprehensive quantitative analysis of these fossils indicates that the oldest Ediacara assemblage—the Avalon assemblage (575 to 565 Ma)—already encompassed the full range of Ediacara morphospace. A comparable morphospace range was occupied by the subsequent White Sea (560 to 550 Ma) and Nama (550 to 542 Ma) assemblages, although it was populated differently. In contrast, taxonomic richness increased in the White Sea assemblage and declined in the Nama assemblage. These diversity changes, occurring while morphospace range remained relatively constant, led to inverse shifts in morphological variance. The Avalon morphospace expansion mirrors the Cambrian explosion, and both events may reflect similar underlying mechanisms.

The evolutionary history of macroscopic organisms in the late Ediacaran Period (circa 575 to 542 Ma) is regarded as a prelude to the Cambrian explosion (*1*). There are >270 described Ediacara species occurrences from >30 localities on several major continents (Fig. 1 and tables S1 to S3), providing an adequate data set for a quantitative analysis of Ediacara taxonomic and morphological evolution. Using cluster analysis of taxonomic composition, Waggoner recognized three Ediacara assemblages: Avalon, White Sea, and Nama (*2*). The Avalon assemblage (575 to 565 Ma) (*3*) is restricted to deep-water environments in the Avalon Province and represents an early evolutionary stage with relatively low taxonomic richness. The subsequent White Sea assemblage (560 to 550 Ma) shows a substantial diversity increase and a notable geographic expansion into Baltica

---

Department of Geosciences, Virginia Polytechnic Institute and State University, Blacksburg, VA 24061, USA.

*To whom correspondence should be addressed. E-mail: xiao@vt.edu

(Winter Coast and adjacent area, Podolia, Finnmark, and Urals) (*4*, *5*), Australia (*6*), Siberia (*4*), and Laurentia (*7*). Diversity drops again in the Nama assemblage (550 to 542 Ma) (*8*, *9*), which includes fossils from the Kalahari Craton (*10*), Yangtze Platform (*11*, *12*), Laurentia (*13*, *14*), and Carolina Terrace (*15*, *16*).

Waggoner (*2*) discussed three possible interpretations of the Ediacara assemblages: They may represent different evolutionary stages, biogeographic provinces, or environmental-ecological associations. These interpretations need not be mutually exclusive, because evolutionary changes could be driven by biogeographic, ecological, and environmental factors. Grazhdankin (*17*) argued that these assemblages represent environmental-ecological associations with little biogeographic provinciality or evolutionary change, although available geochronological data (*1*, *8*, *9*, *18*, *19*) indicate that the assemblages do indeed differ in age.

Previous work on the Ediacara assemblages focused on taxonomic data. We tested whether morphological patterns mirror taxonomic trends and whether there are any temporal, geographic, and environmental effects on Ediacara morphological patterns.

We recorded the presence or absence of 50 morphological characters for 272 occurrences of Ediacara species (or unnamed forms) from 60 publications and one unpublished museum sample (table S4). To maintain taphonomic uniformity, we focused on classical Ediacara assemblages and excluded possible Ediacara fossils preserved as carbonaceous compressions (*20*). Although the coded characters are not exhaustive and exclude some inferred anatomical structures, such as gonads and intestine of some dickinsoniid fossils (*21*), those characters represent the overall shape, first-order symmetry (e.g., unipolar bilateral symmetry in *Charniodiscus*), and central-peripheral differentiation (e.g., central stalk and primary side branches in Ediacara fronds) associated with classical Ediacara specimens. They also include such important features as stems and discoidal holdfasts. The chosen characters are easily recognizable and less likely to be altered beyond recognition by taphonomic processes, which is an important factor, considering that most Ediacara fossils are preserved as casts and molds. A coded character may not be phylogenetically homologous or functionally analogous among different taxa, but we focus on morphological evolution and make no inference on the phylogenetic homology and functional biology of the coded characters.

Our raw diversity estimates (Fig. 2A and table S3)—20, 77, and 15 genera in the Avalon, White Sea, and Nama assemblages, respectively—are broadly similar to Waggoner's estimate. To correct for uneven sampling, we used rarefaction to standardize taxonomic richness estimates. The diversity pattern observed for raw data persisted after rarefaction (Fig. 2, A and B). To further test whether taxonomic synonymy had an impact on the observed diversity pattern, we reclassified all taxa in our database on the basis of distinctive morphotypes using our character-coding system and then conducted rarefaction analysis. Again, the richness pattern remained unchanged (Fig. 2, A and B), indicating minimal impact of taxonomic synonymy. Furthermore, because the quality of fossil preservation is comparable in the three assemblages (table S3), the significant differences in taxonomic diversity are unlikely to have been an artifact of differential preservation of the assemblages.

To compare the realized morphospaces of the three Ediacara assemblages, we first used the nonparametric multidimensional scaling (MDS) method to ordinate the pooled multivariate data set into two dimensions (MDS Dim1 and Dim2), so that each species occurrence can be represented by two MDS scores rather than by 50 characters. The morphospace of each assemblage can then be visualized as a convex "hull" in a scatterplot of the two-dimensional (2D) MDS scores (*22*). Our results show that all three assemblages share similar morphospaces of comparable size (Fig. 2C), and this pattern persisted when the MDS ordination was fitted into three dimensions (fig. S1, A and B). Shared morphospace, calculated as the overlapping area between convex hulls, is on average 81.9% (Avalon–White Sea, 81.9%; Nama–White Sea, 84.1%; Avalon-Nama, 79.7%), as compared with 12.3% for shared genera (Avalon–White Sea, 10.3%; Nama–White Sea, 15.2%; Avalon-Nama, 11.4%) (Fig. 2D). Thus, despite substantial changes in taxonomic diversity throughout the Ediacara history, the overall size and position of the Ediacara morphospace remained markedly static.

Although the morphospace range (Fig. 2C and fig. S1, A and B) is comparable across the three assemblages, the group centroids are statistically distinct for the Avalon–White Sea and Avalon-Nama comparisons (table S5). Thus, the typical (average) morphology of the Avalon assemblage may differ from the typical morphologies of the two subsequent assemblages, perhaps reflecting the intuitive perception that the Avalon assemblage was somewhat distinct. However, the difference is minor: All pairwise distances between centroids are small (table S5), and discriminant analysis misclassifies 59.2% of species occurrences into incorrect assemblages (table S6). These results are consistent with a substantial overlap among the three morphospaces observed on ordination plots (Fig. 2C and fig. S1, A and B).

To test whether Ediacara biotas of similar age from different biogeographic provinces or paleolatitudes have distinct morphospaces, we focused on the White Sea assemblage (i.e., the only assemblage with sufficient geographic coverage) and used MDS to ordinate the Baltica, Flinders Ranges, Siberia, and Wernecke biotas (Fig. 2E and table S2). The Baltica and Flinders Ranges biotas, likely coeval (*2*) but from different paleolatitudes (*23*), share similar morphospaces (90.2% shared morphospace versus 41.3% shared genera) that are comparable to the morphospace of the entire White Sea assemblage [shared morphospace: Baltica–White Sea (86.9%), Flinders Ranges–White Sea (91.9%); shared genera: Baltica–White Sea (75.3%), Flinders Ranges–White Sea (44.2%)]. In contrast, the Siberia and Wernecke biotas occupy smaller morphospaces. However, these smaller morphospaces may reflect inadequate sampling, because these two biotas are represented by only 10 and 13 species occurrences, respectively. Indeed, rarefaction analysis of the White Sea assemblage suggests that at least ~30 species occurrences are required to retain its morphospace size (Fig. 2F). In sum, the comparable morphospaces of the adequately sampled Flinders Ranges and Baltica biotas, the small distances between centroids (table S5), and poor classificatory performance of discriminant analysis (table S6) all suggest that the Ediacara morphospace may have been decoupled from paleobiogeography.

It has been argued that the distribution of Ediacara taxa was primarily controlled by pa-

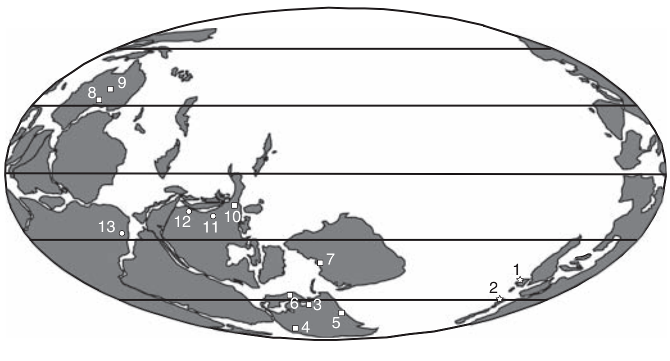

Fig. 1. Ediacaran paleogeographic map and fossil localities. The Avalon assemblage is indicated by stars: 1, Charnwood Forest (England); 2, Avalon Peninsula (Newfoundland). The White Sea assemblage is indicated by squares: 3, Winter Coast and adjacent area (Russia); 4, Podolia (Ukraine); 5, Urals (Russia); 6, Finnmark (Norway); 7, Olenëk Uplift (Siberia); 8, Flinders Ranges (Australia); 9, central Australia; 10, Wernecke Mountains (Canada). The Nama assemblage is indicated by circles: 11, British Columbia (Canada); 12, Great Basin (United States); 13, southern Namibia. Baltica biota refers to Ediacara fossils of the White Sea assemblage from four localities: Winter Coast and adjacent area, Podolia, Urals, and Finnmark. Latitude lines at 30° intervals are indicated. [Modified from Waggoner (*2*)]

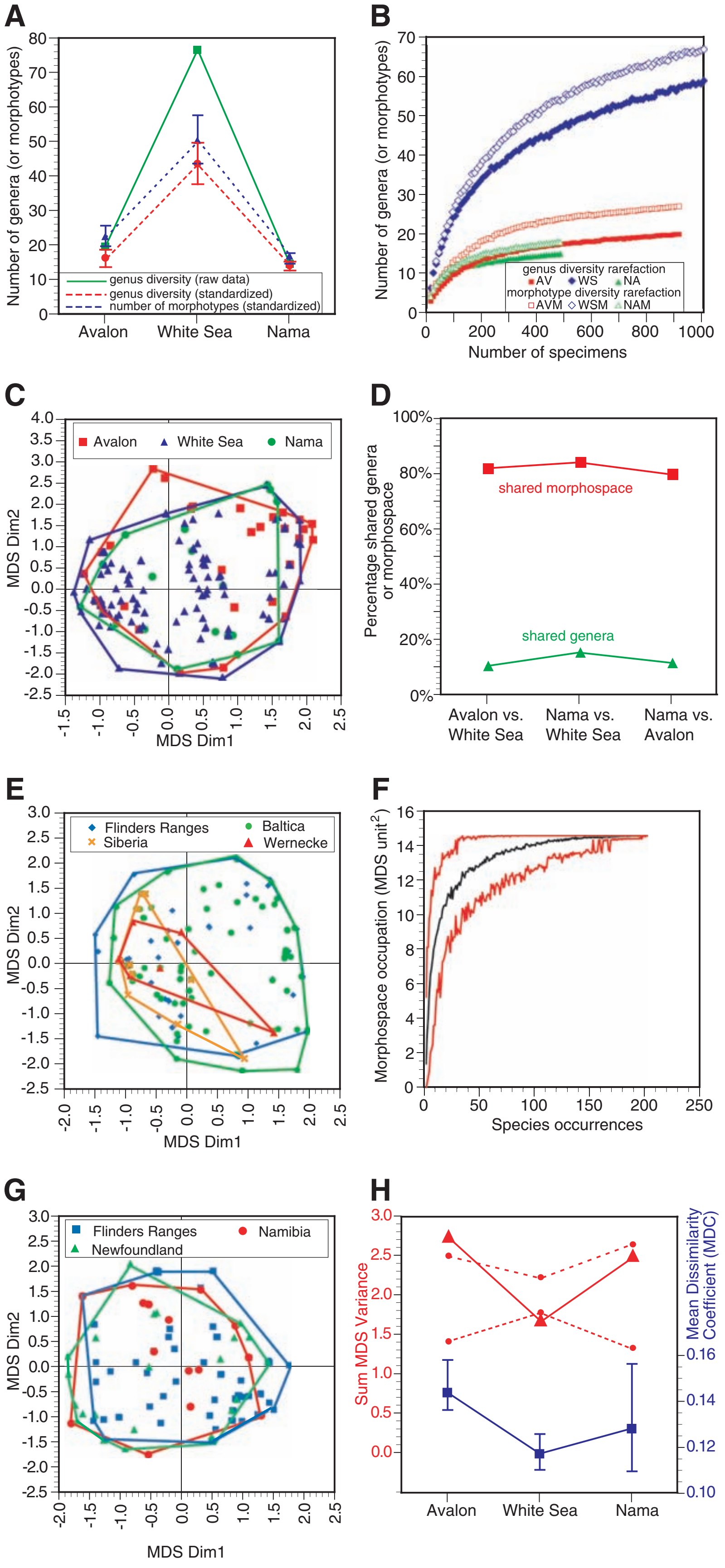

Fig. 2. (**A**) Taxonomic richness measured as the number of genera from raw data, genus-level richness standardized at 400 specimens, and the number of morphotypes standardized at 400 specimens. Error bars represent 95% confidence intervals (CIs), each estimated by 1000 independent rarefaction runs. (**B**) Rarefaction analysis showing relation between sampling intensity and diversity. Mean genus-level diversity and mean morphotype diversity were estimated by 1000 independent rarefaction runs. AV, Avalon; WS, White Sea; NA, Nama. (**C**) MDS ordination plot with convex hulls delineating the morphospace range realized by the three Ediacara assemblages. (**D**) Percentage of shared morphospace or genera among the three Ediacara assemblages. (**E**) MDS ordination plot and convex hulls of four Ediacara biotas within the White Sea assemblage: the Baltica, Flinders Ranges, Siberia, and Wernecke biotas. (**F**) Rarefaction analysis showing the effect of sampling intensity (number of species occurrences) on realized morphospace of the White Sea assemblage. Morphospace size (black line) and 95% CIs (red lines) estimated from 100 independent rarefaction runs. (**G**) MDS ordination plot and convex hulls of the Newfoundland biota of the Avalon assemblage, the Flinders Ranges biota of the White Sea assemblage, and the Namibia biota of the Nama assemblage. (**H**) MDS variance values (solid red line), as compared against predictions of the constant-disparity null model estimated by a Monte Carlo simulation that calculates expected variation in MDS scores if the disparity of the three assemblages was identical (the dashed red lines are the 95% CIs of the null model estimated by 1000 randomization runs). Note that two of the three assemblages are located outside the 95% CIs predicted by the null model of time-invariant disparity. MDC estimates (blue line) with 95% CIs (error bars), which were estimated separately for each of the three Ediacara assemblages by 500 balanced-bootstrap iterations.

leoenvironments (*17*): Avalon-type biotas occur in deep marine habitats, Flinders Ranges–type biotas occur in shallow marine prodeltaic settings, and Nama-type biotas occur in distributary-mouth bar shoals. According to Grazhdankin (*17*), these three biotas represent an environmental-ecological gradient involving little evolutionary change or biogeographic provinciality. We recalculated MDS scores of the Newfoundland, Flinders Ranges, and Namibia biotas that represent these three paleoenvironments (table S2). There are substantial taxonomical differences among the three biotas [shared genera: Flinders Ranges–Newfoundland (11.8%), Newfoundland-Namibia (6.7%), Namibia–Flinders Ranges (12.8%)]. However, the percentage of shared morphospace is high [Flinders Ranges–Newfoundland (86.3%), Newfoundland-Namibia (91.7%), Namibia–Flinders Ranges (89.6%)] (Fig. 2G), and discriminant analysis suggests (tables S5 and S6) that the three groups are indistinguishable or strongly overlapping, indicating that paleoenvironments were not a major factor controlling the extent of Ediacara morphospace.

Although evolutionary change, biogeographic provinciality, and paleoenvironments might have played a role in Ediacara taxonomic evolution, they do not seem to have controlled the overall range of the realized morphospace, which appears to be invariant to notable taxonomic differences. Thus, changes in taxonomic diversity that occurred through time while morphospace range remained relatively constant should affect the internal structure of morphospace. Because of its greater taxonomic diversity, the White Sea assemblage should have a more crowded morphospace. Consequently, the morphological disparity (average morphological distances between taxa) of the White Sea assemblage should be smaller than the disparities of the Avalon and Nama assemblages.

We used three metrics—MDS variance, total character variance, and the mean dissimilarity coefficient (MDC) (*24*–*26*)—to quantify morphological disparity. The MDS variance was estimated by summing the variances of MDS scores along the two MDS dimensions. As expected, the sum of the MDS variance is lower in the White Sea assemblage than the sums of the other two assemblages (Fig. 2H). Results were similar when scores based on the 3D MDS ordination were used (fig. S1C). The total character variance, calculated by summing the variances of the original 50 variables, shows a comparable outcome (fig. S1D). For binary characters, the MDC of an assemblage can be calculated as the fraction of dissimilar characters averaged across all pairwise comparisons. The MDC results are notably consistent with those based on variances, although the difference between the White Sea and Nama assemblages is statistically insignificant (Fig. 2H), perhaps as a result of low statistical power associated with the small sample size of the Nama assemblage (table S3). The inverse relation between taxonomic diversity (Fig. 2A) and morphological disparity, observed for all applied metrics (Fig. 2H and fig. S1, C and D), reflects morphospace saturation: An increase in diversity within the confines of a static morphospace inevitably reduces the average morphological distance between taxa.

Although the three Ediacara assemblages differ in taxonomic composition, their morphospaces overlap strongly and are comparable in size. Ediacara morphospace reached its maximum range already in the Avalon assemblage and was subsequently maintained in the White Sea and Nama assemblages. The morphospace was filled sparsely in the low-diversity, high-disparity Avalon and Nama assemblages but was filled densely in the high-diversity, low-disparity White Sea assemblage. Furthermore, the Ediacara morphospace ranges do not appear to have been controlled by paleobiogeography or paleoenvironments.

What might have led to the rapid morphospace expansion in the Avalon assemblage, and what might have constrained the Ediacara morphospace from further expansion or shift in the subsequent White Sea and Nama assemblages? We consider a long, undocumented period of Ediacara history before the Avalon assemblage to be unlikely. The rapid increase of morphospace at the beginning of Ediacara evolution parallels the disparity patterns of the Cambrian explosion (*27*–*29*): a rapid evolution of body plans followed by taxonomic diversification within the limits of a predefined morphospace. Various environmental, ecological, and developmental factors have been proposed to explain the rapid evolution of animal body plans during the Cambrian explosion, as well as to account for post-Cambrian constraints on modifications of these basic body plans despite taxonomic diversification (*30*). In principle, these explanations may also be applied to the Avalon radiation. Future research should combine paleoecological, paleoenvironmental, developmental, and morphometric data to test (i) whether the Gaskiers glaciation (*3*), Ediacaran oxygenation (*31*, *32*), establishment of a regulatory developmental system (*33*), or sophisticated ecological interactions (*34*) might have been the underlying drivers for the early morphological diversification of Ediacara organisms and (ii) whether the ecological saturation or developmental entrenchment might have constrained Ediacara morphospaces. Regardless of the veracity of these causative explanations, the marked parallels between the Cambrian and Avalon explosions suggest that the decoupling of taxonomic and morphological evolution is not unique to the Cambrian explosion and that the Avalon explosion represents an independent, failed experiment with an evolutionary pattern similar to that of the Cambrian explosion.

References and Notes

1. G. M. Narbonne, *Annu. Rev. Earth Planet. Sci.* **33**, 421 (2005).
2. B. Waggoner, *Integr. Comp. Biol.* **43**, 104 (2003).
3. G. M. Narbonne, J. G. Gehling, *Geology* **31**, 27 (2003).
4. B. S. Sokolov, A. B. Iwanowski, Eds. *The Vendian System, Volume 1: Paleontology* (Springer-Verlag, Heidelberg, Germany, 1990).
5. J. Farmer *et al.*, *Geol. Mag.* **129**, 181 (1992).
6. J. G. Gehling, M. L. Droser, S. R. Jensen, B. N. Runnegar, in *Evolving Form and Function: Fossils and Development*, D. E. G. Briggs, Ed. (Peabody Museum of Natural History, Yale University, New Haven, CT, 2005), pp. 43–66.
7. G. M. Narbonne, H. J. Hofmann, *Palaeontology* **30**, 647 (1987).
8. J. P. Grotzinger, S. A. Bowring, B. Z. Saylor, A. J. Kaufman, *Science* **270**, 598 (1995).
9. J. E. Amthor *et al.*, *Geology* **31**, 431 (2003).
10. D. Grazhdankin, A. Seilacher, *Palaeontology* **45**, 57 (2002).
11. W. Sun, *Precambrian Res.* **31**, 361 (1986).
12. S. Xiao, B. Shen, C. Zhou, G. Xie, X. Yuan, *Proc. Natl. Acad. Sci. U.S.A.* **102**, 10227 (2005).
13. H. J. Hofmann, E. W. Mountjoy, M. W. Teitz, *Can. J. Earth Sci.* **28**, 1541 (1991).
14. J. W. Hagadorn, B. M. Waggoner, *J. Paleontol.* **74**, 349 (2000).
15. G. G. Gibson, S. A. Teeter, M. A. Fedonkin, *Geology* **12**, 387 (1984).
16. P. G. Weaver, M. A. S. McMenamin, R. C. Tacker, *Precambrian Res.* **150**, 123 (2006).
17. D. Grazhdankin, *Paleobiology* **30**, 203 (2004).
18. M. W. Martin *et al.*, *Science* **288**, 841 (2000).
19. S. A. Bowring *et al.*, *Science* **261**, 1293 (1993).
20. S. Xiao, X. Yuan, M. Steiner, A. H. Knoll, *J. Paleontol.* **76**, 347 (2002).
21. J. Dzik, *Integr. Comp. Biol.* **43**, 114 (2003).
22. J. W. Huntley, S. Xiao, M. Kowalewski, *Precambrian Res.* **144**, 52 (2006).
23. A. G. Smith, in *The Ecology of the Cambrian Radiation*, A. Y. Zhuravlev, R. Riding, Eds. (Columbia Univ. Press, New York, 2001), pp. 11–46.
24. M. Foote, *Proc. Natl. Acad. Sci. U.S.A.* **89**, 7325 (1992).
25. M. Foote, *Paleobiology* **19**, 185 (1993).
26. M. Foote, *Paleobiology* **20**, 320 (1994).
27. S. J. Gould, *Paleobiology* **17**, 411 (1991).
28. D. E. G. Briggs, R. A. Fortey, M. A. Wills, *Science* **256**, 1670 (1992).
29. M. Foote *et al.*, *Science* **258**, 1816 (1992).
30. C. R. Marshall, *Annu. Rev. Earth Planet. Sci.* **34**, 355 (2006).
31. D. A. Fike, J. P. Grotzinger, L. M. Pratt, R. E. Summons, *Nature* **444**, 744 (2006).
32. D. E. Canfield, S. W. Poulton, G. M. Narbonne, *Science* **315**, 92 (2007).
33. E. H. Davidson, D. H. Erwin, *Science* **311**, 796 (2006).
34. K. J. Peterson, N. J. Butterfield, *Proc. Natl. Acad. Sci. U.S.A.* **102**, 9547 (2005).

35. Funding was provided by NSF, National Natural Science Foundation of China, NASA Exobiology Program, and Yale University Peabody Museum. We thank two anonymous reviewers for constructive comments.

Supporting Online Material
www.sciencemag.org/cgi/content/full/319/5859/81/DC1
Materials and Methods
Fig. S1
Tables S1 to S6
References

10 September 2007; accepted 16 November 2007
10.1126/science.1150279

Intermittent Plate Tectonics?

Paul G. Silver[1]* **and Mark D. Behn**[2]

Although it is commonly assumed that subduction has operated continuously on Earth without interruption, subduction zones are routinely terminated by ocean closure and supercontinent assembly. Under certain circumstances, this could lead to a dramatic loss of subduction, globally. Closure of a Pacific-type basin, for example, would eliminate most subduction, unless this loss were compensated for by comparable subduction initiation elsewhere. Given the evidence for Pacific-type closure in Earth's past, the absence of a direct mechanism for termination/initiation compensation, and recent data supporting a minimum in subduction flux in the Mesoproterozoic, we hypothesize that dramatic reductions or temporary cessations of subduction have occurred in Earth's history. Such deviations in the continuity of plate tectonics have important consequences for Earth's thermal and continental evolution.

Plate tectonic theory originated to explain how oceanic lithosphere is created at spreading centers and consumed at subduction zones. The continental component of this theory was added by Wilson (*1*), who proposed that there is an cycle of continental breakup and collision that accompanies the opening and closing of ocean basins. One of the most intriguing aspects of this theory is the formation of supercontinents after ocean closure. In particular, supercontinent assembly has the potential to dramatically reduce subduction flux by the termination of subduction via continent-continent collision. For example, consider the Atlantic Ocean basin, which has been growing in area at the expense of the Pacific since its opening at 200 million years ago (Ma). If this trend continues, relative plate-motion models (*2*) predict that in ~350 million years (My), the Pacific will effectively close, leading to widespread continent-continent collisions and the termination of subduction in the Pacific basin. This would eliminate most of Earth's subduction zones, resulting in an order of magnitude reduction in global subduction flux.

Despite the plausibility of such an event, it is commonly assumed that reductions in global subduction flux of this magnitude do not occur (*3*). The goal of this study is to critically evaluate this assumption and to consider the alternative hypothesis that there have been dramatic reductions in subduction flux over Earth's history. There are two main factors that must be considered when evaluating the continuity of subduction flux: the mode of ocean closure and the characteristics of subduction initiation. If the Atlantic closed (A-type closure), instead of the Pacific (P-type closure), then Pacific subduction would survive intact (Fig. 1). A-type closure occurs when an interior ocean closes after the breakup of a previous supercontinent. In contrast, P-type closure represents the closing of an external ocean (*4*). The key distinction between these two modes, in terms of subduction flux, is that P-type closure has the potential to dramatically reduce or even eliminate subduction flux, whereas A-type closure does not (Fig. 1). Closure mode can be determined by dating the former oceanic crust (preserved as ophiolites in sutures) after supercontinent assembly. For A-type closure, the (former) ocean crust from the internal ocean is always younger than the age of breakup of the previous supercontinent (Fig. 1). For P-type closure, this crust can be older (because subduction predates the breakup of the previous supercontinent), as exemplified today by the circum-Pacific ophiolite belts, some of which possess early Paleozoic ages (such as the Trinity ophiolite of northern California) and predate the breakup of Pangaea (*4*).

P-type and A-type closure represent two end-member cases, and in practice the mode of closure is likely to be a mixture of the two. It nevertheless appears that supercontinent assembly is typically predominantly produced by one or the other (*4*). The supercontinent Pangaea, which was formed by the closing of the Iapetus Ocean, appears to have formed primarily by A-type closure (*4*). In contrast, presently available evidence suggests that both the supercontinents Pannotia (*5*, *4*) and Rodinia formed primarily by P-type closure (*6*, *4*). Finally, the earlier hypothesized supercontinent Nuna may have formed by A-type closure, although this is highly uncertain (*4*) (Table 1).

For Rodinia, the evidence for P-type closure is based on (i) the greater age of oceanic-affinity rocks (such as ophiolites), as compared to the age of breakup of Nuna (*4*); (ii) the fact that the Superior province faced an open ocean for ~0.8 billion years (*4*); and (iii) that the Grenville orogen, which ultimately created Rodinia, ap-

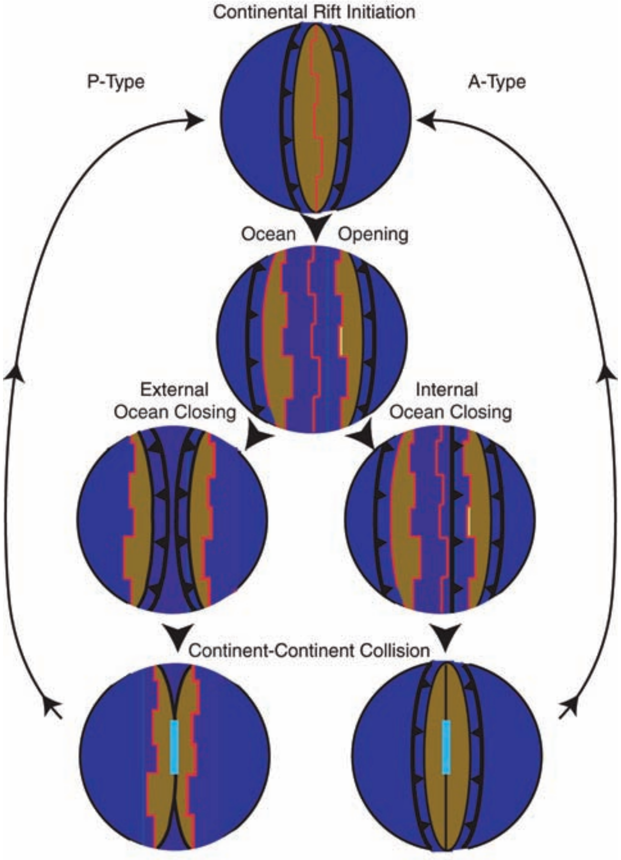

Fig. 1. Schematic of two modes of ocean closure: P-type and A-type (*4*). (**Top**) Supercontinent (brown), surrounded by subduction zones (black), begins rifting, initiating continental breakup and the creation of an internal ocean (red lines). (**Middle top**) Breakup continues, increasing the size of the internal ocean at the expense of the external ocean. (**Middle bottom**) In A-type closure, subduction begins at a passive margin of the internal ocean and the internal ocean begins to close. In P-type closure, the internal ocean continues to grow and becomes the largest ocean basin (the other side of Earth is shown). (**Bottom**) Supercontinent assembly. In A-type closure, the internal ocean closes, shutting down subduction zones in the internal ocean, while subduction (and sea-floor spreading) in the external ocean continues. In P-type closure, the external ocean closes, shutting down all subduction. A-type and P-type closure can be distinguished by the age of former oceanic crustal material (such as ophiolites) that is trapped in the suture zone upon supercontinent assembly (light blue rectangle) (*4*). In A-type closure, it is younger than the age of breakup of the previous supercontinent (because subduction initiation postdates the previous breakup), whereas in the case of P-type closure, oceanic crustal material can predate the breakup of the previous supercontinent (because subduction initiation predates breakup).

---

[1] Department of Terrestrial Magnetism, Carnegie Institution of Washington, 5241 Broad Branch Road, NW, Washington, DC 20015, USA. [2] Department of Geology and Geophysics, Woods Hole Oceanographic Institution, Mail Stop 22, Woods Hole, MA 02543, USA.

*To whom correspondence should be addressed.

pears to have been a collision between two active margins (*6*). These observations suggest that this collision stopped an extensive (~20,000 km) length of active margin stretching from southwestern North America to Baltica (~10,000 km) (*7*) on the western side and an equally long active margin to the east. Thus, the geologic record suggests a predominantly P-type closure mode and points to a drastic reduction in subduction flux.

The second factor in assessing the continuity of subduction flux is subduction initiation, probably the least well-understood aspect of plate tectonic theory (*8*, *9*). The Wilson cycle predicts that the Atlantic will close again to form a second Pangaea through widespread initiation of subduction in the Atlantic basin (*1*, *10*). Yet, with the exceptions of the narrow Caribbean and Scotia arcs, there is no evidence for subduction initiation (either intra-oceanic or at passive margins) within this ocean basin, despite 100– to 200–million-year-old passive margin sequences. From a thermal point of view, for ages greater than ~80 My, the flattening of the sea-floor–age relation (*11*) suggests little further change in passive margin thermal structure (and by extension little change in passive margin stability). Thus, the passage of time does not appear to increase the probability of subduction initiation in the Atlantic basin, suggesting that P-type closure remains a likely closure mode for the future.

If most of the world's subduction zones were indeed lost through P-type ocean closure, roughly constant subduction flux could still be maintained if subduction initiation approximately balanced subduction termination. This requires that there be a causal relationship between the two processes corresponding to an approximate "conservation law" for subduction flux; namely, that order-of-magnitude fluctuations in subduction flux do not occur. Is there such a law? The most likely mechanism would be through a transfer of stress induced by a collision, leading to "forced" subduction initiation elsewhere (*8*). Yet the response to recent collisions suggests otherwise. The formation of the Alpine-Himalayan chain represents the collision of India and Africa with Eurasia at about 35 to 50 Ma in the closure of the Tethys Ocean. If large-scale collisional stress transfer occurred, we would expect subduction to have initiated elsewhere within the Indian and African plates. However, no new subduction zones have initiated south of either India or Africa to compensate for the loss of subduction by this ocean closure. The Indian plate does exhibit extensive internal deformation related to the collision (*12*); yet more than 50 My have elapsed without the initiation of subduction. In fact, the only subduction initiation that has occurred in the past 80 My (with the notable exception of the 600-km-long Scotia Arc) has been intra-oceanic and entirely within the Pacific basin (*8*). As such, it would prevent neither the ultimate closure of the Pacific basin nor the loss of Pacific-basin subduction zones. These examples illustrate that (i) an internal ocean can exist for at least 200 My (and probably much longer) without subduction initiation, and (ii) subduction does not immediately begin in response to a continent-continent collision, lagging by at least tens and perhaps hundreds of millions of years. Given the evidence that supercontinent assembly has occurred by P-type closure in the past and appears to be occurring in the present, and the absence of evidence for a subduction flux "conservation law," we conclude that supercontinent assembly has the potential to substantially reduce subduction flux or even temporarily eliminate it.

Table 1. History (formation age, breakup age, and duration) and ocean closure mode for the last four supercontinents.

Supercontinent	Formation (Ma)	Breakup (Ma)	Duration (My)	Mode	Ref.
Pangaea	350	250	100	Atlantic	(*4*)
Pannotia/Gondwanaland	650	550	100	Pacific	(*4*, *5*)
Rodinia	900	760	140	Pacific	(*4*, *6*, *39*)
Nuna	1800	1500	300	Atlantic?	(*4*)

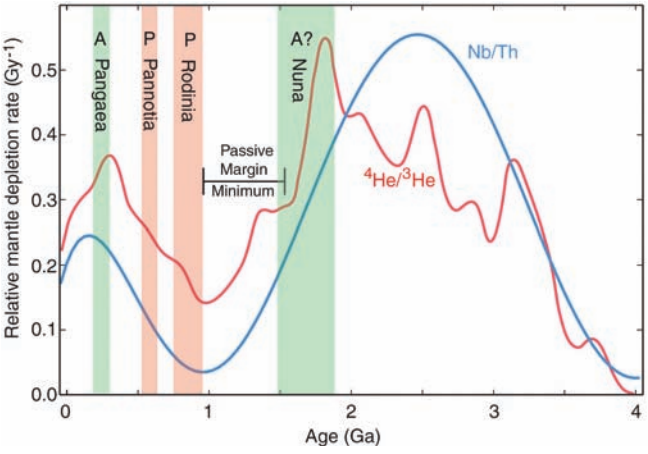

Fig. 2. Estimated mantle depletion-rate curves as inferred from two independent sources. Blue curve: relative mantle depletion rate obtained from a derivative of polynomial fit to measurements of Nb/Th ratios and other geochemical and geophysical estimates (*15*). Red curve: ^{4}He/^{3}He ratios (*16*) of ocean island basalts, with an inferred time scale based on a He evolution model that matches peaks in the distribution of crustal zircons. The two curves are broadly similar, characterized by a peak at ~2.5 Ga, a minimum around 1.0 Ga, and a second maximum in the Phanerozoic. The units of the blue curve are relative mantle depletion rate (Gy^{-1}), whereas the ^{4}He/^{3}He curve has no well-defined units but should also reflect relative mantle depletion. Assuming that the depletion-rate curves are proxies for subduction flux, then they should reflect the rate of plate tectonic activity and predict relatively low tectonic activity in the Mesoproterozoic and early Neoproterozoic. The minimum in passive margin formation (denoted by the black time bracket), thought to be another proxy for plate tectonic activity (*26*), also occurs roughly at this time (black bracket). Also shown are the lifetimes of the known supercontinents, denoting whether they were formed primarily by A-type (A, green) or P-type (P, orange) closure. Grenville collision occurred at the formation time of Rodinia (~1 Ga).

Although a direct record of subduction flux earlier than 200 Ma is not available, we can look for proxies from which to estimate this flux. Here we define subduction flux, F_s, as the globally integrated product of trench length and convergence velocity. One promising approach is to make use of subduction-related magmatism. The primary magmatic product of subduction is arc volcanism, and it is reasonable to assume that the global arc magmatic production rate, M, is proportional to F_s. This assumption is supported by numerical modeling results (*13*), by comparisons with local geology (*14*), and by the positive correlation between magmatic production rates and convergence velocity for several subduction zones in the Pacific (fig. S2). If arc magmatism is reflected in mantle depletion, we can then use the time history of mantle depletion as a proxy for subduction flux.

As an illustration, we choose two geochemical indicators of mantle depletion history proposed in the literature. The first is based primarily on Nb/Th ratios (*15*), whereas the second is based on the statistical distribution of ^{4}He/^{3}He ratios in ocean island basalts (*16*, *17*). These two independent measures exhibit the same overall basic features, namely a maximum in the Neoarchean, a minimum around 1.0 billion years ago (Ga), and a second maximum in the Phanerozoic (Fig. 2). Interpreted as subduction flux, this variation is distinctly different from the expected gradual reduction in subduction flux over the age of Earth inferred from the secular decline in mantle temperature (*18*). These geochemical proxies therefore suggest a minimum in subduction flux corresponding in time to the formation of Rodinia by P-type closure.

Other proxies for plate tectonic activity can also be used. Assuming that continental crust is predominantly derived from arc volcanism, a continental growth-rate curve could be used as a subduction flux proxy. Although there are concerns about biased sampling of the crust, the role of recycling, and the difficulty of distinguishing between juvenile and reworked crust, it has become increasingly clear that continental growth is episodic rather than continuous (*15*, *16*, *19*–*24*). The conventional explanation is that this episodicity reflects dramatic events in the mantle, such as superplumes and mantle overturn events, implicitly arguing that crustal addition is unrelated to subduction. However, we propose that an equally plausible alternative is that the episodicity of crust formation reflects the episodicity of subduction flux (*25*). Another possible proxy for subduction flux is the occurrence of passive margins throughout Earth's history (*26*). It has been found that passive margins do not occur with a higher frequency (that is, with shorter passive margin lifetimes) at earlier times in Earth's history, as would be expected from the secular decline in mantle temperature. Instead, there is a near absence of passive margins in the Mesoproterozoic between 1.75 and 1.0 Ga as compared to periods before and after. The one exception corresponds to the longest-lived passive margin, with a lifetime of 600 My, suggesting a decrease in plate tectonic activity during this period. This timing is broadly consistent with the mantle depletion curves shown in Fig. 2 and provides additional support for a reduction in subduction flux during this time.

A dramatic reduction in subduction flux would have important implications for the thermal history of Earth. For example, an order of magnitude decrease would, from a thermal point of view, constitute a switch to stagnant-lid or sluggish-lid convection, with little or no subduction or sea-floor spreading (*27*). There is increasing evidence that Earth has lost heat much more slowly than is predicted from a backward extrapolation of present-day plate tectonic rates. Indeed, such an extrapolation assuming a present-day Urey ratio, γ_0, of 0.3 leads to unacceptably high mantle temperatures for ages >1 Ga (*28*, *29*) [so-called thermal catastrophe (Fig. 3)]. A value of $\gamma_0 = 0.7$ avoids this problem, although this appears to be an unacceptably high value, given present estimates of the concentration of heat-producing elements (*28*). Although there have been other hypothesized solutions to this problem, such as more sluggish plate tectonics in the past due to thicker chemical boundary layers formed at higher mantle temperature (*29*), a minimum in slab flux would dramatically lower the rate of heat loss and provide a simple means of resolving this paradox (Fig. 3). As an illustration, we have performed a thermal history calculation by parameterizing the heat flux Q as a function of internal temperature (*29*), multiplied by an index of plate tectonic "efficiency" (a value between 0 and 1), based on the gross characteristics of the mantle depletion-rate curves in Fig. 2 (*17*). The curve is scaled so that the two peaks (at the present and at 2.5 Ga) correspond to 100% efficiency, with the greater peak height at 2.5 Ga reflecting higher mantle temperatures at that time. In addition, the minimum in crustal growth rate at 1.0 Ga is constrained to be at 10% efficiency [corresponding to a 90% reduction in subduction flux or ~5000 km of subduction length remaining (fig. S1)]. Using $\gamma_0 = 0.3$, we find that the variable slab-flux model yields a thermal history that does not result in thermal catastrophe back to 4 Ga (Fig. 3).

These global calculations also imply that on shorter time scales, an order of magnitude reduction in slab flux should correspond to a period of increased mantle temperature whose magnitude depends on the assumed radioactive heat production. For $\gamma_0 = 0.3$ (0.7), the heating rate would be about 5°C (12°C)/100 My in the recent past and 18°C (42°C)/100 My in the early Archean, when heat production was thought to be several times greater (*29*). Thus, periods of attenuated plate tectonic activity may also be reflected in increased non–subduction-related magmatic activity. For example, the major emplacement period of "anorogenic" granites at 1.6 to 1.3 Ga corresponds in time to the suggested period of reduced plate tectonic activity in the Mesoproterozoic. These granites are difficult to explain by plate tectonic (orogenic) mechanisms (*30*, *31*), and proposals for their emplacement have appealed to supercontinent formation and subsequent insulation of the underlying mantle (*32*, *33*). Decreased subduction flux constitutes another viable mechanism, and the worldwide occurrence of these granites suggests a global increase in upper mantle temperature.

It has been implicitly assumed that the oceanic and continental components of plate tectonics, namely sea-floor spreading/subduction and the Wilson cycle, interact only weakly. As we have shown, however, supercontinent assembly, through its impact on subduction zones, has the potential to produce a very strong interaction, possibly to the point of temporarily stopping plate tectonics altogether. If this is correct, then the Wilson cycle takes on new meaning, representing a cycle in the operation of plate tectonics itself.

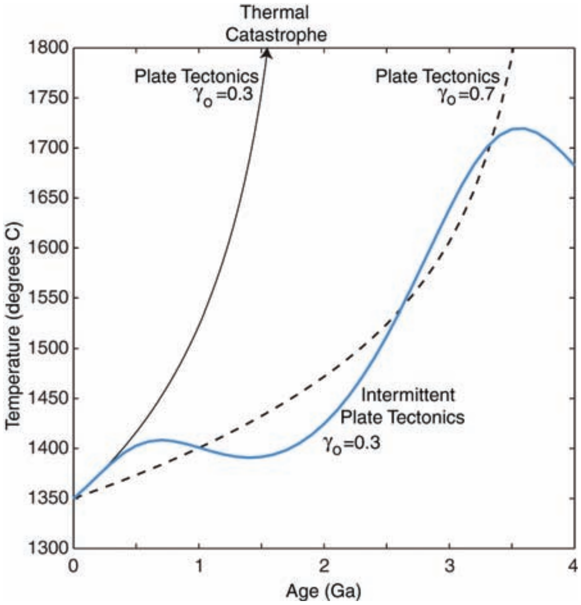

Fig. 3. Estimated thermal history of Earth under variable subduction flux (blue curve). We assume that heat flux Q is the product of a function of internal temperature [used by (*29*)] and a measure of plate tectonic efficiency (between 0 and 1) based on the basic features of the mantle depletion-rate curves (Fig. 2). An initial Urey number, γ_0, of 0.3 is assumed. Also shown are full plate tectonic efficiency with $\gamma_0 = 0.3$ (solid black curve), which leads to a thermal catastrophe (unreasonably high mantle temperatures) before about 1.0 Ga, and $\gamma_0 = 0.70$ (dashed curve), which avoids the catastrophe before 3.0 Ga but is thought to be an unrealistically high value (*29*). A variable slab-flux model predicts reasonable mantle temperatures back to 4.0 Ga (no thermal catastrophe) for plate tectonics working on average at about 50% efficiency and with realistic γ_0.

References and Notes

1. J. T. Wilson, *Nature* **211**, 676 (1966).
2. C. DeMets, R. G. Gordon, D. F. Argus, S. Stein, *Geophys. J. Int.* **101**, 425 (1990).
3. We are assuming that plate tectonics began to operate early in Earth's history. This sidesteps the important problem of plate tectonic initiation. Some have argued that plate tectonics began as late as the Neoproterozoic (*34*–*37*).
4. J. B. Murphy, R. D. Nance, *Int. Geol. Rev.* **47**, 591 (2005).
5. P. F. Hoffman, *Science* **252**, 1409 (1991).
6. I. W. D. Dalziel, S. Mosher, L. M. Gahagan, *J. Geol.* **108**, 499 (2000).
7. K. E. Karlstrom *et al.*, *Precambrian Res.* **111**, 5 (2001).
8. M. Gurnis, C. Hall, L. Lavier, *Geochem. Geophys. Geosys.* **5**, Q07001 (2004).
9. R. J. Stern, *Earth Planet. Sci. Lett.* **226**, 275 (2004).
10. J. F. Casey, J. F. Dewey, *Geol. Soc. Spec. Publ*. **13**, 269 (1984).
11. C. Stein, S. Stein, *Nature* **359**, 123 (1992).
12. M. Gerbault, *Earth Planet. Sci. Lett.* **178**, 165 (2000).
13. A. M. Cagnioncle, E. M. Parmentier, L. T. Elkins-Tanton, *J. Geophys. Res.* **112**, B09402 (2007).
14. P. Clift, P. Vannucchi, *Rev. Geophys*. **42**, RG2001 (2004).
15. K. D. Collerson, B. S. Kamber, *Science* **283**, 1519 (1999).
16. S. W. Parman, *Nature* **446**, 900 (2007).
17. Materials and methods are available as supporting material on *Science* Online.
18. G. F. Davies, *Dynamic Earth: Plates Plumes and Mantle Convection* (Cambridge Univ. Press, Cambridge, 1999).
19. J. D. Kramers, I. N. Tolstikhin, *Chem. Geol.* **139**, 75 (1997).
20. K. C. Condie, *Earth Planet. Sci. Lett.* **163**, 97 (1998).
21. K. C. Condie, *Tectonophysics* **322**, 153 (2000).
22. S. Rino *et al.*, *Physics Earth Planet. Int.* **146**, 369 (2004).
23. A. I. S. Kemp, C. J. Hawkesworth, B. A. Paterson, P. D. Kinny, *Nature* **439**, 580 (2006).
24. C. J. Hawkesworth, A. I. S. Kemp, *Nature* **443**, 811 (2006).
25. C. O'Neill, A. Lenardic, L. N. Moresi, T. H. Torsvik, C.-T. A. Lee, *Earth Planet. Sci. Lett.* **262**, 552 (2007).
26. D. C. Bradley, *Eos* **88**, U44A-03 (2007).
27. N. H. Sleep, *J. Geophys. Res.* **105**, 17563 (2000).
28. J. Korenaga, *Geophys. Res. Lett.* **30**, 1437 (2003).
29. J. Korenaga, *Archean Geodynamics and the Thermal Evolution of Earth,* K. Benn, J. C. Mareschal, K. Condie,

Eds., vol. 164 of *Geophysical Monograph Series: Archean Geodynamics and Environments* (American Geophysical Union, Washington, DC, 2006), pp. 7–32.
30. J. L. Anderson, J. Morrison, *Lithos* **80**, 45 (2005).
31. There is also evidence for anorogenic magmatism associated with Pannotia, the other supercontinent formed by P-type closure (*38*).
32. P. F. Hoffman, *Geology* **17**, 135 (1989).
33. J. L. Anderson, E. E. Bender, *Lithos* **23**, 19 (1989).
34. A. E. J. Engel, S. P. Itson, C. G. Engel, D. M. Stickney, E. J. Cray Jr., *Geol. Soc. Am. Bull.* **85**, 843 (1974).
35. W. B. Hamilton, *Precambrian Res.* **91**, 143 (1998).
36. R. J. Stern, *Geology* **33**, 557 (2005).
37. R. J. Stern, *Chin. Sci. Bull.* **52**, 578 (2007).
38. M. Doblas, J. Lopez-Ruiz, J.-M. Cebria, N. Youbi, E. Degroote, *Geology* **30**, 839 (2002).
39. Z. X. Li *et al.*, *Precambrian Res.* **160**, 179 (2008).

40. We thank S. Shirey, P. Hoffman, D. Rumble, G. Davies, D. Anderson, A. Shaw, W. Bleeker, D. Bradley, B. Kamber, K. Cooper, D. Weereratne, M. Fogel, S. Parman, R. Stern, A. Levander, and three anonymous reviewers. This work is supported by the Department of Terrestrial Magnetism, Carnegie Institution of Washington, and the Woods Hole Oceanographic Institution.

Supporting Online Material
www.sciencemag.org/cgi/content/full/319/5859/85/DC1
SOM Text
Figs. S1 and S2
References

26 July 2007; accepted 27 November 2007
10.1126/science.1148397

A Mosaic of Chemical Coevolution in a Large Blue Butterfly

David R. Nash,[1]* Thomas D. Als,[2]† Roland Maile,[3]‡ Graeme R. Jones,[3] Jacobus J. Boomsma[1]

Mechanisms of recognition are essential to the evolution of mutualistic and parasitic interactions between species. One such example is the larval mimicry that *Maculinea* butterfly caterpillars use to parasitize *Myrmica* ant colonies. We found that the greater the match between the surface chemistry of *Maculinea alcon* and two of its host *Myrmica* species, the more easily ant colonies were exploited. The geographic patterns of surface chemistry indicate an ongoing coevolutionary arms race between the butterflies and *Myrmica rubra*, which has significant genetic differentiation between populations, but not between the butterflies and a second, sympatric host, *Myrmica ruginodis*, which has panmictic populations. Alternative hosts may therefore provide an evolutionary refuge for a parasite during periods of counteradaptation by their preferred hosts.

Social and brood parasites often use mimicry to exploit their hosts (*1*, *2*). These parasites typically affect a small proportion of host populations, so that selection for costly defensive discrimination between kin and parasites by the host (*2*, *3*) may be weak (*4*). This allows social parasites of ants, bees, and wasps to parasitize multiple host species (*5*–*7*). However, when parasites are common enough, selection on hosts to avoid being parasitized fuels coevolutionary arms races, in which parasites evolve better mimicry and hosts improve their recognition of parasites (*8*, *9*).

The dynamics of parasite density and distribution can be explained by geographic mosaic models of coevolution (*10*), which allow different degrees of interaction and adaptation between local populations. In these models, mutual coadaptation is restricted to sites of intense and lasting interactions (hotspots), whereas parasites and hosts may evolve independently in other populations (coldspots). Theoretical studies have explored geographic mosaic models (*11*, *12*), but there have been few empirical tests of ecological systems in which the mechanisms of coevolution and the patterns of interaction were known (*10*).

The Alcon blue butterfly, *Maculinea alcon*, is socially parasitic on two species of *Myrmica* ants in Denmark (*13*). The butterfly's caterpillars initially develop on marsh gentian plants, *Gentiana pneumonanthe* (Fig. 1A), before being "adopted" by a foraging *Myrmica* worker (Fig. 1B). Once inside the host ant nest, caterpillars are fed by the ants in preference to their own larvae (*14*), reducing host fitness, particularly in small colonies (*15*) (Fig. 1C and fig. S2). The overlap in distribution of the widespread host ants and the rare host plant is small, both locally and regionally, and there is geographic variation in the abundance and use of the two host ant species (*13*). Populations of the Alcon blue are therefore patchy, and only a small fraction of host ant populations are parasitized and potentially subject to selection for resistance. The parasite is absent from most host populations, which are therefore coevolutionary coldspots (*10*, *11*). In much of Europe, a third ant species, *Myrmica scabrinodis*, is also a host of the Alcon blue (*16*), but infection of this species has never been observed in Denmark, despite its abundance on Danish *M. alcon* sites (*13*).

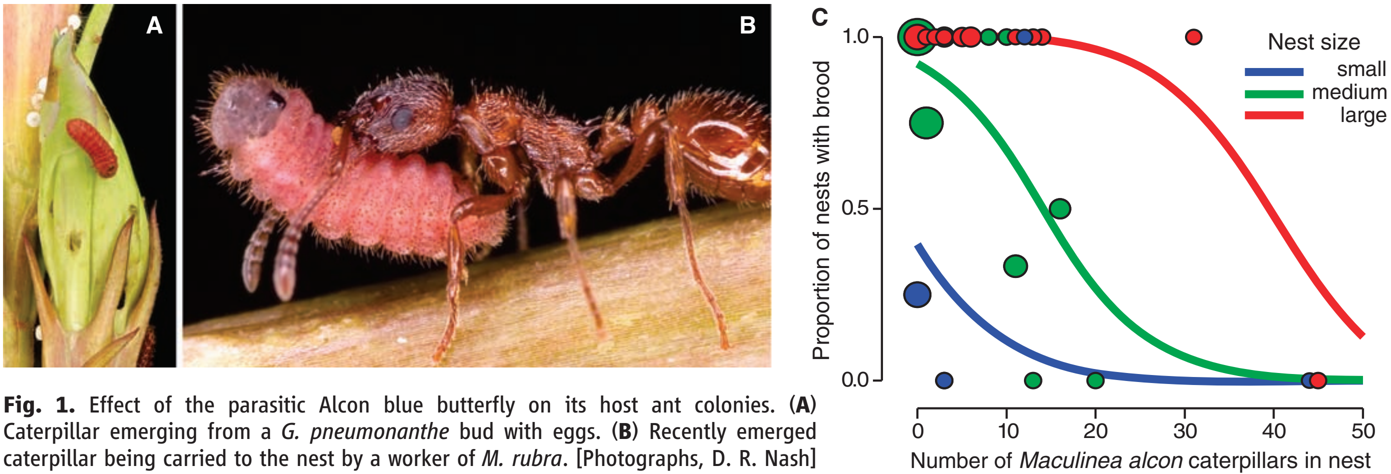

Fig. 1. Effect of the parasitic Alcon blue butterfly on its host ant colonies. (**A**) Caterpillar emerging from a *G. pneumonanthe* bud with eggs. (**B**) Recently emerged caterpillar being carried to the nest by a worker of *M. rubra*. [Photographs, D. R. Nash] (**C**) Relationship between the number of caterpillars present in small, medium, and large *M. rubra* nests (SOM text) in late spring and the probability of ant brood being present. The area of each symbol is proportional to the number of nests observed with that number of caterpillars. Lines are fitted logistic regressions.

---

[1] Institute of Biology, University of Copenhagen, Universitetsparken 15, DK-2100 Copenhagen, Denmark. [2] Department of Genetics and Ecology, University of Aarhus, DK-8000 Århus C, Denmark. [3] School of Chemistry, Keele University, Keele, Staffordshire ST5 5BG, UK.

*To whom correspondence should be addressed. E-mail: DRNash@bi.ku.dk

†Present address: Population Genetics Laboratory, Danish Institute for Fisheries Research, Vejlsoevej 39, DK-8600 Silkeborg, Denmark.

‡Present address: Trivadis GmbH, D-70565 Stuttgart, Germany.

In previous cross-infectivity experiments (*17*), Alcon blue caterpillars were adopted more rapidly by host ants from the populations that they infect than by the alternative host species present in the same area (sympatric). However, local parasite maladaptation (host resistance) was also found, because the most rapid adoption of caterpillars was by *Myrmica rubra* colonies from distant (allopatric) populations (*17*). Adoption time is a good measure of infectivity of the parasite that combines the speed of retrieval of caterpillars and initial integration into the ant colony (*18*).

Maculinea caterpillars are thought to infect *Myrmica* nests by mimicking the surface chemistry of the ant brood (*19*, *20*). We collected samples of pre-adoption parasite caterpillars and host ant larvae from the same three populations that were previously used for the cross-infection experiments and examined their cuticular chemistry (*15*, *17*). Qualitatively, the caterpillars of *M. alcon* and the larvae of *M. rubra* and *Myrmica ruginodis* shared the same set of surface compounds, whereas the nonhost ant *M. scabrinodis* did not (Fig. 2A, fig. S1, and table S1). Quantitatively, however, the relative abundances of the shared compounds varied between populations of *M. alcon* (Fig. 2B) and its two ant hosts (figs. S1 and S3). Chemical similarity was a significant predictor of infectivity, explaining 62% of the variation in adoption time for *M. rubra* and 78% for *M. ruginodis* (Fig. 2, C and D).

Local selection on hosts should favor heritable [Supporting Online Material (SOM) text] changes in ant larval surface chemistry if this allows discrimination between ants and *Maculinea* caterpillars (*21*). Because the patchy *Maculinea* populations are expected to counter host resistance, coevolutionary hotspots are created. Therefore, we hypothesized that the ants and caterpillars are in a coevolutionary arms race in degree of hydrocarbon profile matching and that there are different trajectories in change in surface chemistry between hotspots. However, if substantial gene flow occurs between infected host subpopulations and nearby uninfected subpopulations, any parasite-induced selection on the ants to change recognition compounds is likely to be ineffective, resulting in a coevolutionary coldspot. Previous work suggested that *M. rubra* has levels of gene flow much lower than those of *M. ruginodis* (*22*).

We compared the surface chemistry of ant larvae from uninfected nests of *M. rubra* and *M. ruginodis* from the three sites with *M. alcon* and from three sites where the butterfly has never been recorded (*15*) (Fig. 3A). The chemical profiles of *M. rubra* (Fig. 3B) differed significantly between the six populations (Wilk's $\lambda_{10,40} = 0.159$, $P < 0.0001$) because of divergent chemical profiles among the infected populations ($\lambda_{4,18} = 0.204$, $P = 0.0047$) rather than differences between uninfected populations ($\lambda_{4,20} = 0.899$, $P = 0.891$). In contrast, *M. ruginodis* (Fig. 3C) did not have significantly different surface chemical profiles between populations ($\lambda_{10,48} = 0.612$, $P = 0.414$), and differences between infected populations ($\lambda_{4,22} = 0.960$, $P = 0.976$) were no greater than those between uninfected populations ($\lambda_{4,24} = 0.852$, $P = 0.735$).

We estimated Wright's F_{ST} (*23*), a measure of genetic differentiation between populations, by using three variable microsatellite loci (*15*) to examine whether differences in chemical profiles between and among parasitized *M. rubra* and *M. ruginodis* reflected genetic structure (*22*). Populations of *M. rubra* were strongly genetically differentiated, with an overall F_{ST} of 0.136 [$P < 0.0001$; all loci produced highly significant F_{ST} values (table S3)], whereas populations of *M. ruginodis* were not ($F_{ST} = 0.004$, $P = 0.473$). Our F_{ST} estimate for *M. rubra* over distances >100 km was similar to that found in Finland (*22*) over a few hundred meters, confirming that this species has highly viscous populations with little local gene flow. We also measured Wright's F_{IS}, a measure of inbreeding, and found it was similar for the two ant species, with *M. ruginodis* [$F_{IS} = 0.187$ (table S4)] being somewhat more inbred than *M. rubra* ($F_{IS} = 0.136$). Thus, inbreeding is not associated with the higher hydrocarbon profile differentiation and variability in *M. rubra*. The corresponding values for *M. alcon* were $F_{ST} = 0.182$ and $F_{IS} = 0.132$, estimates very similar to those for *M. rubra*. These data indicate that all three species have patchy populations but that migration is higher in *M. ruginodis* than in either *M. rubra* or *M. alcon*.

We found a relatively constant infection rate for *M. ruginodis* nests (range of 8 to 40%) across all sampled populations (*13*), whereas infection rates of *M. rubra* nests varied from 0 to 72%. For *M. rubra*, the infection rate increased with the prevalence of *M. rubra* (logistic regression, $r^2 = 40.86$, d.f. = 5, $P < 0.0001$), whereas no such relationship existed for *M. ruginodis* ($r^2 = 4.59$, d.f. = 7, $P = 0.71$). This is consistent with the Alcon blue becoming locally adapted to *M. rubra* but not to *M. ruginodis* as host populations become denser.

The changes in host surface chemistry in parasitized *M. rubra* populations indicate that the *M. alcon*–*M. rubra* combination forms a geographic mosaic of coevolutionary hotspots, with a continuing arms race in chemical mimicry, whereas the sympatric *M. alcon*–*M. ruginodis* interaction does not. An alternative interpretation, that the changes in hydrocarbon profiles of *M. rubra* reflect environmental differences between infected and uninfected sites, seems unlikely given the arbitrary direction of profile divergences and the lack of divergence in uninfected populations. If anything, we expect uninfected populations to be more environmentally variable than infected populations because they occur in a range of habitats, whereas infected populations

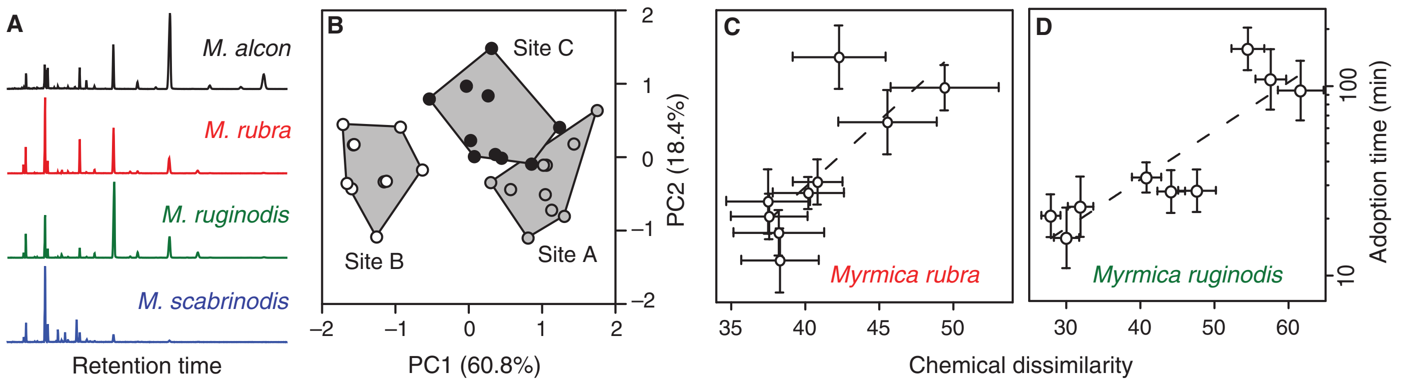

Fig. 2. Chemical mimicry of *Myrmica* ants by Alcon blue caterpillars. (**A**) Representative gas chromatograms for surface extracts of caterpillars of *M. alcon*, larvae of the host ants *M. rubra* and *M. ruginodis*, and larvae of the sympatric nonhost *M. scabrinodis*. (**B**) Ordination plots showing the first two principal components of the chemical profiles of *M. alcon* caterpillars from the three sample sites. Markers show the chemical profiles for individual caterpillars. The data for each study population are enclosed by a minimum convex polygon. (**C** and **D**) Relationship between adoption time (log scale) and dissimilarity in chemical profiles (Mahalanobis distance) between *M. alcon* caterpillars and larvae of *M. rubra* (**C**) and *M. ruginodis* (**D**). Each point is the mean ± SE of five observations for each of the nine combinations of butterflies and ants from the three infected sites (*17*). Lines are major axis regressions: for *M. rubra*, $r^2 = 0.62$, $P = 0.011$; for *M. ruginodis*, $r^2 = 0.78$, $P = 0.002$.

must overlap the niche of *G. pneumonanthe*. Lack of profile variation between uninfected populations has previously been demonstrated for *M. rubra* over much larger distances (*20*). The within-population variation in cuticular hydrocarbon profiles was consistently higher in infected populations than in uninfected populations of *M. rubra* (sum multivariate test; $F_{1,4} = 10.56$, $P = 0.034$) but not *M. ruginodis* ($F_{1,4} = 0.17$, $P = 0.455$), which further supports our interpretation.

M. alcon is a virulent parasite of *Myrmica* ants (Fig. 1C and SOM text) that will reduce the size and density of host colonies. This, coupled with the density-dependent infection rate for one of its hosts, *M. rubra* (Fig. 3D), is likely to lead to dynamic shifts in host use over time. Although *M. rubra* is not a host at site A (*13*), we observed strong divergence in its chemical profiles at this site (Fig. 3B), which may reflect former use of this host. The coevolutionary coldspots provided by *M. ruginodis* may thus allow *M. alcon* to persist during the emergence of resistant forms of *M. rubra* (SOM text), but this may also put an ultimate limit on how far *M. alcon* can diverge from the relatively static chemical profile of *M. ruginodis*. *M. rubra* and *M. ruginodis* are very similar to each other chemically (*20*), so it is unlikely that such a system could exist for parasites that use more distinct hosts.

Our findings are consistent with geographic mosaic models for coevolution (*24*) and confirm that restricted gene flow is a crucial prerequisite for local coevolution (*25*). Our results also have important implications for the conservation of the Alcon blue, which is increasingly threatened throughout much of its range (*26*). Other *Maculinea* species have been reintroduced to areas where native species have gone extinct without prior screening of similarity in genetics or cuticular chemical profiles (*27*, *28*). Our data suggest that this is reasonable for *Maculinea* species that rely on relatively panmictic species of *Myrmica* host ants because successful reintroductions can likely be made from any source population that uses the same host ant. However, for *Maculinea* species that rely on genetically differentiated host ants, the match between the cuticular chemical profiles of caterpillars and ant larvae should be carefully considered.

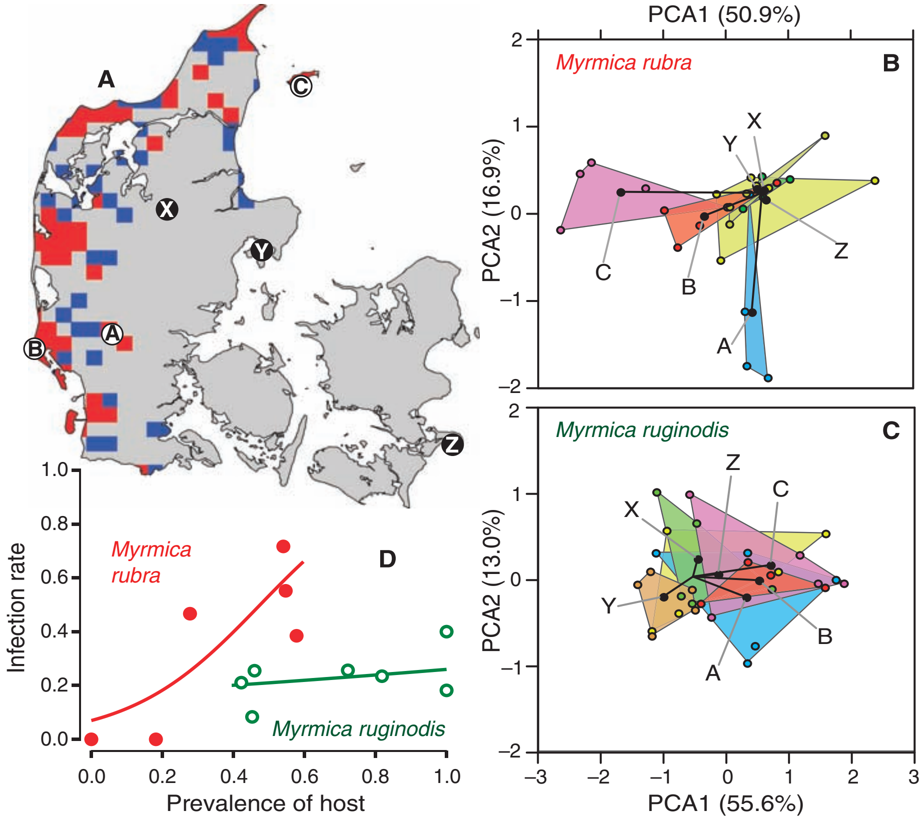

Fig. 3. Adaptation of *Myrmica* host ants to infection by Alcon blue caterpillars. (**A**) The current (after 1990, red) and historical (before 1990 but not since, blue) distribution of *M. alcon* in Denmark plotted on a 10 km–by–10 km grid. The locations of studied infected (points A, B, and C) and uninfected (points X, Y, and Z) populations are marked. (**B** and **C**) Ordination plots showing the first two principal components of the chemical profiles of *M. rubra* (B) and *M. ruginodis* (C). Colored markers show the chemical profiles for individual nests, and the data for each study population are enclosed by a minimum convex polygon. The centroid of each population (black dot) is labeled and linked by a line to the overall centroid of the three uninfected populations. (**D**) Relationship between the infection rate (proportion of nests infected) and the prevalence (proportion of the total host nests that are of that species) for the two host ant species present in each of seven populations of *M. alcon* examined in Denmark (*13*). Lines are fitted logistic regressions.

References and Notes

1. N. B. Davies, M. D. Brooke, *J. Anim. Ecol.* **58**, 225 (1989).
2. P. D'Ettorre, N. Mondy, A. Lenoir, C. Errard, *Proc. R. Soc. London Ser. B Biol. Sci.* **269**, 1911 (2002).
3. N. B. Davies, M. D. Brooke, *J. Anim. Ecol.* **58**, 207 (1989).
4. N. B. Davies, *Cuckoos, Cowbirds and Other Cheats* (Poyser, London, 2000).
5. B. Hölldobler, E. O. Wilson, *The Ants* (Belknap, Cambridge, 1990).
6. C. D. Michener, *The Bees of the World* (Johns Hopkins Univ. Press, Baltimore, 2000).
7. S. Turillazzi, M. J. West-Eberhard, *Natural History and Evolution of Paper-Wasps* (Oxford Univ. Press, Oxford, 1996).
8. S. Foitzik, B. Fischer, J. Heinze, *Behav. Ecol.* **14**, 80 (2003).
9. N. E. Langmore *et al.*, *Behav. Ecol.* **16**, 686 (2005).
10. J. N. Thompson, *The Geographic Mosaic of Coevolution* (Univ. Chicago Press, Chicago, 2005).
11. R. Gomulkiewicz, J. N. Thompson, R. D. Holt, S. L. Nuismer, M. E. Hochberg, *Am. Nat.* **156**, 156 (2000).
12. S. L. Nuismer, *Evol. Int. J. Org. Evol.* **60**, 24 (2006).
13. T. D. Als, D. R. Nash, J. J. Boomsma, *Ecol. Entomol.* **27**, 403 (2002).
14. J. A. Thomas, G. W. Elmes, J. C. Wardlaw, *Proc. R. Soc. London Ser. B Biol. Sci.* **265**, 1895 (1998).
15. Materials and methods are available as supporting material on *Science* Online.
16. G. W. Elmes *et al.*, *Memorabilia Zool.* **48**, 55 (1994).
17. T. D. Als, D. R. Nash, J. J. Boomsma, *Anim. Behav.* **62**, 99 (2001).
18. G. W. Elmes, J. C. Wardlaw, K. Schönrogge, J. A. Thomas, R. T. Clarke, *Entomol. Exp. Appl.* **110**, 53 (2004).
19. T. Akino, J. J. Knapp, J. A. Thomas, G. W. Elmes, *Proc. R. Soc. London Ser. B Biol. Sci.* **266**, 1419 (1999).
20. G. W. Elmes, T. Akino, J. Thomas, R. T. Clarke, J. J. Knapp, *Oecologia* **130**, 525 (2002).
21. N. D. Tsutsui, *Ann. Zool. Fenn.* **41**, 713 (2004).
22. P. Seppä, P. Pamilo, *Heredity* **74**, 200 (1995).
23. S. Wright, *Evolution and the Genetics of Populations - Volume 2: The Theory of Gene Frequencies* (Univ. Chicago Press, Chicago, 1969).
24. J. N. Thompson, *Am. Nat.* **153**, S1 (1999).
25. A. D. Morgan, S. Gandon, A. Buckling, *Nature* **437**, 253 (2005).
26. C. A. M. Van Swaay, M. S. Warren, *Red Data Book of European Butterflies (Rhopalocera)* (Council of Europe Publishing, Strasbourg, France, 1999).
27. J. A. Thomas, *Brit. Wildl.* **11**, 22 (1999).
28. I. Wynhoff, *J. Insect Conserv.* **2**, 47 (1998).
29. We thank P. S. Nielsen for samples; E. D. Morgan, H. Jungnickel, and J. Tentschert for chemical analysis; and J. Frydenberg, J. Ebsen, and A. Lomborg for microsatellite analysis. D.R.N. was supported by European Union (EU) Marie Curie and Carlsberg Foundation fellowships. Collaboration between Denmark and Keele was via the EU research training networks Social Evolution, which supported R.M., and Integrated Studies of the Economy of Insect Societies (INSECTS). Population genetic analysis of *M. alcon* was supported by the EU Research Training and Development network MacMan. The final stages of this study were supported by the Danish National Research Foundation (J.J.B. and D.R.N.).

Supporting Online Material

www.sciencemag.org/cgi/content/full/319/5859/88/DC1
Materials and Methods
SOM Text
Figs. S1 to S3
Tables S1 to S4
References

14 August 2007; accepted 26 November 2007
10.1126/science.1149180

Polymorphic Y Chromosomes Harbor Cryptic Variation with Manifold Functional Consequences

Bernardo Lemos,* Luciana O. Araripe, Daniel L. Hartl

The paucity of polymorphisms in single-copy genes on the Y chromosome of *Drosophila* contrasts with data indicating that this chromosome has polymorphic phenotypic effects on sex ratio, temperature sensitivity, behavior, and fitness. We show that the Y chromosome of *D. melanogaster* harbors substantial genetic diversity in the form of polymorphisms for genetic elements that differentially affect the expression of hundreds of X-linked and autosomal genes. The affected genes are more highly expressed in males, more meagerly expressed in females, and more highly divergent between species. Functionally, they affect microtubule stability, lipid and mitochondrial metabolism, and the thermal sensitivity of spermatogenesis. Our findings provide a mechanism for adaptive phenotypic variation associated with the Y chromosome.

Y chromosomes experience strong selective pressures for increased male fitness due to sexual selection, and they accumulate deleterious mutations owing to the lack of recombination (*1*, *2*). In most species of *Drosophila*, the Y chromosome has few protein-coding loci but shows a high density of transposable elements and other repetitive sequences (*3*, *4*). Only about 10 to 20 single-copy protein-coding loci are known to reside in the *D. melanogaster* Y chromosome, all of which are also exceptional in their megabase-sized introns embedded within heterochromatin of largely unknown sequence (*3*, *5*). This gene content represents less than 0.2% of the *Drosophila* genome [~13,000 coding genes (*6*)]. The small number of genes is particularly noteworthy in that the Y chromosome comprises some 40 Mb of DNA, or 23% of the haploid genome. The Y chromosome is about the same size as the X chromosome, whereas the latter contains >2500 genes. Extremely low levels of DNA sequence polymorphism are observed for single-copy Y-linked genes (*7*), and population genetics theory implies that the Y chromosome can maintain stable polymorphisms only under restrictive conditions (*1*, *2*, *8*). These observations stand in contrast to manifold phenotypic consequences of Y-linked polymorphisms, including effects on sex ratio (*9*, *10*), heat adaptation (*11*), behavior (*12*, *13*), and male fitness (*14*).

To address this apparent contradiction, we examined genome-wide variation in gene expression among lines of *D. melanogaster* differing only in the origin of the Y chromosome (*15*) (figs. S1 to S3). Extraneous sources of variation were minimized by use of a common isogenic genetic background of X chromosome, autosomes, mitochondrial DNA, and cytoplasm, as well as by careful control of environmental variables including temperature, humidity, and light. The five Y chromosomes tested include isolates from diverse geographical origins representing both temperate and tropical climates. The Y chromosomes were originally derived from flies collected in Massachusetts (Ymass) and Ohio (Ycs) in the United States as well as the Democratic Republic of Congo (Ycongo) and Zimbabwe (Yz53) in Africa. The effects of these chromosomes were compared among themselves as well as with those of the Y chromosome (Y4361) in a genetically marked laboratory strain into which the diverse Y chromosomes had been introduced.

A substantial number of genes were differentially expressed between the original Y4361 genotype and the Y-chromosome substitution lines [123 to 1010 genes; Bayesian posterior probability > 0.999 to 0.995; false discovery rate (FDR) < 1 to 15%; Fig. 1A]. This result contrasts with control comparisons between females of the Y-chromosome substitution lines, which showed no differential expression (*15*). Approximately 14%, 37%, 47%, and <1% of the Y-linked regulatory variation can be assigned to genes in the X, second, third, and fourth chromosomes, respectively. Moreover, four Y-linked genes [*Su(Ste)*, *Kl-5*, *Ccy*, and *Occludin-related Y*] themselves showed evidence for differential expression across the Y-chromosome substitution lines (Fig. 1, B to E), a significant enrichment over random expectations ($P < 0.05$; Fisher's exact test). These results indicate that polymorphic variation in the Y chromosome has manifold consequences in the regulation of genes located on the X chromosome and autosomes. Furthermore, the genes affected by Y-linked regulatory elements showed significant patterns in regard to their sex bias in expression, levels of polymorphism and divergence, and association with temperature.

Polymorphic regulatory variation due to the Y chromosome might be expected to affect traits expressed in males. In agreement with this prediction, we found that Y-linked variation is enriched for genes that are more highly expressed in males ($P < 0.0001$, Kruskal-Wallis, and other similar tests below; Fig. 2A). Conversely, genes affected by Y-linked regulatory variation are expressed at significantly lower abundances in females ($P < 0.0001$; Fig. 2B). Such a pattern might be expected of sexually antagonistic variation that is beneficial in one sex while detrimental in the other (*16*), and the pattern suggests a role for Y-linked polymorphisms in mediating the expression of these genes. Moreover, Y-linked regulatory polymorphisms may help to explain some of the diversity in gene expression patterns observed within and between species of *Drosophila* (*17*, *18*). We found that genes whose expression is affected by the Y chromosome show significantly greater divergence in gene expression between *D. melanogaster* and *D. simulans* ($P < 0.0001$; Fig. 2C), as well as higher levels of gene expression polymorphism relative to other genes ($P < 0.0001$; Fig. 2D). These patterns indicate that Y-linked regulation of gene expression may result in dynamic evolutionary histories within and between species of fruit flies.

Evidence for adaptive polymorphism in the Y chromosome comes from its contribution to variation in the sensitivity of *Drosophila* spermatogenesis with respect to temperature (*11*, *19*). Thermal heat sterility thresholds differ across species, from 23°C in heat-sensitive species up to 31°C in heat-tolerant species. In *D. melanogaster*, genetic variation in thermal tolerance is observed among geographical populations. Flies from tropical populations are more tolerant to heat-induced sterility and recover fertility more rapidly than those from temperate populations. Genetic analysis reveals that the Y chromosome alone accounts for about 50% of the difference in heat sensitivity observed between natural populations of *D. melanogaster* (*11*, *19*). We hypothesize that variation in thermal sensitivity may be, at least in part, due to regulatory variation exerted by the Y chromosome. Indeed, we found that genes affected by Y-linked regulatory variation are more responsive to heat shock than are other genes ($P < 0.0001$; Fig. 3A). To investigate this connection in greater detail, we reared flies containing a Y chromosome from a temperate climate (Ymass) with those containing a Y chromosome from a tropical climate (Ycongo) at two temperatures (16°C and 25°C) and assayed their levels of gene expression at both temperatures (fig. S4). We found 14 genes to be up-regulated and 16 genes down-regulated in Ymass relative to Ycongo at both temperatures, whereas fewer than one such gene is expected by chance alone. The genes identified to be up-regulated

---

Department of Organismic and Evolutionary Biology, Harvard University, 16 Divinity Avenue, Cambridge, MA 02138, USA.

*To whom correspondence should be addressed. E-mail: blemos@oeb.harvard.edu

in Ymass include *SOX100B*, a gene known to be associated with male gonadal development (*20*), and *OS-C*, a gene presumably involved in olfactory coding (*21*). The genes identified to be down-regulated in Ymass include *CG7311* and *CG9389*, both of whose products are targeted to the mitochondria and are implicated in the metabolism of lipids. These findings point to consistent differences in gene expression among the isogenic lines that correlate with the Y chromosome independent of temperature.

We also investigated whether Y chromosomes may harbor variation that is apparent at only one temperature. This hypothesis predicts that the Ycongo line (with the tropical Y chromosome) would show, at 16°C, a more disrupted pattern of gene expression than the Ymass line (with the temperate Y chromosome). The opposite pattern would be expected at 25°C. We found that the Ycongo line showed about twice as many genes up-regulated at 16°C relative to Ymass, whereas the Ymass line showed about twice as many genes up-regulated at 25°C relative to Ycongo ($P < 10^{-7}$, Fisher's exact test; Fig. 3B). These findings point to temperature-dependent differences between Y-chromosome substitution lines, including cases in which the sign of the difference between strains was reversed at the two temperatures (Fig. 3, C and D). Taken together, these results suggest that genes responding to Y-linked variation are functionally coherent in showing association with male functions including spermatogenesis and temperature adaptation. These processes have also been linked to lipid metabolism in *Drosophila*, and indeed we found Y-linked variation for genes associated with lipid and fatty acid metabolism as well as with the mitochondria and the cytoskeleton (tables S1 and S2). Our findings indicate that Y-linked regulatory variation is expressed through dynamic interactions with temperature, and they provide a mechanism for understanding the effects of the Y chromosome on the heat sensitivity of spermatogenesis as well as other evolutionary and ecologically relevant phenotypes.

Y chromosomes are known to harbor structural polymorphism in heterochromatic sequences and copy-number polymorphisms in repetitive sequences both in humans and flies (*22–24*), and they can influence transcription epigenetically, as revealed by their ability to modify position-effect variegation in flies (*25–27*). We therefore suggest that structural polymorphisms in the Y chromosome may result in a variety of epigenetic effects, including the differential regulation of autosomal or X-linked transposable elements through such mechanisms as the homology-dependent RNA interference pathways (*28*). In agreement with this prediction, we found that Y-linked polymorphisms result in differential expression of 13 out of 53 families of transposable elements

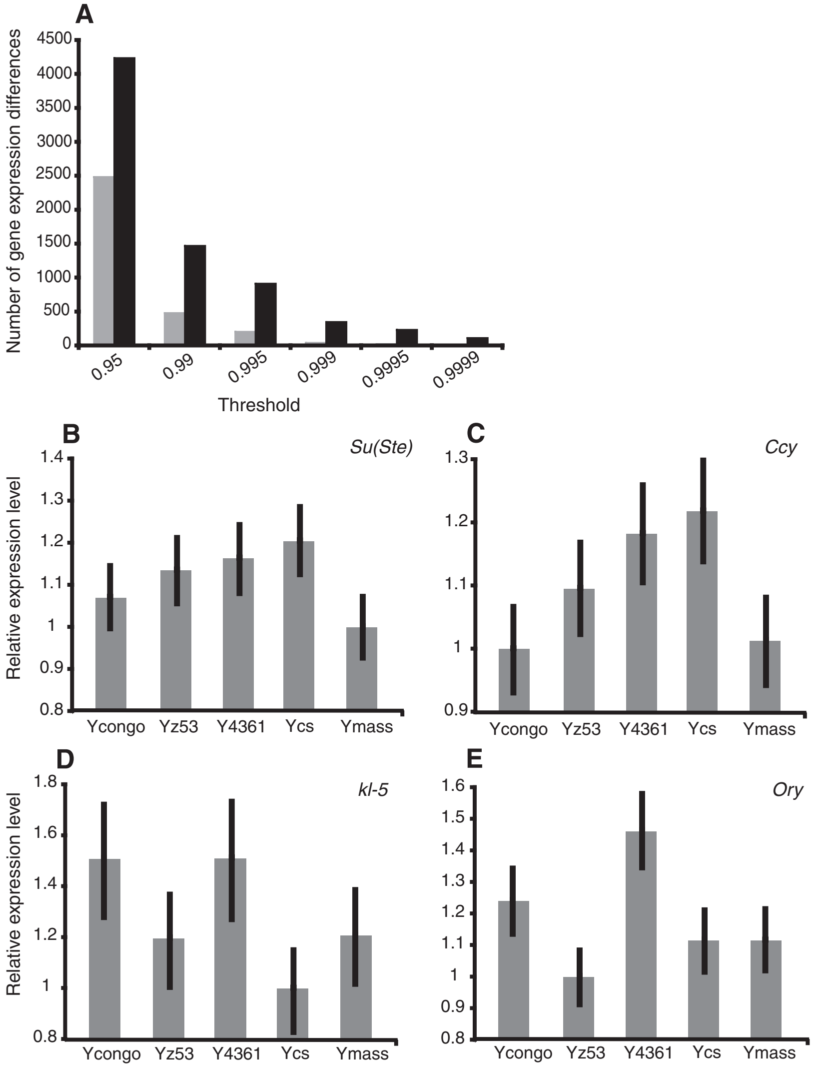

Fig. 1. (**A**) Number of genes differentially expressed among Y-chromosome substitution lines (black bars) as a function of the Bayesian posterior probability of differential expression. Gray bars indicate the estimated number of genes expected by chance. (**B** to **E**) Four Y-linked genes [*Su(Ste)*, *Kl-5*, *Ccy*, and *Occludin-related Y* (*Ory*)] with significant expression variation among Y-chromosome substitution lines. Estimated relative differences in expression are shown. Black bars denote 95% credible interval for estimated relative difference.

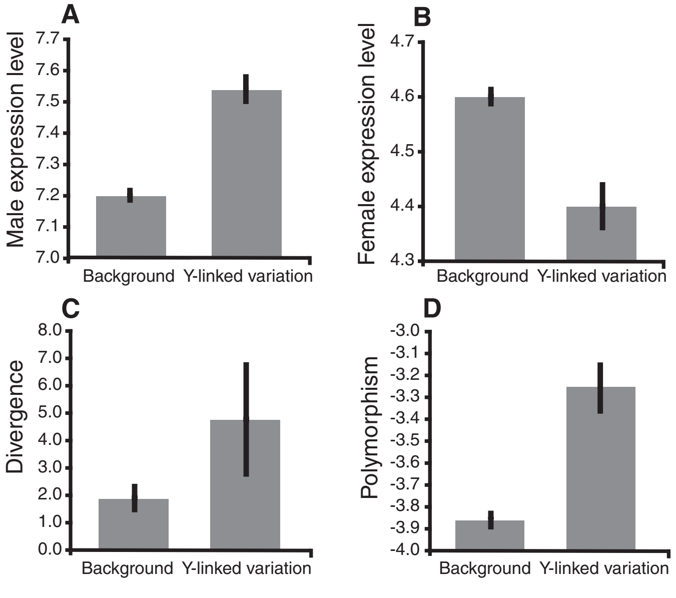

Fig. 2. Genes showing Y-linked regulatory variation are expressed at higher abundances in males (**A**) and lower abundances in females (**B**); they show higher levels of divergence between *D. melanogaster* and *D. simulans* (**C**) and higher levels of polymorphism within *D. melanogaster* (**D**). Error bars denote two SEs around the mean. Background refers to the subset of genes not differentially expressed across Y-chromosome substitution lines.

represented in our data, a highly significant enrichment over random expectations ($P = 0.0003$; Fig. 4, A to D).

Our data reveal substantial levels of Y-chromosome polymorphism with consequences for gene regulation. This diversity is manifested functionally as significant differences in the expression of autosomal and X-linked genes from one Y chromosome to the next. Polymorphic Y-linked regulatory variation appears to be manifold, evolutionarily dynamic, preferential for male-biased genes, and influenced by temperature. One model for the mechanism of these effects is that polymorphisms in the content or lengths of heterochromatic blocks harboring transposable elements and other repetitive sequences might alter the availability of limiting transcription factors or chromatin regulators throughout the genome (*29*). Our results also raise the question of how widespread Y-linked regulatory variation may be in other organisms with similarly heterochromatin-rich Y chromosomes, including humans and other mammals.

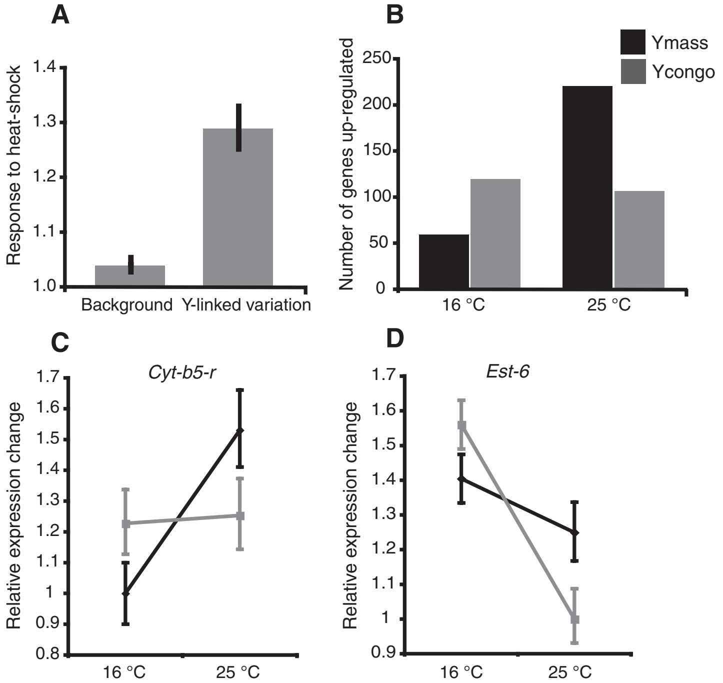

Fig. 3. (**A**) Genes showing Y-linked regulatory variation are more sensitive to heat shock. Gray bars denote two SEs around the mean. (**B**) Number of genes up-regulated in Ymass and Ycongo at 16°C and 25°C. (**C** and **D**) Two genes for which the sign of the difference between Ymass and Ycongo is reversed at the two temperatures assayed.

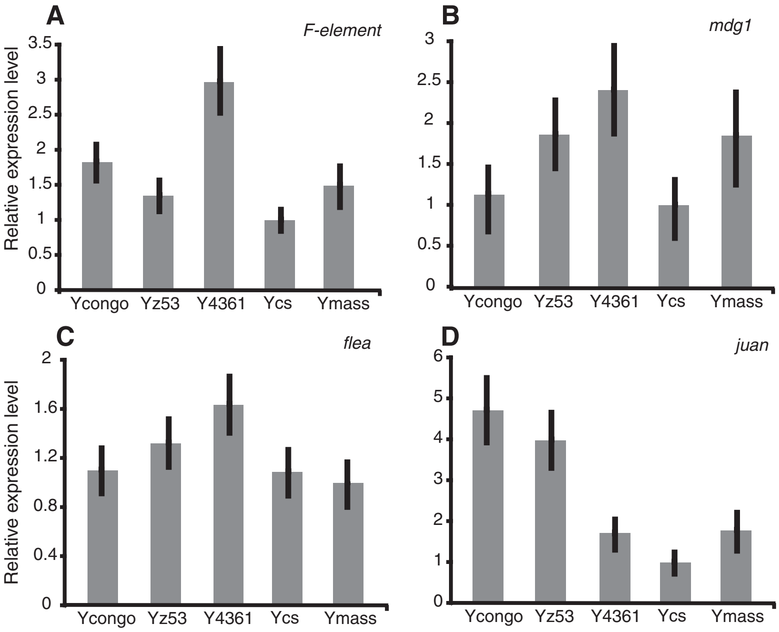

Fig. 4. Four transposable elements [(**A**) *F-element*; (**B**) *mdg1*; (**C**) *flea*; (**D**) *juan*] with significant expression variation across Y-chromosome substitution lines. Estimated relative differences in expression are shown. Black bars denote 95% credible interval for estimated relative difference.

References and Notes

1. D. Charlesworth, B. Charlesworth, *Curr. Biol.* **15**, R129 (2005).
2. D. L. Hartl, A. G. Clark, *Principles of Population Genetics* (Sinauer Associates, Sunderland, MA, ed. 4, 2007).
3. A. B. Carvalho, A. G. Clark, *Science* **307**, 108 (2005); published online 4 November 2004 (10.1126/science.1101675).
4. C. D. Smith, S. Shu, C. J. Mungall, G. H. Karpen, *Science* **316**, 1586 (2007).
5. A. B. Carvalho, *Curr. Opin. Genet. Dev.* **12**, 664 (2002).
6. M. D. Adams *et al.*, *Science* **287**, 2185 (2000).
7. M. Zurovcova, W. F. Eanes, *Genetics* **153**, 1709 (1999).
8. A. G. Clark, *Genetics* **125**, 527 (1990).
9. A. B. Carvalho, S. C. Vaz, L. B. Klaczko, *Genetics* **146**, 891 (1997).
10. C. Montchamp-Moreau, V. Ginhoux, A. Atlan, *Evol. Int. J. Org. Evol.* **55**, 728 (2001).
11. C. Rohmer, J. R. David, B. Moreteau, D. Joly, *J. Exp. Biol.* **207**, 2735 (2004).
12. S. Huttunen, J. Aspi, *Behav. Genet.* **33**, 17 (2003).
13. S. F. Stoltenberg, J. Hirsch, *Anim. Behav.* **53**, 853 (1997).
14. A. K. Chippindale, W. R. Rice, *Proc. Natl. Acad. Sci. U.S.A.* **98**, 5677 (2001).
15. See supporting material on *Science* Online.
16. W. R. Rice, *Proc. Natl. Acad. Sci. U.S.A.* **95**, 6217 (1998).
17. C. D. Meiklejohn, J. Parsch, J. M. Ranz, D. L. Hartl, *Proc. Natl. Acad. Sci. U.S.A.* **100**, 9894 (2003).
18. J. M. Ranz, C. I. Castillo-Davis, C. D. Meiklejohn, D. L. Hartl, *Science* **300**, 1742 (2003).
19. J. R. David *et al.*, *J. Evol. Biol.* **18**, 838 (2005).
20. T. J. DeFalco *et al.*, *Dev. Cell* **5**, 205 (2003).
21. M. P. McKenna, D. S. Hekmat-Scafe, P. Gaines, J. R. Carlson, *J. Biol. Chem.* **269**, 16340 (1994).
22. E. M. S. Lyckegaard, A. G. Clark, *Proc. Natl. Acad. Sci. U.S.A.* **86**, 1944 (1989).
23. E. M. S. Lyckegaard, A. G. Clark, *Mol. Biol. Evol.* **8**, 458 (1991).
24. S. Repping *et al.*, *Nat. Genet.* **35**, 247 (2003).
25. M. Gatti, S. Pimpinelli, *Annu. Rev. Genet.* **26**, 239 (1992).
26. S. Henikoff, P. B. Talbert, *Nat. Rev. Genet.* **7**, 793 (2006).
27. S. R. Schulze, L. L. Wallrath, *Annu. Rev. Entomol.* **52**, 171 (2007).
28. R. K. Slotkin, R. Martienssen, *Nat. Rev. Genet.* **8**, 272 (2007).
29. X. Liu, B. Wu, J. Szary, E. M. Kofoed, F. Schaufele, *J. Biol. Chem.* **282**, 20868 (2007).
30. We thank E. Dopman, P. Fontanillas, Y. Go, S. Kingan, R. Kulathinal, C. Meiklejohn, H. Montenegro, S. Renn, and S. Rifkin for their help during assembly, printing, and annotation of the microarrays as well as helpful discussions. Supported by NIH grants GM068465 and GM065169 (D.L.H.). Raw microarray data have been deposited in the Gene Expression Omnibus database (accession number GSE9457).

Supporting Online Material

www.sciencemag.org/cgi/content/full/319/5859/91/DC1
Materials and Methods
Figs. S1 to S4
Tables S1 and S2
References

7 August 2007; accepted 20 November 2007
10.1126/science.1148861

Heterochromatin and RNAi Are Required to Establish CENP-A Chromatin at Centromeres

Hernan Diego Folco,[1] Alison L. Pidoux,[1] Takeshi Urano,[2] Robin C. Allshire[1]*

Heterochromatin is defined by distinct posttranslational modifications on histones, such as methylation of histone H3 at lysine 9 (H3K9), which allows heterochromatin protein 1 (HP1)–related chromodomain proteins to bind. Heterochromatin is frequently found near CENP-A chromatin, which is the key determinant of kinetochore assembly. We have discovered that the RNA interference (RNAi)–directed heterochromatin flanking the central kinetochore domain at fission yeast centromeres is required to promote CENP-A$^{\mathrm{Cnp1}}$ and kinetochore assembly over the central domain. The H3K9 methyltransferase Clr4 (Suv39); the ribonuclease Dicer, which cleaves heterochromatic double-stranded RNA to small interfering RNA (siRNA); Chp1, a component of the RNAi effector complex (RNA-induced initiation of transcriptional gene silencing; RITS); and Swi6 (HP1) are required to establish CENP-A$^{\mathrm{Cnp1}}$ chromatin on naïve templates. Once assembled, CENP-A$^{\mathrm{Cnp1}}$ chromatin is propagated by epigenetic means in the absence of heterochromatin. Thus, another, potentially conserved, role for centromeric RNAi-directed heterochromatin has been identified.

Metazoan centromeres are mostly composed of repetitive DNA upon which the kinetochore assembles to mediate chromosome segregation. Epigenetic factors contribute to the establishment and maintenance of kinetochores at particular sites, which are composed of CENP-A chromatin (*1*–*4*). However, the primary signals specifying the site of CENP-A chromatin, and thus kinetochore assembly, are unknown.

In *Drosophila*, human, and fission yeast, kinetochores are embedded in heterochromatin (*5*–*7*). Fission yeast centromeres have two distinct domains: outer repeats (*otr*) that flank the central kinetochore domain composed of innermost repeats (*imr*) and central core (*cnt/cc*) DNA (*3*, *8*) (Fig. 1A). Heterochromatin, containing Swi6 (heterochromatin protein 1 or HP1) bound to histone H3 dimethylated on lysine 9 (H3K9me2), forms over the *otr*, whereas CENP-A$^{\mathrm{Cnp1}}$ replaces histone H3 in the central domain (*5*, *7*, *9*–*11*). Centromeric heterochromatin contributes to centromere function by recruiting cohesin and mediating cohesion between sister centromeres (*12*, *13*). Here, we test the idea that heterochromatin marks sites for CENP-A chromatin assembly (*14*).

Fission yeast minichromosomes must contain at least part of an *otr* and a large portion of central domain (*imr*-*cc*) DNA to allow kinetochore assembly, segregation function, and minichromosome retention (*3*, *14*–*17*). Small interfering RNAs (siRNAs) originating from noncoding *otr* transcripts direct H3K9 methylation and heterochromatin formation on these repeats (*8*, *18*). Defects in various components cause loss or reduction in H3K9 methylation, Swi6, and centromeric cohesin (*5*, *9*, *13*). Endogenous chromosomes segregate without centromeric heterochromatin, because sister chromatids remain tethered by arm cohesin. However, mitotic stability of small circular minichromosomes is obliterated (*19*).

Minichromosomes containing *otr* and *cc* DNA have centromere activity, resulting in a low loss rate compared with acentrics (*15*, *16*). Here, two minichromosomes were initially used (Fig. 1A) [described in (*15*, *20*)]: pH-cc2 and pHH-cc2 (H denotes an *otr* heterochromatic element, cc denotes central domain DNA). pcc2 lacks *otr* repeats. These plasmids carry *ura4*$^+$ and *sup3-5* (suppressor of *ade6-704*) selection systems. Formation of a functional centromere on transformation of naked DNA into cells requires both *otr* and *cc* sequences (*3*, *14*). Thus, the acentric pcc2 plasmid is mitotically unstable and rapidly lost but is maintained in selective media, whereas pH-cc2 and pHH-cc2 are mitotically stable and segregate in wild-type cells (*15*). Heterochromatin is not essential for cell viability; to determine whether it is required to establish CENP-A$^{\mathrm{Cnp1}}$ chromatin on *cc* DNA, we compared the association of CENP-A$^{\mathrm{Cnp1}}$ with minichromosomes after establishment in wild type and transmission, by crossing, into a *clr4*Δ background with minichromosome DNA transformed directly into *clr4*Δ cells (fig. S1).

Wild-type cells containing pH-cc2 and pHH-cc2 minichromosomes were crossed (indicated by X) to *clr4*Δ (*clr4*Δ*::LEU2*) cells, and wild-type (leu$^-$) or *clr4*Δ (leu$^+$) progeny were selected that contained the minichromosomes. In addition, pcc2, pH-cc2, and pHH-cc2 plasmids were transformed into wild-type and *clr4*Δ strains, and primary ura$^+$ ade$^+$ transformants (indicated by T) with intact minichromosome DNA were selected for further analyses (Fig. 1A and fig. S2) (*20*). Chromatin immunoprecipitation (ChIP) showed the presence of H3K9me2 on the *otr* of pH-cc2 and pHH-cc2 in wild-type cells derived from crosses or primary transformants (Fig. 1, B and C). However, this heterochromatic modification is lost in *clr4*Δ. CENP-A$^{\mathrm{Cnp1}}$ is associated with endogenous *cen1*/*cen3* central core DNA (*cc1/3*) relative to the euchromatic *fbp1*$^+$ locus in all strains (Fig. 1, B and C, and fig. S3). However, no CENP-A$^{\mathrm{Cnp1}}$ was detected on pcc2 in either wild type or *clr4*Δ (Fig. 1D and fig. S3). Thus, CENP-A$^{\mathrm{Cnp1}}$ cannot associate with *cc* DNA when introduced alone on a plasmid, and Clr4 does not act through *cc* DNA to recruit CENP-A$^{\mathrm{Cnp1}}$. This is consistent with the formation of normal nucleosomal ladders on pcc2 rather than the unusual *cc* chromatin seen at active centromeres (*16*, *17*).

In contrast, CENP-A$^{\mathrm{Cnp1}}$ is enriched on *cc* of pH-cc2 or pHH-cc2 transformed into wild type (wt-T) or crossed into wild type (wt-X) or *clr4*Δ (*clr4*Δ-X). However, no CENP-A$^{\mathrm{Cnp1}}$ is detected on pH-cc2 or pHH-cc2 when transformed directly into *clr4*Δ, even though enrichment of endogenous *cc1/3* is seen (Fig. 1, B and C, and fig. S3). Thus, the presence of CENP-A$^{\mathrm{Cnp1}}$ on identical minichromosomes in genetically identical *clr4*Δ cells is dependent on whether the minichromosome entered these cells in a preassembled or naked state. This suggests that Clr4-dependent centromeric heterochromatin influences establishment of CENP-A$^{\mathrm{Cnp1}}$ within the central domain.

Small pH-cc2 or pHH-cc2 minichromosomes with partial centromeric DNA elements and *otr* heterochromatin on only one side of a central core may be particularly sensitive to the absence of heterochromatin in such CENP-A$^{\mathrm{Cnp1}}$ establishment assays. Therefore, we used a 36-kb minichromosome containing two nearly complete *otr* repeats flanking an entire *cen3* central domain [pH-icc3i-H (Fig. 2A)] (*16*, *20*). Compared with *cen1* structure, this minichromosome contains an almost complete centromere with 32.5 kb of contiguous *cen3* DNA. pH-icc3i-H was crossed into wild type or *clr4*Δ, and colonies retaining pH-icc3i-H were selected. In addition, total DNA from wild-type cells containing pH-icc3i-H was used to transform wild type and *clr4*Δ to select cells that directly received pH-icc3i-H. Using specific primer pairs to distinguish minichromosome from endogenous sequences, we observed the same pattern of H3K9me2 and CENP-A$^{\mathrm{Cnp1}}$ association seen for the smaller minichromosomes (Figs. 1 and 2A). Thus, the association of CENP-A with pH-icc3i-H in genetically identical *clr4*Δ cells depended on its route of introduction. This indicates that the Clr4 H3K9 methyltransferase and intact *otr* heterochromatin are required to establish CENP-A$^{\mathrm{Cnp1}}$ chromatin on centromeric *cc* DNA even on pH-icc3i-H which resembles a complete *cen1* (*16*, *19*).

Use of different primers on minichromosomes indicates that CENP-A$^{\mathrm{Cnp1}}$ and H3K9me2 are generally found only at *cc* and *otr* sequences,

---

[1] Wellcome Trust Centre for Cell Biology, Institute of Cell Biology, School of Biological Sciences, The University of Edinburgh, 6.34 Swann Building, Edinburgh EH9 3JR, Scotland, UK. [2] Department of Biochemistry 2, Nagoya University Graduate School of Medicine, Nagoya 466-8550, Japan.

*To whom correspondence should be addressed. E-mail: robin.allshire@ed.ac.uk

respectively, with no evidence of intermingling (fig. S4). A relative reduction in CENP-A^{Cnp1} levels at endogenous centromeres in *clr4*Δ cells can be detected, but only in selective minimal media (fig. S5). This provides some indication that intact heterochromatin may affect CENP-A^{Cnp1} recruitment at centromeres in their normal context. Heterochromatin may become critical for establishing CENP-A^{Cnp1} chromatin under particular conditions, for example, on germination of spores that have remained dormant for prolonged periods. Heterochromatin-directed CENP-A^{Cnp1} chromatin assembly may act as a backup system that is redundant with other mechanisms of CENP-A^{Cnp1} deposition and is only revealed by establishment assays.

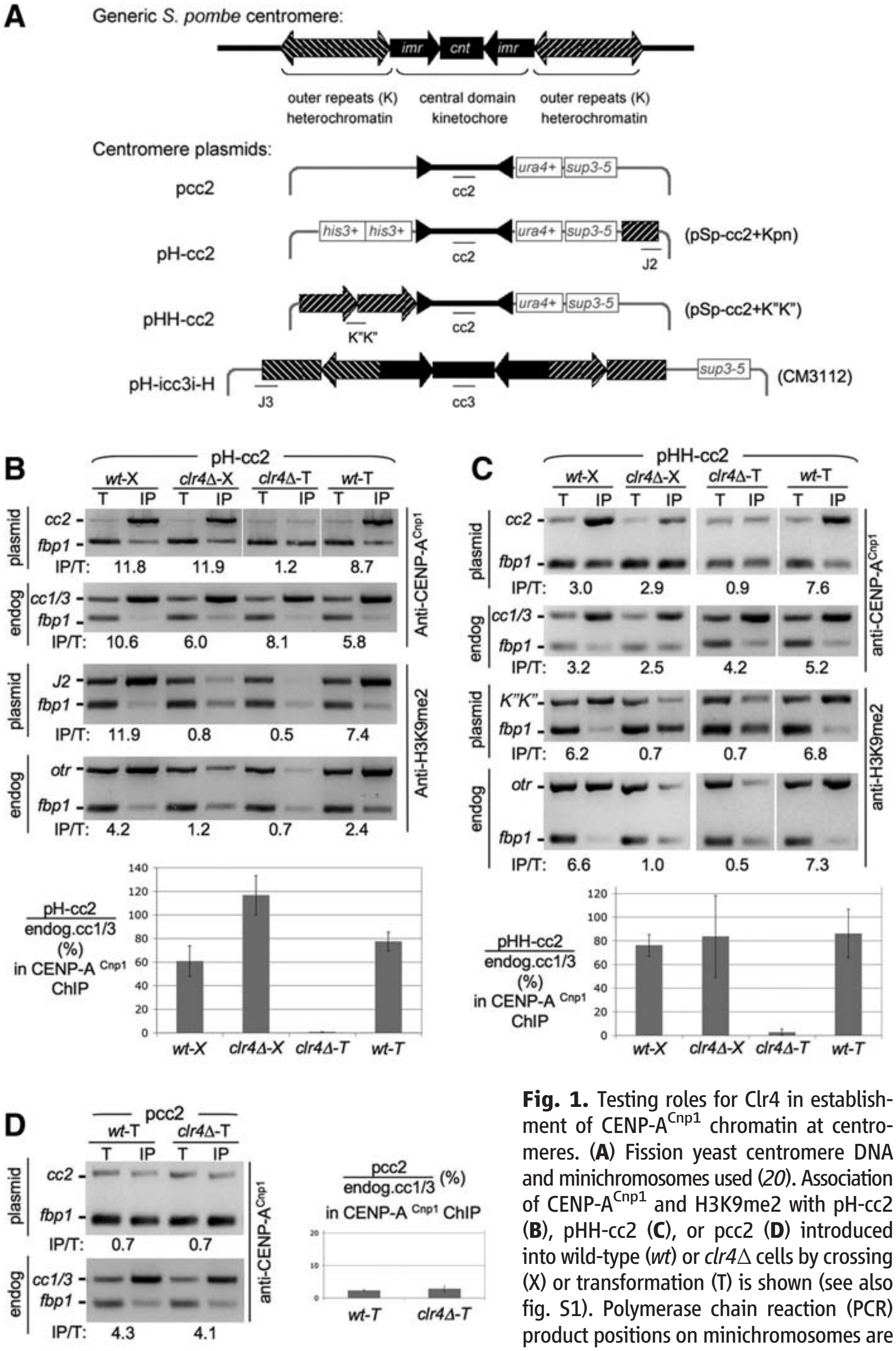

Fig. 1. Testing roles for Clr4 in establishment of CENP-A^{Cnp1} chromatin at centromeres. (**A**) Fission yeast centromere DNA and minichromosomes used (*20*). Association of CENP-A^{Cnp1} and H3K9me2 with pH-cc2 (**B**), pHH-cc2 (**C**), or pcc2 (**D**) introduced into wild-type (*wt*) or *clr4*Δ cells by crossing (X) or transformation (T) is shown (see also fig. S1). Polymerase chain reaction (PCR) product positions on minichromosomes are indicated (A). *fbp1* is the control noncentromeric locus. In CENP-A^{Cnp1} ChIP, enrichment of p*cc2* product was compared with input DNA (T) relative to *fbp1*. Enrichment of endogenous *cc1/3* relative to *fbp1* was also assessed. In H3K9me2 ChIP, enrichment at plasmid–outer repeats J2 (B) or K″K″ (C) products was compared with the PCR of input DNA relative to the *fbp1* product. Enrichment of endogenous *otr* sequences was also assessed (B and C). Quantitative PCR confirms these results [lower panels (B) and (C) and right (D) and fig. S3] (*20*). Histograms show percent enrichment on plasma relative to endogenous *cc1/3*.

The CENP-A^{Cnp1} detected on unstable minichromosomes in *clr4Δ-X* cells might be a remnant of a once-functional kinetochore, but other kinetochore proteins might be lost from such minichromosomes, regardless of their derivation. CENP-C is a conserved inner kinetochore component (*21*). Sim4 is a component of a conserved multisubunit kinetochore complex (*10*, *22*). CENP-C^{Cnp3} and Sim4 are detected at endogenous *cc1* and *cc3* (*cc1/cc3*), relative to a control locus (*act1*) (Fig. 2B), by ChIP and were also present on pH-icc3i-H derived by crossing or transformation. CENP-C^{Cnp3} and Sim4 were retained on *cc* DNA of pH-icc3i-H when crossed into *clr4*Δ, but neither was recruited to pH-icc3i-H on transformation into *clr4*Δ. Thus, these genetically identical cells (*clr4*Δ−X, *clr4*Δ−T) differ in the association of two additional kinetochore proteins with *cc3*, depending on whether the DNA molecule was initially propagated in wild type before transmission into cells lacking Clr4.

These analyses demonstrate that, once CENP-A^{Cnp1} chromatin and kinetochore proteins assemble on centromeric DNA, they are propagated without flanking heterochromatin. However, heterochromatin influences the establishment of CENP-A^{Cnp1} chromatin and, consequently, a kinetochore on naked centromeric DNA. The addition of functional Clr4 to *clr4*Δ cells containing a minichromosome derived by DNA transformation should induce heterochromatin assembly on *otr* sequences and, thus, CENP-A^{Cnp1} assembly. To test this, we reintroduced the *clr4*$^+$ gene into *clr4*Δ cells propagating pH-icc3i-H derived by crossing or DNA transformation (*clr4*$^+$↺*clr4*Δ−X, *clr4*$^+$↺*clr4*Δ−T; Fig. 3A). H3K9me2 appears on endogenous outer repeats and the plasmid-*otr* junction (J3) of pH-icc3i-H after *clr4*$^+$ reintroduction. Moreover, CENP-A^{Cnp1} is now detected on the *cc* of pH-icc3i-H [compare *clr4*Δ−T with *clr4*$^+$↺*clr4*Δ−T (Fig. 3A)]. To determine whether Clr4 reintroduction concomitantly restored full centromere-kinetochore function, we assessed minichromosome stability. In *clr4*Δ−X and *clr4*Δ−T cells, pH-icc3i-H does not segregate and is rapidly lost. *clr4*$^+$ reintroduction allowed the minichromosome to acquire centromere activity and to segregate normally. *clr4*$^+$↺*clr4*Δ−X and *clr4*$^+$↺*clr4*Δ−T cells are no longer sensitive to thiabendazole (TBZ), which indicates that full centromere function has been restored (Fig. 3B). Thus, centromeric epialleles that lack or retain CENP-A^{Cnp1} can be created depending on the history of the centromeric DNA; a nonfunctional centromeric epiallele without CENP-A^{Cnp1} can switch to the functional state, which contains CENP-A^{Cnp1}, upon provision of Clr4 methyltransferase.

Intact *otr* heterochromatin requires a functional RNAi pathway (*8*, *23*–*25*). To further dissect the process of CENP-A^{Cnp1} establishment, we transformed pHH-cc2 into cells lacking Swi6 or RNAi components Chp1 or Dcr1. Consistent with other analyses (*26*), no H3K9me2 was established on pHH-cc2 in *chp1*Δ or *dcr1*Δ

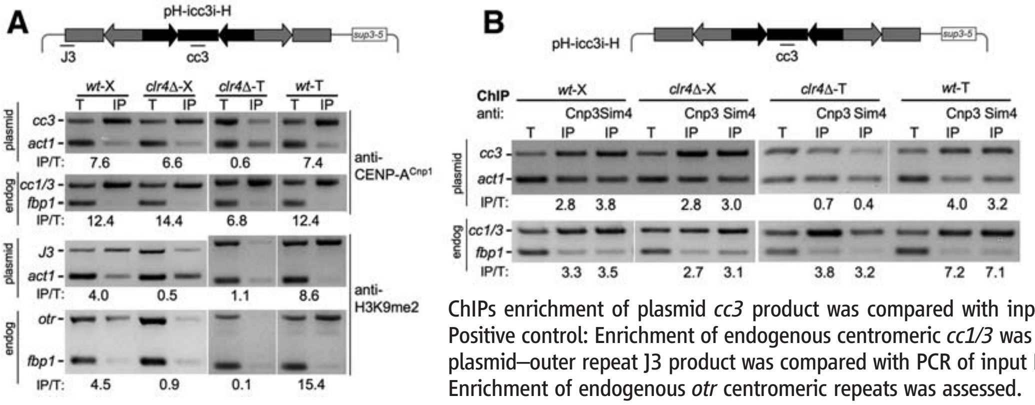

Fig 2. Clr4 is required to establish, but not to maintain CENP-A^{Cnp1} and kinetochore proteins on the large *cen3* minichromosome. Association of CENP-A^{Cnp1} and H3K9me2 in (**A**), and CENP-C^{Cnp3} and Sim4 in (**B**) were determined by ChIP in wild-type and *clr4*Δ strains containing pH-icc3i-H introduced by crossing (X) or transformation (T). *fbp1* or *act1* are control noncentromeric loci. In CENP-A^{Cnp1}, CENP-C^{Cnp3}, and Sim4 ChIPs enrichment of plasmid *cc3* product was compared with input DNA (T) relative to the *act1* product. Positive control: Enrichment of endogenous centromeric *cc1/3* was assessed. H3K9me2 ChIP: Enrichment of plasmid–outer repeat J3 product was compared with PCR of input DNA (T) relative to *act1*. Positive control: Enrichment of endogenous *otr* centromeric repeats was assessed.

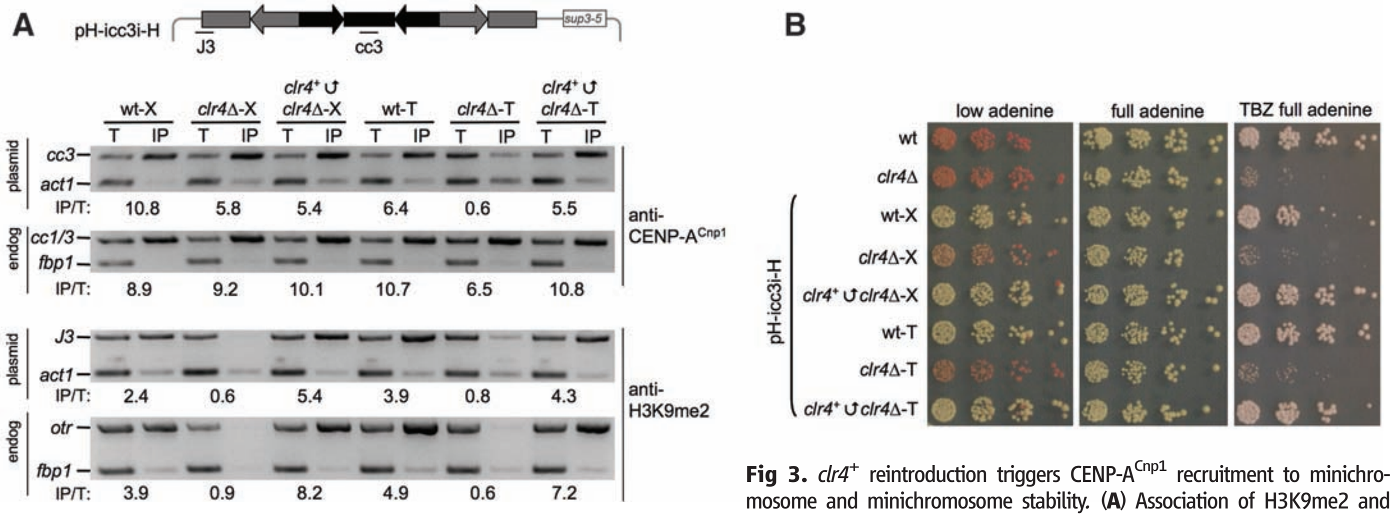

Fig 3. *clr4*$^+$ reintroduction triggers CENP-A^{Cnp1} recruitment to minichromosome and minichromosome stability. (**A**) Association of H3K9me2 and CENP-A^{Cnp1} with pH-icc3i-H in *clr4*Δ before and after *clr4*$^+$ reintroduction (*clr4*$^+$↺*clr4*Δ). Primers and conditions as in Fig. 2. (**B**) Wild-type (*wt*) and *clr4*$^+$↺*clr4*Δ cells containing pH-icc3i-H, are indistinguishable. Serial dilution assay on 1/10th adenine assesses minichromosome stability [red colonies (lost); white colonies (retained)] or full adenine ± 10 μg/ml TBZ.

cells (Fig. 4). Moreover, CENP-A^{Cnp1} did not associate with *cc2* DNA on these minichromosomes even though CENP-A^{Cnp1} is associated with endogenous centromeres (Fig. 4 and fig. S3). Thus, an active RNAi pathway is required to establish CENP-A^{Cnp1} chromatin on naked centromere DNA. The RNAi pathway is still active in the absence of Swi6; *swi6*Δ cells produce siRNAs and retain H3K9me2 on centromere repeats (*26*, *27*). However, although *otr* chromatin of pHH-cc2 becomes H3K9-methylated when introduced into *swi6*Δ, no CENP-A^{Cnp1} is detected on its *cc2* region. Thus, H3K9me2, and presumably the targeting of RITS to *otr* chromatin, is not sufficient to induce the assembly of CENP-A^{Cnp1} within the central domain of minichromosomes when introduced as naked DNA. We conclude that a patch of fully intact centromeric heterochromatin is required to establish, but not to maintain, CENP-A^{Cnp1} on the nearby central kinetochore domain of fission yeast centromeres [see our model(fig. S6)]. It is possible that centromeric cohesin, which is intimately associated with heterochromatin, may also play a role in establishing CENP-A chromatin.

These analyses demonstrate that, in fission yeast, heterochromatin integrity is essential for

Fig 4. Swi6 and RNAi components are required for CENP-A establishment. CENP-A^{Cnp1} and H3K9me2 ChIP on pHH-cc2 after direct transformation with plasmid DNA and selection in *dcr1*Δ, *chp1*Δ, *swi6*Δ, and wild-type (*wt*) strains. Primers and conditions as in Fig 1C. Quantitative PCR confirms these results (lower panel and fig. S3) (*20*).

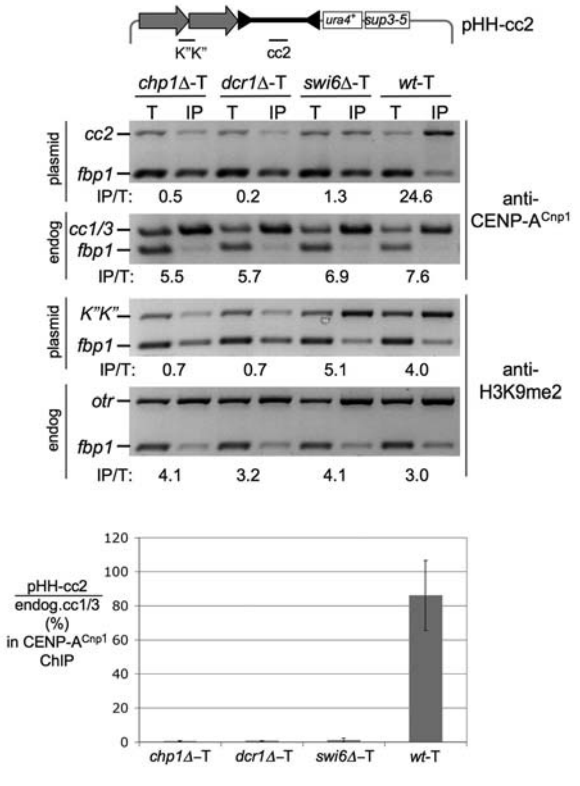

establishment of the CENP-A chromatin that underlies kinetochores. It is noteworthy that HP1 heterochromatin is formed 800 kb from the CENP-A chromatin of a human neocentromere (*28*); thus, it is conceivable that heterochromatin might play a similar role at metazoan centromeres.

References and Notes

1. D. W. Cleveland, Y. Mao, K. F. Sullivan, *Cell* **112**, 407 (2003).
2. B. A. Sullivan, M. D. Blower, G. H. Karpen, *Nat. Rev. Genet.* **2**, 584 (2001).
3. C. A. Morris, D. Moazed, *Cell* **128**, 647 (2007).
4. K. Mythreye, K. S. Bloom, *J. Cell Biol.* **160**, 833 (2003).
5. J. F. Partridge, B. Borgstrom, R. C. Allshire, *Genes Dev.* **14**, 783 (2000).
6. B. A. Sullivan, G. H. Karpen, *Nat. Struct. Mol. Biol.* **11**, 1076 (2004).
7. K. Takahashi, E. S. Chen, M. Yanagida, *Science* **288**, 2215 (2000).
8. S. I. Grewal, S. Jia, *Nat. Rev. Genet.* **8**, 35 (2007).
9. J. Nakayama, J. C. Rice, B. D. Strahl, C. D. Allis, S. I. Grewal, *Science* **292**, 110 (2001).
10. A. L. Pidoux, W. Richardson, R. C. Allshire, *J. Cell Biol.* **161**, 295 (2003).
11. S. Saitoh, K. Takahashi, M. Yanagida, *Cell* **90**, 131 (1997).
12. P. Bernard *et al.*, *Science* **294**, 2539 (2001).
13. N. Nonaka *et al.*, *Nat. Cell Biol.* **4**, 89 (2002).
14. A. L. Pidoux, R. C. Allshire, *Philos. Trans. R. Soc. London B Biol. Sci.* **360**, 569 (2005).
15. M. Baum, V. K. Ngan, L. Clarke, *Mol. Biol. Cell* **5**, 747 (1994).
16. K. Takahashi *et al.*, *Mol. Biol. Cell* **3**, 819 (1992).
17. L. G. Marschall, L. Clarke, *J. Cell Biol.* **128**, 445 (1995).
18. A. Verdel, D. Moazed, *FEBS Lett.* **579**, 5872 (2005).
19. R. C. Allshire, E. R. Nimmo, K. Ekwall, J. P. Javerzat, G. Cranston, *Genes Dev.* **9**, 218 (1995).
20. Materials and methods are available as supporting material on *Science* Online.
21. H. Saitoh *et al.*, *Cell* **70**, 115 (1992).
22. X. Liu, I. McLeod, S. Anderson, J. R. Yates 3rd, X. He, *EMBO J.* **24**, 2919 (2005).
23. T. A. Volpe *et al.*, *Science* **297**, 1833 (2002).
24. A. Verdel *et al.*, *Science* **303**, 672 (2004).
25. K. Noma *et al.*, *Nat. Genet.* **36**, 1174 (2004).
26. M. Sadaie, T. Iida, T. Urano, J. Nakayama, *EMBO J.* **23**, 3825 (2004).
27. M. Buhler, A. Verdel, D. Moazed, *Cell* **125**, 873 (2006).
28. R. Saffery *et al.*, *Mol. Cell* **12**, 509 (2003).
29. We thank A. Bird, A. Buscaino, E. Choi, W. Earnshaw, and M. Vogelauer for comments; M. Baum, D. Moazed, O. Niwa, J. Partridge, and M. Yanagida for materials; and the Allshire lab for discussions. The Epigenome Network of Excellence (NoE) is acknowledged for support (EC-FP6). H.D.F. and A.L.P. are funded by Wellcome Trust program grant 065061/Z. R.C.A. is a Wellcome Trust Principal Research Fellow.

Supporting Online Material
www.sciencemag.org/cgi/content/full/319/5859/94/DC1
Materials and Methods
SOM Text
Figs. S1 to S6
Tables S1 and S2
References

25 September 2007; accepted 26 November 2007
10.1126/science.1150944

Assembly Mechanism of the Contractile Ring for Cytokinesis by Fission Yeast

Dimitrios Vavylonis,[1,2,3]* Jian-Qiu Wu,[2]*† Steven Hao,[4]
Ben O'Shaughnessy,[1] Thomas D. Pollard[2,4,5]‡

Animals and fungi assemble a contractile ring of actin filaments and the motor protein myosin to separate into individual daughter cells during cytokinesis. We used fluorescence microscopy of live fission yeast cells to observe that membrane-bound nodes containing myosin were broadly distributed around the cell equator and assembled into a contractile ring through stochastic motions, after a meshwork of dynamic actin filaments appeared. Analysis of node motions and numerical simulations supported a mechanism whereby transient connections are established when myosins in one node capture and exert force on actin filaments growing from other nodes.

Cytokinesis is the final step in cell division, when a dividing cell physically separates into two. Assembly and constriction of a contractile ring of actin, myosin, and associated proteins cleaves cells in many organisms, including animals and yeast. Analysis of budding and fission yeast identified ~50 participating proteins (*1*), the temporal sequence of events (*2*), and local concentrations of many proteins (*3*). A major challenge is to understand how the network of proteins functions, ultimately at the level of a testable quantitative model of the entire system.

Fission yeast assembled a cytokinetic contractile ring by condensation of a broad band of membrane-associated nodes (Fig. 1, A and B, and Movie S1). The nucleus determines the initial location of the zone with these nodes by releasing the anillin-like protein Mid1p (*4*), which recruits to nodes the motor protein myosin-II, followed by other proteins, including formin Cdc12p (*2*). Actin filaments nucleated by Cdc12p (*5*, *6*) are proposed to establish a network between the nodes, allowing myosin-II to pull the nodes together (*7*–*10*) into a ring (Fig. 1C).

Numerical simulations of a simple model, with nodes pulling on their nearest neighbors in a network of fixed connections, moved nodes along linear trajectories into clusters (Fig. 1I) rather than in a continuous ring around the equator (*11*). Thus, additional features must be present, which we explored using confocal microscopy to follow myosin-II and actin filaments with high temporal and spatial resolution in live cells. Cells expressed the myosin-II light chain Rlc1p fused to three copies of green fluorescent protein (GFP) or tdTomato from its native promoter (Fig. 2). We used the calponin homology domain of *S. pombe* IQGAP Rng2p tagged with GFP calponin homology domain (GFP-CHD) (*12*) to mark actin filaments (Fig. 3) because actin tagged with yellow fluorescent protein (YFP) did not incorporate into contractile rings (*3*, *10*).

We discovered that nodes make many starts, stops, and changes of direction as they condense into a contractile ring (Fig. 2, C and D, and Movie S2). The highly stochastic pattern of node motions suggested that the connections between nodes were unstable (Fig. 1, G and H). A model with traction between nodes depending on transient connections established by stochastic search-and-capture produced simulations in which nodes condense into a continuous ring through lifelike stop-go movements (Fig. 1J and Movies S3 and S4) (*11*). The success of this model depends on its parameter values, so we observed live cells to measure parameters and test assumptions and predictions.

Wild-type cells assembled 63 ± 10 ($n = 22$) nodes located close to the plasma membrane in a band ~1.8 μm wide around the middle of the cell (Fig. 1A and Movie S1). Nodes were distributed randomly around the equator and in a Gaussian manner along the long axis of the cell (fig. S1A). Rlc1p-3GFP accumulated in individual nodes over ~1 min (Fig. 2A, fig. S1B, and Movie S5). The Rlc1p-3GFP fluorescence intensities of nodes varied ~fourfold within a cell (fig. S1C), fluctuated over time (Fig. 2B), and recovered with a half-time of about 30 s after photobleaching (*11*), indicating that the protein exchanges dynamically with the cytoplasmic pool.

When first formed, nodes moved relatively little for ~10 min (Movies S5 and S6), but the mean square displacement (MSD) of the center

---

[1]Department of Chemical Engineering, Columbia University, New York, NY 10027, USA. [2]Department of Molecular, Cellular, and Developmental Biology, Yale University, New Haven, CT 06520, USA. [3]Department of Physics, Lehigh University, Bethlehem, PA 18015, USA. [4]Department of Molecular Biophysics and Biochemistry, Yale University, New Haven, CT 06520, USA. [5]Department of Cell Biology, Yale University, New Haven, CT 06520, USA.

*These authors contributed equally to this work.

†Present address: Department of Molecular Genetics and Department of Molecular and Cellular Biochemistry, The Ohio State University, Columbus, OH 43210, USA.

‡To whom correspondence should be addressed. E-mail: thomas.pollard@yale.edu

of each node increased over time (Fig. 2E, black), consistent with 2-dimensional diffusion: $\mathrm{MSD}(t) = \mathrm{MSD}(0) + 4Dt$. The diffusion constants D distributed around 20 nm^2/s in control cells and cells treated with Latrunculin A to depolymerize actin (fig. S2). Node motions appeared uncorrelated, because the slopes of relative MSD between pairs of nodes (Fig. 2E, gray, and fig. S2B) were on average equal to the sum of the slopes of individual node MSD curves. Diffusive behavior implies that any anchors or cross-links of nodes were dynamic or very soft on minute time scales. The large mass [>22,000 kD (*10*)] of nodes may contribute to D being orders of magnitude smaller than D of transmembrane proteins (*13*).

Nodes began to move about the time a dynamic meshwork of actin filaments appeared around the equator, 2.3 ± 1.9 min (n = 29 cells) after spindle pole bodies separated and Cdc12p joined the nodes (*2*) (fig. S3 and Movies S7 to S9). Nodes moved in 20-s bursts (Fig. 2G) at velocities of ~30 nm/s (Fig. 2F and Movie S2). Node movements terminated in pauses or by merger with another node. Many motions could be clearly attributed to pairwise attractions, and a few nodes switched partners during these directed motions (Fig. 2D and fig. S4). Although most node motions were toward the final location of the contractile ring, the distribution of orientations was broad (Fig. 2G, inset) and the velocities and durations of movements were uncorrelated within our resolution (fig. S4J).

We used fluorescence microscopy to verify actin filament connections between nodes. Linear elements marked with GFP-CHD extended in all directions from Rlc1p nodes and established connections among them (Fig. 3, B to D, fig. S5, and Movies S10 to S15). The GFP-CHD fluorescent intensity of mature contractile rings [with ≥20 filaments in wild-type cells (*3*, *14*)] was 10 to 20 times as high as the least intense linear elements in the broad band; thus, the faintest elements probably represent small bundles of actin filaments or perhaps even single actin filaments. Contractile ring actin filaments grew normally from nodes in vegetative cells lacking the formin For3p that nucleates interphase actin cables (*12*) (Movies S12, S13, and S16).

The dense actin filament network among the nodes obscured details of their relationships, but in favorable cases (e.g., during early stages of node condensation) we observed linear elements elongating at ~0.2 μm/s (75 actin subunits/s) (Fig. 3C, fig. S5, and Movie S15). Some growing linear structures were aimed directly at a target node; others appeared to move laterally to associate with a node (Movies S11 and S13). When growing actin filaments buckled [as observed in vitro (*15*)], their contour lengths also increased at ~0.2 μm/s (Movie S17). Some nodes connected by actin filaments moved along the direction of the linear element (Movies S12 to S14).

Filaments growing at 0.2 μm/s generally remained in a zone of full width ~4 μm on both margins of contractile rings (Fig. 3, A and B), suggesting filament lifetimes of <20 s. We observed two processes that contribute to filament turnover. Long-growing filaments could break and short filaments could disappear rapidly (Movies S10, S15, and S16), which resembled severing of growing actin filaments by cofilin in vitro (*16*). Figure 3D (Movie S14) shows a node stopping when its actin connection apparently broke, and Movie S18 shows the ends of a broken filament recoiling as if under tension.

Monte Carlo simulations (*11*) of a model with search, capture, pull, and release (Fig. 1, D to H) reproduced the start-stop motion of nodes and over ~10 min assembled a continuous ring with nonuniform fluorescence intensities (Fig. 1J and Movies S3 and S4) as observed in cells (Fig. 1B). We assume that nodes nucleate actin filaments that grow in random directions parallel to the membrane. Myosin-II binds filaments passing within 100 nm and exerts constant tensile force on the filament, tending to reduce node separation. The total force $\mathbf{F}_{\mathrm{tot}}$ from all connections results in a node velocity $\mathbf{v} = \mathbf{F}_{\mathrm{tot}}/\zeta$, where the friction coefficient $\zeta = k_BT/D \approx 0.2$ pN s/nm from the Einstein relation, using D ~20 nm^2/s. Because nodes move at 30 nm/s, $\mathbf{F}_{\mathrm{tot}}$ ~ 6 pN. A force of 4 pN per connection reproduced the observed distribution of node speeds (fig. S6). This force value is a lower bound, because sources other than thermal motion may contribute to the observed translational diffusion of nodes. An average of 40 Myo2p heads per node (*3*), with each producing ~2 pN force (*17*), should produce force in this range. Node velocities are low compared with the ability of *S. pombe* Myo2 to move unloaded actin filaments at 400 nm/s (*18*), so we expect that node-bound myosin-II operates near stall, consistent with our lower estimate. We assume a short-range (150 nm) repulsive radial force to prevent nodes from overlapping. We assume that nodes pause when they lose connections with neighboring nodes after mean time τ_{break}. Connections fail when the filament breaks or the filament dissociates from myosin-II, as expected for motors with low duty cycles (*17*). Filaments searching for nodes also break

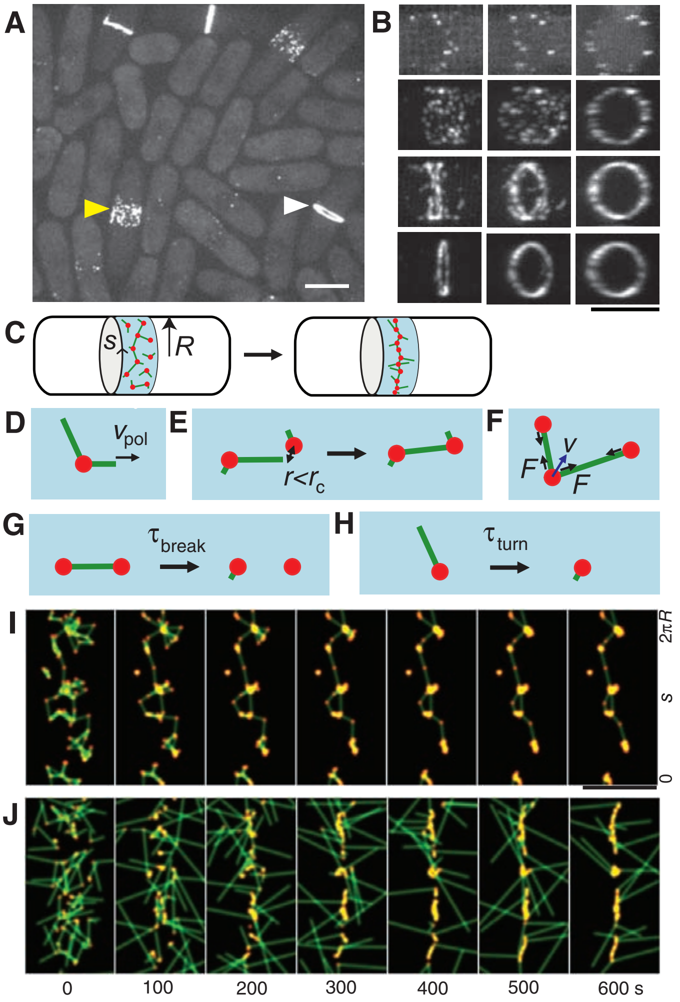

Fig. 1. Formation of contractile rings from bands of nodes. (**A**) Confocal maximum intensity projection of cells expressing Rlc1p-3GFP. Bands of nodes (yellow arrow) condense into rings (white arrow). (**B**) 3D reconstructions showing cells expressing Rlc1p-3GFP at progressive stages of ring formation (rows). Columns show successive 45° *y*-axis rotations. (**C**) Model for ring formation via actin connections between nodes (*s*, arc length; *R*, radius). (**D** to **H**) Search, capture, pull, and release mechanism. (D) Actin filaments polymerize out of nodes with pointed ends leading at rate v_{pol}. (E) Pointed ends passing within r_c of another node form connections. (F) Each connection produces an attractive force F. Nodes move in the direction of the total force with velocity $\mathbf{v} = \mathbf{F}_{\mathrm{tot}}/\zeta$. (G) The lifetime of connections is τ_{break}, and (H) the lifetime of unconnected actin filaments is τ_{turn}; in both cases, a new filament grows immediately. (**I** and **J**) Simulated images of condensing bands (*11*). The *y* axis is the arc length *s*. (I) A model with permanent connections between each two nearest neighbors generates clumps. (J) Model with reactions in (D) to (H) (v_{pol} = 0.2 μm/s; F/ζ = 20 nm/s; $\tau_{\mathrm{turn}} = \tau_{\mathrm{break}}$ = 20 s; r_c = 100 nm) condenses nodes into rings over 550 s (Movies S3 and S4). Scale bars, 5 μm.

Fig. 2. Node formation and motions in cells expressing Rlc1p-3GFP. (**A**) Time course (seconds) of node formation (Movie S5). (**B**) Position of a newly formed node at 1-s intervals. (**C**) Time course (seconds) of movements as nodes condense into a ring (Movie S2). (**D**) Details of node motions [1-s intervals from the series shown in (C)]. Node 1 (filled arrowhead) moves toward a node in the upper right corner and stops. Node 2 (open arrowhead) moves toward node 1. (**E**) MSD of newly formed nodes. Black curves, MSD of three nodes in the same cell versus time; gray lines, relative MSD between the three nodes. (**F**) Distribution of node velocities during condensation (data from 10 cells). Unresolved node motions in regions of high node density are not included. (**G**) Durations of node movements. (Inset) Directions of node motions with respect to the long axis of the cell (absolute values). In (A), (C), and (D), each frame is a moving average of six successive frames at 1-s intervals. Scale bars, 5 μm.

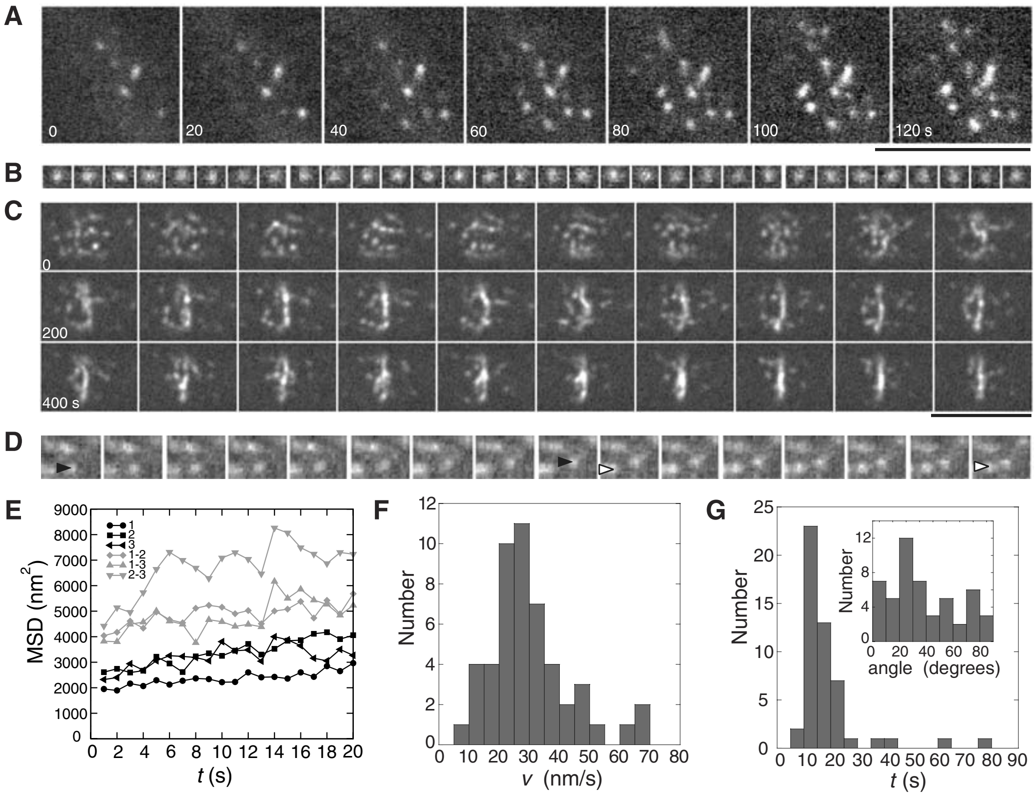

Fig. 3. Actin filament and node dynamics in cells expressing GFP-CHD to mark actin filaments (A to D) and Rlc1p-mRFP1 (B) or Rlc1p-tdTomato (C and D) to mark nodes. Time in minutes in (A) and seconds in (C) and (D). (**A**) Time series showing actin patches at both ends of the cell and assembly of a contractile ring from a meshwork of actin filaments (Movie S8). (**B**) Six cells from the same field arranged according to cell-cycle stage showing networks of actin filaments connecting nodes. Movie S9 shows 3D projections of cells b to d. (**C**) Time series showing actin filaments transiently connecting two nodes (arrow) and regrowing from this node (arrowhead) (Movie S15). (**D**) Time series of actin filaments in the boxed region capturing a lagging node and pulling it toward the contractile ring until the filament apparently breaks (arrow). Kymograph of the moving node with time horizontal. See Movies S11 to S14. Scale bars, 5 μm [(A) and (B)], 1 μm [(C) and (D)].

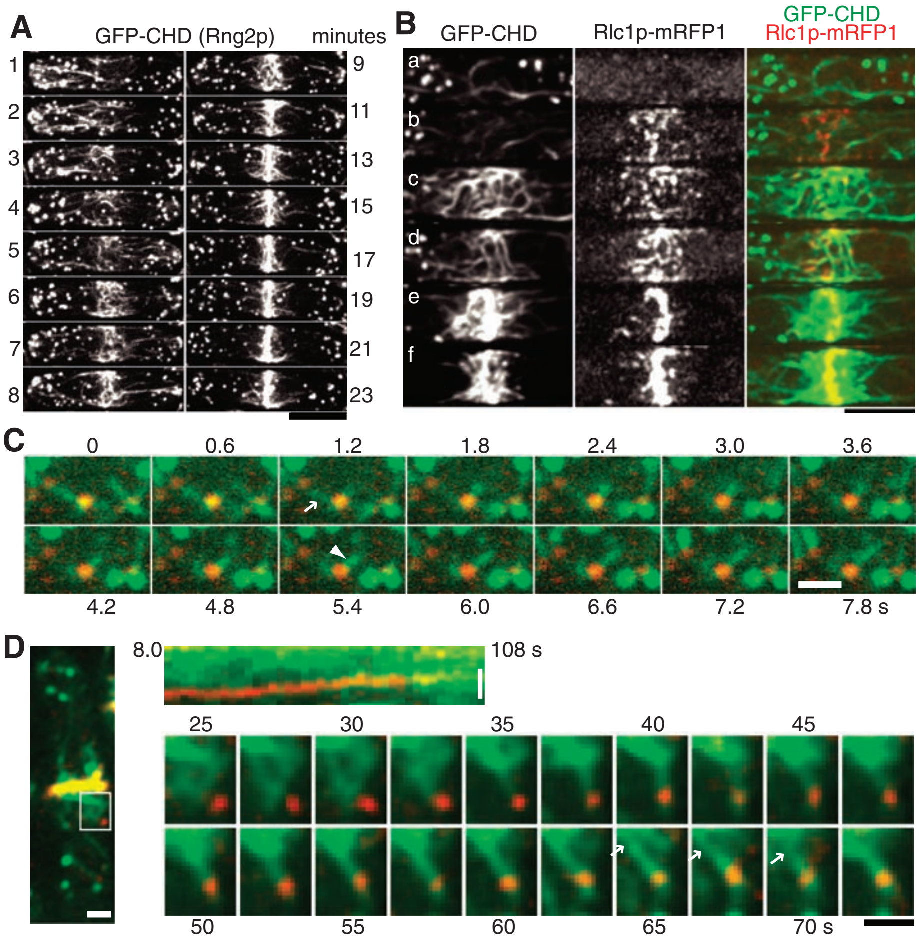

randomly after τ_{turn}. After breaks, a new filament grows in a new direction. We assume that tension switches off elongation of filaments anchored by Cdc12p and that a filament connecting two nodes does not accrete additional nodes (*11*).

The model was robust over a large range of parameter values (Fig. 4, A to D, and figs. S7 to S16). Using experimental parameter values, simulations generated rings with few gaps (Fig. 4, B and D) in the same time (Fig. 4, A and C) as live cells. Reliable avoidance of large gaps among disconnected clumps of nodes requires >50 nodes distributed in a zone <2.8 μm wide and τ_{break} < 80 s. Clumps tend to form in a search-and-capture mechanism, because nodes find close neighbors more efficiently than distant ones and collapse locally. Condensation of the nodes in 10 min also depended on 1 to 4 actin elongating from nodes and active formins in >50% of nodes. Nodes had time to find their neighbors within τ_{turn} and complete condensation in ~10 min if they grew >20 subunits/s. In agreement with this, inhibiting actin polymerization with Latrunculin A or by depleting profilin results in clumps of nodes (*10*, *19*).

The search, capture, pull, and release model reproduces two classic experiments. When *cdc25-22* cells are arrested in the G2 phase of the cell cycle for 4 hours at the restrictive temperature, they continue to grow in length and assemble 97 ± 17 nodes (*n* = 17) in a band ~3.5 μm wide. When released into mitosis at the permissive temperature, they form a contractile ring in ~25 min. In simulations using the standard parameters but arrays of 100 nodes in a band 3.5 μm wide, the nodes condense into somewhat irregular rings in 15 to 30 min (Fig. 4E and fig. S17). The model with standard parameters also reproduces the fusion of pairs of contractile rings (*20*) separated by up to 8 μm at velocities comparable to experiments (Fig. 4F and fig. S18).

The success of this random search-and-capture mechanism without feedback suggests that its inherent randomness may endow the mechanism with an advantageous plasticity, aiding navigation of the complex landscape of kinetic barriers and traps separating a broad band of nodes from a completed contractile ring. The model attempts to capture the essential components of the mechanism, but additional features such as spatial, temporal, and orientational control of actin polymerization and myosin activity cannot be excluded. Thus, the precise mechanistic role of many regulatory proteins such as tropomyosin and cofilin remains to be established. Most important, formation of actin filament bundles clearly contributes to ring assembly (Fig. 3, A and B, and Movie S19) (*9*, *20*). Our observations suggest that transient bundles stabilize tenuous initial connections between nodes rather than leading ring assembly (*9*, *14*). Cytokinesis by animal cells also involves formins (*4*) and mobile clusters of myosin-II (*21*), so our model may represent a conserved module used in contractile networks.

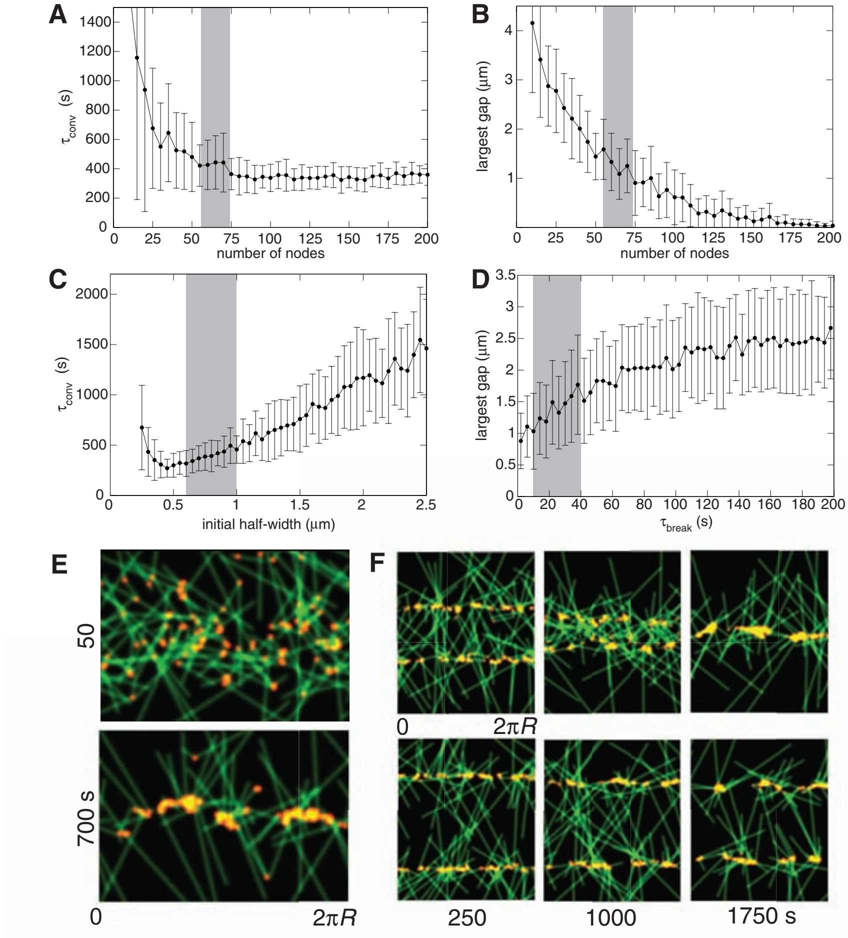

Fig. 4. Simulations of contractile ring assembly by the model in Fig. 1, D to H, using parameters in Fig. 1J unless noted otherwise. Graphs plot averages of 50 simulations ±SD. Gray regions indicate physiological parameter range. (**A**) Time (τ_{conv}) for the band of nodes to condense 50% versus number of nodes. (**B**) Largest circumferential gap between nodes 500 s after the onset of condensation versus number of nodes. (**C**) As (A), but as a function of the initial half-width of the broad band. (**D**) As (B), but as a function of the lifetime of connections. (**E**) Snapshots of simulations of ring formation in *cdc25-22* cells (100 nodes, initial half-width 1.6 μm). (**F**) Simulations of attraction between two condensed rings (70 nodes each), as in (*20*). (Top) Rings separated by 4 μm fuse within 20 min. (Bottom) Rings separated by 10 μm fail to converge.

References and Notes

1. D. A. Guertin, S. Trautmann, D. McCollum, *Microbiol. Mol. Biol. Rev.* **66**, 155 (2002).
2. J.-Q. Wu, J. R. Kuhn, D. R. Kovar, T. D. Pollard, *Dev. Cell* **5**, 723 (2003).
3. J.-Q. Wu, T. D. Pollard, *Science* **310**, 310 (2005).
4. D. R. Burgess, F. Chang, *Trends Cell Biol.* **15**, 156 (2005).
5. F. Chang, D. Drubin, P. Nurse, *J. Cell Biol.* **137**, 169 (1997).
6. D. R. Kovar, J. R. Kuhn, A. L. Tichy, T. D. Pollard, *J. Cell Biol.* **161**, 875 (2003).
7. N. I. Naqvi, K. Eng, K. L. Gould, M. K. Balasubramanian, *EMBO J.* **18**, 854 (1999).
8. F. Motegi, K. Nakano, I. Mabuchi, *J. Cell Sci.* **113**, 1813 (2000).
9. R. Arai, I. Mabuchi, *J. Cell Sci.* **115**, 887 (2002).
10. J.-Q. Wu *et al.*, *J. Cell Biol.* **174**, 391 (2006).
11. Materials and methods are available as supporting material on *Science* Online.
12. S. G. Martin, F. Chang, *Curr. Biol.* **16**, 1161 (2006).
13. A. Kusumi *et al.*, *Annu. Rev. Biophys. Biomol. Struct.* **34**, 351 (2005).
14. T. Kamasaki, M. Osumi, I. Mabuchi, *J. Cell Biol.* **178**, 765 (2007).
15. D. R. Kovar, T. D. Pollard, *Proc. Natl. Acad. Sci. U.S.A.* **101**, 14725 (2004).
16. A. Michelot *et al.*, *Curr. Biol.* **17**, 825 (2007).
17. J. Howard, *Mechanics of Motor Proteins and the Cytoskeleton* (Sinauer Associates Publishers, Sunderland, MA, 2001).
18. M. Lord, T. D. Pollard, *J. Cell Biol.* **167**, 315 (2004).
19. D. R. Kovar, E. S. Harris, R. Mahaffy, H. N. Higgs, T. D. Pollard, *Cell* **124**, 423 (2006).
20. R. R. Daga, F. Chang, *Proc. Natl. Acad. Sci. U.S.A.* **102**, 8228 (2005).
21. M. Werner, E. Munro, M. Glotzer, *Curr. Biol.* **17**, 1286 (2007).
22. We thank T. Kamine and M. Manix for help and D. McCollum, S. Martin, F. Chang, M. Balasubramanian, V. Sirotkin, and K. Sawin for strains and plasmids. This work was supported by NIH research grants GM-26338 and GM-26132.

Supporting Online Material

www.sciencemag.org/cgi/content/full/1151086/DC1
Materials and Methods
Figs. S1 to S18
Table S1
References
Movies S1 to S19

28 September 2007; accepted 21 November 2007
Published online 13 December 2007;
10.1126/science.1151086
Include this information when citing this paper.

Ongoing in Vivo Experience Triggers Synaptic Metaplasticity in the Neocortex

Roger L. Clem,[1] Tansu Celikel,[2]* Alison L. Barth[1]†

In vivo experience can occlude subsequent induction of long-term potentiation and enhance long-term depression of synaptic responses. Although a reduced capacity for synaptic strengthening may function to prevent excessive excitation, such an effect paradoxically implies that continued experience or training should not improve and may even degrade neural representations. In mice, we examined the effect of ongoing whisker stimulation on synaptic strengthening at layer 4-2/3 synapses in the barrel cortex. Although *N*-methyl-D-aspartate receptors were required to initiate strengthening, they subsequently suppressed further potentiation at these synapses in vitro and in vivo. Despite this transition, synaptic strengthening continued with additional sensory activity but instead required the activation of metabotropic glutamate receptors, suggesting a mechanism by which continued experience can result in increasing synaptic strength over time.

N-methyl-D-aspartate receptor–dependent synaptic strengthening is the most common and best-understood form of plasticity in the central nervous system, found in brain areas ranging from the hypothalamus to the cerebral cortex and in species including amphibians, birds, and mammals. Because NMDARs are required for both learning in vivo and synaptic potentiation in vitro, it is likely that synaptic strengthening that occurs during the course of normal behavioral experience requires NMDARs (*1*). The occlusion of NMDAR-dependent long-term potentiation (LTP) after in vivo experience has been taken as evidence that the signaling pathways employed in behaving animals to increase synaptic strength are the same as those underlying LTP (*2*–*4*).

How NMDARs influence plasticity after the initiation of synaptic strengthening in vivo has not been well studied. Because experience-dependent plasticity is cumulative over time in many behaviorally relevant contexts, understanding how synaptic plasticity is modified or enhanced after its induction is critical to our ability to understand and facilitate learning (*5*). These questions may be especially important in the context of development and the maturation of sensory responses.

In slices from control mice, pairing-induced potentiation of cortical layer 4-2/3 synapses in vitro is NMDAR-dependent [Fig. 1A; protocol modified from (*6*); control, percent of baseline excitatory postsynaptic current (EPSC) amplitude: 162.5 ± 21.2%, n = 18 cells; + D,L-2-amino-5-phosphonovaleric acid (APV) 114.5 ± 8.8%, n = 10 cells; a scatter plot of all LTP experiments is shown in fig. S1]. This LTP was accompanied by an increase in AMPAR-EPSC rectification that lasted for the duration of recording (>30 min after induction; fig. S2), suggesting that it is accompanied by an increase in current through glutamate receptor 2–lacking, Ca^{2+}-permeable AMPA receptors (CP-AMPARs). Single-whisker experience (SWE), in which all but a single large facial whisker have been removed from the animal's snout (*7*, *8*), induces synaptic potentiation by CP-AMPAR addition to layer 4-2/3 synapses after 24 hours (*7*). Using c*fos*–coupled green fluorescent protein (fosGFP) transgenic mice to visualize the location of the spared whisker barrel (*9*), we examined whether synaptic potentiation could occur when NMDARs were blocked during SWE.

The competitive NMDAR antagonist carboxypiperazin-4-yl-propyl-1-phosphonic acid (CPP) has been used to block NMDARs in vivo (*10*, *11*). Although NMDAR antagonists can have sedative effects that might reduce levels of activity reaching the cortex and thereby influence SWE plasticity, we found that CPP injection did not alter whisker-evoked responses in vivo but did confer a mild motor impairment in control undeprived animals (fig. S3).

Animals injected with CPP throughout SWE (–2 hours and +12 hours after SWE onset) showed no increase in the ratio of AMPAR- to NMDAR-mediated EPSCs (A:N) versus control (Fig. 1, E to G; A:N ratio: control 1.01 ± 0.08, n = 11 cells; SWE 1.69 ± 0.12, n = 9 cells; SWE + CPP 1.01 ± 0.16, n = 6 cells). Additionally, the amplitude of quantal AMPAR-EPSCs (Sr^{2+}-mEPSC, in which Sr^{2+} was used to induce asynchronous glutamate release) was unchanged in animals receiving CPP (Fig. 1, H to J; Sr^{2+}-mEPSC amplitude: control 9.79 ± 0.35 pA, n = 11 cells; SWE 12.0 ± 0.46 pA, n = 10 cells; SWE + CPP 10.6 ± 0.39 pA, n =

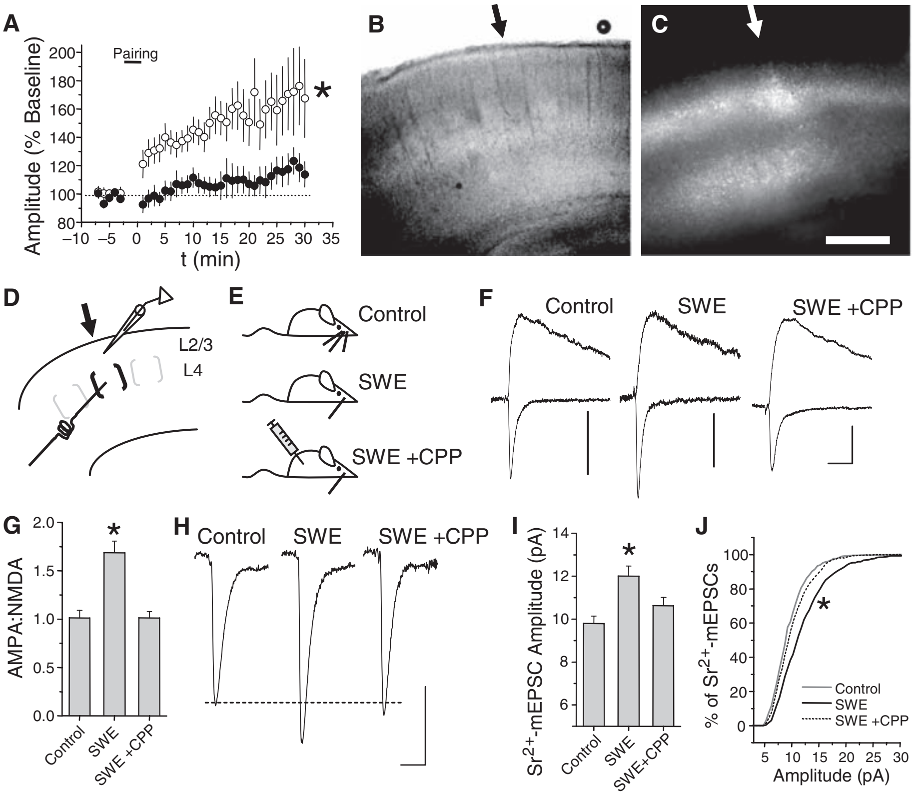

Fig. 1. LTP and SWE-induced synaptic strengthening require NMDARs. (**A**) Pairing (0 mV, 2 Hz, 360 pulses) induces LTP at layer 4-2/3 synapses from control undeprived mice (white circles) that is abolished in APV-treated cells (black circles). *t*, time. *$P < 0.01$. (**B**) Coronal slice of the barrel cortex under brightfield illumination. (**C**) Fluorescence illumination of (B) showing fosGFP expression in the spared barrel column (arrow). Scale bar, 500 μm. (**D**) Electrode positions. (**E**) Experimental groups for (F) to (J): control, whisker intact; SWE, 24 hours of SWE; SWE + CPP, 24 hours of SWE with recurrent CPP treatment. (**F**) Representative EPSCs at membrane holding potential (V_h) = –70 mV and +40 mV, scaled to +40 mV. Scale bars, 25 pA, 20 pA, and 25 pA × 20 ms, respectively. (**G**) Mean A:N ratio for all groups. *$P < 0.001$. (**H**) Group-averaged quantal Sr^{2+}-mEPSCs. Scale bar, 5 pA × 5 ms. (**I**) Mean Sr^{2+}-mEPSC amplitude. *$P < 0.001$. (**J**) Cumulative histogram of Sr^{2+}-mEPSC amplitude for all groups. *$P < 0.001$.

---

[1] Department of Biological Sciences and Center for the Neural Basis of Cognition, Carnegie Mellon University, Pittsburgh, PA 15213, USA. [2] Department of Cell Physiology, Max Planck Institute for Medical Research, Jahnstrasse 29, 69120 Heidelberg, Germany.

*Present address: Laboratory of Neural Circuits and Plasticity, University of Southern California, 3641 Watt Way, HNB 501, Los Angeles, CA 90089-2520, USA.

†To whom correspondence should be addressed. E-mail: barth@cmu.edu

12 cells). Despite the fact that in vitro LTP and in vivo synaptic strengthening occur over different time courses and may take advantage of different cellular mechanisms, these data indicate that both processes require NMDAR activation.

A common test of whether LTP-like processes have occurred in vivo is to see whether after in vivo stimulation, LTP can still be induced by artificial stimuli (*2–4*). If the intracellular pathways used to induce synaptic strengthening were maximally activated by in vivo experience, then further LTP should be difficult or impossible to elicit, a result that has been observed in previous studies (*2–4*). However, the mechanisms underlying LTP suppression and its physiological relevance remain poorly understood.

After 24 hours of SWE, pairing was no longer effective in inducing LTP and instead produced a mild depression at spared column layer 4-2/3 synapses in vitro (Fig. 2, D to F; 84.0 ± 5.5%, *n* = 7 cells). These data suggest that, coincident with an increase in quantal AMPAR-mediated EPSC amplitude (*7*), in vivo experience saturates or fundamentally alters NMDAR-dependent LTP at these synapses. The magnitude of LTP of deprived 4-2/3 synapses was similar to that of the control (Fig. 2, B and F; 150.2 ± 9.7%, *n* = 8 cells) and was eliminated after treatment with APV (Fig. 2, C and F; 97.1 ± 5.8%, *n* = 7 cells).

Because we observed a mild depression of synaptic responses after pairing in the spared column, it seemed possible that NMDAR activation induced long-term depression (LTD), a possible homeostatic response to the saturation of synaptic strengthening (*5*). Unexpectedly, APV application revealed a strong potentiation of spared column 4-2/3 synapses (Fig. 3, B and F; 179.1 ± 31.2%, *n* = 8 cells). This result indicated that LTP was not merely saturated at these synapses but NMDARs had acquired the ability to suppress pairing-induced synaptic strengthening in vitro.

We next sought to characterize this NMDAR-independent form of LTP at layer 4-2/3 synapses in the spared column. In the presence of APV, inclusion of the Ca^{2+} chelator BAPTA (10 mM) in the recording electrode blocked LTP (Fig. 3, C and F; 91.3 ± 3.7%, *n* = 7 cells), indicating that potentiation requires postsynaptic Ca^{2+} entry. At excitatory synapses onto interneurons (*12*, *13*), as well as at glutamatergic contacts on some glial cells (*14*), activation of CP-AMPARs is required for LTP. Previous work has shown that these receptors are trafficked to and maintained at layer 4-2/3 synapses by sensory-evoked activity in the spared barrel column (*7*). Thus, it was conceivable that this Ca^{2+}-dependent form of NMDAR-independent LTP required activation of CP-AMPARs. However, pharmacological blockade of CP-AMPARs with the specific antagonists philanthotoxin-433 (PhTX) or joro spider toxin (JsTX) did not reduce LTP induced at spared 4-2/3 synapses treated with APV (Fig. 3, D and F; 167.3 ± 22.7%, *n* = 5 cells, pooled).

Metabotropic glutamate receptor (mGluR) activation can support LTP in some types of interneurons (*15*, *16*) and at excitatory synapses in the cerebellum (*17*), amygdala (*18*), and hippocampus (*19*, *20*), although it usually complements NMDAR-mediated plasticity. In order to investigate whether these receptors might be responsible for the APV-resistant LTP in the spared barrel column, we bath-applied the broad-spectrum mGluR antagonist MCPG [(RS)-α-methyl-4-carboxyphenylglycine] together with APV. Under these conditions, pairing-induced LTP was fully eliminated (Fig. 3, E to F; MCPG + APV, 95.2 ± 3.3%, *n* = 8 cells). Thus, after the onset of experience-dependent plasticity in the spared barrel column, mGluRs can oppose NMDAR-mediated synaptic depression in vitro.

These experiments indicate that, at least in brain slices for pairing-induced LTP, the rules governing the induction of synaptic strengthening are altered by sensory experience. Does this switch in

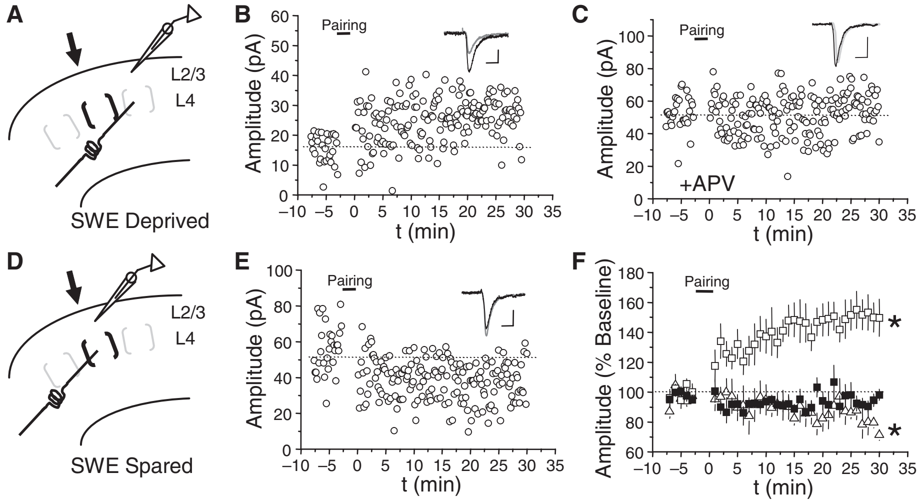

Fig. 2. SWE occludes pairing-induced LTP in vitro. (**A** and **D**) Electrode positions for recording in deprived (A) or spared (D) columns. (**B** and **C**) Representative experiments showing pairing-induced LTP in a deprived column (B) that is abolished in APV-treated cells (C). Inset in (B), (C), and (E) shows averaged EPSC before pairing (gray) and 30 min after pairing (black). Scale bar in (B), 10 pA × 10 ms; in (C), 20 pA × 10 ms. (**E**) Representative experiment showing that LTP is not elicited in the spared column. Scale bar, 30 pA × 10 ms. (**F**) Summary of LTP experiments at 4-2/3 synapses in spared (triangles), deprived (white squares), and deprived + APV (black squares) columns. $P < 0.01$.

Fig. 3. NMDAR block reveals mGluR- and Ca^{2+}-dependent LTP at spared column synapses. (**A**) Electrode positions. (**B** to **E**) For pairing at 4-2/3 synapses within the spared column of slices from SWE animals, representative experiments for (B) APV, (C) APV + BAPTA, (D) APV + JsTX or PhTX (data pooled), and (E) APV + MCPG are shown. Scale bars in (B), 40 pA × 10 ms; in (C), 30 pA × 10 ms; in (D), 60 pA × 10 ms; in (E), 20 pA × 10 ms. (**F**) Summary of pairing-induced plasticity experiments. APV-only (white squares), APV + BAPTA (black squares), APV + PhTX or JsTX (black circles), and APV + MCPG (white triangles). $^*P < 0.01$.

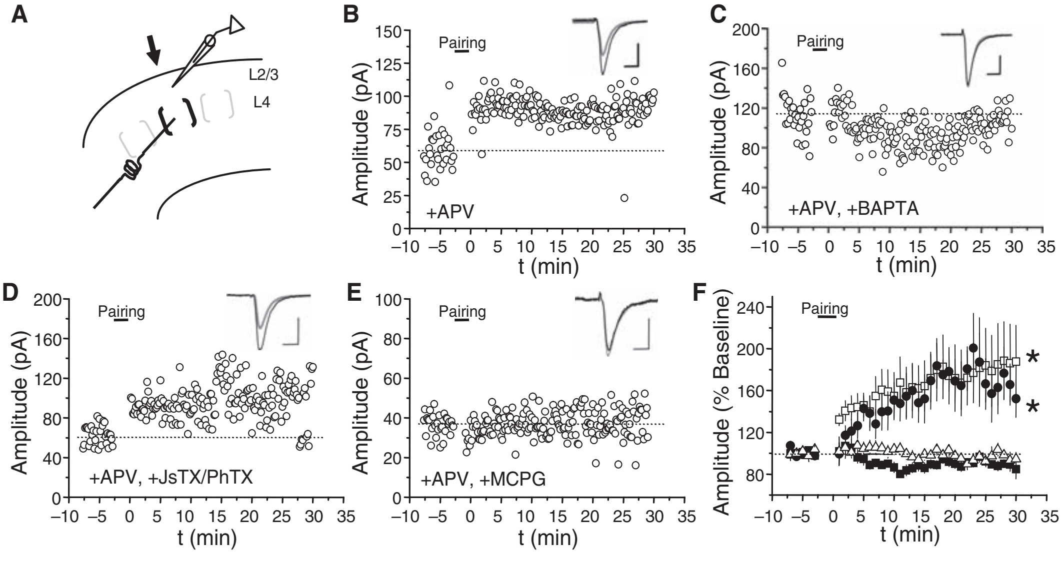

NMDAR function also occur in vivo, suppressing SWE-induced potentiation after its initial NMDAR-dependent induction? To address this, mice were subjected to 18 hours of SWE and then injected with CPP. At 24 hours after SWE onset (6 hours after CPP injection), acute brain slices were prepared and the properties of layer 4-2/3 synapses were assessed (Fig. 4A). The A:N ratio was significantly increased in CPP-treated as compared to SWE-only mice (Fig. 4, B and C; SWE/no drug 1.69 ± 0.12, $n = 9$ cells; SWE + CPP 2.24 ± 0.20, $n = 11$ cells; $P < 0.001$), and this increase could be attributed at least partly to an increase in Sr^{2+}-mEPSC amplitude (Fig. 4, D to F; spared/no drug 12.0 ± 0.46 pA, $n = 10$ cells; spared + CPP 13.98 ± 0.30 pA, $n = 14$ cells). Our results are consistent with at least one other study showing that NMDAR antagonists prevent the decay of LTP induced in vivo (*11*) and show that synaptic strengthening can be enhanced by precisely timed treatment with NMDAR antagonist.

In vivo treatment with the competitive mGluR group I antagonist 1-aminoindan-1,5-dicarboxylic acid (AIDA), 18 hours after the onset of SWE and 6 hours before slice preparation (Fig. 4A), resulted in the reduction of both the A:N ratio and Sr^{2+}-mEPSC amplitudes to control values (Fig. 4, B and C; A:N ratio: spared + AIDA 0.98 ± 0.07, $n = 9$ cells; Fig. 4, D to F; Sr^{2+}-mEPSC amplitude: spared + AIDA 9.56 ± 0.25 pA, $n = 11$ cells), indicating that mGluR activation is required at least for the maintenance of increased synaptic strength induced by in vivo sensory experience. Neither drug had any effect in control animals when administered 6 hours before animals were killed (Fig. 4, B and C; A:N ratio: control + CPP 1.02 ± 0.07, $n = 8$ cells; control + AIDA 1.02 ± 0.08, $n = 7$ cells; Fig. 4, D to F; Sr^{2+}-mEPSC amplitude: control + CPP 10.6 ± 0.26 pA, $n = 10$ cells; control + AIDA 10.12 ± 0.34 pA, $n = 9$ cells).

NMDAR subunit composition can be altered by sensory deprivation (*21*), with increased decay-time constants and heightened sensitivity to the NMDAR 2B subunit–specific antagonist ifenprodil at excitatory synapses (*7*, *22*). However, we found no evidence for an alteration in NMDAR properties at spared column layer 4-2/3 synapses with respect to decay kinetics, ifenprodil sensitivity, and current/voltage relations (fig. S3). Thus, the switch in NMDAR function probably occurs at the level of coupling to intracellular signaling cascades.

If NMDARs and mGluRs act simultaneously both to oppose and promote potentiation after its initiation, which process dominates with ongoing in vivo experience? To address this, we looked at the amplitude of quantal layer 4-2/3 AMPAR-EPSCs after 48 hours of SWE. Mean amplitude significantly increased with longer SWE treatment (48 hours of SWE: 14.25 ± 0.46 pA, $n = 12$ cells; versus 24 hours of SWE: 12.0 ± 0.46 pA, $n = 10$ cells; fig. S5). Thus, despite a switch in the ability of NMDARs to support potentiation, a physiologically relevant capacity for LTP is maintained in vivo, and cumulative experience can continue to increase synaptic strength. This augmentation probably depends on continued mGluR activation, because AIDA injection 6 hours before slice preparation abolished SWE-induced potentiation (Fig. 4, D to F).

These results do not rule out presynaptic modifications that could contribute to LTP or LTD in

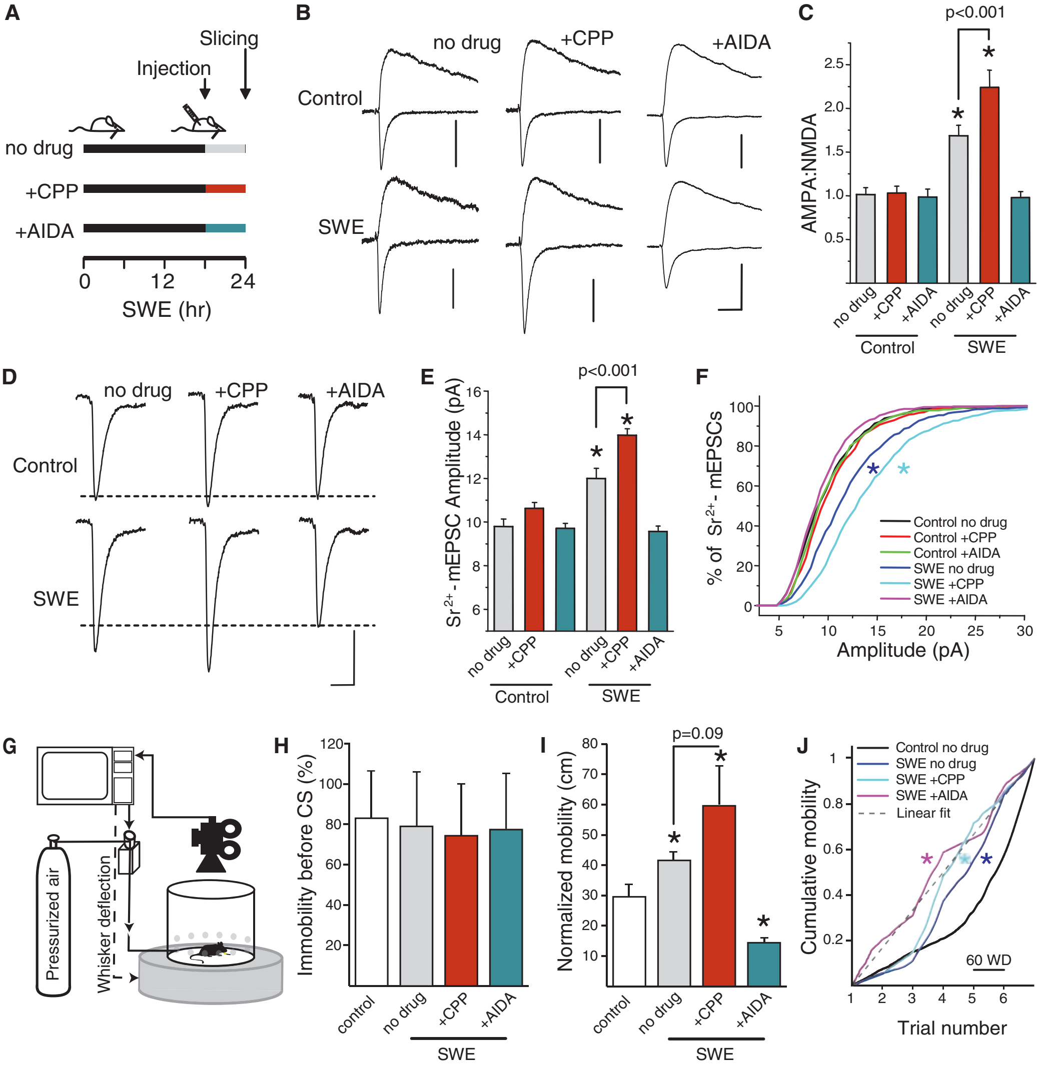

Fig. 4. NMDARs and mGluRs oppositely regulate synaptic strength and behavioral plasticity in vivo after SWE initiation. (**A**) Experimental timeline for joint SWE and in vivo drug delivery. CPP or AIDA was injected 18 hours after SWE onset. Slices were prepared 6 hours later. (**B**) Representative layer 4-2/3 EPSCs at $V_h = -70$ mV and +40 mV for each experimental group, scaled to peak current at +40 mV. Scale bars: control, 25 pA; control + CPP, 25 pA; control + AIDA, 40 pA; SWE spared, 20 pA; SWE spared + CPP, 30 pA; SWE spared + AIDA, 60 pA × 20 ms. (**C**) Mean A:N ratio for all groups. (**D**) Group-averaged Sr^{2+}-mEPSCs. Scale bar, 5 pA × 10 ms. (**E**) Mean Sr^{2+}-mEPSC amplitude. (**F**) Cumulative histogram of Sr^{2+}-mEPSC amplitude. $*P < 0.001$ versus control. (**G**) Experimental setup for associative tactile conditioning. Whisker deflections [CS, 100 ms (up) and 400 ms (down) at 2 Hz for 30 s] were paired with air-puff stimuli (US, 3 bars, 5 s overlapping with last 5 s of CS), and animal mobility was quantified from video recordings during conditioning by custom-written software. As animals learned to associate the whisker deflections with the air-puff stimuli, they tended to increase their mobility to avoid the upcoming US. (**H**) Fraction of time spent immobile in test chamber immediately before CS onset did not differ between test groups, indicating that whisker deprivation or drug treatment did not influence mobility. (**I**) Animal mobility normalized to movement before CS. $*P < 0.05$ versus control. (**J**) Cumulative distribution of mobility over all trials shows that SWE mice learned faster than controls and that SWE + CPP mice learned faster than SWE and control animals. SWE + AIDA animals failed to acquire the task, with equal mobility responses for each training trial (linear fit for cumulative mobility). $*P < 0.01$ for all pairwise comparisons across groups.

vitro (*23*); however, increased quantal amplitude after SWE and pharmacological treatments in vivo identify a clear postsynaptic component for the plasticity observed. Although the in vitro pairing protocol is a crude approximation of the kind of activity that layer 2/3 neurons experience in vivo, it combines a physiological frequency (*24*, *25*) of afferent stimulation (2 Hz) with NMDAR activation and predicts with remarkable accuracy the effects of in vivo SWE and pharmacological treatment.

Is this increase in synaptic strength correlated with learning behavior? To test this, we used an associative tactile conditioning task that pairs whisker deflection [conditioned stimulus (CS)] with a nonaversive, habituating air-puff stimulus [unconditioned stimulus (US); Fig. 4G and movies S1 and S2]. SWE mice showed increased mobility after whisker deflection as compared to controls, indicating that the SWE enhanced CS-US association (Fig. 4I). In parallel with their effects on synaptic strength in SWE mice, treatment with CPP and AIDA further enhanced or reduced associative learning (Fig. 4I). Analysis of changes in mobility over the course of task acquisition shows that SWE + CPP–treated animals acquired the CS-US association significantly faster than did SWE animals (Fig. 4J). These data indicate that increased synaptic strength in the barrel cortex is associated with enhanced performance in a whisker-dependent learning task, and that NMDAR and mGluR antagonists similarly affect synaptic strength and behavioral output.

Why doesn't normal sensory experience (that is, when all whiskers are intact) result in a similar occlusion of NMDAR-dependent LTP? Compared to SWE, this stimulus may not be sufficiently strong to induce a switch in NMDAR and mGluR properties. However, in both our experiments and many others [see, for example (*26*, *27*)], a fraction of neurons failed to demonstrate NMDAR-dependent LTP. It is tempting to speculate that in these cells, an mGluR-dependent form of LTP might be observed in the presence of NMDAR antagonists.

Our results indicate that after the initiation of LTP-like processes by sensory experience, a capacity for further synaptic strengthening is preserved and depends on mGluR activation. Because mGluR-mediated synaptic strengthening was observed both in vitro and in vivo, this is likely to be a physiologically relevant mechanism that may explain why an apparent "ceiling" for LTP does not negate the benefits of cumulative experience in enhancing response properties in the neocortex.

References and Notes

1. R. C. Malenka, M. F. Bear, *Neuron* **44**, 5 (2004).
2. M. S. Rioult-Pedotti, D. Friedman, J. P. Donoghue, *Science* **290**, 533 (2000).
3. B. Sacchetti *et al.*, *Eur. J. Neurosci.* **15**, 143 (2002).
4. J. R. Whitlock, A. J. Heynen, M. G. Shuler, M. F. Bear, *Science* **313**, 1093 (2006).
5. W. C. Abraham, W. P. Tate, *Prog. Neurobiol.* **52**, 303 (1997).
6. N. Hardingham *et al.*, *J. Neurosci.* **23**, 4428 (2003).
7. R. L. Clem, A. Barth, *Neuron* **49**, 663 (2006).
8. S. Glazewski, B. L. Benedetti, A. L. Barth, *J. Neurosci.* **27**, 3910 (2007).
9. A. L. Barth, R. C. Gerkin, K. L. Dean, *J. Neurosci.* **24**, 6466 (2004).
10. C. Kentros *et al.*, *Science* **280**, 2121 (1998).
11. D. M. Villarreal, V. Do, E. Haddad, B. E. Derrick, *Nat. Neurosci.* **5**, 48 (2002).
12. J. G. Gu, C. Albuquerque, C. J. Lee, A. B. MacDermott, *Nature* **381**, 793 (1996).
13. N. K. Mahanty, P. Sah, *Nature* **394**, 683 (1998).
14. W. P. Ge *et al.*, *Science* **312**, 1533 (2006).
15. C. J. McBain, T. J. DiChiara, J. A. Kauer, *J. Neurosci.* **14**, 4433 (1994).
16. Y. Perez, F. Morin, J. C. Lacaille, *Proc. Natl. Acad. Sci. U.S.A.* **98**, 9401 (2001).
17. E. D'Angelo, P. Rossi, S. Armano, V. Taglietti, *J. Neurophysiol.* **81**, 277 (1999).
18. O. Lee, C. J. Lee, S. Choi, *Neuroreport* **13**, 685 (2002).
19. Z. I. Bashir *et al.*, *Nature* **363**, 347 (1993).
20. Y. M. Lu *et al.*, *J. Neurosci.* **17**, 5196 (1997).
21. E. M. Quinlan, D. H. Olstein, M. F. Bear, *Proc. Natl. Acad. Sci. U.S.A.* **96**, 12876 (1999).
22. B. D. Philpot, A. K. Sekhar, H. Z. Shouval, M. F. Bear, *Neuron* **29**, 157 (2001).
23. V. A. Bender, K. J. Bender, D. J. Brasier, D. E. Feldman, *J. Neurosci.* **26**, 4166 (2006).
24. T. Celikel, B. Sakmann, *Proc. Natl. Acad. Sci. U.S.A.* **104**, 1395 (2007).
25. T. Celikel, V. A. Szostak, D. E. Feldman, *Nat. Neurosci.* **7**, 534 (2004).
26. A. L. Barth, R. C. Malenka, *Nat. Neurosci.* **4**, 235 (2001).
27. C. C. Petersen, R. C. Malenka, R. A. Nicoll, J. J. Hopfield, *Proc. Natl. Acad. Sci. U.S.A.* **95**, 4732 (1998).
28. Research was supported by grant DA017188-01 from the National Institutes of Health. We thank B. Benedetti for in vivo recording data and P. Castillo, M. Wheeler, and K. Velanova for helpful discussions.

Supporting Online Material
www.sciencemag.org/cgi/content/full/319/5859/101/DC1
Materials and Methods
Figs. S1 to S6
References
Movies S1 and S2

16 April 2007; accepted 2 November 2007
10.1126/science.1143808

Small Circuits for Large Tasks: High-Speed Decision-Making in Archerfish

Thomas Schlegel and Stefan Schuster*

The enormous progress made in functional magnetic resonance imaging technology allows us to watch our brains engage in complex cognitive and social tasks. However, our understanding of what actually is computed in the underlying cellular networks is hindered by the vast numbers of neurons involved. Here, we describe a vertebrate system, shaped for top speed, in which a complex and plastic decision is performed by surprisingly small circuitry that can be studied at cellular resolution.

It is widely accepted that cognitive abilities such as making complex decisions require the enormous densities of highly interconnected cortical neurons. However, not all neurons within the areas labeled by functional magnetic resonance imaging (fMRI) as active during complex cognitive tasks [e.g., (*1*–*4*)] might be crucial for the performance, and perhaps much smaller "minimum circuitry" would suffice. Here, we provide evidence for this view in a vertebrate system, in which a highly complex decision is made by surprisingly compact neural circuitry.

Archerfish are renowned for their ability to down aerial insect prey with precisely aimed shots of water. As soon as their successful shots dislodge their prey from the substrate, the fish must make an important decision (Fig. 1). On the basis of at least three independently varying initial parameters of prey motion, they must initiate an adapted open-loop start that, without requiring any further sensory information, rotates the fish toward where their prey will later land and pushes them off with a speed matched to distance (*5*–*7*). Due to heavy competition from peers and other surface-feeding fish, this decision must be made rapidly and accurately. The decision requires learning and is absent when competition is lacking, and its tuning appears to involve high levels of generalization and abstraction (*8*–*10*).

In principle, archerfish could use a priori information to prime and speed up their decisions: Observing the shot would signal all school members when aerial motion needs to be responded to and could perhaps even signal the likelihood of particular trajectories. To test the importance of such contextual information, we completely deprived the fish of it. In these experiments prey was initially invisible to the fish, and the experimenter could at any time elicit a prey trajectory with speed and angle randomly selected from large ranges (matching the corresponding ranges in naturally dislodged prey) (fig. S1). Surprisingly, even when shooting-related information was thus not available for priming the decisions, the minimum and average latencies required for accurate responses were not longer than in the control, and average latency appeared to be even slightly reduced (by about 5 ms, $P = 0.034$; Fig. 2B; table S1). Furthermore, with only target motion available, the fish were just as accurate as when additional contextual information was freely available ($P = 0.212$; Fig. 2C; table S1). These findings show that motion cues are necessary and sufficient to trigger the archerfish's high-speed decisions and this, in turn, places full control over all decision-relevant parameters in the hands of the experimenter.

Prospective shooters must precisely pinpoint the location of their aerial prey (*11*) and could thus focus

---

Universität Erlangen-Nürnberg Institut für Zoologie II, Staudtstrasse 5, D-91058 Erlangen, Germany.

*To whom correspondence should be addressed. E-mail: sschuste@biologie.uni-erlangen.de

the processing of aerial motion signals to the region around their prey. To test whether such a focus, set a priori, was critical to the performance, we cued the fish to one of three platforms, but then started prey motion from any of the other platforms, a set distance from where the fish would assume motion to occur (Fig. 3A). Surprisingly, even substantial horizontal offsets of 20 cm—34° seen from below the cue platform—did not affect response latency ($P = 0.103$; table S1). Latency increased only at an offset between expected and actual takeoff of 40 cm, or about 53° of visual angle (Fig. 3B; $P < 0.001$; table S1). Minimum latency, observed in the fastest responses, was also only affected at this large offset (table S2). Furthermore, accuracy was completely unaffected by displacing the start point of the prey's course (Fig. 3C; $P > 0.3$ in all cases). Hence, the fish did not a priori limit or enhance the processing of target motion to a region of interest.

Yet the fish do exploit selective attention—however, not based on a priori information but rather as an integral part of their complex decision. To test whether the fish averaged motion signals over extended regions, as suggested by the findings of Fig. 3, B and C, we simultaneously blew off two similar-sized, initially invisible flies from the start platform. Both flies moved at approximately equal speed but in opposing directions (Fig. 3D), and averaging would make the fish choose the point of impact of the flies' center of mass. However, when challenged in this way, the fish immediately and highly selectively decided which of the two conflicting motion signals to take into account. Starts were directed not at the point predicted by averaging or any intermediate point but right at the point of impact of the chosen fly (Fig. 3F; error distributions not significantly different in one-fly and two-flies conditions, $P = 0.10$). Furthermore, the added decision which of the two targets to choose did not increase latency (Fig. 3E; $P = 0.13$; table S1). The decision which fly to attend to was not made at random: Although the choices were not per se explained by differences in the speed of the two flies or by the angle between the fly's motion and the fish's initial orientation, the fish significantly preferred that fly whose later landing point lay closer: Chosen flies had an average distance of 266 mm (SEM = 14.7 mm; range: 26 to 624 mm; $n = 80$), whereas rejected flies were significantly ($P < 0.001$) farther away (average distance: 353 mm; SEM = 12.6 mm; range: 73 to 597 mm, $n = 80$). If it saved the fish at least 1 cm of travel (which it did in 77 cases), then the fish chose the closer fly with a probability of 68%.

The decisions showed a further interesting element of complexity. When changes in latency occurred, these were not accompanied by changes in accuracy. Figure 4A illustrates this finding for experiments in which changes in the visual contrast did affect latency (Fig. 4B) but not accuracy. This implies that latency is adjusted so as to guarantee a minimum in precision, thus avoiding energy being wasted with prematurely initiated inaccurate responses.

In the previous experiments, we noted accurately aimed responses at latencies down to 40 ms (table S2). To explore whether this value sets the limit of the archerfish's decision-speed, we increased the visual contrast between the moving fly and its background (Fig. 4B). Average latencies obtained at lower visual contrast lay in the range reported previously (*6*, *7*), but the highest contrast level produced a high proportion of precisely aimed predictive starts that were initiated after only a 40-ms latency (table S2 and Fig. 4A). However, the minimum decision time of about 40 ms could not be reduced further.

Our findings place a considerable upper bound on the neuronal circuitry that underlies the archerfish's complex decision-making. The fish initiated adapted fast-starts as rapidly as 40 ms after the onset of the motion signals that were necessary and sufficient (Figs. 2 and 3) to trigger the decisions. The starts recruit the archerfish's C-start escape network (*5*), which in most teleosts (*12*–*14*), including cichlids (*15*), consists of Mauthner's cell–associated identified reticulospinal neurons and drives life-saving escapes but also voluntary behaviors (*16*). In goldfish, the known path from the retina over the tectum to the ventral dendrite of the Mauthner's cell to the onset of muscle contraction involves a sensomotor delay of 35 ms (*17*, *18*). Even if timing was slightly different in archerfish [and constrained mainly by phototransduction (*19*-*21*)], to leave a more realistic 10 to 15 ms of sampling before the decision, the computations that underlie its decision must be done in the retina and the fastest output pathway. Retinal computations have already elegantly explained a range of

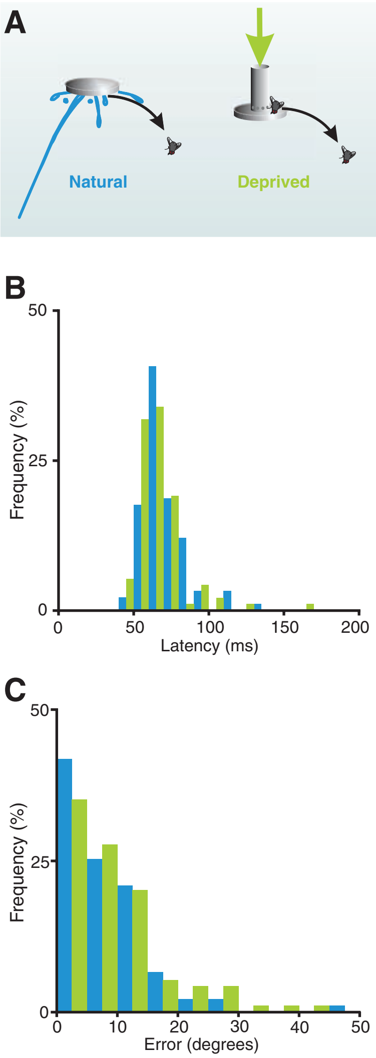

Fig. 2. Archerfish high-speed decisions do not require contextual a priori information. (**A**) In the "natural condition" (blue), fish dislodged a target fly from the bottom of a small disk. In the "deprived condition" (green), the fly was placed on top of the disk where it could not be seen by the fish. Motion then was triggered not by a fish's shot but by an airstream (green arrow) commanded by the experimenter. Depriving the fish from shooting-related contextual cues did not increase latency (**B**) nor decrease accuracy (**C**) of the responses (table S1). Histograms are based on $n = 91$ (natural) and $n = 94$ (deprived) responses. Binning starts at zero and counts relating to the natural (deprived) condition are shown in blue (green) in the left (right) half of each bin. Bin widths are 10 ms (B) and 5° in (C).

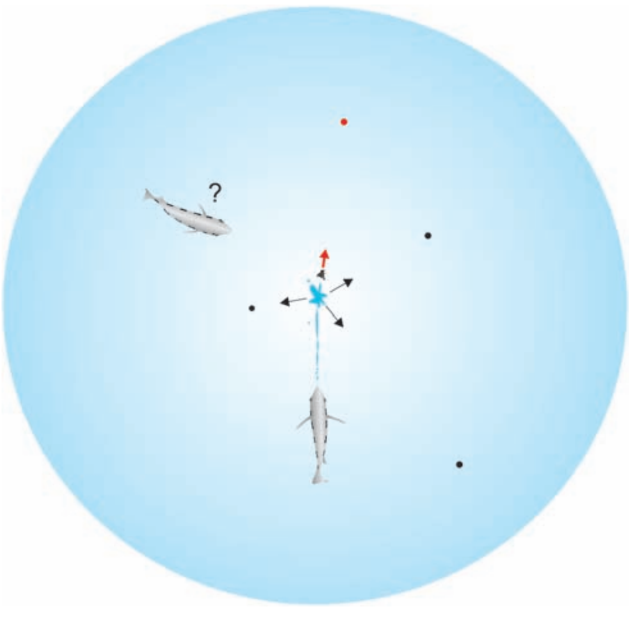

Fig. 1. High-speed decision-making in hunting archerfish. At the time a shot (blue) is on its way toward an insect prey, the insect's later point of impact may be anywhere within a large area (blue circle; drawn to scale as appropriate for the present experiments). Previous work has shown that the fish quickly watch their prey's initial motion to decide how much to turn and at what speed to start so as to be at the right spot at the right time. The decision is made on the basis of at least three variables that vary independently over large ranges: the initial speed, direction, and height of the insect prey. Arrows and dots indicate possible initial motion of the prey and corresponding impact points.

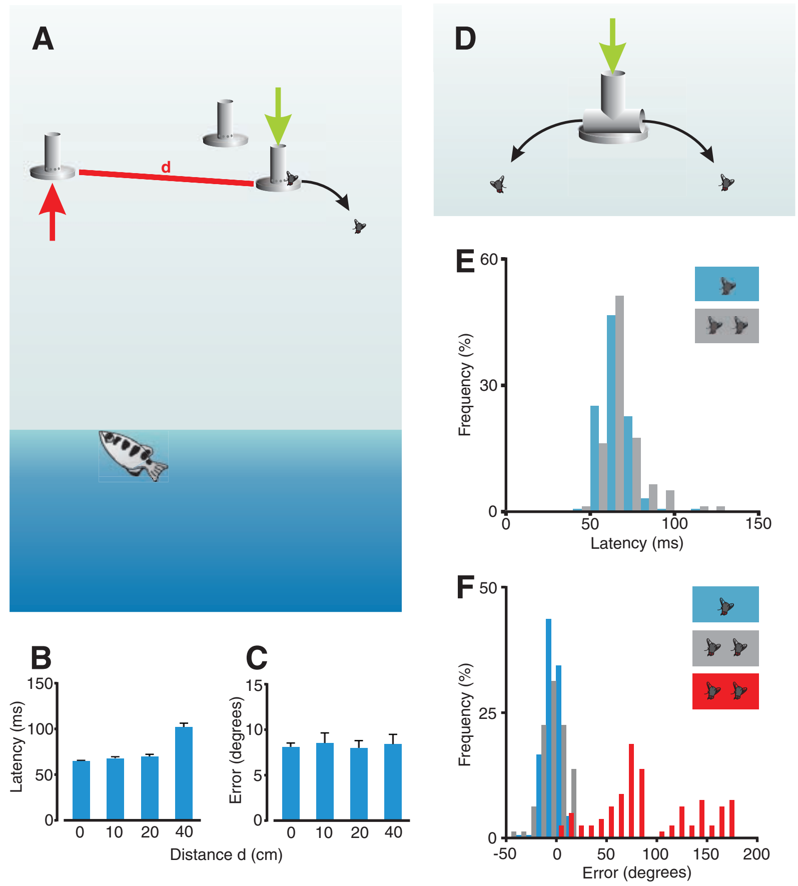

Fig. 3. Selective attention is part of the high-speed decision. (**A**) Fish were cued to one of three start disks (red arrow), but the initially invisible fly was started a set, randomly assigned, distance *d* from that disk. Response latency increased only at substantial distances (**B**), and the accuracy of the response was unaffected (**C**). Total of $n = 556$ responses. (**D**) When two flies were simultaneously sent from the disk into opposing directions, the fish immediately and selectively attended to just one of the two flies. Latency (**E**) and aims taken (**F**) in the two-fly experiments were not statistically different from those in controls with just one fly leaving the start platform (blue). (E) Bins as in Fig. 2B. (F) Direction of aim relative to the later impact point of the chosen fly (gray; control: blue) and with respect to the point predicted by motion-averaging (red). Negative signs indicate errors in directions toward the start platform. First positive bin 0° to 10°, blue (gray) columns shown in first (second) half of bin, red columns placed in bin's center. Analysis of $n = 163$ (80) single (two) fly starts.

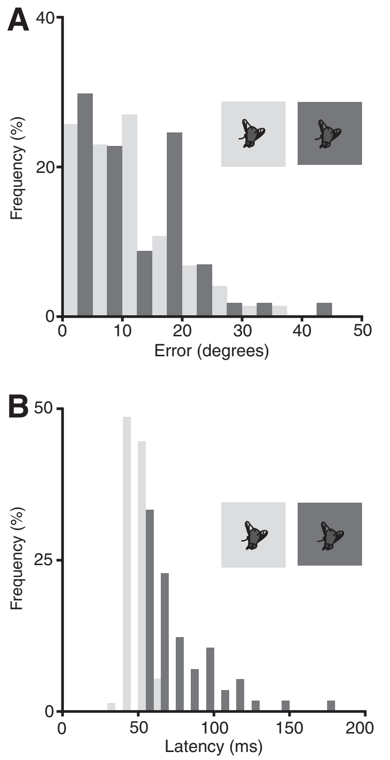

Fig. 4. Top decision speed pins down the underlying network. Although changing the visual contrast between the prey and its immediate background did not significantly affect accuracy (**A**), it strongly affected latency (**B**). (A) Histogram showing the magnitude of the fish's error in aiming at high contrast ($C = 0.51$) and low contrast ($C = 0.061$). Both contrasts were different from the contrast used in the previous experiments. (B) High contrast shifts the distribution of latency and enables responses only 40 ms after the onset of prey motion. Binning as in Fig. 2, B and C, and based on $n = 74$ starts at high (light) and $n = 57$ at low (dark) contrast.

complex visual tasks (*22*–*24*) and could be the building blocks of the complex processing that would provide the archerfish's decision circuitry with quick and yet accurate estimates of speed, direction, and height of aerial prey. The later part of the circuitry must then combine the signals from the two eyes with signals coding for the fish's spatial position, accommodation, and gaze direction to transform them into an adapted motor pattern. Given our knowledge on teleost Mauthner's cell–associated C-start escape circuitry (*12*–*18*), it is likely that a small network of six identified neurons plays a key role in the initial decision, with the further (accessible) (*12*) set of serially repeated identified cells in the hindbrain contributing to its fine-tuning (*10*).

In conclusion, our data show that even complex decisions can be made rapidly and accurately by a relatively small number of neurons that are likely to offer outstanding opportunities for an approach at the cellular level (*10*, *12*–*14*). Furthermore, because the circuitry does not require shooting-related inputs (Figs. 2 and 3), it can be studied in vivo, targeting both the ongoing processing and the ways in which the fish tunes its decision-making circuitry to the laws of its outer world. Minimum circuits such as that used in archerfish decision-making might be much more widespread and could provide us with simpler systems to explore the neuronal mechanisms of decision-making and other "cognitive" computations, opening up a way of understanding how cognitive networks have evolved.

References and Notes

1. S. M. Tom, C. R. Fox, C. Trepel, R. A. Poldrack, *Science* **315**, 515 (2007).
2. K. Nelissen, G. Luppino, W. Vanduffel, G. Rizzolatti, G. A. Orban, *Science* **310**, 332 (2005).
3. A. G. Sanfey, J. K. Rilling, J. A. Aronson, L. E. Nystrom, J. D. Cohen, *Science* **300**, 1755 (2003).
4. S. Dehaene, E. Spelke, P. Pinel, R. Stanescu, S. Tsivkin, *Science* **284**, 970 (1999).
5. S. Wöhl, S. Schuster, *J. Exp. Biol.* **210**, 311 (2007).
6. S. Rossel, J. Corlija, S. Schuster, *J. Exp. Biol.* **205**, 3321 (2002).
7. S. Wöhl, S. Schuster, *J. Exp. Biol.* **209**, 141 (2006).
8. S. Schuster, S. Rossel, A. Schmidtmann, I. Jäger, J. Poralla, *Curr. Biol.* **14**, 1565 (2004).
9. S. Schuster, S. Wöhl, M. Griebsch, I. Klostermeier, *Curr. Biol.* **16**, 378 (2006).
10. Supporting data are available on *Science* Online.
11. L. M. Dill, *Behav. Ecol. Sociobiol.* **2**, 169 (1977).
12. J. R. Fetcho, D. H. Bhatt, *Curr. Opin. Neurobiol.* **14**, 707 (2004).
13. H. Korn, D. S. Faber, *Neuron* **47**, 13 (2005).
14. J. R. Fetcho, D. M. O'Malley, *Curr. Opin. Neurobiol.* **7**, 832 (1997).
15. J. G. Canfield, *Brain Behav. Evol.* **67**, 188 (2006).
16. J. G. Canfield, *J. Comp. Physiol. A* **193**, 1055 (2007).
17. S. J. Zottoli, A. T. Hordes, D. S. Faber, *Brain Res.* **401**, 113 (1987).
18. T. Preuss, P. E. Osei-Bonsu, S. A. Weiss, C. Wang, D. S. Faber, *J. Neurosci.* **26**, 3454 (2006).
19. P. Lennie, *Vision Res.* **21**, 815 (1981).
20. J. L. Schnapf, T. W. Kraft, D. A. Baylor, *Nature* **325**, 439 (1987).
21. D. M. Guthrie, J. Banks, *Vis. Neurosci.* **4**, 367 (1990).
22. B. P. Ölveczky, S. A. Baccus, M. Meister, *Nature* **423**, 401 (2003).
23. T. Hosoya, S. A. Baccus, M. Meister, *Nature* **436**, 71 (2005).
24. M. J. Berry II, I. H. Brivanlou, T. A. Jordan, M. Meister, *Nature* **398**, 334 (1999).
25. Supported by grants Schu 1470/2 and 5 from the Deutsche Forschungsgemeinschaft. We thank the referees, H. Wagner, J. Hemmi, A. Reichenbach, H. Brandstätter, and P. Übel for their help.

Supporting Online Material

www.sciencemag.org/cgi/content/full/319/5859/104/DC1
Materials and Methods
SOM Text
Fig. S1
Tables S1 and S2
References

15 August 2007; accepted 23 November 2007
10.1126/science.1149265

Debubbler Series

The Systec Debubbler Series for low-pressure diagnostic and life science instruments improves on passive bubble-trap technology with active bubble removal and transfer-line degassing. Three configurations—active debubbler, degasser/debubbler, or transfer-line degasser—offer the choice of removing bubbles with or without also removing dissolved system gasses. Highly efficient online active debubbling helps equipment manufacturers improve dispensing precision, reduce sample loss and reagent usage, and improve analytical accuracy in high-throughput applications. The new series features an innovative semi-permeable degassing membrane to remove gases from dispensed liquids.

IDEX Health & Science
For information 360-679-2528
www.idex-hs.com

Gel Documentation System

The next generation DigiGenius budget gel documentation system features a high-resolution, computer-controlled camera, allowing molecular biologists to easily view images in real time on any computer. The 10-megapixel camera can separate even the closest band images. The camera can be linked via an interface to a computer in order to automate the camera's set up and images can be captured on either a flash card or computer. Users can choose to add compatible components to the basic system such as an ultraviolet transilluminator or white or blue conversion screens. It comes with a safety hood upgradeable to a full mini-darkroom.

Syngene
For information 800-686-4407
www.syngene.com

Sulfur-Compound Measurement

A sensitive new analytical system enables routine measurement of thiols, thioesters, disulfides, and other sulfur-containing compounds. Sulfur-containing compounds are critical to a variety of biologically and clinically important processes, from oxidative metabolism, to cardiovascular and neurodegenerative-disease mechanisms, to signal transduction, but measuring them has been difficult. The new system incorporates a specially developed electrochemical cell with a unique boron-doped diamond (BDD) working electrode coupled with the Coulochem III ECD system. The electrode provides excellent sensitivity and durability, while eliminating the problems of fouling, high background, and mobile phase oxidation associated with earlier electrochemical detection (ECD) systems.

ESA Analytical
For information +44 1844-239381
www.esainc.com

Literature

Precision Optical Filters for Fluorescence Microscopy is a new catalog that includes 15 new high-performance sets for fluorescent proteins and 10 new sets for fluorescence resonance energy transfer. These new products complement an extensive selection of dye-specific filter sets for all single-label and multi-label microscopy applications, including quantum dots, multiplex fluorescence in situ hybridization, ratio imaging, confocal, and multi-photon. Other resources include a fluorophore reference table, light source and detector spectral data, an explanation of filter nomenclature, guidelines for choosing the optimal filter sets, and a list of components organized by wavelength.

Omega Optical
For information 802-254-2690
www.omegafilters.com

Distillation System

The Lab-Crest Midi-Dist Distillation System saves space and time in laboratory testing and analysis requiring distillation. Designed to allow replacement of costly macro distillation techniques, these compact units allow multiple samples to be prepared for analysis quickly and easily. The heater, holder, manifolds, tubing, couplings, and controls are integrated and designed to simplify set-up and use. It is comprised of 10 complete borosilicate glass units and a 10-position aluminum heat block and apparatus holder, coated with Teflon for corrosion resistance. Glassware, heater, water, and vacuum manifolds, controls, and connections are integrated into a single compact system. The system can handle up to 10 50-ml liquid or sludge samples.

Andrews Glass Co
For information 800-845-0026
www.andrews-glass.com

Multi-Parameter System

Version 2.0 of the LiQC multi-parameter system is for simultaneous determination of density, refractive index, pH/conductivity, and color. The instrument combines single measurements into one automated process. A sample vial is filled, placed on an automatic sample changer, and assigned a barcode label. The LiQC automatically completes every subsequent step: choosing the appropriate method, pumping the sample into the various flow-through cells, and performing all measurements. The instrument evaluates results statistically, compares them to specifications, and transfers them to laboratory information systems. The LiQC thoroughly cleans and dries the measuring cells before moving on to the next sample.

Mettler Toledo
For information 614-438-4505
www.mt.com

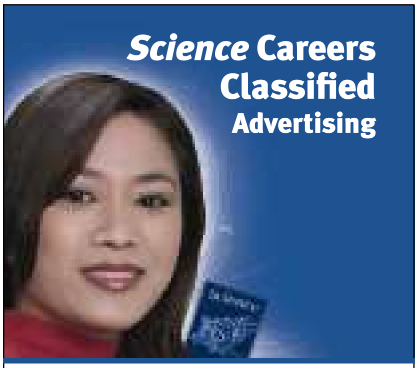

We've got **Careers** down to a **Science**.

For full advertising details, go to **www.sciencecareers.org** and click on **For Advertisers,** or call one of our representatives.

United States & Canada

E-mail: advertise@sciencecareers.org
Fax: 202-289-6742

IAN KING
Recruitment Sales Manager/
Industry – US & Canada
Phone: 202-326-6528

ALEXIS FLEMING
Northeast Academic
Phone: 202-326-6578

TINA BURKS
Southeast Academic
Phone: 202-326-6577

DARYL ANDERSON
Midwest/Canada Academic
Phone: 202-326-6543

NICHOLAS HINTIBIDZE
West Academic
Phone: 202-326-6533

Europe & International

E-mail: ads@science-int.co.uk
Fax: +44 (0) 1223 326532

TRACY HOLMES Sales Manager
Phone: +44 (0) 1223 326525

ALEX PALMER
Phone: +44 (0) 1223 326527

ALESSANDRA SORGENTE
Phone: +44 (0) 1223 326529

MARIUM HUDDA
Phone: +44 (0) 1223 326517

LOUISE MOORE
Phone: +44 (0) 1223 326528

To subscribe to *Science*:
In US/Canada call 202-326-6417 or 1-800-731-4939
In the rest of the world call +44 (0) 1223-326-515

Science Careers
From the journal *Science* AAAS

POSITIONS OPEN

POSITION DESCRIPTION: LIMNOLOGIST

Southern Illinois University Carbondale (SIUC). The College of Science seeks an outstanding scientist in the general area of limnology/freshwater ecology as an ongoing part of SIUC's commitment to enhance interdisciplinary research **(website: http://news.siu.edu/s150/).** Southern Illinois University Carbondale is a large, public, comprehensive research-intensive university situated in a pleasant, small town setting southeast of St. Louis.

The Department of Zoology at SIUC invites applications for a tenure-track position as an **ASSISTANT PROFESSOR** with a start date of August 16, 2008. Applicants must hold a Ph.D. or other appropriate doctoral degree and have a record of relevant postdoctoral research training by the time of appointment. The applicant must also have an externally funded research program that employs modern research techniques or the potential for developing one, as well as a significant record of peer-reviewed publications. The successful candidate will enhance and complement existing programmatic strengths in the areas of ecology, fisheries biology, conservation, biodiversity, and evolutionary biology. Possible research areas include (but are not limited to) trophic interactions, population or community ecology, ecosystem dynamics, ecological stoichiometry, or watershed/landscape-level processes. Modern research facilities and startup funds are available. The successful applicant is expected to teach a limnology course, and undergraduate/graduate courses dependent upon the individual's expertise and program needs. The Department of Zoology, with a faculty of 25, offers B.S., M.S., and Ph.D. degrees **(website: http://www.science.siu.edu/zoology/).**

Applications: Review of applications will begin February 15, 2008, and continue until the position is filled. Applicants should submit curriculum vitae, a statement of teaching and research interests, and the names and addresses of at least three references to: **Limnology Search Committee Chair, Department of Zoology, Mail Code 6501, Southern Illinois University Carbondale, 1125 Lincoln Drive, Carbondale, IL 62901. E-mail: zoology@zoology.siu.edu.**

SIUC is an Affirmative Action/Equal Opportunity Employer that strives to develop a diverse faculty and staff and to increase its potential to serve a diverse student population. All applications are welcomed and encouraged and will receive consideration.

BIOLOGICAL SCIENCE PEDAGOGIST

Saint Louis University, a Catholic, Jesuit institution dedicated to student learning, research, health care, and service, is seeking applicants for a tenure-track appointment in the Department of Biology, beginning fall 2008. We seek a **PEDAGOGIST** in the biological sciences at the **ASSISTANT PROFESSOR** level possessing strong teaching and research skills and a publication record commensurate with a Ph.D program. The successful candidate is expected to contribute to existing introductory, undergraduate, and graduate courses in the Department, advise and mentor undergraduate and graduate students, and conduct research, and develop new pedagogical programs in the area of biological sciences. Development of programs on campus or at the Reis Biological Station in the Ozark Mountains is desirable. The candidate is expected to develop a record of external funding in the field of science education research. A Ph.D. degree is required and postdoctoral experience desirable. Interested candidates must submit their application, statements of teaching philosophy and research plans, and curriculum vitae to **website: http://jobs.slu.edu.** Three letters of recommendation and reprints are to be sent to: **Dr. Nevin Aspinwall, Chair, Biological Science Pedagogist Search Committee, Department of Biology, 3507 Laclede Avenue, St. Louis, MO 63103.** Review of applications will commence January 30, 2008, and continue until the position is filled. *Saint Louis University is an Affirmative Action, Equal Employment Employer and encourages nominations of and applications from women and minorities.*

POSITIONS OPEN

FACULTY POSITION in EPITHELIAL BIOLOGY

Department of Cell Biology and Center for Respiratory Health
Emory University School of Medicine

Applications are invited for a tenure-track faculty position at the **ASSISTANT, ASSOCIATE, or FULL PROFESSOR** level in epithelial biology. All aspects of epithelial biology are welcome as is the use of model genetic systems. Relevant faculty research programs include epithelial cell junctions, epithelial polarity, ion channel biology, membrane transport, flagellar dynamics, and molecular motors, among many others in cell, developmental, and neurobiology. The successful applicant will be a member of the Department of Cell Biology as well as the Emory Center for Respiratory Health. Within the past ten years, the Department of Cell Biology has recruited ten new investigators, including a new Chair, and is housed in the new Whitehead Biomedical Research Building. Emory bioscience faculty participate in one or more of eight rapidly growing, interdisciplinary predoctoral training programs. For questions contact **e-mail: search@cellbio.emory.edu.** Applications will be considered until the position is filled, with interviews beginning in early 2008. Send curriculum vitae, a brief research plan, representative reprints, and three reference letters to:

Epithelial Biology Search Committee
Department of Cell Biology
Emory University
School of Medicine, Room 400
Whitehead Research Building
615 Michael Street, Atlanta, GA 30322

Emory University is an Equal Opportunity Employer. Women and members of underrepresented racial and ethnic groups are encouraged to apply.

VISITING ASSISTANT PROFESSOR, BIOLOGY

The Biology Department at Loyola College is offering a one-year Visiting Assistant Professor position to begin in the fall of 2008. The position is intended to be a training program in which the successful applicant will be given the opportunity to teach introductory and upper-level courses in biology, be engaged in research involving undergraduate students, participate in departmental and college-wide service, and to receive guidance and mentoring from faculty that will prepare the candidate for a future career in academia. The successful applicant will be expected to teach introductory courses in cell and molecular biology, and organismal biology, upper-level courses in one or more of the following areas: neurobiology, vertebrate morphology, and cell biology. Candidates should have a Ph.D in biology or a related discipline.

To apply, please apply electronically at **website: http://www.loyola.edu/careers** and include curriculum vitae, statement of teaching and research interests, a teaching philosophy, and contact information for three references.

For more information please contact: **Monika Matthews (e-mail: mmatthews@loyola.edu, telephone: 410-617-2642), Administrative Assistant to the Biology Department,** or **Dr. David Rivers (e-mail: drivers@loyola.edu), Chair of the Biology Department.** Applications received by March 15, 2008, will receive full consideration.

For more information about Loyola, please review our **websites: http://www.loyola.edu/** and **http://www.loyola.edu./biology/.**

Loyola College is a selective comprehensive, Jesuit Catholic Institution that welcomes applicants from all backgrounds who can contribute to its educational mission. Our University values campus diversity and demonstrates this in campus initiatives; we particularly encourage members of historically underrepresented groups to apply.

Industrial Biotechnology at DuPont India

E.I. du Pont de Nemours and Company is expanding its technical and engineering capabilities and is locating a Research and Development facility within its wholly-owned subsidiary, DuPont, India, in Hyderabad. As part of this plan, we are establishing an Industrial Biotechnology Research and Development group, which will focus on a broad range of activities associated with the production of fuels, chemicals, and materials from renewable resources using modern tools of molecular biology, biochemistry, and fermentation sciences. DuPont has recently been named one of the best employers in the biotechnology and pharmaceutical industry in the 2007 Science Magazine Top Employers Survey.

Presently, we are looking for self-motivated and energetic individuals with relevant backgrounds to become a part of this exciting global R&D effort based in India.

RESEARCH SCIENTIST/PRINCIPAL INVESTIGATOR

BIOCHEMIST

The successful candidate will use knowledge of biochemistry while working in teams to develop biocatalytic routes for making chemicals and materials. The role of the biochemist will be:

- To identify potential enzyme catalysts in the design phase of the project, to troubleshoot and to solve problems associated with the function of those enzymes in the process
- To work with molecular biologists to carry out directed evolution by designing and implementing screens for improved biocatalysts, and perform follow-up characterization of hits

Minimum Skills/Qualifications:

- PhD in Biochemistry, Chemistry or a related discipline
- 2+ years of postdoctoral experience
- Advanced knowledge of Biochemistry with emphasis on enzyme function and analysis
- Demonstrated ability in Analytical Biochemistry

MOLECULAR BIOLOGIST

This position involves working in multidisciplinary teams to engineer microbes (bacteria, yeast or fungi) for the economic production of industrial compounds. The successful applicant will have expertise in molecular biology and genetics as well as microbial metabolism and biochemistry. The work may include working with biochemists to evaluate biocatalyst performance, and carry out directed evolution to improve native biocatlysts.

Minimum Skills/Qualifications:

- PhD in Biotechnology, Biochemistry, Biology, Microbiology or a related discipline
- 2+ years of postdoctoral experience
- Advanced knowledge of Molecular Biology

FERMENTATION SCIENTIST

The successful candidate will interact with a larger multi-disciplinary group including microbial physiologists, enzymologists, molecular geneticists and engineers in support of metabolic engineering and biocatalysis programs within DuPont. The successful candidate will possess a strong background in biochemistry, analytical chemistry and microbial physiology.

Minimum Skills/Qualifications:

- PhD in Chemical or Biochemical Engineering, Biology, Microbiology or a related discipline
- 2+ years of postdoctoral experience
- Demonstrated ability to design, execute and analyze fermentation experiments

RESEARCH ASSOCIATE

BIOCHEMIST

We seek associate scientists to work in teams to develop biological routes for making chemicals and materials. The role of the associate biochemist is to generate, purify, and assay enzyme catalysts in the design and implementation phases of the project. The work may include working with molecular biologists to carry out directed evolution by implementing screens for improved biocatalysts and doing follow-up characterization of hits. The candidate will be expected to maintain expertise within multiple technologies in the areas of biochemistry.

Minimum Skills/Qualifications:

- MS in Biochemistry, Chemistry or a related discipline
- Knowledge of Biochemistry with emphasis on protein purification, analysis of protein purity and expression levels, and analytical methods or enzyme activity
- Demonstrated ability in Analytical Biochemistry

MOLECULAR BIOLOGIST

This position involves engineering microbes (bacteria, yeast or fungi) for the economic production of industrial compounds. The work may include working with biochemists to evaluate biocatalyst performance. The candidate will be expected to maintain expertise within multiple technologies in the areas of molecular biology.

Minimum Skills/Qualifications:

- MS in Biochemistry, Biology, Microbiology or a related discipline
- Knowledge of Molecular Biology with emphasis on purification of bacterial plasmids, PCR, primer design, restriction analysis, gel purification, cloning, transformation and growth of bacteria (including preparation of competent cells and electroporation), analysis and manipulation of DNA of sequences (i.e. Vector NTI)

FERMENTATION SCIENTIST

The successful candidate will interact with a larger multidisciplinary group including biochemists and molecular biologists, in support of metabolic engineering and biocatalysis programs. The candidate will be expected to maintain state-of-the-art knowledge in fermentation science and maintain expertise within multiple technologies in the areas of biocatalysis and metabolic engineering.

Minimum Skills/Qualifications:

- BTech/MTech/MS in Chemical or Biochemical Engineering, or MS in Biology, Microbiology or a related discipline
- Demonstrated ability to execute and analyze fermentation experiments

---

For all research scientist/principal investigator positions, the person shall be expected to maintain state-of-the-art knowledge in Biochemistry/Molecular Biology/Fermentation Science and integrate that into DuPont programs where appropriate, and to maintain expertise within multiple technologies in the areas of biocatalysis and metabolic engineering.

For all of the above position, the candidate will be expected to participate in multi-functional research teams, and to communicate effectively with their peers both in Hyderabad and in the US via presentations and written reports. Candidates should also be able to thrive in a fast-paced global research team environment and be committed to the use of biotechnology.

Qualified candidates should apply through DuPont's career web-page: http://careers.dupont.com
Click on: jobs by region/Asia Pacific/India.

DUPONT

The miracles of science™

Division of Cancer Biology
Cancer Etiology Branch
Microbiologist/Chemist/Biologist

With nation-wide responsibility for improving the health and well being of all Americans, the Department of Health and Human Services (DHHS) oversees the biomedical research programs of the National Institutes of Health and those of NIH's research Institutes.

The National Cancer Institute (NCI) at the NIH is seeking a Microbiologist, Chemist, or Biologist to fill the position of Chief in the Cancer Etiology Branch (CEB). This branch administers a large portfolio of research grants covering a broad spectrum of topics directed at understanding the biological basis of cancer, emphasizing cancer etiology, biological and chemical carcinogenesis. The Branch Chief uses expert knowledge of the research field and administrative experience to provide the Branch with leadership, direction, coordination and perspective as well as to respond to NCI leadership. The Chief develops initiatives in the area of scientific responsibility, establishes program priorities, evaluates program effectiveness, provides information, advice and consultation to individual scientists and institutional management officials relative to NIH and NCI funding, provides NCI leadership with recommendations concerning funding needs, priorities and strategies, and organizes meetings and workshops to further program objectives.

A full Civil Service package of benefits (including health and life insurance options, retirement, paid holidays, vacation and sick leave) is available.

The NCI vacancy announcement for this position contains complete application procedures and lists all mandatory information, which you must submit with your application. To obtain the vacancy announcement for this position which will be available on **12/11/2007** and posted under announcement **#NCI-08-235571-DE&MP**, you may visit the website **https://careerhere.nih.gov** OR you can have it faxed to you by calling **1-800-728-JOBS (for local calls, 301-402-5057) and enter the "FAX ID Number 1899"**. You will be prompted for your fax machine number. Applications must be postmarked by **01/29/2008**.

Tenure Track/Tenured Position
Basic Biomedical Research

Division of Intramural Research (DIR) of the National Heart, Lung and Blood Institute is seeking an outstanding scientist to initiate and direct an independent research program on the NIH campus in Bethesda, MD. The area of expertise of the candidate is less important than his/her demonstrated ability to conduct outstanding independent research in areas within the broad interests of the DIR. The areas of expertise may include but are not limited to: molecular and cellular biology, biophysics, biochemistry, immunology, systems biology, physiology, signal transduction, developmental biology, and molecular imaging. Potential candidates are welcome to view the NHLBI DIR web pages (http://dir.nhlbi.nih.gov/) to review the research programs and support available within the DIR. The existing faculty is an outstanding group of internationally recognized biomedical researchers covering a wide range of basic and clinical research topics complemented by the other DIR programs within NIH. Strong research core support in optical and electron microscopy, transgenic and knockout mouse production, mouse phenotyping, proteomics, genomics, and flow cytometry/cell sorting is available to the DIR faculty. Candidates can also train Ph.D. students by participating in the Graduate Partnership Programs (http://gpp.nih.gov/) with many academic programs around the world.

The candidate must have an M.D., Ph.D., or both and have an outstanding record of research accomplishments as evidenced by publications in major peer-reviewed journals. The position can be filled as a tenure-track or tenured position, but preference will be given to senior post-doctoral fellows or faculty who are still in the early stages of their research careers. The successful candidate will be offered a competitive salary commensurate with experience and qualifications, and will be assigned ample research space, supported positions, and an operating budget. Appointees may be US citizens, resident aliens, or non-resident aliens with or eligible to obtain a valid employment authorized visa. Applications must be received by **February 1, 2008**. Please submit a curriculum vitae and brief statement of research interests along with three letters of reference to:

"Robert S. Balaban, Ph.D., Scientific Director, NHLBI
c/o Mary McMahon
Administrative Officer, NHLBI
10 Center Drive, MSC 1670
Building 10, Room 7N220
Bethesda, MD 20892-1670"
mcmahonm@nhlbi.nih.gov

Clinical Tenure-Track Position
National Institute of Allergy and Infectious Diseases

The National Institute of Allergy & Infectious Diseases (NIAID), Division of Intramural Research (DIR), is seeking an outstanding tenure-track investigator to develop a clinical research program to better understand, treat, and ultimately prevent infectious, immunologic, and/or allergic diseases. The scope of the NIAID research portfolio has expanded considerably in recent years in response to new challenges such as bioterrorism; emerging and reemerging infectious diseases, including acquired immunodeficiency syndrome (AIDS), influenza, severe acute respiratory syndrome (SARS), West Nile virus, malaria, and tuberculosis; immunologic diseases and the increase in asthma prevalence among children in this country.

The successful candidate will implement and direct an independent clinical research program with research emphasis on clinical research but may include translational or basic research. The incumbent will have the opportunity to choose the Laboratory in which he/she would like to be affiliated. It is expected that clinical protocols developed will complement the research goals of the Laboratory selected. In addition, the candidate will be paired with a Senior Investigator who will serve as a clinical mentor.

An outstanding postdoctoral record of research accomplishment and M.D., M.D./Ph.D. or equivalent degree is required for this position; board eligibility/board certification is also required. The incumbent will be expected to be qualified for credentialing by the NIH Clinical Center.

Candidates will be assigned independent resources to include clinical and/or laboratory support personnel, equipment, space, and an allocated annual budget for services, supplies, and salaries to ensure success. This is a tenure-track appointment under Title 42. Salary is dependent on experience and qualifications.

Interested candidates may contact **Dr. Karyl Barron, Deputy Director, DIR, NIAID at 301/402-2208 or email (kbarron@nih.gov)** for additional information about the position. To apply for the position, send your curriculum vitae, bibliography, and an outline of your proposed research program (no more than two pages), by **January 31, 2008** via email to **Ms. Wanda Jackson at jacksonwa@niaid.nih.gov**. In addition, three letters of recommendation must be sent to **Chair, NIAID DIR Clinical Tenure Track Search Committee, c/o Ms. Wanda Jackson at jacksonwa@niaid.nih.gov or 10 Center Drive MSC 1356, Building 10, Rm. 4A-26, Bethesda, Maryland 20892-1356**. E-mail is preferred. Please note search **#018** when sending materials.

Further information regarding the DIR laboratories is available at: **http://www3.niaid.nih.gov/about/organization/dir/default.htm** and information on working at NIAID is available on our website at: **http://healthresearch.niaid.nih.gov**.

OFFICE OF PORTFOLIO ANALYSIS AND STRATEGIC INITIATIVES
DIRECTOR, DIVISION OF EVALUATION AND SYSTEMIC ASSESSMENTS

The Office of the Director, National Institutes of Health (NIH) in Bethesda, Maryland, is seeking a Director of the Division of Evaluation and Systemic Assessments (DESA) within the Office of Portfolio Analysis and Strategic Initiatives (OPASI). If you are an exceptional candidate with an M.D. and/or Ph.D. and the vision and ability to integrate evaluation systems and programs across multiple disciplines and organizations, we encourage your application.

The OPASI's primary objective is to develop: a transparent process of planning and priority-setting characterized by a defined scope of review with broad input from the scientific community and the public; valid and reliable information resources and tools, including uniform disease coding and accurate, current and comprehensive information on burden of disease; an institutionalized process of regularly scheduled evaluations based on current best practices; the ability to weigh scientific opportunity against public health urgency; a method of assessing outcomes to enhance accountability; and a system for identifying areas of scientific and health improvement opportunities and supporting regular trans-NIH scientific planning and initiatives.

As the DESA Director, you will be responsible for planning, conducting, supporting, and coordinating, specific program evaluations and projects of NIH Institutes and Centers such as the Roadmap, Obesity, and Neuroscience Blueprint initiatives. In addition, you will serve as the liaison for conducting governmentally required assessments according to the Government Performance and Results Act (GPRA) and OMB Program Assessment Rating Tool (PART). You will also serve as a member of the OPASI Steering Committee involved in oversight of institution-wide planning and analysis.

Salary is commensurate with experience and includes a full benefits package. A detailed vacancy announcement with the mandatory qualifications and application procedures can be obtained on **USAJOBS at www.usajobs.gov (announcement number OD-08-230779-T42) and the NIH Web Site at http://www.jobs.nih.gov**. Questions on the application procedures may be addressed to **Brian Harper on 301-594-5332**. Applications must be received by midnight eastern standard time on **January 15, 2008**.

CHAIR

DEPARTMENT OF CELL BIOLOGY AND PHYSIOLOGY
UNIVERSITY OF PITTSBURGH SCHOOL OF MEDICINE

The University of Pittsburgh School of Medicine is seeking a chair for the Department of Cell Biology and Physiology. The Department comprises 22 tenure/tenure-stream faculty with a research focus on cell polarity and the trafficking of proteins and lipids, on the function and dysfunction of ion channels, on reproductive biology, and on signal transduction in diabetes and metabolism. The successful candidate must demonstrate an outstanding record of scholarship commensurate with appointment at the rank of Full Professor with tenure. An outstanding startup package has already been committed for this position, and the person who holds this position will occupy the fully endowed Richard King Mellon Chair in Cell Biology and Physiology.

The new chair will lead a significant expansion of the department and will benefit from interactions with the Center for Biological Imaging and the University of Pittsburgh Cancer Institute, and the recently established Clinical and Translational Science Institute and Drug Discovery Institute, as well as with other research units within the School of Medicine. The University of Pittsburgh School of Medicine is enjoying unparalleled growth in its research, clinical, and academic missions. The University is currently ranked 7th among educational and research institutions in NIH funding and has doubled its NIH support in the last 10 years.

Please send curriculum vitae and bibliography to the head of the CBP Chair Search Committee (**Jeffrey L. Brodsky, Ph.D.**) at: **jbrodsky@pitt.edu**.

The University of Pittsburgh is an Affirmative Action, Equal Opportunity Employer. Women and members of minority groups under-represented in academia are especially encouraged to apply.

FACULTY POSITION
Genetics/Skeletal Biology

The Department of Genetics at Harvard Medical School and the Department of Orthopaedic Surgery at Children's Hospital Boston invite applications for a tenure-track appointment at the Assistant Professor level. The appointee will be a full member and active participant in the Department of Genetics (**http://genetics.med.harvard.edu**) and be given laboratory space in the Orthopaedic Research Laboratories at Children's Hospital Boston (**http://www.childrenshospital.org**).

The successful candidate is expected to direct innovative and independent research in the field of skeletal biology, preferably addressing questions related to pediatric skeletal health and disease, and to participate in the teaching activities of the Department of Genetics and the Department of Orthopaedic Surgery. Applicants must hold a Ph.D., M.D./Ph.D., or M.D. degree, have completed post-doctoral training, and have a strong record of research accomplishments.

Applicants should submit electronically (pdf format only) a curriculum vitae, bibliography, and a 3-page description of research accomplishments/future research interests by **February 29, 2008**, and ask 3 references to provide letters of recommendation (also in pdf format). All these materials should be sent to the following email address:

faculty_search@genetics.med.harvard.edu

Harvard Medical School and Children's Hospital Boston are Equal Opportunity/Affirmative Action Employers. Applications from women and minorities are encouraged.

OLD DOMINION UNIVERSITY
COLLEGE OF SCIENCES
FACULTY POSITIONS

The College of Sciences at Old Dominion University under the leadership of the newly appointed Dean Chris D. Platsoucas, Ph.D., is pursuing a major expansion of its research base. Applications are invited for over twenty tenure/tenure track faculty positions at all ranks to support this initiative of focused hiring in strategic areas. Areas of interest include the following:

1. **Biology** (immunology, molecular pathogenesis, virology, cancer research, ecology).
2. **Computer Sciences** (information retrieval, security and encryption, data mining and visualization, digital media, digital libraries, bioinformatics, medical imaging and applications, modeling and simulation).
3. **Chemistry** (organic chemistry).
4. **Psychology** (human factors); health, quantitative and clinical psychology).
5. **Mathematics & Statistics** (computational sciences and applied mathematics, statistics).
6. **Physics** (condensed matter, accelerator physics).
7. **Oceanography** (chemical, physical and geological oceanography).

Applications should include a curriculum vita, statement of research accomplishments and future research plans and names and addresses (including e-mails) of four references. Applications should be sent by e-mail (**science@odu.edu**) or regular mail to the **Chair, Search Committee (please specify the position of interest) c/o Ms. Andrea Stephen, Dean's Office, College of Sciences, Oceanography & Physics Building, Norfolk, VA 23529.**

Old Dominion University is an Affirmative Action/Equal Opportunity institution and requires compliance with the Immigration Reform and Control Act of 1986.

Why not
change the world?

TWO FACULTY POSITIONS
Department of Biology

The School of Science at Rensselaer Polytechnic Institute is seeking two exceptionally qualified scientists to work in an exciting, interdisciplinary environment as full-time tenure-track or tenured faculty positions at any rank (assistant, associate, or full professor) in the Department of Biology. The Department of Biology is in a period of rapid expansion with many new faculty appointments anticipated in the next five years. We are seeking candidates in a wide spectrum of areas, including but not limited to

- Ecology and Evolution including Evo/Devo
- Microbiology including host-pathogen interactions
- RNA Biology
- Single Molecule Mechanics
- Structural Biology
- Systems Biology

The successful candidates must have a Ph.D. or equivalent degree, postdoctoral experience, and will be expected to establish an extramurally funded research program, train graduate students, and participate in undergraduate education. Applicants should email a single PDF document containing curriculum vitae, a three-page statement of research accomplishments and goals, and a brief description of teaching interests to **biology-chair@rpi.edu**. In addition, applicants should arrange to have at least three letters of recommendation forwarded by email. Consideration of candidates will begin upon receipt of applications and will continue until the positions are filled.

Rensselaer

We welcome candidates who will bring diverse intellectual, geographical, gender and ethnic perspectives to Rensselaer's work and campus communities. Rensselaer Polytechnic Institute is an Affirmative Action/Equal Opportunity Employer.

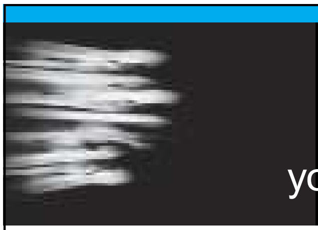

your job at **TUDelft**

CHALLENGE THE FUTURE

Assistant/Associate Professor of Physics Confocal Electron-Light Microscopy

Department:	**Imaging Science & Technology**
Level:	**PhD**
Working hours:	**Full-time**
Term of contract:	**Tenure-track or tenured as applicable**
Salary:	**Maximum of € 5670 per month gross with a full-time appointment**

The department is part of the Faculty of Applied Sciences. The professor should strengthen our research in imaging science and technology, specifically in instrumentation and applications for high resolution microscopy. The first challenge is to lead the development of a combined electron and light microscope, where lab-on-a-chip technology will be used to manipulate biological specimens in the sample chamber. We seek a physicist with proven skills in instrumentation and in networking with users who have a biology background. Other responsibilities will include teaching and coaching students.

Information and application

For more information about the position please visit:

www.jobsinDelft.nl

TUDelft

Delft University of Technology

ENVIRONMENTAL BIOTECHNOLOGY

Geobacter Project

www.geobacter.org

POSTDOCTORAL POSITIONS available in the following areas:

Adaptive Evolution: *Geobacter* species and other environmentally relevant organisms can be evolved for enhanced performance in energy production, bioremediation, etc. Identify beneficial mutations and evaluate their role in contributing to processes of interest.

Metagenomics and Molecular Ecology: Evaluate the function and activity of *Geobacter* and other organisms involved in groundwater bioremediation through the analysis of environmental genomic and proteomic data as well as elucidation of *in situ* gene expression.

Genome-Scale *In Silico* Modeling of Bioremediation: Develop constraint-based models based on the genome sequences of environmentally relevant organisms and couple these models with hydrological and geochemical models.

Reductive Dechlorination: Investigate novel methods of improving bioremediation of chlorinated contaminants with new strategies for stimulating this process and genome-scale modeling and genetic manipulation of dechlorinating microorganisms.

Microbial Fuel Cells: Investigate mechanisms of electron transfer between microorganisms and electrodes; model functioning of microbial fuel cells; and improve power output via adaptive evolution and genetic engineering.

For research program details please visit **www.geobacter.org**. Minimum qualifications are a PhD in Microbiology or a related field. Salary is commensurate with experience. Please email curriculum vitae and names of three references to: **Dr. Derek Lovley, Environmental Biotechnology Center, Department of Microbiology, University of Massachusetts, Amherst, MA. Email: dlovley@microbio.umass.edu or send information to Search Committee Chair, R30904 Microbiology, 203N Morrill IVN, UMASS, Amherst, MA 01003**. Review of applications will begin **January 18, 2008** and continue until the positions are filled.

UMASS is an Affirmative Action/Equal Opportunity Employer.
Women and members of minority groups are encouraged to apply.

RUPRECHT-KARLS-
UNIVERSITÄT
HEIDELBERG

The Medical Faculty Mannheim of the University of Heidelberg
is seeking qualified applicants for the following positions of

Professor of Psychiatry and Psychotherapy (W3)

The incumbent will be appointed

Deputy Medical Director

of the Department of Psychiatry and Psychotherapy at the Central Institute of Mental Health, Mannheim (Medical Director: Andreas Meyer-Lindenberg, MD, PhD, MSc). The department presently has 128 inpatient beds and 32 day hospital beds. The responsibilities of the position include research, teaching and patient care.

Qualifications and requirements: Applicants should show a high quality research profile and excellent scientific achievements on an international level. A postdoctoral thesis (habilitation) or the equivalent as well as several years of experience in a senior clinical position are prerequisites. Additionally, the incumbent's main research interests should be in biological psychiatry. Candidates are expected to have extensive teaching experience, to be accredited in the area of psychiatry and psychotherapy or show an equivalent educational background.

Professor of Child and Adolescent Clinical Neurophysiology (W3)

The incumbent will represent the field as a whole in terms of research and teaching.

Research facilities are provided at the Central Institute of Mental Health in Mannheim (Foundation under Public Law, Director: Andreas Meyer-Lindenberg, MD, PhD, MSc) within the Department of Child- and Adolescent Psychiatry and Psychotherapy (Medical Director: Tobias Banaschewski, MD, PhD).

Applicants should show a high quality research profile and excellent scientific achievements on an international level in the area of neurophysiological research in child and adolescent development as well as sound experience in multimodal imaging. Candidates should be able to represent the field of child- and adolescent psychiatry with an interdisciplinary approach linking medicine, biology, psychology and behavioural science. A postdoctoral thesis (habilitation) or its equivalent as well as experience in soliciting third party funding and participating in multicenter cooperations are expected.

In addition to fulfilling its university and clinical functions and to its role as a university teaching hospital (Dept. of Psychiatry and Psychotherapy, Dept. of Child and Adolescent Psychiatry and Psychotherapy, Dept. of Psychosomatic and Psychotherapeutic Medicine, Dept. of Addictive Behavior and Addiction Medicine as well as the Chair for Neuropsychology and Clinical Psychology) the Central Institute of Mental Health is known as a research institute of international standing (WHO Collaborating Center, Member of the Association for Clinical and Biomedical Research, as well as recipient of centre grant research funding – presently SFB 636). The institute is home to a wide range of research areas such as the departments/working groups on Biostatistics, Community Psychiatry, Genetic Epidemiology, Geriatric Psychiatry, Clinical Psychology, Molecular Biology, Neuroimaging, NMR research and Psychopharmacology.

Applications containing all pertinent information should be sent within two weeks to: **Medical Faculty Mannheim, University of Heidelberg, Dean's Office, Klaus van Ackern, MD, PhD hon., University Hospital Mannheim, Theodor-Kutzer-Ufer 1-3, 68167 Mannheim, Germany**

The positions are available indefinitely. By law, however, first appointments to a professorship must initially be limited to a set time period. However, if necessary, exceptions may be made in order to win outstanding candidates from outside Germany or from outside the academic community for the position. If the appointment is to be continued after the initially set time-limit a second round of application proceedings is not required for permanent tenure.

The University of Heidelberg is seeking to increase the percentage of female scientists and is explicitly encouraging qualified female scientists to apply. The University is an equal opportunity employer. Applications from qualified disabled persons will be given priority.

UNIVERSITY OF CALIFORNIA
UC RIVERSIDE

DEAN—COLLEGE OF NATURAL AND AGRICULTURAL SCIENCES

The University of California, Riverside, invites inquiries, applications, and nominations for the position of Dean of the College of Natural and Agricultural Sciences. The College is unique among land-grant institutions, combining the physical, mathematical, biological, and agricultural sciences under one administrative umbrella with 13 academic departments and 12 research centers and institutes. This distinctive structure enables the kind of cross-department collaborations and interdisciplinary linkages that have established the national and international reputation of the College in many fields of scientific inquiry.

As the chief academic and administrative leader for the College, the Dean reports to the Provost and is responsible for promoting excellence in all aspects of the College's teaching, research, and public service missions; oversight and leadership for long-range planning and implementation; allocation and overall management of resources; and leadership in external relations and development activities in support of the College's aspirations. The College awards over 4,000 undergraduate and graduate degrees annually and has 242 tenure-track faculty and almost 300 researchers and other academics. Grants and contracts currently exceed $50 million a year. Additional information and a detailed position profile may be found at www.cnas.ucr.edu.

The successful candidate will have a distinguished record qualifying for appointment at the rank of Professor in the College; an abiding commitment to academic excellence; prior successful administrative experience in a research university or its equivalent; the ability to work effectively with faculty, staff, students, alumni, and friends of the College; and the talent to represent the College to its many constituencies. The University of California, Riverside, has a strong institutional commitment to the achievement of diversity among its faculty, staff, and students and seeks an individual who shares that commitment.

The start date for the position will be July 1, 2008 or as negotiated. Candidates should provide a curriculum vitae and statement of interest, along with the names and contact information for five references who will not be contacted without prior approval. Candidate materials should be received by January 30, 2008 to ensure full consideration; the position will remain open until filled. Applications, nominations and inquiries should be submitted electronically, in confidence, to the committee's consultant, Dr. Sally P. Springer of Storbeck/Pimentel and Associates, at s.springer@storbeckpimentel.com.

The University of California is an Equal Opportunity/Affirmative Action Employer

---

nature nanotechnology

Associate Editors

Nature Nanotechnology is a prestigious journal covering all areas of nanoscience and technology. We have exciting opportunities available for a chemist and a physicist/materials scientist to join our editorial team as Associate Editors.

These are demanding and intellectually stimulating positions. Applicants should have a PhD and preferably post-doctoral experience in an area of chemistry or physics/materials science related to nanoscience and technology. Broad scientific knowledge and good Word skills are essential.

The successful candidates will work closely with the Editor on all aspects of the journal including manuscript selection, and commissioning, editing and writing other content for the journal and its website. Liaising with the international nanoscience and technology community is a central part of both jobs and the successful candidates will be expected to attend conferences and visit laboratories around the world. The positions will be based in our London or Boston offices.

Applicants should send a covering letter (including their salary expectations), a CV, and a News & Views style piece (500 words or less) about a recent paper (or papers) in the literature to Denise Pitter, Personnel Assistant at londonrecruitment@macmillan.co.uk
Please quote reference number NPG/LON/788

Closing date: 31st January 2008

nature publishing group npg

BROOKLYN COLLEGE
The City University of New York

11 TENURE TRACK FACULTY POSITIONS

In support of the College's targeted signature programs in research and to supporting both high quality research and teaching in the sciences, Brooklyn College is seeking applications for 11 tenure track faculty positions in the Sciences to begin Fall 2008.

Brooklyn College is one of the nation's leading public liberal arts colleges and a principal teaching and research institution of The City University of New York. Applicants should have a strong record of scholarly productivity, including the ability or potential to develop and sustain a program of research supported by outside funding, and a commitment to teaching at the undergraduate, masters and Ph.D. levels when applicable.

Please visit
http://www.brooklyn.cuny.edu/bc/offices/personnel/jobs/index.php
for more details.

BROOKLYN COLLEGE IS CUNY

An AA/EO/IRCA/ADA Employer

FACULTY POSITION in BOTANY

The Department of Biological Sciences at National Sun Yat-Sen University, Taiwan is seeking for a tenured/tenure-track faculty member in the area of Field Botany. Appointment rank is open and dependent upon the applicant qualifications. The minimum requirements include a Ph.D. or equivalent degree in plant ecology, plant systematics or a related field with at least one year of postdoctoral experience preferred. The ability to communicate and teach in Mandarin and English is also required. Applicants should submit a statement of career goals, a resume, the graduate transcript, publication reprints, and three letters of recommendation by January 31, 2008 to: **Prof. Hsueh-Wen Chang, Chairperson, Department of Biological Sciences, National Sun Yat-sen University, 70, Lien-Hai Road, Kaohsiung, Taiwan 80424** www.uni-frankfurt.de

JOHANN WOLFGANG GOETHE
UNIVERSITÄT
FRANKFURT AM MAIN

Professorship (W2)
Macromolecular Complexes in Cell Biology

The Cluster of Excellence “Macromolecular Complexes“ at the Johann Wolfgang Goethe University in Frankfurt is seeking to appoint an outstanding scientist with a strong research profile in functional and molecular analysis of macromolecular complexes in key areas of cell biology. The successful candidate will complement and strengthen the current research topics of the Cluster, which comprise membrane biology and transport, bioenergetics, RNA/protein complexes, signalosomes and nuclear complexes. The candidate should have a profound background in molecular and cell biology and should take advantage of the Cluster’s oustanding infrastructure for structural analysis including X-ray, cryo-EM, NMR, MS and spectroscopic analyses.
Start-up funds as well as substantial funding for personnel und running costs are available. There will be ample opportunities for interactions with leading research groups at the University and the Max Planck Institutes of Biophysics and Brain Research. Excellent, state-of-the-art core facilities, including imaging, proteomics, genomics, and bioinformatics will be available to all groups in the Cluster. For further information, including the positions filled in the first round of appointments, see www.cef-mc.de. Participation in new or existing DFG-funded Collaborative Research Centres (SFBs) in Frankfurt is expected. The successful candidate will develop a highly competitive research program in an area related to the interests of the Cluster and participate in teaching.
The designated salary for the position is W2 (tenure track; initially for 5 years) on the German university scale. The Goethe University is committed to a pluralistic campus community through affirmative action and equal opportunity.
For details, see **http://www.uni-frankfurt.de/aktuelles/ausschreibung/professuren/ index.html**
Applications including a curriculum vitae, pdf files of 5 key publications, statements of research achievements (1 page) and future plans (3 pages), as well as the names and addresses of 5 academic referees should be sent within **four weeks** after publication of this advertisement via e-mail to: **Director, Cluster of Excellence Macromolecular Complexes, Goethe University Frankfurt, e-mail: office@cef-mc.de**
Further information: **http://www.cef-mc.de/index.php?id=2**

Hier wird Wissen Wirklichkeit

The Ohio State University
Assistant Professor
Plant Ecology, Tenure-Track

The Ohio State University at Mansfield seeks a **Tenure-Track Aassistant Professor** in terrestrial or aquatic **Plant Ecology** who will contribute to the Introductory Biology Program and the development of an Environmental Studies Program. Teaching responsibilities will likely include courses in Local Flora, Introductory Biology, and Data Analysis.

The successful applicant will begin in autumn 2008 and teach at the Mansfield regional campus. In addition, this person will be a member of the Department of Evolution, Ecology, & Organismal Biology on the main campus in Columbus. Regional campus faculty are expected to maintain active research programs and are able to advise graduate students on the main campus. Candidates must have a Ph.D. in plant ecology or related field, and postdoctoral experience is desirable.

THE OHIO STATE UNIVERSITY
MANSFIELD

Please send curriculum vitae, statements of teaching philosophy and research interests, and three letters of reference by **January 25, 2008 to: Dr. Ted Dahlstrand, The Ohio State University at Mansfield, 1760 University Dr., Reidl Hall, Rm. 206, Mansfield, OH 44906.**

To build a diverse workforce Ohio State encourages applications from individuals with disabilities,minorities, veterans,and women. EEO/AA employer.

U.S. MILITARY HIV RESEARCH PROGRAM

HIV Diversity and Neutralization

The U.S. Military HIV Research Program, supported by the Henry M. Jackson Foundation for the Advancement of Military Medicine, is a key contributor to the global effort to develop HIV vaccines. The internationally recognized Molecular Virology/Global Epidemiology component of the program has initiated a new effort to evaluate the impact of HIV diversity on serum neutralization of viral infectivity, through development and standardization of virus innocula for *in vitro* evaluation of HIV neutralization in primary target cells. This research is expected to facilitate the development of HIV vaccines that elicit strong neutralizing antibodies against the broad range of HIV variants in the global epidemic. Opportunities to participate in this new initiative have opened at multiple levels.

Scientist: Incumbent will contribute to HIV vaccine development and research will have high visibility in the scientific community. Applicant must have a PhD in Molecular Biology with 2-4 years laboratory experience in molecular cloning, DNA sequencing, and PCR. Will plan, manage, and execute a major program component in HIV neutralization. Experience with viral systems in general and HIV in particular are desirable. Must have demonstrated scientific productivity and strong organizational, leadership, and communication skills, experience with supervising technical staff. **Job No: 203000**.

Postdoctoral: Seeking a laboratory scientist with a recent PhD in Molecular Biology, Virology, or related discipline. Incumbent will perform molecular cloning of HIV genomes, targeted genetic modification of molecular clones to produce standardized viral reagents for HIV neutralization assays. Must have demonstrated ability to organize and execute laboratory efforts, manage and analyze data, and prepare professional quality manuscripts. **Job No: 203010**.

Laboratory Technician: Seeking individuals to perform laboratory research in support of studies in HIV diversity. The applicant will provide technical support to senior technical and professional staff and should possess a working knowledge of standard Molecular Biology techniques. Duties include laboratory experiments, preparation of technical reports, maintaining clear and accurate laboratory records, and other duties as assigned. Applicants should have a Bachelors degree in Biology, Chemistry, or related discipline. **Job No: 203057 or 203058**.

Please e-mail resumes to **careers@hjf.org** or fax to **240-314-7334** with **Job No. in subject line**. The **Henry M. Jackson Foundation for the Advancement of Military Medicine** offers a competitive salary and generous benefits package.

AA/EEO

CHAIR

DEPARTMENT OF MICROBIOLOGY AND MOLECULAR GENETICS

UNIVERSITY OF PITTSBURGH SCHOOL OF MEDICINE

The University of Pittsburgh School of Medicine is seeking a chair for the Department of Microbiology and Molecular Genetics. The department comprises 32 primary faculty members with a focus on basic research in Microbiology, Molecular Biology, Virology, Biochemistry and Developmental Biology. In particular, candidates working within any area of Microbiology and Molecular Genetics are encouraged to apply for the chair. The successful candidate will have an outstanding record of scholarship commensurate with appointment at the rank of Full Professor with tenure, and as the William S. McEllroy Professor.

The University of Pittsburgh School of Medicine is enjoying unparalleled growth in its research, clinical, and academic missions. Of more than 3,000 institutions nationwide, the University of Pittsburgh is currently ranked 7th among educational and research institutions in NIH funding. The chair of Microbiology and Molecular Genetics will have an outstanding opportunity to add further to the growth of the basic biomedical sciences in the School of Medicine.

Please send a full curriculum vitae and bibliography to the MGG Chair Search Committee at: **mmg@medschool.pitt.edu**.

The University of Pittsburgh is an Affirmative Action, Equal Opportunity Employer. Women and members of minority groups under-represented in academia are especially encouraged to apply.

Dartmouth College

Endowed Position in the Environmental Sciences

Sherman Fairchild Chair in Sustainability Science

Dartmouth College invites applications for a newly endowed Chair in Sustainability Science, an emerging field that examines the dynamic interactions between environment and society. The successful candidate will be committed to interdisciplinary research, and teaching at the undergraduate and graduate levels. We seek candidates with outstanding records in a relevant field in the natural sciences. Candidates in the social sciences with crosscutting expertise will also be given strong consideration. Research areas might include: global environmental change, earth systems science, conservation ecology or resource ecology, biocomplexity, environmental health or other relevant topics. The Sherman Fairchild Professor will have a leading role in developing new research and curriculum initiatives as part of an expanding program in the study of human-environment relations reaching across several departments and involving the professional schools of engineering, medicine and business. Strong preference will be given to those candidates with proven leadership skills as well as experience in the application of scientific knowledge in policy making and problem solving at the intersections of environmental, technological and social change. We intend to hire at the rank of associate or full professor with tenure, and the successful candidate will be located in Environmental Studies (with possible affiliation with another department or program).

The Search Committee will begin reviewing applications after **January 31, 2008**. Applications will be considered until the position is filled. Please send letter of application, CV, and the names of three references to: **Ross A. Virginia, Chair, Search Committee in Sustainability Science, Environmental Studies Program, 6182 Steele Hall, Dartmouth College, Hanover, NH 03755 USA.**

Dartmouth College combines a commitment to innovative scholarship and excellent teaching. Dartmouth College is an Equal Opportunity/Affirmative Action Employer and has a strong commitment to diversity. We welcome applications from a broad spectrum of people, including women, persons of color, persons with disabilities, and veterans.

TEMPLE UNIVERSITY®

Developmental/Cell Biologist Associate/Full Professor

The Department of Biology at Temple University is expanding its research programs and anticipates multiple faculty hires over each of the next several years. The Department invites applications for an Associate/Full Professor (tenured/tenure-track) position in the area of Developmental/Cell Biology. We are especially interested in individuals who are using current molecular genetic approaches to study basic mechanisms of developmental pathways and/or cell function. Individuals whose research programs complement and extend the department's strengths in vertebrate development, developmental neuroscience, RNA biology, molecular virology, and cancer biology are especially urged to apply. However, outstanding candidates in other areas also will be given full consideration. Applicants are expected to have a significant track record of funded research, as well as teaching at the graduate and undergraduate levels. Applicants should submit their curriculum vitae, a research program summary, and the names and contact information of three references to: **Dr. Richard Waring, Developmental/Cell Biologist Search Committee Chair, Department of Biology, Temple University, 1900 North 12th Street, Philadelphia, PA 19122. E-mail: waring@temple.edu.** Review of applications will begin immediately and will continue until the position is filled.

Temple University is an equal opportunity, equal access, affirmative action employer committed to achieving a diverse community (AA, EOE, m/f/d/v).

DTU

PROFESSOR

IN WASTEWATER ENGINEERING

The Institute of Environment & Resources seeks to fill the position of Professor in Wastewater Engineering. The candidate examines and advances wastewater treatment processes based on fundamental process engineering understanding, guides an externally funded research program, and partakes in the leadership of the new PhD school UrbanWaterTech.

Further information may be obtained from Head of Department Mogens Henze, tel. +45 4525 1477, e-mail: moh@er.dtu.dk

The full text of the announcement can be seen on DTU's homepage.

Application deadline: 1st April 2008 at 12.00.

The Technical University of Denmark is one of the largest technical research and educational institutions in Northern Europe with 7,000 students, 4,500 employees and a yearly turnover of DKK 3.1 billion. As of January 1, 2007, DTU has merged with the Danish Institute for Food and Veterinary Research, Risø National Laboratory, the Danish Institute for Fisheries Research, the Danish National Space Centre and the Danish Transport Research Institute.

Further details www.dtu.dk/vacancy

www.uni-frankfurt.de

JOHANN WOLFGANG GOETHE
UNIVERSITÄT
FRANKFURT AM MAIN

Professorship (W2)
Membrane Transport Machineries

The Cluster of Excellence "Macromolecular Complexes" at the Johann Wolfgang Goethe University in Frankfurt is seeking an outstanding individual with a proven track record in the field of membrane biochemistry, whose research efforts should integrate with and complement the present areas of research in the field of transport across cellular membranes (e.g. structure and function of transport complexes, protein translocation, lipid transport, assembly or biogenesis of transport machineries).

Start-up funds as well as substantial funding for personnel and running costs are available. The candidate's research group will be accommodated at the Biocenter of the university and provided with state-of-the-art facilities and infrastructure. Ample opportunity is available for interaction on the Riedberg Campus and several Collaborative Research Centers (SFBs) as well as with research groups at the Max Planck Institutes of Biophysics and Brain Research.

The successful candidate will develop a highly competitive research program in an area related to the interests of the Cluster of Excellence and participate in teaching of the biochemistry curriculum. The group will be integrated into the Department of Biochemistry, Chemistry and Pharmacy, which provides access to all core facilities, including imaging, proteomics, genomics, and bioinformatics. The designated salary for the position is W2 (tenure track; initially for 5 years) on the German university scale. The Goethe University is committed to a pluralistic campus community through affirmative action and equal opportunity.

For details, see **http://www.uni-frankfurt.de/aktuelles/ausschreibung/professuren/index.html**

Applications including a curriculum vitae, pdf files of 5 key publications, statements of research achievements (1 page) and future plans (3 pages), as well as the names and addresses of 5 academic referees should be sent within **four weeks** after publication of this advertisement via e-mail to: **Director, Cluster of Excellence Macromolecular Complexes, Goethe University Frankfurt, e-mail: office@cef-mc.de**

Further information: **http://www.cef-mc.de/index.php?id=2**

Hier wird Wissen Wirklichkeit

UNIVERSITY OF
ALBERTA
EDMONTON, ALBERTA, CANADA

www.careers.ualberta.ca

Assistant or Associate Professor, Fisheries Ecology

We invite applications for a tenure-track position at the Assistant or Associate Professor level in Fisheries Ecology. We welcome individuals with strong credentials in fisheries biology/conservation, whose research focus can address fisheries challenges in Alberta and northern Canada, including the effects of resource development and other environmental perturbations. The successful candidate will be expected to build a field research program with external funding and encouraged to develop collaborations with federal and provincial agencies, other universities, and private-sector scientists, as well as with established departmental groups in freshwater and northern ecology, conservation biology, and environmental physiology. Applicants must have a PhD and demonstrated potential for excellence in teaching, research, and for working successfully with the public and/or private sector.

The Department of Biological Sciences (http://www.biology.ualberta.ca/), with 72 faculty and 275 graduate students, offers an exciting environment for collaborative research. It has ready access to lakes and rivers in boreal, mountain, and parkland regions and in Canada's northern territories. Exceptional infrastructure includes a field station near Athabasca, a biogeochemical laboratory, and aquatics, molecular biology and microscopy/imaging services.

Candidates should submit, preferably electronically (positions@biology.ualberta.ca), a CV, a one-page summary of research plans, a statement of teaching interests, and reprints of their three most significant publications to:

Dr. L. S. Frost, Chair
Department of Biological Sciences
CW 405 Biological Sciences Bldg.
University of Alberta
Edmonton, Alberta, Canada T6G 2E9

Applicants must also arrange for three letters of reference to be sent electronically to the Chair (positions@biology.ualberta.ca).

Deadline: February 7, 2008.
The earliest date of employment will be July 1, 2008. The University of Alberta offers a competitive salary commensurate with experience and has an excellent benefits plan.

All qualified candidates are encouraged to apply; however, Canadians and permanent residents will be given priority. The University of Alberta hires on the basis of merit. We are committed to the principle of equity in employment. We welcome diversity and encourage applications from all qualified women and men, including persons with disabilities, members of visible minorities, and Aboriginal persons.

TENURE TRACK FACULTY POSITION IN NEW YORK

HUMAN GENETICS

The Departments of Molecular Genetics and Pediatrics, jointly invites applications for two tenure-track positions at the **Assistant or Associate Professor** level.

We are seeking candidates working in the fields of human genetics and genomics. The focus would be on genome wide studies and human disease. Candidates with shared clinical and basic science programs are encouraged to apply.

Start-up packages will be provided to build the laboratories of successful candidates. The Albert Einstein college of medicine offers numerous state-of-the-art core facilities (http://www.aecom.yu.edu/home/shared.asp) for genomics and epigenomics, mouse gene targeting, analytical imaging, open to all investigators, as well as several NIH-funded programs to support graduate student and postdoctoral training.

Albert Einstein is located in a pleasant, tree-lined residential area of the northeast corner of the Bronx, with easy access to, Manhattan and the suburbs of Westchester County and Connecticut.

Please submit a curriculum vitae, a statement if research interests and future plans, and have three reference letters sent to: **Search Committee/Vivian Gradus, Department of Molecular Genetics, Albert Einstein College of Medicine, Jack and Pearl Resnick Campus, 1300 Morris Park Avenue, Bronx, NY 10461. Inquiries should be sent electronically to gradus@aecom.yu.edu** EOE

http://www.aecom.yu.edu/home/

ALBERT EINSTEIN COLLEGE OF MEDICINE OF YESHIVA UNIVERSITY

Marine Fisheries Specialist in Cooperative Extension Department of Wildlife, Fish, and Conservation Biology, University of California, Davis

We are recruiting a Marine Fisheries Specialist at Assistant Specialist rank to work with Sea Grant Extension colleagues and diverse groups on research and education needs in marine fisheries, conduct research on biological and human dimensions of fisheries, and provide information on harvest and conservation of marine fish and shellfish to policy makers and stakeholders. **Qualifications:** Ph.D. in Biological Sciences or related fields with background in ecology, marine biology, and/or resource management. Evidence of leadership, team-building, and strong communication skills.

Information and applications:
http://recruitments.caes.ucdavis.edu

Inquiries: Dr. John Eadie, Committee Chair, **(530) 754-9204**, **jmeadie@ucdavis.edu**. Applications should be received by **February 29, 2008**.

UC Davis is an Affirmative Action/Equal Employment Opportunity Employer and is dedicated to recruiting a diverse faculty community. We welcome all qualified applicants, including women, minorities, veterans, and individuals with disabilities.

POSITIONS OPEN

UAB THE UNIVERSITY OF ALABAMA AT BIRMINGHAM

POSTDOCTORAL POSITIONS at the UNIVERSITY of ALABAMA at BIRMINGHAM

The University of Alabama at Birmingham (UAB) is one of the premier research universities in the United States with internationally recognized programs in AIDS and bacterial pathogenesis, bone biology and disease, cancer, diabetes and digestive and kidney diseases, free radical biology, immunology, lung disease, neuroscience, trauma and inflammation, and basic and clinical vision science among others. UAB is committed to the development of outstanding postdoctoral scientists and has been consistently ranked in recent years as one of the top 10 locations among U.S. universities for training postdoctoral scholars.

UAB is recruiting candidates for postdoctoral positions in a variety of research areas. UAB faculty are well-funded (20th in 2005 NIH funding), utilize multidisciplinary approaches, and provide excellent research training environments that can lead exceptional candidates to entry-level positions in academia, government, or the private sector. Full medical coverage (single or family), competitive salaries/stipends, sick leave, vacation, and maternity/paternity leave are offered with every position. Depending on the source of funding, other benefits may be available. Birmingham is a mid-size city centrally located in the southeast near beaches and mountains, and enjoys a moderate climate for year-round outdoor activities and a cost of living rate lower than most metropolitan areas.

Visit our **website: http://www.postdocs.uab.edu,** under Postdoctoral Opportunities to view posted positions. Send your curriculum vitae and cover letter to the contact name for those positions for which you are qualified and which interest you. **University of Alabama at Birmingham, Office of Postdoctoral Education, telephone: 205-975-7020.**

UAB is an Equal Employment Opportunity Employer.

The University of Texas Southwestern Medical Center at Dallas. Division of Nephrology seeks **CLINICAL RESEARCH FELLOW** for a one-year clinical fellowship in dialysis-related clinical research beginning in July 2008 at the Dallas VA. This program offers the opportunity to follow a chronic hemodialysis shift for a year, participate in transplant evaluation clinic, and carry out clinical research in patients with advanced kidney disease. The applicant also has the opportunity to audit classes in the Clinical Sciences Graduate Program.

To apply, contact:

Robert F. Reilly, M.D.
Professor of Medicine, University of Texas Southwestern
Chief, Section of Nephrology
VA North Texas Healthcare System
4500 S. Lancaster Road
Dallas, TX 75216
Telephone: 214-857-1908
E-mail: robert.reilly2@va.gov

UT Southwestern is an Equal Opportunity/Affirmative Action Employer.

TECHNICIAN wanted. The University of Georgia (UGA) Complex Carbohydrate Research Center (CCRC) is seeking a Research Technician to assist in studies of the roles of carbohydrates in memory. The Technician will participate in the synthesis of fluorescent tags and will chromatographically separate the tagged carbohydrates. The position requires a B.S.; laboratory experience in analytical and/or organic chemistry is desired. Send application letter, curriculum vitae, and names and e-mail addresses of two references to **Christian Heiss, e-mail: cheiss@ccrc.uga.edu.** All applications received by January 31, 2008, will be considered. *Equal Employment Opportunity/Affirmative Action.*

STONY BROOK UNIVERSITY MEDICAL CENTER

Stony Brook University Medical Center seeks highly qualified physician scientists (Assistant/Associate/Professor) to participate in developing the new Long Island Center for Clinical and Translational Sciences (LICCATS). This center will bring together clinicians and scientists from a consortium of major clinical and research institutions throughout Long Island to catalyze the translation of innovative ideas into improved clinical practice and human health. As the lead institution for this center, Stony Brook University has an extensive research portfolio. Ongoing initiatives include the recent launching of the New York Supercomputing Center and a newly created 246-acre Research and Development Park configured to house the Center of Excellence in Wireless and Information Technology and the Center for Advanced Energy, among other initiatives. LICCATS will leverage existing strengths in computational and structural biology, drug discovery and medical device design, nanotechnology, and imaging to expand its translational medicine capacities. Selected candidates will hold faculty appointments in the appropriate School of Medicine department based on the incumbents' area of expertise. **Required:** The successful candidate must have an M.D., be board eligible in their medical specialty, qualified for New York State licensure, and engaged in clinical/ translational research. **Preferred:** Preference will be given to candidates with a track record of peer-reviewed NIH or similar source of funding. Qualified candidates with demonstrated abilities may be able to assume leadership positions within the institution. To qualify for an appointment as an Associate Professor or Professor, the candidates must meet the School of Medicine's criteria for Appointment, Promotion, and Tenure and must have an established reputation and record of research or scholarly activity. Competitive packages commensurate with qualifications and level of appointment will be offered with salary, protected time for research, laboratory space, and funds to initiate research programs. Review of applications will begin in January 2008 and will continue until positions are filled. Electronic submissions are preferred.

To apply online visit *www.stonybrook.edu/jobs* or send a cover letter, C.V., names, and contact information for four references to:
Marie Gelato, M.D., Ph.D., Professor of Medicine, Department of Medicine
T15-060 Health Sciences Center Stony Brook University, SUNY
Stony Brook, NY 11794-8154

Equal Opportunity/Affirmative Action Employer.

上海交通大学

Distinguished Professor/Professor/Associate Professor Positions at the Med-X Research Institute, Shanghai Jiao Tong University, Shanghai, China

The newly established Med-X Research Institute at the Shanghai Jiao Tong University (SJTU), Shanghai, China, is one of the key open collaborative research platforms integrating the strengths in science, engineering and medicine of the university. It supports innovative and groundbreaking multi-interdisciplinary research in emerging medical and technological fields, as well as modern clinical instrumentation, equipment and systems.

The Institute invites applicants for 20 full-time tenure/tenure-track positions, at distinguished professor, professor or associate professor levels, who will undertake international research leadership in, but not limited to, each of the following general fields:

1. Biomedical imaging and image informatics
2. Neural biomedical engineering and other biomedical instrumentation
3. Novel technology for preventive, predictive and personalized medicine, and early diagnosis and treatment
4. Digital medicine, tele-medicine, and medical informatics

The applicants will collaborate with the best faculty in our Medical, Engineering, Sciences and other Schools, and in our 12 affiliated hospitals. The Institute will provide an intellectually stimulating research environment, conduct cutting-edge research in Med-X areas, and train the next generation of researchers.

Applicants should have doctoral level qualifications in a relevant academic discipline, outstanding international reputation in research and scholarship, and strong track record or potential in securing funding. Applicants should be willing to work with a team and possess a dedication to research and education. Remuneration packages will be competitive and will match the candidate's qualifications and experiences. (Visiting and contract positions will also be considered.)

Please send a detailed curriculum vitae with names and contact details of three referees, statement of intended research, and copies of three publications, by **February 28, 2008** to: **Professor Jiufu Luo, Associate Director, The Med-X Research Institute, Shanghai Jiao Tong University, Shanghai 200030, China; E-mail: jfluo@sjtu.edu.cn; Tel: 0086-21-62932359 (office); 0086-13501622305 (mobile)**.

---

nature geoscience

Associate Editor

Nature Publishing Group, the publisher of *Nature*, is pleased to announce the launch of *Nature Geoscience*. This international monthly journal will launch in January 2008 providing in-depth coverage of the Earth Sciences. In December 2007, *Nature Geoscience* has started publishing research related to the understanding of the Earth as a system, including relevant investigations of the solid Earth, hydrosphere, atmosphere, cryosphere and climate, as well as the planets of the solar system.

We seek an **Associate Editor** to establish *Nature Geoscience* as the essential publication for the Earth Science community.

The ideal candidate will have (or expect shortly to receive) a Ph.D. or equivalent degree in one of the disciplines of the geosciences. Postdoctoral experience is preferred (but not required), but emphasis will be placed on broadly trained applicants. The successful candidate will play an important role in determining the representation of their field in the journal. Key elements of the position include the selection of manuscripts for publication, as well as commissioning, editing and writing for the journal. Close contact with related research communities, through conferences and laboratory visits, will be an essential component of this position.

This is a demanding and intellectually stimulating role, which calls for a keen interest in the practice and communication of science. The successful candidate will therefore be highly motivated and outgoing, and must possess excellent interpersonal skills. The salary and benefits are competitive, reflecting the critical importance and responsibilities of this position, based in our London or Boston offices.

Applicants should send a CV (including a brief account of their research and other relevant experience), a research highlight in *Nature Geoscience* style (200 words or less) on a recent relevant *Nature* paper, and a brief cover letter explaining their interest in the post and their salary expectations.

Applications should be sent to Denise Pitter, Personnel Assistant at
londonrecruitment@macmillan.co.uk
Applicants should clearly mark on their submissions reference number NPG/LON/795.
Incomplete applications will not be considered.

Closing date: 18th January 2008.

nature publishing group npg

FACULTY POSITIONS in TERRESTRIAL BIOGEOCHEMISTRY and CLIMATE CHANGE

The Appalachian Laboratory (AL) of the University of Maryland Center for Environmental Science (UMCES) seeks two individuals for full-time faculty positions at either the **ASSISTANT or ASSOCIATE PROFESSOR** level to enhance our strengths in terrestrial and aquatic ecology, landscape and watershed ecology, and remote sensing. Excellent research and computing facilities are available at AL, including plant, soil, and water analysis laboratories with state-of-the-art analytical instrumentation, growth chambers, and a greenhouse. The main responsibility of these positions is research, but UMCES faculty also participate in graduate education, outreach, and application of basic science to regional (e.g., restoration of Chesapeake Bay) and global (e.g., land use and climate change) environmental problems. We will interview candidates who are interested in collaborative research, are published in top scientific journals, and can acquire external funding to support their research.

We are particularly interested in: (1) Effects of climate change on terrestrial and/or aquatic ecosystems. We seek an **ECOLOGIST** who applies climate change data and forecasts to address the problem of ecosystem change, including issues such as invasive species, mitigation of ecosystem impacts, ecosystem restoration, adaptation of land and aquatic resource management, and ecosystem/climate feedback processes.

(2) Terrestrial biogeochemistry in multiuse landscapes. We seek an outstanding researcher who may address topics such as carbon sequestration by soils, forest nutrient transformations, and effects of land use change and ecosystem disturbances on elemental cycles.

Applicants should send curriculum vitae; statement of research interests; brief discussion of how the applicant's research would complement ongoing research at AL/UMCES; selected reprints; and list of four references (name, title, mailing address, telephone, fax, and e-mail address) to either the: **Climate Change** or **Terrestrial Biogeochemistry Search Committee, Appalachian Laboratory, University of Maryland Center for Environmental Science, 301 Braddock Road, Frostburg, MD 21532.** Review of applications will begin on December 1, 2007. Information about AL and UMCES can be found at **websites: http://www.al.umces.edu/** and **http://www.umces.edu/.** *UMCES is an Affirmative Action/Equal Opportunity Employer. Women and minorities are strongly encouraged to apply.*

ASSISTANT/ASSOCIATE/FULL PROFESSORS in COGNITIVE NEUROSCIENCE

Cognitive Neuroscience Center
Medical University of South Carolina

The Department of Neurosciences and the Neuroscience Institute at the Medical University of South Carolina seek applications for several tenure-track faculty positions in cognitive neuroscience. Candidates will partake in the development of a new Cognitive Neuroscience Center, located on the medical school campus in Charleston. Applicants must have a strong academic record of independent research with a Ph.D. or M.D. degree and expertise in neurophysiology in behaving animals, neuroimaging in animals or humans, or other cognitive neuroscience approach. Newly renovated laboratory space, new animal and human research imaging facilities, and attractive startup packages and benefits are available.

Applicants must apply online at **website: http://www.musc.edu/hrm/careers/faculty.htm.** Position requisition number is 044299 and review of applications will begin on February 1, 2008, and continue until the positions are filled. Applicants should also submit online a cover letter expressing their interest and qualifications, curriculum vitae, and names of three references addressed to: **Gary Aston-Jones, Ph.D., Department of Neurosciences, Medical University of South Carolina, 173 Ashley Avenue, BSB 403, Charleston, SC 29425**. (Please note: all documents must be submitted online.)

MUSC is an Equal Employment Opportunity/Affirmative Action Employer.

RUTGERS
CAMDEN

The Biology Department of Rutgers University in Camden, New Jersey seeks a broadly trained **EXPERIMENTAL GENETICIST** for a tenure-track **ASSISTANT PROFESSOR** position beginning fall 2008. Research interests in systems or computational/integrative biology are desirable. Ph.D. required and postdoctoral experience preferred. This position entails teaching undergraduate and graduate courses in the area of the applicant's expertise and participation in introductory biology courses. Please send curriculum vitae, statement of research interests, and three letters of recommendation to: **Dr. Joseph V. Martin, Biology Department, Rutgers University, Camden, NJ 08102.** Review of applications will begin January 25, 2008, and continue until the position is filled. *Rutgers is an Equal Opportunity/Affirmative Action Employer. Women and minorities are encouraged to apply.*

The Faculty of Biological Sciences of the Pontificia Universidad Católica de Chile has opened applications for three tenure-track **ASSISTANT PROFESSOR** positions, at the Department of Cell and Molecular Biology (two positions) and the Department of Physiology (one position). Candidates should possess the capacity to develop an independent research program in their respective field, complementing the departmental orientation towards the fundamental mechanisms which sustain biological function and the variations that cause disease, either at the molecular, cellular, tissue, organ, or individual level, as well as their translational possibilities for medicine or biotechnology. Please refer to **website: http://www.bio.puc.cl/departamentos/home.asp?id_section=75** and **website: http://www.bio.puc.cl/departamentos/home.asp?id_section=76.**

The position will involve teaching activities directed to undergraduate and graduate students, including research training.

Candidates must hold a Ph.D., or combined M.D./Ph.D. degrees, and should accredit research expertise in cellular and/or molecular biology or physiology, supported by postdoctoral training.

Applications will be received until March 31, 2008. Please send curriculum vitae, a brief description of previous and anticipated research, and three reference letters. The positions will be immediately available, but should start not later than March 2009.

Application packages should be sent either via regular mail or e-mail (in PDF format) to the following address:

Dr. Rodrigo Iturriaga
Secretario Académico
Facultad de Ciencias Biológicas
Casilla 114-D
Santiago, Chile
E-mail: riturriaga@bio.puc.cl

HERBARIUM CURATOR/ ASSISTANT PROFESSOR of GEOGRAPHY

The Utah Museum of Natural History and Department of Geography at the University of Utah invite applications for a tenure-track joint position as Herbarium Curator and Assistant Professor of Geography beginning 1 July 2008. Complete job description and application instructions can be found at the following **website: http://www.umnh.utah.edu/pageview.aspx?menu=4257&id=16046.**

The University of Utah values candidates who have experience working in settings with students from diverse backgrounds, and possess a strong commitment to improving access to higher education for historically underrepresented students.

The University of Utah is an Equal Opportunity/Affirmative Action Employer, encourages applications from women and minorities, and provides reasonable accommodation to the known disabilities of applicants and employees.

FACULTY POSITION in VACCINE and INFECTIOUS DISEASES INSTITUTE and CLINICAL RESEARCH DIVISION

Fred Hutchinson Cancer Research Center and the University of Washington

The Vaccine and Infectious Disease Institute and Clinical Research Division of the Fred Hutchinson Cancer Research Center (FHCRC) and the University of Washington (UW) are jointly recruiting a full-time faculty position at the **ASSISTANT or ASSOCIATE MEMBER/PROFESSOR** level as an **ASSOCIATE LABORATORY DIRECTOR** with the HIV Vaccine Trials Network Laboratory Program, in the Clinical Research Division of the FHCRC and the Department of Global Health at the UW, with preference being given to those who study molecular immunology as it relates to HIV vaccines, pathogenesis, and immunology. M.D. or Ph.D. qualification is required. The individual will be expected to develop an independent research program. Excellent collaborations with scientists in clinical, molecular medicine, and basic sciences at FHCRC and the UW are available. Salary depending on experience plus excellent benefits. Application review will continue until the position is filled. Interested candidates may submit curriculum vitae, a concise statement of research plan, and three reference letters to:

Julie McElrath, M.D., Ph.D.
Co-Director, Vaccine and Infectious Disease Institute
Associate Head, Program in Infectious Diseases
Fred Hutchinson Cancer Research Center
1100 Fairview Avenue N., LE-500
P.O. Box 19024
Seattle, WA 98109-1024

The University of Washington and the Fred Hutchinson Cancer Research Center are Affirmative Action, Equal Opportunity Employers. We are dedicated to the goal of building a culturally diverse and pluralistic faculty and staff committed to teaching and working in a multicultural environment and strongly encourage applications from women, minorities, individuals with disabilities, and covered veterans.

MOLECULAR PSYCHIATRIST

University of California, Irvine
School of Medicine
Department of Psychiatry and Human Behavior

The Department of Psychiatry is seeking to identify qualified individuals for a Molecular Psychiatry Program. This position is half of a full-time equivalent (FTE) **ASSOCIATE or FULL PROFESSOR,** tenure and half FTE **ASSOCIATE or FULL PROFESSOR IN RESIDENCE,** senate. Level and salary are commensurate with qualifications. The position involves the application of molecular techniques to understand psychiatric illness.

The UCI School of Medicine is committed to the development of a major program in molecular medicine and a psychiatric component is considered an essential part of this research agenda. Successful candidates must have an M.D. and/or Ph.D. degree with expertise and experience in the field of molecular psychiatry. Methodological, statistical genetic experience, and laboratory skills are desirable. The successful candidate should have a proven record of research funding and scholarly activity/publications.

Please send curriculum vitae to:

Barry F. Chaitin, M.D.
Chairman and Professor
University of California, Irvine
Department of Psychiatry and Human Behavior
c/o Academic Personnel Manager
19722 MacArthur Boulevard, RM 13B
Irvine, CA 92612

Submission via electronic mail can be made to **e-mail: bhobart@uci.edu.**

Closing date: December 31, 2007.

The University of California, Irvine has an active career partner program and a National Science Foundation ADVANCE Program for Gender Equality and is an Equal Opportunity Employer committed to excellence through diversity.

THE UNIVERSITY OF SOUTHERN MISSISSIPPI
DEPARTMENT OF BIOLOGICAL SCIENCES
TENURE-TRACK FACULTY POSITION ENTOMOLOGY

The University of Southern Mississippi Department of Biological Sciences invites application for a nine-month, tenure-track assistant professor position in entomology. The successful candidate will join our growing department with strong research programs in cellular and molecular biology, organismal biology and ecology. Although preference will be given to applicants whose research complements existing research programs, work in any area of applied or basic research will be considered. A competitive salary commensurate with qualifications and experience, competitive startup package, modern lab space, and state-of-the-art facilities will be provided.

The University of Southern Mississippi, a Carnegie Research High Activity institution with 15,000 students, is located in Hattiesburg, Miss., near the Gulf Coast and has abundant opportunities for outdoor recreation. Hattiesburg is the medical, commercial and cultural center of southern Mississippi and is ranked in the top five small metropolitan areas in the United States. The Department of Biological Sciences comprises twenty-nine faculty and offers baccalaureate, Master of Science and Ph.D. degrees. Over 60 graduate students currently pursue masters and doctoral degrees. Further information about the department may be found at **http://www.usm.edu/biology/**.

The successful candidate will be expected to establish an active, extramurally funded research program, mentor graduate students and participate in undergraduate and graduate teaching in his or her area of expertise. Postdoctoral research experience is required. Applicants should submit a letter of application, curriculum vitae, statement of research plans, copies of pertinent reprints and three letters of reference to: **Micheal Davis, Entomology Search Committee, Dept. of Biological Sciences, The University of Southern Mississippi, 118 College Drive #5018, Hattiesburg, MS 39406-0001**. Electronic submission accepted (**Mike.Davis@usm.edu**). Review of applications will begin on **January 31, 2008**, and continue until the position is filled.

The University of Southern Mississippi is an Affirmative Action/Equal Opportunity Employer/Americans with Disabilities Act Institution.

CONFERENCE

2nd International Congress on Stem Cells and Tissue Formation

July 6-9 2008

International Congress Center Dresden

Speakers:

Arturo Alvarez-Buylla
Yves A. Barde
Thomas Braun
Oliver Brüstle
Gerald De Haan
Michele De Luca
Stefanie Dimmeler
Yuval Dor
Reinhard Fässler
Jonas Frisén
Margaret A. Goodell
Jürgen Hescheler
Ryoichiro Kageyama
Arnold R. Kriegstein
Evert Kroon
Achim Leutz
Shin-Ichi Nishikawa
Shahin Rafii
Hans R. Schöler
Martin E. Schwab
Austin Smith
Kirsty L. Spalding
Gustav Steinhoff
Andrew F. Stewart
Derek van der Kooy
Valeri Vasioukhin
Fiona Watt
Marius Wernig
Anna M. Wobus
Pamela C. Yelick
Peter W. Zandstra

More information:
www.stemcellcongress-dresden.org

---

nature chemistry

Associate Editors

The Nature Publishing Group is pleased to announce the launch of *Nature Chemistry* in 2009. Following the success of *Nature Materials, Nature Chemical Biology* and *Nature Physics*, and given the strength of the parent journal *Nature*, we fully expect *Nature Chemistry* to seize the commanding heights of the chemistry-publishing landscape.

Alongside the highest-quality original research, *Nature Chemistry* will cover news, commentary and analysis from and for the chemistry community, as well as striving to develop a voice that chemists care about.

As part of this exciting new publishing venture, we are now seeking three Associate Editors for *Nature Chemistry*, to be based in our London, Boston and Tokyo offices.

Applicants should have a PhD in a chemistry-related discipline, with demonstrable research achievements. Although postdoctoral experience is preferred (not required), emphasis will be placed on broadly trained applicants with a good knowledge of the chemistry community. Key elements of the position include the selection of manuscripts for publication, and commissioning, editing and writing other content for the journal. Candidates who wish to be considered for the role in our Japan office must demonstrate a good understanding of the East Asian research communities (in particular Japan, China and Korea) as well as being fluent in English and preferably an Asian language (Japanese, Chinese or Korean).

These are demanding and extremely stimulating roles, which call for a keen interest in the practice and communication of science. The successful candidates will, therefore, be dynamic, motivated and outgoing, and must possess excellent interpersonal skills. The salary and benefits, will be competitive, reflecting the critical importance and responsibilities of each position.

Applicants should send a CV (including their class of degree and a brief account of their research and other relevant experience), a News & View style piece (no more than 500 words) on a recent paper from the chemical literature, and a brief cover letter explaining their interest in the post, salary expectations, and indicating whether they wish to be considered for a position in London, Boston or Tokyo.

To apply please send your CV and covering letter, quoting reference number NPG/LON/797 to Denise Pitter at londonrecruitment@macmillan.co.uk

Closing date: 31st January 2008.

nature publishing group npg

FACULTY POSITION
Exercise and Nutrition Translational Obesity/Metabolic Syndrome/ Diabetes Research
University of Missouri, Columbia
Department of Nutritional Sciences

The Department of Nutritional Sciences at the University of Missouri, Columbia invites applications for a tenure-track position at the **ASSISTANT PROFESSOR** level from investigators whose interests focus on obesity and the metabolic syndrome. The newly expanded Department of Nutritional Sciences now spans three colleges within the University and has a mission focused on an interdisciplinary approach to the obesity epidemic with broad application from pipette to patient to population to policy. The University is noted for interdisciplinary research programs. We are seeking an outstanding scientist to work in our expanding human exercise and nutrition academic and research programs. Position qualifications include an M.D./Ph.D., M.D., or a Ph.D. with postdoctoral experience and a translational research focus. The successful applicant will be expected to develop an outstanding translational research program and contribute to Department teaching activities. This person would be involved in campus-wide research initiatives relative to exercise and nutrition in obesity, metabolism, and the metabolic syndrome. Located midway between St. Louis and Kansas City, Columbia is a vibrant university town that is consistently ranked among the top small cities to live in America.

Please send curriculum vitae, a narrative of research and educational interests, and the names and contact information of three references to:

Chair, Nutritional Sciences Search Committee
Department of Nutritional Sciences
217 Gwynn Hall
University of Missouri-Columbia
Columbia, MO 65211

Or by electronic submission (strongly preferred) to **e-mail: umchesnsjobs@missouri.edu.** Active review of applications will begin January 15, 2008, and the search will continue until the position is filled.

Visit the University of Missouri, Columbia's **website: http://www.missouri.edu/.** *Please direct ADA accommodation requests to our* ***Coordinator*** *at* ***telephone: 573-884-7278*** *(V/TTY). The University of Missouri, Columbia is an Equal Opportunity Employer, Affirmative Action Employer, and complies with the guidelines set forth in the Americans with Disabilities Act of 1990.*

POSTDOCTORAL RESEARCH - MENTORED TEACHING FELLOWSHIPS available: Office for Diversity in Science Training, University of Kansas, NIH-Institutional Research and Academic Career Development Award (IRACDA) Program. Postdoctoral fellowships are available through the NIH-IRACDA Program. This comprehensive Program offers three years of support to outstanding candidates seeking postdoctoral research training along with an opportunity to obtain mentored teaching experience in a four-year tribal college in preparation for an academic career. Ph.D. in biomedical sciences or related field required. For complete description and application instructions go to **website: https://jobs.ku.edu,** position #00061772. Review of applications will begin March 15, 2008, for appointments beginning August 1, 2008, and will continue until positions are filled. *Equal Opportunity/Affirmative Action Employer.*

COMPUTATIONAL BIOCHEMISTRY CONSULTANT

The University of Minnesota Supercomputing Institute seeks to hire a person with a computational biochemistry/biophysics background to join a dynamic group that provides high level of technical support for researchers. The candidate must have expertise in computational aspect of molecular modeling, structural chemistry, drug design, and/or structural biology.

Please see the employment section at **website: http://www.msi.umn.edu** for details.

The U of M is an Equal Opportunity Educator and Employer.

UNIVERSITY OF MINNESOTA

RESEARCH ASSISTANT PROFESSOR
Cryo-electron Microscopy
University of Minnesota

The University of Minnesota, Twin Cities invites applications for a research-track faculty position in the area of cryo-electron microscopy. Full position description is available online.

Ph.D. or equivalent degree with minimum of five years of experience in the field of cryo-electron microscopy is required. Applications are accepted through the University of Minnesota online employment **website: http://employment.umn.edu/applicants/Central?quickFind=68717.**

Equal Opportunity Educator and Employer.

FACULTY POSITION in VACCINE and INFECTIOUS DISEASES INSTITUTE
Fred Hutchinson Cancer Research Center and the University of Washington

The Vaccine and Infectious Disease Institute and Clinical Research Division of the Fred Hutchinson Cancer Research Center (FHCRC) and the University of Washington (UW) are jointly recruiting one or more full-time faculty positions at the level of **ASSISTANT MEMBER/PROFESSOR** without tenure in the Clinical Research Division of the FHCRC and the Department of Global Health at the UW. Preference is being given to those who study molecular immunology as it relates to HIV vaccines, pathogenesis, and mucosal immunology. M.D. or Ph.D. qualification is required. University of Washington faculty engage in teaching, research, and service. The individual will be expected to develop an independent research program. Excellent collaborations with scientists in clinical, molecular medicine, and basic sciences at the Fred Hutchinson Cancer Research Center and the University of Washington are available. Salary depending on experience plus excellent benefits. Interested candidates may submit curriculum vitae, a concise statement of research plan, and three reference letters to:

Julie McElrath, M.D., Ph.D.
Co-Director, Vaccine and Infectious Disease Institute
Associate Head, Program in Infectious Diseases
Fred Hutchinson Cancer Research Center
1100 Fairview Avenue N., LE-500
P.O. Box 19024
Seattle, WA 98109

Application review will continue until the position is filled.

The University of Washington and the Fred Hutchinson Cancer Research Center are Affirmative Action, Equal Opportunity Employers. We are dedicated to the goal of building a culturally diverse and pluralistic faculty and staff committed to teaching and working in a multicultural environment, and strongly encourage applications from women, minorities, individuals with disabilities, and covered veterans. The University of Washington, a recipient of the 2006 Alfred P. Sloan award for Faculty Career Flexibility, is committed to supporting the work-life balance of its faculty.

POSTDOCTORAL POSITIONS
Molecular Cellular Imaging

Two Postdoctoral positions are available to study the relationship between protein subnuclear localization and transcriptional regulation. Our research combines molecular biological approaches with live cell imaging to address these questions. The ideal candidate will have a background in molecular biology and cellular imaging, and will be qualified for NIH training grant support. Send curriculum vitae and three references to: **Richard N. Day, Departments of Medicine and Cell Biology, Box 800578 HSC, University of Virginia, Charlottesville, VA 22908-0578; e-mail: rnd2v@virginia.edu; website: http://faculty.virginia.edu/rday/.**

EVOLUTIONARY FUNCTIONAL MORPHOLOGIST
FACULTY POSITION at the UNIVERSITY of MONTANA

The Organismal Biology and Ecology Program seeks a tenure-track **ASSISTANT/ASSOCIATE PROFESSOR in VERTEBRATE FUNCTIONAL MORPHOLOGY.** The successful candidate will take a strong experimental approach that is both laboratory and field-based and integrates ecological and evolutionary perspectives in the study of animal performance. Areas of interest are open, but could encompass comparative anatomy and physiology, evolution of locomotor morphology and performance, or evolution of feeding morphology and function. Teaching responsibilities will include an undergraduate course in comparative vertebrate morphology, an undergraduate course to be identified, and a graduate seminar. Shared animal-holding pens, flight tunnels, and a fully equipped laboratory for research in functional morphology are housed at a near-campus research facility. Candidates at the Associate Professor level should possess a highly regarded research program, with a strong publication record, excellence in teaching, and success at obtaining competitive funding. Assistant Professor applicants should show strong evidence of the potential to develop a vigorous, externally funded research program and teaching excellence. Applicants must have a Ph.D. and ideally postdoctoral experience.

Applicants should send application materials (curriculum vitae, statements of research and teaching interests, representative examples of publications, and names of three references) to: **Thomas E. Martin, Chair, Functional Morphologist Search Committee, Division of Biological Sciences, University of Montana, Missoula, MT 59812;** or by **e-mail: morph.search@mso.umt.edu.** Review of materials will begin on 8 February 2008. Additional information on this position may be obtained at **website: http://morphologist.dbs.umt.edu.**

The University of Montana is an Affirmative Action/Equal Opportunity Employer. DBS is interested in hiring candidates who will enhance the ethnic and gender diversity of its faculty. UM is an Equal Employment Opportunity/Affirmative Action Employer and the recipient of an active National Science Foundation PACE Award.

POSTDOCTORAL POSITION
Baylor College of Medicine

Postdoctoral Research position is available immediately to study estrogen receptor action in bladder cancer focusing on therapeutic uses of selective estrogen receptor modulators (SERMs). We use a combination of state-of-the-art cell and molecular biology techniques in conjunction with in vivo bioluminescence imaging and ultrasonography of mouse bladder tumor models. For details of the Laboratory's research see **website: http://public.bcm.tmc.edu/mcb/faculty/smith_c.html.**

Required qualifications: Ph.D. in biological science with a strong background in molecular and/or cancer biology. Experience with mouse tumor models is desired. Salary commensurate with experience.

To apply send (e-mail preferred; **e-mail: carolyns@bcm.tmc.edu**) a letter of application including a short description of research experience and interests, curriculum vitae, and names and contact information for three references to **Carolyn Smith, Ph.D.** at the following address: **Department of Molecular and Cellular Biology, BCM130, Baylor College of Medicine, Houston, TX 77030.** *BCM is an Equal Opportunity, Affirmative Action, Equal Access Employer.*

University of Florida College of Public Health and Health Professions/Emerging Pathogens Institute seeks a **PROFESSOR and DIRECTOR,** Environmental Health Program; a doctoral degree in appropriate discipline required. View the complete job posting at **website: http://www.phhp.ufl.edu/services/humanresources/** and click on job vacancies. *The University of Florida is an Equal Opportunity Employer.*

In good company...

Official photograph of T.R.H. the Prince and Princess of Asturias with the Laureates. Bottom row starting from the left, Michael Schumacher, Prince of Asturias Award Laureate for Sports; Felix Zandman, Avner Shalev, chairman of the directorate of Yad Vashem, Prince of Asturias Award Laureate for Concord; Al Gore, Prince of Asturias Award Laureate for International Cooperation; Amos Oz, Prince of Asturias Award Laureate for Letters; Lady Christiane Dahrendorf, wife of Ralf Dahrendorf, Prince of Asturias Award Laureate for Social Sciences; Ginés Morata and Peter Lawrence, Prince of Asturias Award Laureate for Scientific and Technical Research; second row, David Azrieli, Moshe Haelion, Mazaltov Behar Mordoh, Isaac Querub Caro, president of Yad Vashem Spain; Perla Bittan Hazan, director of Yad Vashem's Ibero-America, Spain and Portugal Desk; **Colin Norman, News Editor and Andrew Sugden, International Managing Editor of *Science*, Prince of Asturias Award Laureate for Communication and Humanities**; third row Andrèe Geulen-Herscovici, Baruch Shub, Jaime Vándor Koppel, Zygmunt Rotter Fleischer, Anna Rzechte de Rotter, Max Mazin, honorary president of Yad Vashem Spain, Prince of Asturias Award Laureate for Concord; Philip Campbell, editor-in-chief of *Nature* and Annette Thomas, CEO of Macmillan Ltd, Prince of Asturias Award Laureate for Communication and Humanities.

Science is proud to be co-recipient, with *Nature*, of Spain's 2007 Prince of Asturias Foundation Award – Communication and Humanities. Since 1981, the foundation has recognized world leaders in scientific, technical, cultural, social, and humanitarian work. We are honored to be in their company.

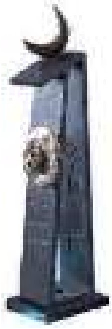

Congratulations to all the 2007 winners.

Arts – Bob Dylan
Communication and Humanities – Journals *Science* and *Nature*
Concord – Yad Vashem, the Holocaust Museum in Jerusalem
International Cooperation – Al Gore
Letters – Amos Oz
Scientific and Technical Research – Ginés Morata and Peter Lawrence
Social Sciences – Ralf Dahrendorf
Sports – Michael Schumacher

Photos courtesy of the Prince of Asturias Foundation.

Science
AAAS

PLANT COMMUNITY ECOLOGIST (ASSISTANT PROFESSOR)

The Department of Ecology at Montana State University seeks a Plant Community Ecologist (tenure track) to teach and study plant community ecology with a focus on plant/animal interaction, plant community biodiversity, and/or climate change/disturbance response, preferably in the greater Yellowstone ecosystem and Montana. Collaborative research with existing strengths in animal ecology, quantitative ecology, land use change, and landscape ecology is desirable. See **website: http://www.montana.edu/ecology/** for more information. Start date negotiable; August 2008 preferred. Applicants should submit a letter of interest addressing the required and preferred qualifications, curriculum vitae, description of research accomplishments and future directions, statement of teaching experience and interests, copies of three publications, and names and contact information of three references to: **Plant Community Ecology Search Committee, Department of Ecology, Montana State University, Bozeman, MT 59717.** Screening of applications will begin February 15, 2008, and continue until a suitable candidate is found. *Montana State University and the Department of Ecology are committed to faculty diversity, and women and minority candidates are especially encouraged to apply. MSU is an Equal Opportunity/Affirmative Action Employer.*

ASSISTANT or ASSOCIATE PROFESSOR of MOLECULAR, CELLULAR, and INTEGRATED PHARMACOLOGY/TOXICOLOGY. Salary dependent on qualifications and experience. Ph.D. or equivalent with advanced training in pharmacology/toxicology or related field; teaching aptitude/experience/potential; potential to develop outstanding independent research program that applies modern molecular, cellular, and in vivo technologies toward understanding gene-environment interactions that influence susceptibility to complex disorders of humans and animals; ability/potential to acquire extramural funding; excellent interpersonal and communication skills; ability to work with others in a collegial, team atmosphere. Desired (not required): D.V.M., M.D., or equivalent with strong research focus. To receive fullest consideration, apply by February 25, 2008; open until filled. Submit (1) letter of intent outlining special interest in the position, overall related qualifications and experience and career goals; (2) curriculum vitae; (3) three reprints; and (4) names and addresses of three professional references to: **Isaac Pessah, Department Chair (e-mail: vm-mb@vetmed.ucdavis.edu), Department of Molecular Biosciences, School of Veterinary Medicine, 1 Shields Avenue, University of California, Davis, CA 95616.** E-mail applications preferred. *UCD is an Affirmative Action/Equal Opportunity Employer.*

PHARMACOLOGY TENURE-TRACK FACULTY POSITION
University of Wisconsin, Madison

A tenure-track faculty position as an **ASSISTANT PROFESSOR** is available in the Department of Comparative Biosciences, School of Veterinary Medicine. Qualifications include Ph.D., postdoctoral experience, and potential to develop an outstanding, extramurally funded research program in pharmacology that complements existing departmental strengths. Teaching responsibilities include instruction in fundamentals of pharmacology. To apply, send curriculum vitae, brief statements of research interests and teaching philosophy, and three reference letters to: **Gordon S. Mitchell, Chair, Department of Comparative Biosciences, University of Wisconsin, 2015 Linden Drive, Madison, WI 53706.** Apply by March 1, 2008. For additional information, see **website: http://www.vetmed.wisc.edu/jobs.html.** *Equal Opportunity/Affirmative Action Employer.*

Material Intelligence has the following positions open.

(1) **SENIOR SCIENTIST.** Requires Ph.D. in physics or closely related field and working knowledge of scalar diffraction and inverse scattering in nonuniform media. Duties will include both theory and experiments. Software, electronic design, or mechanical skills are desirable.

(2) **PROGRAM MANAGER.** Requires degree in engineering or physical science, experience in similar job function, and competency in office and project management software. Duties include administering a government contract; preparing and submitting reports and data items; and coordinating meetings, program reviews, and field tests.

(3) **ELECTRICAL ENGINEER/DESIGNER.** Requires degree plus five years of experience in electrical engineering, analog circuit design for instrumentation, digital design with field-programmable gate array, layout, and test. Degree in a physical science with relevant experience may be accepted. Also desirable are ultrasound, microwave, and video experience.

(4) **SOFTWARE ENGINEER.** Requires degree in engineering, or physical science, plus five years of experience designing and programming real time systems, device drivers, signal processing, data acquisition, graphics, and video.

(5) **MECHANICAL ENGINEERING TECHNICIAN.** Requires degree in mechanical engineering, or physical science, and relevant experience. Duties include light mechanical design, machining and assembly, and assisting in experiments. Experience in environmental testing is desirable.

(6) **TECHNICAL ASSISTANT/COMPUTER SUPPORT.** Requires degree in engineering or physical science, experience in system management, and software programming skills. Mechanical and electrical skills are desirable. Duties include maintaining computer systems and assisting the senior technical staff.

All positions are located near Morristown, New Jersey.

Please send resumes to **e-mail: jobs@mi-llc.com.**

BIOLOGICAL OCEANOGRAPHER TENURE-TRACK FACULTY POSITION
Florida State University
Department of Oceanography

The Department of Oceanography is seeking to fill a tenure-track faculty position in biological oceanography. We are looking for excellent candidates who are expected to become leaders in their respective fields. The Department actively collaborates with the Department of Biological Sciences **(website: http://www.bio.fsu.edu/),** the Geophysical Fluid Dynamics Institute **(website: http://www.gfdi.fsu.edu),** and supports the Florida State University Coastal and Marine Laboratory **(website: http://www.marinelab.fsu.edu/),** a facility with coastal vessels and laboratories, focusing on research in the pristine ecosystems of the northeastern Gulf of Mexico. The search will continue until the position is filled, but applications received by March 1, 2008, are guaranteed full consideration. Applicants are asked to send separate PDF files containing curriculum vitae, a statement of research/teaching interests, and the names of three references via e-mail to **Dr. Joel Kostka (e-mail: jkostka@ocean.fsu.edu), Department of Oceanography, Florida State University, 117 N. Woodward Avenue, P.O. Box 3064320, Tallahassee, FL 32306-4320. Telephone: 850-644-6700; fax: 850-644-2581.** *FSU is an Equal Opportunity Employer; applications from underrepresented groups are encouraged.*

POSTDOCTORAL POSITION available at the University of California, Los Angeles, to study regulatory T cells development and function (*Nature Immunology* **8**:359-68, 2007, *Journal of Immunology* **178**:2961-72, 2007). Experience in molecular biology and immunology desirable. Send curriculum vitae, a brief description of research experience, and names of three references to **Dr. Talal Chatila (e-mail: tchatila@mednet.ucla.edu).**

POSTDOCTORAL POSITIONS
Lovelace Respiratory Research Institute
Giving the Gift of Breath

Lovelace Respiratory Research Institute (LRRI), the only research Institute fully dedicated to curing respiratory disease, is seeking motivated individuals for two Postdoctoral Fellow appointments in the area of lung mucus biology. These immediately available positions will focus on the elucidation of the molecular mechanism of the anti-inflammatory role of Muc1 mucin (*Journal of Immunology* **176**:3890, 2006) using both in vivo and in vitro systems. Applicants should have a Ph.D., at least two years of directly related experience, and a strong research background in molecular/cell biology, preferably in lung physiology and cell signaling. Opportunities for growth into independent research areas are available.

Please send a cover letter, curriculum vitae, and names of three references to: **Job #N4307, Human Resources Office, Lovelace Respiratory Research Institute, 2425 Ridgecrest Drive S.E., Albuquerque, NM 87108** or **e-mail: hrmail@lrri.org,** or send via **fax: 505-348-4976.**

Equal Opportunity/Affirmative Action Employer. Minorities and Females.

AQUATIC ECOLOGY POSTDOCTORAL

The U.S. Environmental Protection Agency Office of Research and Development seeks applications for a Postdoctoral position supporting causal and risk assessments. The successful applicant will be part of a vibrant team that provides web-based tools to help environmental managers identify the probable causes of biological impairments in aquatic ecosystems. Examples of our work can be viewed at **website: http://www.epa.gov/caddis**.

This is a three-year, federal appointment in Arlington, Virginia. Salary is approximately $50,000 to $70,000 commensurate with qualifications, plus benefits. *Citizenship restrictions apply.* Additional information and application instructions may be found at **website: http://www.epa.gov/ncea**, or by contacting **Jeffrey Frithsen, e-mail: frithsen.jeff@epa.gov**. Application deadline is January 29, 2008. *The USEPA is an Equal Opportunity Employer.*